

# **Synthesis and Evaluation of Benzoyl containing compounds as potential anti-cancer agents**

**Saqib Munir Ahmed**

**School of Science, Engineering & Environment**

**University of Salford, Salford, UK**

**Submitted in Partial Fulfilment of the requirements of the Degree of Philosophy,**

**July 2020**

## Contents

List of Figures .....	7
List of Tables .....	18
Acknowledgements.....	20
Declaration.....	21
Abstract.....	22
Abbreviations.....	24
<b>1. Introduction.....</b>	<b>27</b>
<b>1.1 Cancer .....</b>	<b>27</b>
1.1.1 What is cancer?.....	27
1.1.2 Data Statistics.....	27
<b>1.2 Types of Cancer.....</b>	<b>28</b>
1.2.1 Blastoma .....	28
1.2.2 Carcinoma .....	28
1.2.3 Sarcoma.....	29
1.2.4 Melanoma .....	29
1.2.5 Lymphoma .....	29
1.2.6 Leukaemia .....	29
<b>1.3 Causes of Cancer .....</b>	<b>30</b>
1.3.1 Environmental Factors .....	30
1.3.2 Infection .....	31
1.3.3 Genetics .....	32

1.4	The Cell.....	33
1.4.1	Cell Division.....	33
1.4.2	G0 Phase .....	34
1.4.3	G1 Phase .....	34
1.4.4	S Phase .....	34
1.4.5	G2 Phase .....	34
1.4.6	M Phase.....	34
1.4.7	Mutations.....	35
1.5	Cancer treatment/s.....	44
1.5.1	Surgery .....	45
1.5.2	Radiotherapy.....	45
1.5.3	Chemotherapy .....	47
1.6	Medicinal Anti-Cancer Drugs .....	50
1.6.1	DNA Reactive Agents .....	51
1.6.2	Platinum based Agents including Cisplatin .....	52
1.7	Antimetabolites.....	57
1.8	Antimitotics.....	60
1.9	$\beta$ -Diketones.....	60
1.9.1	Properties of $\beta$ -diketones .....	62
1.10	Absorption, Distribution, Metabolism and Excretion (A.D.M.E).....	63
1.10	Protein coding and kinases .....	65
1.10.1	Proliferating Cell Nuclear Antigen (PCNA) .....	65

1.10.2	Cyclin-dependent kinase 4 (CDK4) .....	66
1.10.3	Cyclin-dependent kinase 6 (CDK6) .....	67
<b>1.11</b>	<b>Aims of the project</b> .....	<b>69</b>
<b>2</b>	<b>Material and Methods</b> .....	<b>71</b>
<b>2.1</b>	<b>Synthesis and purification</b> .....	<b>71</b>
2.1.1	General procedures for compound purification and determination .....	71
2.1.2	General Procedures for synthetic approach .....	73
2.1.3	Synthesis of $\beta$ -Diketone derivatives .....	77
2.1.4	Synthesis of 2-Azido-Diketone derivatives .....	88
2.1.5	Synthesis of <i>N</i> -benzoyl- <i>N'</i> -phenylurea derivatives .....	91
<b>2.2</b>	<b>Experimental – Biological Assays</b> .....	<b>94</b>
2.2.1	Subculture and cell maintenance .....	94
2.2.2	Cell Lines .....	96
2.2.2.1	HepG2 .....	96
2.2.2.2	HCT-116 .....	97
2.2.2.3	HeLa .....	97
2.2.2.4	A549 .....	98
2.2.2.5	CaCo-2 .....	98
2.2.3	Drug Dilution .....	99
2.2.4	MTT Assay .....	99
2.2.5	RNA isolation .....	100
2.2.5.1	RNA Quantification .....	101

2.2.5.2	cDNA Synthesis.....	102
2.2.5.3	qRT-PCR.....	102
<b>2.3</b>	<b>Experimental – Pharmacological Assays .....</b>	<b>104</b>
2.3.1	Plasma Stability Assay.....	104
2.3.2	Liver S9 Fraction Stability Assay.....	107
<b>3</b>	<b>Results &amp; Discussion.....</b>	<b>111</b>
3.1	Synthesis of compounds and analogues.....	111
3.1.1	Dibenzoylmethane.....	113
3.1.2	$\beta$ -Diketones and Synthesis.....	114
3.1.2.1	Baker-Venkataraman Route.....	115
3.1.3	$\beta$ -Diketones as scaffoldings for different targets.....	119
3.1.4	Keto-Enol Tauterism.....	121
3.2	Biological Evaluation.....	124
3.2.1	Cytotoxicity – MTT Assay.....	124
3.2.2	Cytotoxicity – Cisplatin.....	128
3.2.3	Cytotoxicity - DBM and Derivatives (Compounds 1-10) .....	130
3.2.4	Cytotoxicity - 2-Azido Derivatives (Compounds 11-13) .....	149
3.2.5	Cytotoxicity on Benzoylurea Derivatives (Compounds 14-16) .....	155
3.3	Plasma Stability Assay.....	161
3.3.1	Plasma Stability – DBM and Derivatives (Compounds 1-10) .....	166
3.3.2	Plasma Stability – 2-Azido Derivatives (Compounds 11 -13) .....	179
3.3.3	Plasma Stability – Benzoylurea Derivatives (Compounds 14 - 16) .....	183

3.4	S9 Fraction Stability.....	192
3.4.1	S9 Fraction Stability – DBM And Derivatives (Compounds 1 – 10).....	195
3.4.2	S9 Fraction Stability – 2-Azido and Benzoylurea Derivatives (Compounds 11 – 16) .....	202
3.5	PCR and qPCR.....	210
3.5.1	Polymerase Chain Reaction (PCR).....	210
3.5.2	Real-Time PCR.....	212
3.6	Conclusion and Future Work .....	221
4	References .....	223
	Appendix A.....	249
	Raw Data – <sup>1</sup> HNMR spectra .....	249
	Raw Data – IR Spectra.....	256

## List of Figures

Figure 1 A comparison showing the process of cell division between normal and cancerous cells as they divide (adapted from (Shirzadfar, Riahi & Ghaziasgar, 2017)) .....	38
Figure 2 The 10 distinguished Hallmarks of Cancer (adapted from (Hanahan & Weinberg, 2011)) ....	39
Figure 3 Showing how Tumours can stimulate neighbouring cells to harvest angiogenesis signalling molecules resulting in the formation of new blood vessels to occur (Nishida, 2006).....	41
Figure 4 Selective differences between normal healthy cells and cancerous cells. (adapted from (Nishida-Aoki and Ochiya, 2015)) .....	43
Figure 5 The process of cell division. Adapted from Cancer Research UK (Skeel et al., 2011) and (Tobis, Hochhauser & Souhami, 2010). .....	48
Figure 6 Chemical structures of Platinum containing compounds, Cisplatin, Carboplatin and Oxaliplatin, which are widely used as anti-cancer agents .....	51
Figure 7 Chemical structures of Aminopterin and Methotrexate (MTX), which block the production of folic acid .....	58
Figure 8 Chemical structures of Vincristine and Vinblastine, common vinca alkaloids which inhibit the assembly of microtubules .....	60
Figure 9 Overview of the canonical Wnt signalling pathway (adapted from (Khan et al., 2018)) .....	61
Figure 10 Structure of synthetic polymers which includes the common, acrylonitrile butadiene styrene (ABS). ( <a href="https://www.researchgate.net/figure/Formula-of-acrylonitrile-butadiene-styrene-ABS_fig1_307546266">https://www.researchgate.net/figure/Formula-of-acrylonitrile-butadiene-styrene-ABS_fig1_307546266</a> ).....	62
Figure 11 Scheme to show general synthetic route for 1,3-Diketone production using the base/acid method via reflux .....	74
Figure 12 Scheme to show general synthetic route for 2-Azido-Diketone production .....	75
<b>Figure 13: 1-(2-hydroxyphenyl)-3-phenylpropane-1,3-dione (1)</b> .....	77
<b>Figure 14: 1-(2,4-dihydroxyphenyl)-3-phenylpropane-1,3-dione (2)</b> .....	78
<b>Figure 15: 1-(5-chloro-2-hydroxyphenyl)-3-phenylpropane-1,3-dione (3)</b> .....	79

<b>Figure 16: 2-bromo-1,3-diphenylpropane-1,3-dione (4)</b> .....	80
<b>Figure 17: 1-(2-hydroxy-4-methoxyphenyl)-3-phenylpropane-1,3-dione (5)</b> .....	81
<b>Figure 18: 1,3-bis(4-methoxyphenyl)propane-1,3-dione (6)</b> .....	82
<b>Figure 19: 1-(3-(dimethyloxidanyl)-4,5-dimethoxyphenyl)-3-(2-flouro-4-methoxyphenyl)propane-1,3-dione (7)</b> .....	83
<b>Figure 20: 1-(3-(dimethyloxidanyl)-4,5-dimethoxyphenyl)-3-3-flouro-4-methoxyphenyl)propane-1,3-dione (8)</b> .....	84
<b>Figure 21: 1-(3-(dimethyloxidanyl)-4,5-dimethoxyphenyl)-3-(3,4,5-trimethoxyphenyl)propane-1,3-dione (9)</b> .....	85
<b>Figure 22: 1-(phenyl-3-(3,4,5-trimethoxyphenyl)propane-1,3-dione (10)</b> .....	86
<b>Figure 23: 1,3-diphenylpropane-1,3-dione (DBM)</b> .....	87
<b>Figure 24: 2-Azido-1,3-diphenylpropane-1,3-dione (11)</b> .....	88
<b>Figure 25: 2-Azido-1-(2-hydroxyphenyl)-3-phenylpropane-1,3-dione (12)</b> .....	89
<b>Figure 26: 2-Azido-1-(5-chloro-2-hydroxyphenyl)-3-phenylpropane-1,3-dione (13)</b> .....	90
<b>Figure 27: 4-methoxy-N-((4-(trifluoromethyl)phenyl)carbamothioyl)benzamide (14)</b> .....	91
<b>Figure 28: 4-methoxy-N-((3,4,5-trimethoxyphenyl)carbamothioyl)benzamide (15)</b> .....	92
<b>Figure 29: 4-methoxy-N-((4-methoxyphenyl)carbamothioyl)benzamide (16)</b> .....	93
<b>Figure 30 The equilibrium balance formed between the Keto and Enol Tautomer during rapid excitation</b> .....	113
<b>Figure 31 A modified mechanism of Baker-Venkataraman for the synthesis of <math>\beta</math>-diketones, highlighting ring closure</b> .....	116
<b>Figure 32 NHC stimulated synthesis of <math>\beta</math>-diketones (Singh et al., 2011)</b> .....	118
<b>Figure 33 Microwave-assisted production of <math>\beta</math>-diketone with silyl enol ether (Wiles, Watts, Haswell &amp; Pombo-villar, 2002)</b> .....	119
<b>Figure 34 Naturally occurring <math>\beta</math>-Diketone, Curcumin, which has been tested for potential anti-cancerous activity</b> .....	120

Figure 35 7,12-dimethylbenz[ $\alpha$ ]anthracene (DMBA) ..... 120

Figure 36 A graph showing the % Cell Viability of Cisplatin when tested on all 5 cells lines, which include HepG2, HeLa, HCT-116, A549 and Caco-2. Cells were incubated at periods of 24, 48, 72 and 96 hours, and dosed at concentrations; 100uM, 50uM, 25uM, 12.5uM, 6.25uM ..... 129

Figure 37 A graph showing the % Cell Viability of DBM when tested on all 5 cells lines, which include HepG2, HeLa, HCT-116, A549 and Caco-2. Cells were incubated at periods of 24, 48, 72 and 96 hours, and dosed at concentrations; **100uM, 50uM, 25uM, 12.5uM, 6.25uM and 3.125uM** ..... 135

Figure 38 A graph showing the % Cell Viability of Compound 1 when tested on all 5 cells lines, which include HepG2, HeLa, HCT-116, A549 and Caco-2. Cells were incubated at periods of 24, 48, 72 and 96 hours, and dosed at concentrations; **100uM, 50uM, 25uM, 12.5uM, 6.25uM and 3.125uM** ..... 136

Figure 39 A graph showing the % Cell Viability of Compound 2 when tested on all 5 cells lines, which include HepG2, HeLa, HCT-116, A549 and Caco-2. Cells were incubated at periods of 24, 48, 72 and 96 hours, and dosed at concentrations; **100uM, 50uM, 25uM, 12.5uM, 6.25uM and 3.125uM** ..... 137

Figure 40 A graph showing the % Cell Viability of Compound 3 when tested on all 5 cells lines, which include HepG2, HeLa, HCT-116, A549 and Caco-2. Cells were incubated at periods of 24, 48, 72 and 96 hours, and dosed at concentrations; 100uM, 50uM, 25uM, 12.5uM, ..... 138

Figure 41 A graph showing the % Cell Viability of Compound 5 when tested on all 5 cells lines, which include HepG2, HeLa, HCT-116, A549 and Caco-2. Cells were incubated at periods of 24, 48, 72 and 96 hours, and dosed at concentrations; 100uM, 50uM, 25uM, 12.5uM, ..... 139

Figure 42 A graph showing the % Cell Viability of Compound 4 when tested on all 5 cells lines, which include HepG2, HeLa, HCT-116, A549 and Caco-2. Cells were incubated at periods of 24, 48, 72 and 96 hours, and dosed at concentrations; **100uM, 50uM, 25uM, 12.5uM, 6.25uM and 3.125uM** ..... 141

Figure 43A graph showing the % Cell Viability of Compound 6 when tested on all 5 cells lines, which include HepG2, HeLa, HCT-116, A549 and Caco-2. Cells were incubated at periods of 24, 48, 72 and 96 hours, and dosed at concentrations; 100uM, 50uM, 25uM, 12.5uM, ..... 143

Figure 44 A graph showing the % Cell Viability of Compound 7 when tested on all 5 cells lines, which include HepG2, HeLa, HCT-116, A549 and Caco-2. Cells were incubated at periods of 24, 48, 72 and 96 hours, and dosed at concentrations; **100uM, 50uM, 25uM, 12.5uM, 6.25uM and 3.125uM** ..... 144

Figure 45 A graph showing the % Cell Viability of Compound 8 when tested on all 5 cells lines, which include HepG2, HeLa, HCT-116, A549 and Caco-2. Cells were incubated at periods of 24, 48, 72 and 96 hours, and dosed at concentrations; **100uM, 50uM, 25uM, 12.5uM, 6.25uM and 3.125uM** ..... 145

Figure 46A graph showing the % Cell Viability of Compound 9 when tested on all 5 cells lines, which include HepG2, HeLa, HCT-116, A549 and Caco-2. Cells were incubated at periods of 24, 48, 72 and 96 hours, and dosed at concentrations; 100uM, 50uM, 25uM, 12.5uM, ..... 147

Figure 47 graph showing the % Cell Viability of Compound 10 when tested on all 5 cells lines, which include HepG2, HeLa, HCT-116, A549 and Caco-2. Cells were incubated at periods of 24, 48, 72 and 96 hours, and dosed at concentrations; 100uM, 50uM, 25uM, 12.5uM, ..... 148

Figure 48 A graph showing the % Cell Viability of Compound 11 when tested on all 5 cells lines, which include HepG2, HeLa, HCT-116, A549 and Caco-2. Cells were incubated at periods of 24, 48, 72 and 96 hours, and dosed at concentrations; 100uM, 50uM, 25uM, 12.5uM, ..... 152

Figure 49 A graph showing the % Cell Viability of Compound 12 when tested on all 5 cells lines, which include HepG2, HeLa, HCT-116, A549 and Caco-2. Cells were incubated at periods of 24, 48, 72 and 96 hours, and dosed at concentrations; 100uM, 50uM, 25uM, 12.5uM ..... 153

Figure 50 A graph showing the % Cell Viability of Compound 13 when tested on all 5 cells lines, which include HepG2, HeLa, HCT-116, A549 and Caco-2. Cells were incubated at periods of 24, 48, 72 and 96 hours, and dosed at concentrations; 100uM, 50uM, 25uM, 12.5uM ..... 154

Figure 51 A graph showing the % Cell Viability of Compound 14 when tested on all 5 cells lines, which include HepG2, HeLa, HCT-116, A549 and Caco-2. Cells were incubated at periods of 24, 48, 72 and 96 hours, and dosed at concentrations; **100uM, 50uM, 25uM, 12.5uM, 6.25uM and 3.125uM** ..... 158

Figure 52 A graph showing the % Cell Viability of Compound 15 when tested on all 5 cells lines, which include HepG2, HeLa, HCT-116, A549 and Caco-2. Cells were incubated at periods of 24, 48, 72 and 96 hours, and dosed at concentrations; 100uM, 50uM, 25uM, 12.5uM ..... 159

Figure 53A graph showing the % Cell Viability of Compound 16 when tested on all 5 cells lines, which include HepG2, HeLa, HCT-116, A549 and Caco-2. Cells were incubated at periods of 24, 48, 72 and 96 hours, and dosed at concentrations; 100uM, 50uM, 25uM, 12.5uM ..... 160

Figure 54 Above; Plotted data curves to show the % of RMP remaining over the different incubation periods, when tested with 50% and 100% Plasma concentrations. The graphs have been plotted using data from Table 14 & 15. Below; HPLC spectra obtained after running a sample containing RMP and 100% Plasma concentration after an incubation period of 120 minutes. HPLC system was injected with an 80:20 MeOH/H2O ratio ..... 165

Figure 55 Plotted data curves to show the % of DBM remaining over the different incubation periods, when tested with 50% and 100% Plasma concentrations. The graphs have been plotted using data from Table 14 & 15 ..... 166

Figure 56 Plotted data curves to show the % of Compound 1 remaining over the different incubation periods, when tested with 50% and 100% Plasma concentrations. The graphs have been plotted using data from Table 14 & 15. Below; HPLC spectra obtained after running a sample containing Compound 1 and 50% Plasma concentration at incubation period 120 min. HPLC system was injected with an 80:20 MeOH/H2O ratio ..... 168

Figure 57 Plotted data curves to show the % of Compound 2 remaining over the different incubation periods, when tested with 50% and 100% Plasma concentrations. The graphs have been plotted using data from Table 14 & 15. Below; HPLC spectra obtained after running a sample containing Compound 2 and 100% Plasma concentration at incubation period 120 min. HPLC system was injected with an 80:20 MeOH/H2O ratio ..... 169

Figure 58 Plotted data curves to show the % of Compound 3 remaining over the different incubation periods, when tested with 50% and 100% Plasma concentrations. The graphs have been plotted

using data from Table 14 & 15. Below; HPLC spectra obtained after running a sample containing Compound 3 and 50% Plasma concentration at incubation period 120 min. HPLC system was injected with an 80:20 MeOH/H<sub>2</sub>O ratio ..... 170

Figure 59 Plotted data curves to show the % of Compound 5 remaining over the different incubation periods, when tested with 50% and 100% Plasma concentrations. The graphs have been plotted using data from Table 14 & 15. Below; HPLC spectra obtained after running a sample containing Compound 5 and 100% Plasma concentration at incubation period 120 min. HPLC system was injected with an 80:20 MeOH/H<sub>2</sub>O ratio ..... 171

Figure 60 Plotted data curves to show the % of Compound 4 remaining over the different incubation periods, when tested with 50% and 100% Plasma concentrations. The graphs have been plotted using data from Table 14 & 15. Below; HPLC spectra obtained after running a sample containing Compound 4 and 50% Plasma concentration at incubation period 120 min. HPLC system was injected with an 80:20 MeOH/H<sub>2</sub>O ratio ..... 173

Figure 61 Plotted data curves to show the % of Compound 6 remaining over the different incubation periods, when tested with 50% and 100% Plasma concentrations. The graphs have been plotted using data from Table 14 & 15..... 175

Figure 62 Plotted data curves to show the % of Compound 9 remaining over the different incubation periods, when tested with 50% and 100% Plasma concentrations. The graphs have been plotted using data from Table 14 & 15. Below; HPLC spectra obtained after running a sample containing Compound 9 and 50% Plasma concentration at incubation period 120 min. HPLC system was injected with an 80:20 MeOH/H<sub>2</sub>O ratio ..... 176

Figure 63 Plotted data curves to show the % of Compound 10 remaining over the different incubation periods, when tested with 50% and 100% Plasma concentrations. The graphs have been plotted using data from Table 14 & 15 ..... 177

Figure 64 Plotted data curves to show the % of Compound 7 remaining over the different incubation periods, when tested with 50% and 100% Plasma concentrations. The graphs have been plotted using data from Table 14 & 15..... 177

Figure 65 Plotted data curves to show the % of Compound 8 remaining over the different incubation periods, when tested with 50% and 100% Plasma concentrations. The graphs have been plotted using data from Table 14 & 15. Below; HPLC spectra obtained after running a sample containing Compound 8 and 50% Plasma concentration at incubation period 120 min. HPLC system was injected with an 80:20 MeOH/H2O ratio ..... 178

Figure 66 Plotted data curves to show the % of Compound 11 remaining over the different incubation periods, when tested with 50% and 100% Plasma concentrations. The graphs have been plotted using data from Table 14 & 15. Below; HPLC spectra obtained after running a sample containing Compound 11 and 100% Plasma concentration at incubation period 120 min. HPLC system was injected with an 80:20 MeOH/H2O ratio..... 180

Figure 67 Plotted data curves to show the % of Compound 12 remaining over the different incubation periods, when tested with 50% and 100% Plasma concentrations. The graphs have been plotted using data from Table 14 & 15. Below; HPLC spectra obtained after running a sample containing Compound 12 and 100% Plasma concentration at incubation period 120 min. HPLC system was injected with an 80:20 MeOH/H2O ratio..... 181

Figure 68 Plotted data curves to show the % of Compound 13 remaining over the different incubation periods, when tested with 50% and 100% Plasma concentrations. The graphs have been plotted using data from Table 14 & 15. Below; HPLC spectra obtained after running a sample containing Compound 13 and 50% Plasma concentration at incubation period 120 min. HPLC system was injected with an 80:20 MeOH/H2O ratio ..... 182

Figure 69 Plotted data curves to show the % of Compound 14 remaining over the different incubation periods, when tested with 50% and 100% Plasma concentrations. The graphs have been plotted using data from Table 14 & 15. Below; HPLC spectra obtained after running a sample

containing Compound 14 and 100% Plasma concentration at incubation period 120 min. HPLC system was injected with an 80:20 MeOH/H<sub>2</sub>O ratio ..... 184

Figure 70 Plotted data curves to show the % of Compound 15 remaining over the different incubation periods, when tested with 50% and 100% Plasma concentrations. The graphs have been plotted using data from Table 14 & 15. Below; HPLC spectra obtained after running a sample containing Compound 15 and 100% Plasma concentration at incubation period 120 min. HPLC system was injected with an 80:20 MeOH/H<sub>2</sub>O ratio ..... 185

Figure 71 Plotted data curves to show the % of Compound 16 remaining over the different incubation periods, when tested with 50% and 100% Plasma concentrations. The graphs have been plotted using data from Table 14 & 15. Below; HPLC spectra obtained after running a sample containing Compound 16 and 50% Plasma concentration at incubation period 120 min. HPLC system was injected with an 80:20 MeOH/H<sub>2</sub>O ratio ..... 186

Figure 72 Plotted data curves to show the % of Compound RMP (left) and DBM (right) remaining over the different incubation periods, when tested in the presence of the S9 Fraction. Below; HPLC spectra obtained after running a sample containing RMP and S9 Fraction at time intervals of 10 min and 45 min respectively. HPLC system was injected with an 80:20 MeOH/H<sub>2</sub>O ratio ..... 195

Figure 73 Plotted data curves to show the % of Compound 1 (a) and Compound 2 (b) remaining over the different incubation periods, when tested in the presence of the S9 Fraction. Below; HPLC spectra obtained after running a sample containing Compound 1 and S9 Fraction after an incubation period of 45 minutes. HPLC system was injected with an 80:20 MeOH/H<sub>2</sub>O ratio ..... 197

Figure 74 Plotted data curves to show the % of Compound 3 (a) and Compound 4 (b) remaining over the different incubation periods, when tested in the presence of the S9 Fraction. Below; HPLC spectra obtained after running a sample containing Compound 4 and S9 Fraction after an incubation period of 45 minutes. HPLC system was injected with an 80:20 MeOH/H<sub>2</sub>O ratio ..... 198

Figure 75 Plotted data curves to show the % of Compound 5 (a) and Compound 6 (b) remaining over the different incubation periods, when tested in the presence of the S9 Fraction. Below; HPLC

spectra obtained after running a sample containing Compound 5 and S9 Fraction after an incubation period of 45 minutes. HPLC system was injected with an 80:20 MeOH/H<sub>2</sub>O ratio ..... 199

Figure 76 Plotted data curves to show the % of Compound 9 (a) and Compound 10 (b) remaining over the different incubation periods, when tested in the presence of the S9 Fraction. Below; HPLC spectra obtained after running a sample containing Compound 9 and S9 Fraction after an incubation period of 45 minutes. HPLC system was injected with an 80:20 MeOH/H<sub>2</sub>O ratio ..... 200

Figure 77 Plotted data curves to show the % of Compound 7 (a) and Compound 8 (b) remaining over the different incubation periods, when tested in the presence of the S9 Fraction. Below; HPLC spectra obtained after running a sample containing Compound 7 and S9 Fraction after an incubation period of 45 minutes. HPLC system was injected with an 80:20 MeOH/H<sub>2</sub>O ratio ..... 201

Figure 78 Plotted data curves to show the % of Compound 11 (a) and Compound 12 (b) remaining over the different incubation periods, when tested in the presence of the S9 Fraction. Below; HPLC spectra obtained after running a sample containing Compound 12 and S9 Fraction after an incubation period of 45 minutes. HPLC system was injected with an 80:20 MeOH/H<sub>2</sub>O ratio ..... 203

Figure 79 Plotted data curves to show the % of Compound 13 (a) and Compound 14 (b) remaining over the different incubation periods, when tested in the presence of the S9 Fraction. Below; HPLC spectra obtained after running a sample containing Compound 13 and S9 Fraction after an incubation period of 45 minutes. HPLC system was injected with an 80:20 MeOH/H<sub>2</sub>O ratio ..... 204

Figure 80 Plotted data curves to show the % of Compound 15 (a) and Compound 16 (b) remaining over the different incubation periods, when tested in the presence of the S9 Fraction. Below; HPLC spectra obtained after running a sample containing Compound 15 and S9 Fraction after an incubation period of 45 minutes. HPLC system was injected with an 80:20 MeOH/H<sub>2</sub>O ratio ..... 205

Figure 81 Graphical illustration/s plotted to show the Intrinsic Clearance for each compound tested in the presence of S9 Fraction. Graphs were plotted using data from Table 16 and show the following compounds respectively; a). RMP, DBM and derivatives b). RMP and the 2-Azido derivatives c) RMP and the Benzoylurea derivatives ..... 209

Figure 82 – <sup>1</sup> H NMR spectra for 2-bromo-1,3-diphenylpropane-1,3-dione (4) .....	249
Figure 83 - <sup>1</sup> H NMR spectra for 1-(3-(dimethyloxidanyl)-4,5-dimethoxyphenyl)-3-(3,4,5-trimethoxyphenyl)propane-1,3-dione (9).....	249
Figure 84 - <sup>1</sup> H NMR spectra for 1-(3-(dimethyloxidanyl)-4,5-dimethoxyphenyl)-3-(2-flouro-4-methoxyphenyl)propane-1,3-dione (7) .....	250
Figure 85 - <sup>1</sup> H NMR spectra for 1-(5-chloro-2-hydroxyphenyl)-3-phenylpropane-1,3-dione (3) .....	250
Figure 86 - <sup>1</sup> H NMR spectra for 1-(3-(dimethyloxidanyl)-4,5-dimethoxyphenyl)-3-3-flouro-4-methoxyphenyl)propane-1,3-dione (8) .....	251
Figure 87 - <sup>1</sup> H NMR spectra for 2-Azido-1,3-diphenylpropane-1,3-dione (12).....	251
Figure 88 - <sup>1</sup> H NMR spectra for 4-methoxy-N-((4-methoxyphenyl)carbamothioyl)benzamide (16)..	252
Figure 89 - <sup>1</sup> H NMR spectra for 1,3-bis(4-methoxyphenyl)propane-1,3-dione (6).....	252
Figure 90 - <sup>1</sup> H NMR spectra for 1-(phenyl-3-(3,4,5-trimethoxyphenyl)propane-1,3-dione (10) .....	253
Figure 91 - <sup>1</sup> H NMR spectra for 4-methoxy-N-((4-(trifluoromethyl)phenyl)carbamothioyl)benzamide (14).....	253
Figure 92 - <sup>1</sup> H NMR spectra for 1-(2-hydroxyphenyl)-3-phenylpropane-1,3-dione (1) .....	254
Figure 93 - <sup>1</sup> H NMR spectra for 1,3-diphenylpropane-1,3-dione (DBM) .....	254
Figure 94 - <sup>1</sup> H NMR spectra for 4-methoxy-N-((3,4,5-trimethoxyphenyl)carbamothioyl)benzamide (15).....	255
Figure 95 - <sup>1</sup> H NMR spectra for 1-(2,4-dihydroxyphenyl)-3-phenylpropane-1,3-dione (2) .....	255
Figure 96 – Infrared Spectroscopy (IR) for 2-bromo-1,3-diphenylpropane-1,3-dione (4).....	256
Figure 97 - Infrared Spectroscopy (IR) for 2-Azido-1-(2-hydroxyphenyl)-3-phenylpropane-1,3-dione (12).....	256
Figure 98 - Infrared Spectroscopy (IR) for 1,3-bis(4-methoxyphenyl)propane-1,3-dione (6) .....	257
Figure 99 - Infrared Spectroscopy (IR) for 1-(3-(dimethyloxidanyl)-4,5-dimethoxyphenyl)-3-3-flouro-4-methoxyphenyl)propane-1,3-dione (8).....	257

Figure 100 - Infrared Spectroscopy (IR) for 1-(3-(dimethyloxidanyl)-4,5-dimethoxyphenyl)-3-(3,4,5-trimethoxyphenyl)propane-1,3-dione (9).....	258
Figure 101 - Infrared Spectroscopy (IR) for 1-(3-(dimethyloxidanyl)-4,5-dimethoxyphenyl)-3-(2-flouro-4-methoxyphenyl)propane-1,3-dione (7) .....	258
Figure 102 - Infrared Spectroscopy (IR) for 1-(5-chloro-2-hydroxyphenyl)-3-phenylpropane-1,3-dione (3) .....	259
Figure 103 - Infrared Spectroscopy (IR) for 1,3-diphenylpropane-1,3-dione (DBM).....	259
Figure 104 - Infrared Spectroscopy (IR) for 1-(2-hydroxyphenyl)-3-phenylpropane-1,3-dione (1)....	260

## List of Tables

Table 1 Reagents provided within the cDNA synthesis kit and the working volumes used. RTase was added prior to the addition of RNA as the RTase contains an RNase inhibitor within. The cDNA was created with a maximum RNA concentration of 200ng/ $\mu$ l.....	102
Table 2 Primer sequences used for qRT-PCR.....	103
Table 3 Table shows the synthesised compounds as mentioned in the methods section 2.1.3, 2.1.4 & 2.1.5, including all $\beta$ -Diketone, 2-Azido and Benzoylurea derivatives.....	111
Table 4 IC50 values calculated for Cisplatin. Cytotoxicity was observed on HepG2, HeLa, HCT-116, A549 and Caco-2 cell lines, with the standard deviation being calculated based on triplicate results .....	128
Table 5 IC50 values of Beta-Diketone derivatives. Cytotoxicity was observed on HepG2 and HeLa cell lines, with the standard deviation being calculated based on triplicate results .....	131
Table 6 IC50 values of Beta-Diketone derivatives. Cytotoxicity was observed on A540 and HCT-116 cell lines, with the standard deviation being calculated based on triplicate results.....	132
Table 7 IC50 values of Beta-Diketone derivatives. Cytotoxicity was observed on the Caco-2 cell line, with the standard deviation being calculated based on triplicate results.....	133
Table 8 IC50 values of 2-Azido-Diketone derivatives. Cytotoxicity was observed on HepG2 and HeLa cell lines, with the standard deviation being calculated based on triplicate results.....	150
Table 9 IC50 values of 2-Azido-Diketone derivatives. Cytotoxicity was observed on A540 and HCT-116 cell lines, with the standard deviation being calculated based on triplicate results.....	150
Table 10 IC50 values of 2-Azido-Diketone derivatives. Cytotoxicity was observed on the Caco-2 cell lines, with the standard deviation being calculated based on triplicate results .....	151
Table 11 IC50 values for the Benzoylurea derivatives. Cytotoxicity was observed on HepG2 and HeLa cell lines, with the standard deviation being calculated based on triplicate results.....	156
Table 12 IC50 values for the Benzoylurea derivatives. Cytotoxicity was observed on A549 and HCT-116 cell lines, with the standard deviation being calculated based on triplicate results.....	156

Table 13 IC50 values for the Benzoylurea derivatives. Cytotoxicity was observed on the Caco-2 cell lines, with the standard deviation being calculated based on triplicate results. .... 157

Table 14 Containing the data obtained from all compounds when tested at conditions containing 50% Plasma concentration, incubated over time intervals from 0 – 120 minutes. Data highlights % compound remaining from 100% and an overall % decrease from first incubation to last ..... 162

Table 15 Containing the data obtained from all compounds when tested at conditions containing 100% Plasma concentration, incubated over time intervals from 0 – 120 minutes. Data highlights % compound remaining from 100% and an overall % decrease from first incubation to last. .... 163

Table 16 Data values for all compounds calculating pharmacokinetic parameters such as Half life (t1/2) in minutes, Intrinsic Clearance and the overall % decrease of the starting compound tested with the S9 Fraction contained after an incubation period of 0-45 minutes ..... 193

Table 17 Gene expression was obtained on HepG2 cells after 48 hours with the standard deviation being calculated based on triplicate results. .... 214

Table 18 Gene expression was obtained on HepG2 cells after 72 hours with the standard deviation being calculated based on triplicate results. .... 215

Table 19 Gene expression was obtained on HeLa cells after 48 hours with the standard deviation being calculated based on triplicate results. .... 216

Table 20 Gene expression was obtained on HeLa cells after 72 hours with the standard deviation being calculated based on triplicate results. .... 217

Table 21 Gene expression was obtained on A549 cells after 48 hours with the standard deviation being calculated based on triplicate results. .... 218

Table 22 Gene expression was obtained on A549 cells after 72 hours with the standard deviation being calculated based on triplicate results. .... 219

## Acknowledgements

***'In the name of the Almighty, the Most Gracious, the Ever Merciful.'***

Undertaking this Postgraduate degree has been a life shifting experience for me, one that I will treasure and apply in my personal and professional endeavours. This would not have been possible without the help and support of many individuals. Firstly, I would like to direct my sincere and humble gratitude to my advisor Dr. Patricia Raggazon for the continuous support of my study and related research. Not only that but also for her patience, motivation, and immense knowledge. Besides my advisor, I would like to thank the rest of my thesis committee: Dr. John Hadfield, for their insightful comments and encouragement as I know how hard it is stepping in at the last minute to help. My sincere thanks to the technicians who gave access to the laboratory and research facilities. Without their precious care it would not be possible to conduct this research. I thank my fellow lab-mates for the stimulating discussions, and for all the fun we have had in the last four years.

**I would like to thank my family: my Ami & Abu, my brothers and sisters for supporting me spiritually throughout writing this thesis. Every mother is there in the shadows for her child and my Ami has always been behind me, but more importantly this 'victory' is for my dad. The man who has grafted tirelessly day and night with complaining or asking for anything in return. I may not have told him, but he is definitely my role model in life. Abu...I wish I can become even 10% of the man you are and have been. I wish I can overcome struggles and see success the same way you have. A special mention to my 2<sup>nd</sup> Mama and Papa, plus two new sisters. I know how much you guys have prayed for me, and that is something I will always be indebted to. My success is the blessings I cannot repay back from ALL my FAMILY.**

**Above all, I would like to thank my wife Bareera for her unconditional love and constant support, for all the late nights and early mornings, and for keeping me sane the past few months. Thank you for being my muse, editor, proof-reader and sounding board. But most of all, thank you for being my best friend. I owe you everything. I Love You soo much!!! <3 <3 <3**

**Finally, I thank the Almighty, for the opportunities and the blessings.**

**BAREERA, AMI, ABU, MAMA, PAPA, AQIB, RASHDA, SALMA, AROOJ, MUBASHAR, GHALIB & SAMEEN...we have done it guys!!! This is Dr Saqib Munir Ahmed signing off now. I Love You Guys!!!**

## Declaration

The work described in this thesis was carried out within the laboratories at the University of Salford between September 2016 and June 2020 by the author. No part of this thesis has previously been submitted for a degree or any other qualification within the University of Salford or any other institution.

## Abstract

Seen as one of the major causes of death worldwide, Cancer requires the development of effective treatments to combat the disease. However, pharmaceutical companies are faced by the challenge of finding and developing a suitable compound that can override the barriers of the human body and operate effectively in its pharmacological properties.

This thesis and the research look at a naturally occurring compound, Dibenzoyl methane (DBM), its derivatives, and a few additional synthesised compounds with similar chemical properties and their unique activities demonstrated. DBM and its derivatives are classified as  $\beta$ -diketones and were synthesised using two different chemical schemes; the Baker-Venkataraman rearrangement and the Claisen acylation.

In comparison to this, a recently discovered synthetic class of compounds, *N*-benzoyl-*N'*-phenylurea and derivatives were also studied during the period of this investigation. The cytotoxicity of the drug candidates was determined on live mammalian cell lines including HepG2, HeLa and HCT 116 amongst a few supplementary cell lines using the MTT assay. Furthermore, as the final stage of a potential drug compound is associated with different mechanisms of the human body such as A.D.M.E, pharmacological factors such as stability within plasma and metabolic stability were measured. These are responsible for measuring the degradation of the compound over time and looking at the ability of the liver to remove the administered drug respectively. In addition, proceedings of the investigation led to quantitative real time PCR (qPCR) being conducted to analyse levels of gene expression. Observations were made with regards to gene expression on the cyclin-dependent kinase family which are involved in processes such as cell division and differentiation The data was

collected, plotted, and analysed to assess the efficacy of the drug candidates as potential anti-cancer agents.

It was found that several of the synthesised compounds exerted better activity than others, with DBM and compounds containing the O-H hydroxyl group performing better in screening for stability and toxicity. In addition, it was seen that the bulkier compounds, such as the -benzoyl-*N'*-phenylurea derivatives performed better in the assay for plasma stability. Therefore, it can be hypothesised that increasing the size of a compound to make it bulky can in turn improve pharmacological factors however the presence of different functional groups can lead to better toxicity and stability, thus when designing or synthesizing a compound, the approach of using heavier compounds, with many functional groups should be considered.

## Abbreviations

$^{13}\text{C}$ NMR	Carbon-13 nuclear magnetic resonance
$^1\text{H}$ NMR	Proton nuclear magnetic resonance
aq.	Aqueous
Brine	Aqueous sodium chloride solution (saturated)
$\text{CH}_3\text{CN}$	Acetonitrile
CuAAC	Copper (I)-catalyzed alkyne-azide cycloaddition
DCM	Dichloromethane
dd	double doublet
DMF	Dimethylformamide
DMSO	Dimethyl Sulfoxide
EDTA	ethylenediaminetetraacetic acid
EG	ethylene glycol
eq.	equivalent(s)
$\text{Et}_2\text{O}$	Diethyl ether
EtOAc	Ethyl Acetate

EtOH	ethanol
H <sub>2</sub> SO <sub>4</sub>	sulphuric acid
HCl	Hydrochloric Acid
HeLa	immortal cervical cancer cells derived from Henrietta lacks
IC <sub>50</sub>	half maximum inhibitory concentration
<i>J</i>	coupling constant (Hz)
logP	octanol-water partition coefficient
m	multiplet
MeCN	acetonitrile
MeOH	methanol
MgSO <sub>4</sub>	Magnesium Sulfate
MTT	3-(4,5-Dimethylthiazol-2-yl)-2,5-diphenyltetrazolium bromide
NADH	nicotinamide adenine dinucleotide
OMe	methoxy group (-OCH <sub>3</sub> )
PBS	phosphate buffer-solution
Pet.	Petroleum ether
R <sub>f</sub>	retention factor (in TLC)
s	singlet

SiO <sub>2</sub>	silica (silicon dioxide)
t	triplet
THF	tetrahydrofuran
TMS	tetramethyl silane

# 1. Introduction

## 1.1 Cancer

### 1.1.1 What is cancer?

“Everything is poisonous, and nothing is harmless. The dose (amount) alone defines whether something isn't poison” Paracelsus, 1493-1541.

The term cancer, present in every corner of the world, be it rich or poor, is used to describe a disease which has become a thorn to mankind. Here, cancer is defined whereby cells, classified as abnormal, divide uncontrollably and hence invade other healthy tissues within the body. Through systems readily available in the body such as blood and lymph, these newly formed cancer cells can spread in the body, affecting the body so much that it will ultimately lead to death.

### 1.1.2 Data Statistics

Cancer is one of the leading causes of mortality in the developing countries and throughout the world. In the United States of America. Cancer is currently the 2<sup>nd</sup> leading cause of death after heart disease and is predicted over the next few years to surpass heart disease (Siegel, Miller, & Jemal, 2015). In addition, there are more than 360,000 new cases of cancer reported in the UK every year and an estimated 14 million worldwide. In respect of the preceding decade, the incidence rate for cancer has increased by 7% and is projected to increase by a further 2% over the next two decades across the globe, resulting in 23.6 million new cases of cancer globally each year by 2030. There are more than 22 types of cancers (Marshall et al., 2016), thus regardless of numerous efforts, the disease still demands improved treatments (Liu, Miyoshi, & Nakamura, 2007).

Every year there are 164,000 cancer deaths recorded in the UK out of which 88,200 are accounted for by males, but on a global scale there are 8.2 million deaths recorded due to cancer. Common organ cancers such as breast, prostate and lung are responsible for more than a quarter of the deaths which occur in the UK. However, bowel cancer equates to half of those deaths, thus being the dominating type, as informed by Gundem and colleagues in 2015. Although individuals at any age can be diagnosed with cancer, Bassily and colleagues (2010) distinguished those reports show tendencies of escalation from the age of 55 and further established that individuals over the age of 75 account for over a third of all cancer cases in the UK. The cellular natural ageing process and a prolonged time of accrued mutations are the main causes of this increase.

## 1.2 Types of Cancer

There are numerous kinds of cancer that affect cells all over the body. The different types of cancer can be classified according to the type of cell or tissue where the cancer originates. There are six major types of cancer (Danø et al., 2005).

### 1.2.1 Blastoma

This type of cancer is derived from embryonic tissue and most found in children (Indolfi et al., 2007).

### 1.2.2 Carcinoma

This is the most common type of cancer. Carcinoma starts in epithelial cells and cells that make up the skin or the tissue lining organs, like the liver or kidneys. Like other types of cancer, carcinomas are abnormal cells that divide without control. They can spread to other parts of the body, but do not always do so. "*Carcinoma in situ*" remains in the cells where it started. Common forms are breast, lung and colon (Pannathur et al., 2013).

### 1.2.3 Sarcoma

This is a rare kind of cancer. These are tumours of the connective tissue. All sarcomas initiate from mesenchymal cells from the bone marrow. Examples of inclined tissues include cartilage, bone, muscle, and fat (Danø et al., 2005, Miller & Mihm, 2006).

### 1.2.4 Melanoma

This is a type of skin cancer. Melanoma initiates in skin cells that are positioned in the deep layer of the epidermis amid the layer of the basal cells called melanocytes. These cells make a pigment called melanin; this is responsible for giving the skin its natural colour but also delivers protection to the body from ultraviolet radiation from the sun (Miller & Mihm, 2006).

### 1.2.5 Lymphoma

This cancer starts in the lymph glands or other glands belonging to the lymphatic system. Though there are many different types of lymphoma, there are 2 main ones 1). Hodgkin lymphoma – cancer of a type of white blood cell called lymphocytes. This type of lymphoma contains cells called Reed Sternberg cells. Treatment for this type of lymphoma is very different to other lymphomas (Küppers, Engert & Hansmann, 2012). 2). Non-Hodgkin Lymphoma (NHL) – is a cancer of the lymphatic system. There are over 60 different types of NHL (Nossal, 1994).

### 1.2.6 Leukaemia

This cancer starts in blood, forming tissue which is usually the bone marrow. This cancer leads to the over-production of abnormal white blood cells, this affects the part of the immune system, that protects the body against infection. Leukaemia can be classified by

the type of white cell that is affected (myeloid or lymphatic) and by the way this disease progresses (acute or chronic) (Pui, Robison & Look, 2008).

### 1.3 Causes of Cancer

Cancer is a risk to most multicellular organisms, and inherent defence mechanisms have established throughout time in the pursuit to stop or prevent the occurrence and progression of cancer. Cell cycle regulation programmed cell death, immune responses, replicative aging limits, DNA mismatch repair, and the differentiation of cells and architecture of varied tissues are processes that cause the natural resistance to cancer (Hochberg & Noble, 2017). There are large variety of influences that play a role in the development of cancer. These can be in the form of genetic predisposition, age and lifestyle categorised as host factors, lengthy infection, the agents one is exposed to in their daily lives and finally environmental factors one resides in. As cancer cannot be classified as a single disease triggered and caused by a single factor, it becomes a challenge to single out the cause of development in individual cases (Danaei et al., 2005).

#### 1.3.1 Environmental Factors

There are multiple external environmental factors combined with genetic mutations that can lead to and cause human cancers, thus meaning that cancers originate from both environmental and genetic influences. Mutations of certain genes can cause cancer, and some of the mutations are due to natural occurrences amidst the process of DNA replication during cell division. Whereas others are a result of environmental exposures that damage the DNA. These exposures include chemicals in tobacco smoke or radiation found in ultraviolet rays from the Sun (Holick, 2008).

There have been links established between the consumption of alcohol and exposure to pesticides with likes of dichlorodiphenyltrichloroethane (DDT) and dichlorodiphenyldichloroethylene (DDE) and the development of breast cancer. Consumption of red meat and folic acid intake have been linked to a rise in colorectal cancer and UV exposure and use of photosensitising drugs have been heavily linked with melanoma incidences (Chan et al., 2011). Studies have also shown that 97% of all cancers are caused by environmental and man-made influences such as red meat, tobacco, chemicals, and environmental pollutants including radiation spills, exhaust fumes and the burning of fossil fuels (Parkin, Boyd & Walker, 2011). The largest contributor and cause of cancer is smoking in the UK, with a figure equating to 15%.

### 1.3.2 Infection

Infection has also been associated with cancer development, with an approximate 17.8% of all cancer incidences being accounted for by some type of infection. Of this 12.1% are attributed to viral infections. Infections in the form of bacterial, parasitic, and viral have all been linked to tumour occurrence due to their triggering of prolonged and chronic inflammation, which are ideal conditions needed for the proliferation of neoplastic cells (Collins, Hogan & Winter, 2011).

When an infection, such as hepatitis C, attacks the body, then the immune system will thrive to eliminate and destroy the infection. This is performed by prompting localised, acute inflammation which only persists for a brief period. If this is not successful, prolonged acute inflammation may occur, this is then what causes the optimum conditions promoting neoplasms (Danaei et al., 2005). These conditions also heighten the generation of large numbers of inflammation causing cells, these release cytokines, nitric oxide, isoforms of nitric

oxide synthase and reactive species that are derivatives of nitric oxide. All these excretions possess the ability to cause direct damage to DNA and impact proliferation and neoangiogenesis (Collins, Hogan & Winter, 2011).

With regards to bacterial infections, there are two non-specific mechanisms that are linked by belief to carcinogenesis; inflammation, witnessed in the *Helicobacter pylori* (*H. pylori*) infection, and bacterial metabolism leading to the generation of mutagenic compounds (Graham, 2000).

*H. pylori* present as a gram-negative rod-shaped bacterium, is positioned in the mucus layer, situated amid the stomach and the gastric epithelium, and has demonstrated to not migrate or invade neighbouring tissues such as penetrating the basement membrane. *H. pylori* is classified as a group 1 carcinogen and highlights a direct link to cancer formation. This is due to *H. pylori* infection triggering chronic superficial gastritis which then causes an increase in adenocarcinoma incidence 2-fold. In addition, statistics dictate that 3.5% of chronic superficial gastric victims will then progress to develop chronic atrophic gastritis instigating an increase in adenocarcinoma incidence a further 9-fold (Graham, 2000, Polk & Peek, 2010).

### 1.3.3 Genetics

Genetics also establish a crucial role in carcinogens with mutations in genetic material taking place both naturally and being passed down genetically. While naturally occurring, mutations are very challenging to predict and treat, as they are unintentional and often associated with the exposure to environmental stimuli such as radiation or mutagenic agents. However, it is possible to act preventively if the mutation is inherited (Hong et al., 2013). A prime example of inherited defects includes the BRCA1 and BRCA2 tumour suppressor genes, these are significant in the preservation of genomic stability by enabling the homologous

recombination (HR) restoration of DNA double strand breaks, proliferation control and growth regulation. Mutations in the BRCA1 and BRCA2 genes are directly associated with an increased risk of developing breast cancer and ovarian cancers. Nevertheless, for tumorigenesis to happen, the incidence of two events is vital; the first is that the patient must have acquired the mutated BRCA allele, and the second is that the patient must undertake somatic inactivation of the second BRCA allele (Moyer, 2014).

## 1.4 The Cell

Albeit the human body is a complex system which takes specific depth to understand, the foundation is purely based upon a small component, the cell. The cell predominantly is the unit of life within the human body, and all cancers begin within this component, the cell. A small structural unit consisting of biological and functional information, the cell, which is often described as a building block of life, can replicate independently hence make an abundant number of copies of themselves. As well as providing structure, energy and carrying out localised specialized function, contained within a cell can be found the hereditary material such as DNA, RNA, and chromosomes.

### 1.4.1 Cell Division

To maintain and grow, cells within the human body undergo a process in which a parent cell will divide into two or more daughter cells. This process is called Cell Division and usually occurs as part of the mammalian cell cycle.

To form new, fully functioning cells, both normal and cancer cells must undergo a series of phases, 5 to be specific. This chain of events is given the term, the cell cycle, and shown in schematic literature annotated using the characters G<sub>0</sub>, G<sub>1</sub>, S, G<sub>2</sub>, M which describe each phase. The cell cycle is a set of events which result in cell growth and division into two

daughter cells (Huang et al., 2013). After an initial reproduction stage, the newly formed cells, 2 to be precise, are identical to each other. When a new pair of cells is required by the body, the 2 cells formed from the initial cell can undergo the cell cycle, to produce more cells. The way the phases work is briefly outlined below, with all 5 phases mentioned.

#### 1.4.2 G0 Phase

Also called the 'Resting stage' the cell has not yet initialised the splitting process. A cell will spend most of its maturing life within this stage, with the length of this phase lasting from anywhere between a few hours to a few years for specific cells. Upon receiving a signal, the cell will progress to the G1 phase, where it will undergo reproduction.

#### 1.4.3 G1 Phase

Lasting around a period of between 18 to 30 hours, the cell in this phase starts to produce more protein, thus increasing its mass in size, forming cells of a normal size. Preparation for DNA replication occurs in this stage (Huang et al., 2013).

#### 1.4.4 S Phase

Containing the genetic information (DNA), the chromosomes undergo replication, whereby matching DNA strands are present as a template in both new cells formed. Named the S phase, the duration for this stage is between 18 to 20 hours.

#### 1.4.5 G2 Phase

After the DNA is defiantly checked, the cell will now start a process of splitting the cell into 2 different cells. This can take anywhere from between 2 to 10 hours.

#### 1.4.6 M Phase

Given the term the 'M Phase', this is the final stage where Mitosis takes place. Lasting a very small amount of time, in comparison to the other phases, this process takes around 30 to 60

minutes. During this phase, the cell essentially splits itself into 2 new different cells, which are identical to each other. Nuclear and cytoplasmic division also occurs.

#### 1.4.7 Mutations

Though many variations/mutations of cancer are present there is one simple mechanism followed by all types. This phenomenon is dictated when the normal cycle of old cells dividing and being replaced by new ones is taken over to an uncontrollable rate of abnormal cell growth, invading and spreading to various locations sites in the human body. Programmed cell death, commonly referred as apoptosis, has been defined by many, including Chiu and colleagues in 2013, as a process which controls the development and homeostasis of multicellular organisms by the elimination of damaged, aged, or mutated cells. When a mutation arises, the process of apoptosis does not occur thus leading to a great influx of new cells forming, an amount that the body does not require. This formation of extra cells leads onto produce the mass production of cells for masses of tissue that develop into a tumour (Ikediobi et al., 2006).

However, tumours which exist in the body are not all cancerous, there are some cancers that do not involve the formation of a tumour such as leukaemia. Defined as non-cancerous, benign tumours are often removed in several cases, and do not return. The cells which are involved with a benign tumour do not spread to different parts of the body. On the other hand, described as cancerous, malignant tumours do spread throughout the body. This is mediated through a process called metastasis, where the cells invade nearby tissues and are often circulated around the body (Rahbar et al., 2013, Tward et al., 2007).

During the process of cell division, there are a variety of processes that can occur either separately or as a collection which identify whether there is any damage to DNA that

necessitates correction (Finn, 2008). However, a cell that has suffered and gathered a large amount of DNA damage or a cell that no longer possesses the capability to effectively repair the damage, is able to enter one of the following three possible states:

- i. Senescence: this state will cause the cell to become dormant.

This phenomenon is also known as the 'Hayflick limit' and was explained by Hayflick and Moorhead (1961) as one where a normal cell can no longer divide. In an investigation that was conducted, it was discovered that in normal human fibroblasts in culture, achieve approximately 50 cell population doublings at maximum before becoming senescent. Hayflick discovered that all cultured cells are mortal, and the only immortal cultured cells are the cancer cells.

- ii. Apoptosis: this state crusades programmed cell death

Apoptosis advances as a speedy and permanent process to proficiently eliminate the cells that are dysfunctional (Letai, 2008). A trademark of cancer is the ability of malignant cells to avoid apoptosis (Hanahan & Weinberg 2011). Cancer cells can reveal many features that would encourage apoptosis in healthy functioning cells. Examples include that they disturb certain stages of a cell cycle that aid in the enduring of cytotoxic agents' exposure. Due to these disruptions, cancer cells hold the tendency to subsist (Letai, 2008). Therefore, apoptosis is an important barrier to growing cancer, avoiding apoptosis is a crucial fragment to the development of tumour (Cory & Adams, 2005, Plati et al., 2011).

- iii. Cancerous Tumours: this state emerges due to unregulated cell division.

This when cancerous cells have the capability to divide without suitable external signals and do not exhibit contact inhibition. This leads to the continuous dividing of the

cancerous cells in the presence of genetic damage. Finally, this continuous division of genetically damaged cells can lead to the formation of tumours (Castonguay et al., 2017).

In the instance where the cell enters the third state and becomes a tumour, the mutation is passed on the next cell during the process of cell division as shown in Figure1. (Shirzadfar, Riahi & Ghaziasgar, 2017)

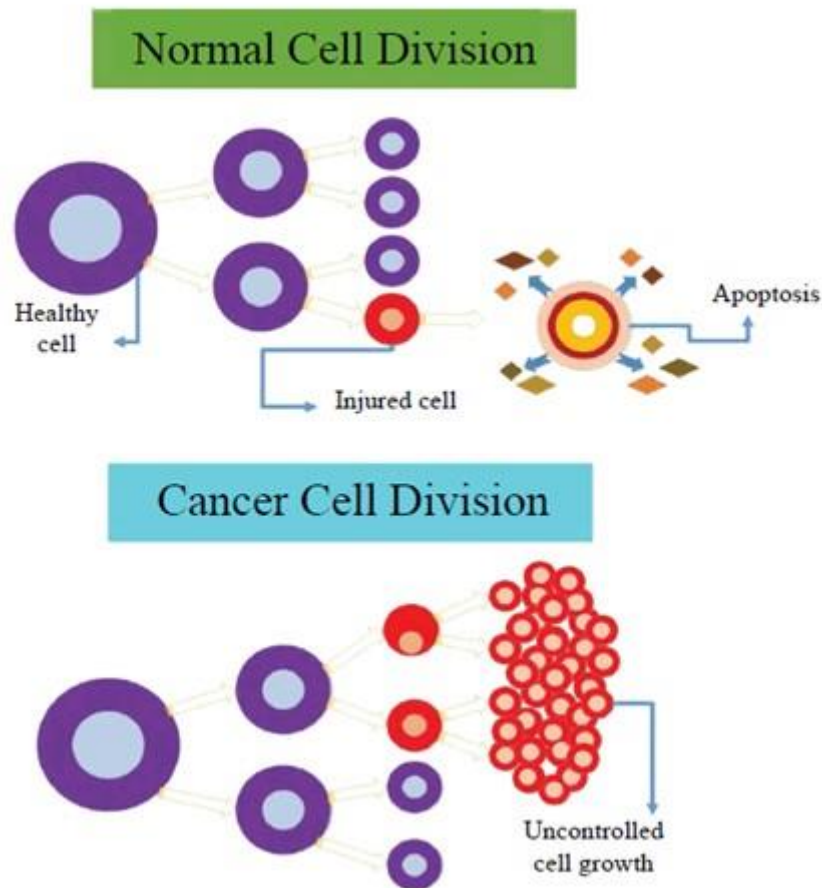


Figure 1 A comparison showing the process of cell division between normal and cancerous cells as they divide  
(adapted from (Shirzadfar, Riahi & Ghaziasgar, 2017))

The Human body is made up of approximately 37.2 trillion human cells. These cells perform as the body's foundation of the building blocks and have fixed features that permit them to endure accurate functioning of tissues, organs, and organ systems (Kusmartsev et al., 2008).

In the initial stages of cell division, the molecular regulatory and biochemical mechanisms in cancer cells possess a lot of similarities when compared to those of 'normal' cells, hence, they are not recognised as being foreign by the body's defence system. The immune system is only triggered partially, and the growth of the tumour becomes overwhelming for the response to be effective. For this very reason, early diagnosis and prompt treatment of cancers are vital

for the success of anticancer treatment and lasting survival of patients (Pantel, Brakenhoff & Brandt, 2008).

‘Hallmarks of Cancer’ is a term used to describe the specific characteristics which differentiate a cancerous cell from a normal one (Fig 2) (Hanahan & Weinberg, 2011).

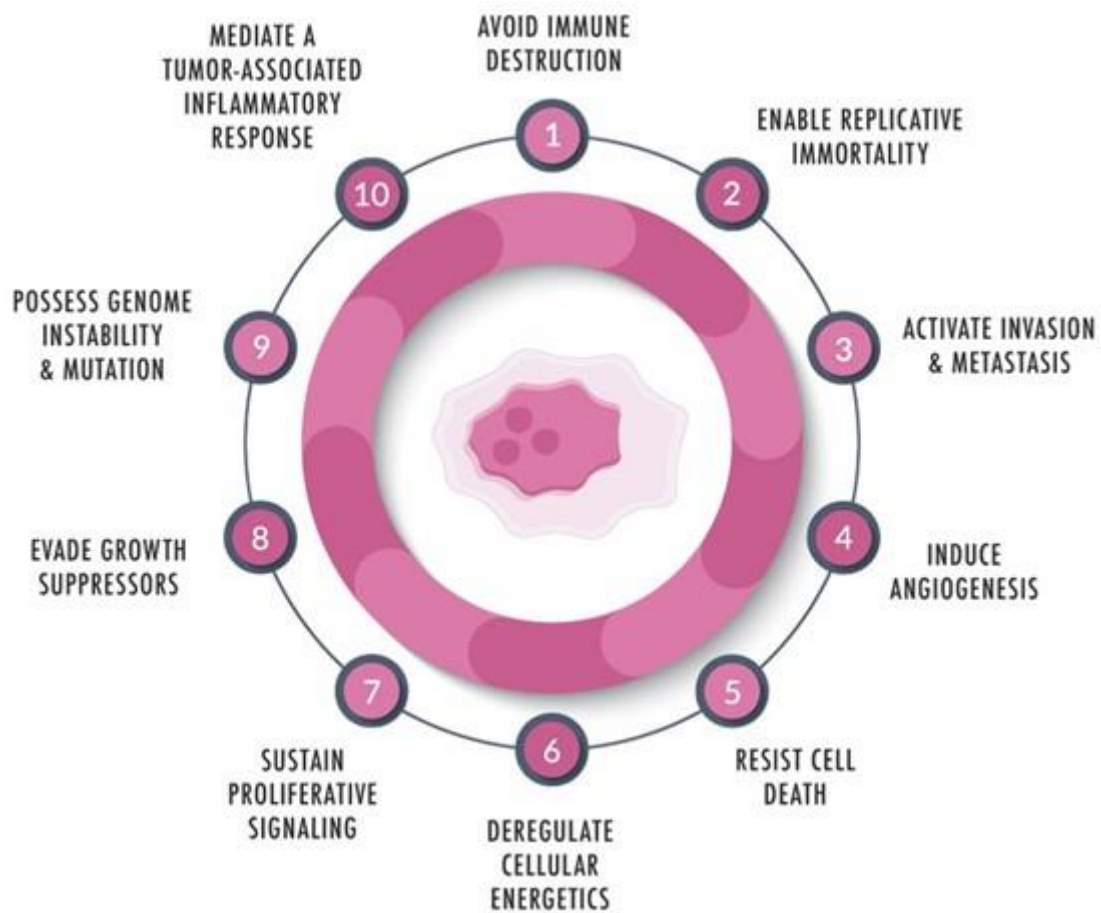


Figure 2 The 10 distinguished Hallmarks of Cancer (adapted from (Hanahan & Weinberg, 2011))

- 1) Cell shape - Normal human cells come in many shapes and sizes due to their ability to adopt and differentiate specialised roles. Unlike cells do not look identical, but, if cells were examined of the identical cell type, they will look enormously similar, sustaining a uniform shape. Cancer cells on the other hand, are misshapen and look like a chaotic assembly of cells, as a selection of shapes and sizes (Bizzarri et al., 2011).

- 2) Nucleus - In normal cells the nucleus has a smooth appearance and preserves a uniform, spheroidal shape. The nucleus in a cancer cell is misshapen and bulges defined as 'blebs' can commonly be distinguished in the cells' nuclear membrane (Barua & Mitragotri, 2013).
- 3) Chromatin - In normal cells, chromatin is fine and evenly distributed but transformed into coarse in cancer cells, it is aggregated into irregular clumps that vary in size and shape (Bizzarri et al., 2011).
- 4) Nucleolus - In cancer cells the nucleolus becomes increasingly enlarged and further irregular, they can have multiple nucleoli within the nucleus (Barua & Mitragotri, 2013, Bizzarri et al., 2011).
- 5) Blood supply - In normal cells Angiogenesis (development of new blood vessels that form from pre-existing vasculature) is a vital process. This occurs during development, growth, and wound healing. In the growth of cancer this is implicated, through the tumours ability to secrete chemical signals that arouse angiogenesis (Figure 3) (Nishida, 2006).

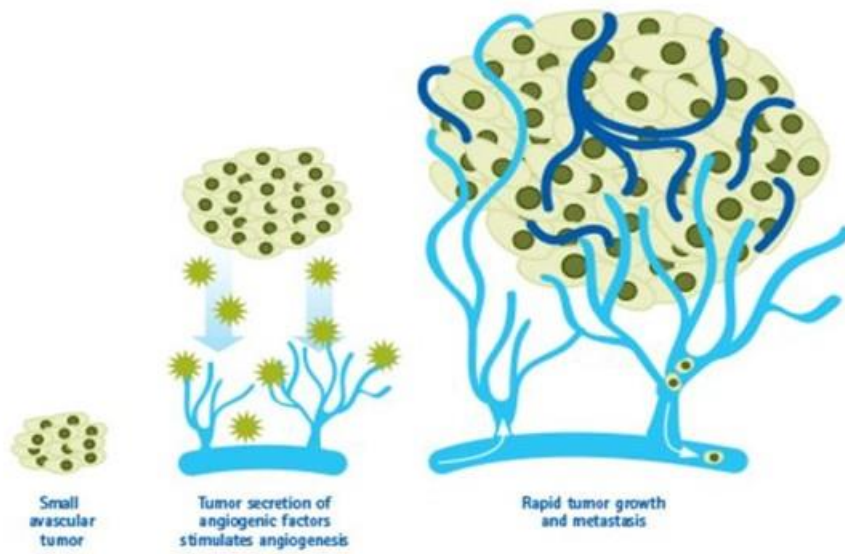
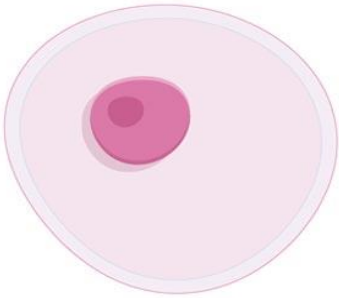


Figure 3 Showing how Tumours can stimulate neighbouring cells to harvest angiogenesis signalling molecules resulting in the formation of new blood vessels to occur (Nishida, 2006).

	Normal Cell	Cancer cell
(Images Adapted from Cancer Research UK 2018)		
<b>Cell Shape</b>	Uniform	Irregular
<b>Nucleus</b>	Spheroid, single nucleus	Misshapen, common to have multiple nuclei
<b>Chromatin</b>	Fine and evenly distributed	Coarse, aggregated
<b>Nucleolus</b>	Single, inconspicuous nucleolus	Multiple and enlarged nucleoli
<b>Cytoplasm</b>	Large volume of cytoplasm	Small volume of cytoplasm
<b>Growth</b>	Controlled	Uncontrolled
<b>Maturation</b>	Mature into specialised cells	Remain immature and undifferentiated
<b>Blood Supply</b>	Normal angiogenesis which occurs during healing and development.	Tumour induced angiogenesis
<b>Oxygen</b>	Favoured but will undergo anaerobic respiration if necessary.	Not needed and favour anaerobic respiration

<b>Location</b>	Remain in intended location	Can spread to various locations in the body (metastasis)
-----------------	-----------------------------	--

*Figure 4 Selective differences between normal healthy cells and cancerous cells. (adapted from (Nishida-Aoki and Ochiya, 2015))*

There are individuals born with a higher susceptibility of acquiring cancer and that is due to the genetic predisposition with the inherited mutations that contribute towards the formation of cancer (Boffetta & Nyberg, 2003).

A leading instance is individuals born with BRCA11, BRCA2 and p53 modifications are less able in the successful suppression of cancer growth (Vogelstein & Kinzler, 2004). This is because these proteins aid in the repair of damaged DNA, hence ensure the stability of each cell's genetic material. The mutation, or alteration of either of those proteins, where the protein product is not made or does not function appropriately, DNA damage may not be restored correctly, causing cancer (Abdul, Santo & Hoosein, 2003).

Various forms of tumours can develop through tissues that are susceptible to malignancies, even though all tumours have distinctive features, the underlying mechanisms are similar. The healthy and functioning cells present in the human body exist in a multifaceted co-dependent system that orders their spread. The existing healthy and functioning cells will only reproduce with the instructions received from neighbouring cells, this ensures the preservation of a suitable tissue size and structure (Dawson & Kouzarides, 2012). Cancerous cells on the other hand perform metastasis. This when they divide very rapidly at an abnormal rate, causing a change in structure of tissue along with evading controls on development with the potential to spread throughout the body. The deviations that occur in a cell which lead to cancer ensue due to widespread of mutations genes within the cell (Lamb et al., 2003).

Eukaryotic cells those which contain a nucleus also contain genes. These genes are present in the nucleus of the cell and comprise of specific sequences of DNA that are arranged as chromosomes. Every single of the genes within the nucleus, codes for a specific protein, this code determining the order in which the amino acids are joined together. The mutations in these genes can consequently cause a change in the functioning or the amount of the protein product (Caraglia et al., 2001). Proto-oncogenes (a normal gene that is mutated to become an oncogene and is then an active participant towards the contribution to cancer) and anti-oncogenes (a category of gene that makes tumour suppressor proteins which aids in the governing of cell growth) are the two types of genes that determine cancer. In other words, proto-oncogenes regulate differentiation and cell growth while anti-oncogenes suppress the growth of cells, as explained by Croce in 2008 then further supported by Smith and colleagues in 2011.

## 1.5 Cancer treatment/s

Cancer is a disease that has an unpredictable nature, different means of diagnosis are considered for a different type of cancer. There are multiple types of treatment in combination recommended for certain types of cancer, but this is dependent on the location in the body and its severity. There are three traditional methods to treating cancer and these are surgery, radiotherapy and systemic therapy. These well established and different approaches are sometimes applied in combination or even as a separate entity (Wust et al., 2002).

### 1.5.1 Surgery

One of the cancer treatment approaches is surgery. Cancer surgery is one of the oldest types of cancer treatment and is still effective for many cancers today. Despite the advancement and alternatives existing in treating tumours, surgical intervention has sustained to be in the lead, especially, when other treatment possibilities could not stand as a cure. The concept behind this method is that eliminating the affected part would hinder the cancerous cells from performing metastasis (Gudmundsson et al., 2009). Thus, Cancer surgery removes the tumour itself and entails removal of the neighbouring tissue during the procedure. There are several factors that determine whether surgery is an option, and this includes the type of cancer an individual has; the size and stage of cancer, where the cancer is in the body and the general health of the patient (Pastan et al., 2007).

Surgery only treats the part of the body that it is operated on, thus, surgery has the possibility of curing cancer that is completely confined to one specific area. It is possible to increase the life expectancy with surgery for individuals with certain type of cancer. This can ultimately lead to cure. If, however, the cancer has spread to additional parts of the body, then surgery can not cure it. Surgery in combination with chemotherapy or radiotherapy bids an option to reduce aggressive intervention and aids in countering microscopic levels of a tumour that cannot be removed through surgical means (Paun et al., 2010).

### 1.5.2 Radiotherapy

Radiotherapy also known as radiation therapy is a cancer treatment that involves exposing the tumour to high doses of radiation to shrink or ultimately kill them. This therapy includes concentrating an ionising radiation medium on the portion affected with cancer or a benign

tumour (Woodhead et al., 2016). This is done by slowly damaging the cancers DNA to the extent beyond repair, stop dividing or die. When damaged cells die, they are broken down and removed by the natural processes of the body (Formenti & Demaria, 2013). Radiation can be applied on tissue through direct or indirect means. The direct method entails ionising an atom by losing an electron from its outer shell, creating a positive charge. Photons of light focused on particles also result in emitting high energy radiation. Molecules producing radicals is a result of indirect radiation. In both cases, a photon colliding with an atom or molecule is skilled at expunging an electron from DNA. This results in damaging the tissue, which is the principle underlying radiotherapy (Mayadev et al., 2018).

Delaney and colleagues in 2005 explain that radiotherapy is not able to destroy cancer straight away. It can take a period of days even weeks of treatment before the DNA of the cancer cells itself is damaged. This is then followed by cancer cells dying for weeks and months after the end of radiotherapy. The type and timing of radiotherapy being administered on the patient is dependent on the type of cancer being targeted and whether the goal of radiation is to treat the cancer or ease the symptoms associated.

Radiotherapy can be combined with other treatments for cancer, where it is used in several stages. The first stage is before surgery where the size of the cancer is shrunk, allowing the surgical removal to be more efficient and minimising the likelihood of the cancer to return. The second would be during surgery- so that the cancer is radiated without having to pass the radiation through the skin (Bosset et al., 2006). Radiotherapy implemented in this manner is called 'intraoperative radiation'. Through this procedure, doctors can protect neighbouring tissue easily from radiation. Finally, the third stage of administration would be after surgery – to destroy any cancer cells that remain (Forastiere et al., 2003).

Radiotherapy is an effective treatment for cancer patients. The Royal college of Radiologists (2015) explained that four of ten patients with cancer are treated with radiotherapy. Radiotherapy has also proven to be cost effective as it equates to only 5% of the total cost of the treatment available to cancer patients (Sharma et al., 2016, Muirhead et al., 2015).

### 1.5.3 Chemotherapy

Chemotherapy is a term which defines as the use of chemical to treat disease. Chemotherapy is circulated through the bloodstream in the body; therefore, it can treat cancer located almost anywhere in the body. Hence, this is known as systemic treatment. Chemotherapy targets cells for damage as they divide. The nucleus of the cell, which is seen as the control centre, contains chromosomes, a thread-like structure made up of DNA. The genes present must be copied exactly each time cell division occurs to make two new cells as highlighted from Figure 5. (Skeel & Khleif, 2011, Shah et al., 2019).

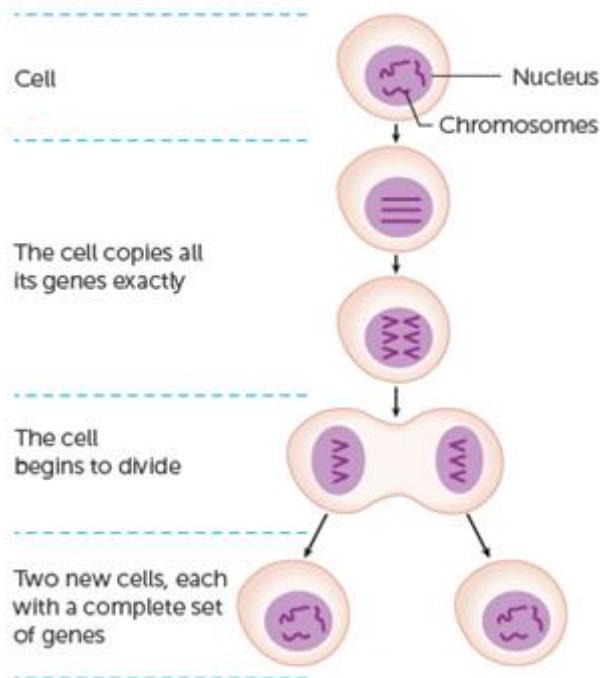


Figure 5 The process of cell division. Adapted from Cancer Research UK (Skeel et al., 2011) and (Tobis, Hochhauser & Souhami, 2010).

Figure 5 illustrates the way a cell will copy its genes and then divide to form two completely new cells. Called Mitosis, via stages such as prophase, metaphase, anaphase, and telophase, one cell, called the mother cell, divides into two cells, called daughter cells. These cells are genetically identical to each other. Drugs depending on their nature will damage cells at the point of splitting, while others when they are making copies of genes before the process of splitting. This is when the drugs will inhibit the division of the cell to form two new cells. Chemotherapy, in comparison is much less likely to effect cells that are at the rest stage (Skeel et al., 2011, Tobis, Hochhauser & Souhami, 2010).

Farber and his peers in 1948 researched methods with respect to enabling measures to decrease the risk of acute lymphocytic leukaemia in children, thus marking the beginning of chemotherapy. Since then, interests for the search and development of drugs and therapies

aimed at cancer established rapidly (Bowder et al., 2000). The mechanism of chemotherapy drugs or chemical agents destroying dividing cells aids to explain why this very traditional approach to cancer treatment also causes side effects. However, chemotherapy is often preferred because you can focus on specific targets in question, such as cells, enzymes or biological pathways, an example would include blocking targeted pathways within the phases of cell cycle. This approach also affects healthy and well-functioning body tissues where the cells are continuously growing and dividing (Smith & Pewett, 2017).

Chemotherapy can impact hair, bone marrow and skin. These tissues are affected because they have dividing cells. However, normal functioning cells can replace or restore the cells that are damaged by chemotherapy. Thus, the conflict subsists, as chemotherapy drugs are known for their role in attacking DNA in cancerous cells, but subsequently, the toxic effect of the drug is a possible threat to the microenvironment (Scharovsky, Mainetti & Rozados, 2009). Furthermore, Marijen et al., (2002) describe that the damage occurred by the healthy cells is not permanent, as most of the side effects disappear once the treatment with chemotherapy is completed, however, side effects such as sickness and diarrhoea might occur but are most likely to subside once the intake of drugs has been stopped (Hickok et al., 2005). The damage is not classified as permanent since the damage to healthy cells does not last. This is because the normal cells in the body can either replace or repair the healthy cells which have been damaged.

Moreover, chemotherapy plays a substantial part in gynaecological malignancies amid female patients suffering from peritoneal cancer as the epithelial tissue on the ovaries and linings that shield the organs in the abdominal cavities are targeted due to cancer (Smith & Pewett, 2017, Webber & Friedlander, 2017). This shows that certain types of chemotherapy can

sometimes cause delayed effects, which may mean that a second cancer can show up, either immediately or many years later. This is when cancer cells settle in a part of the body, thus forming a new tumour. However, even though this new tumour is growing in a different part of the body, it is said to be the same type of cancer as the initial primary tumour. An example would be, if breast cancer cells were to spread to another organ, such as the liver, then they grow and behave like breast cancer cells. The treatment for this cancer would most likely be with the same drugs, and not treated the same way as cancer cells which start in the liver itself.

There are several mediums of administering chemotherapy to the patient, the management of dose and administration of drugs emerged from the ongoing dilemma of cure and danger of chemotherapy (Kareva, Waxman & Klement, 2015). It can be given as an injection into the bloodstream, a drip into the bloodstream, tablets, or capsules, at varied times and doses. These are classified as systemic treatment, because the managing of chemotherapy drugs in this way allows them to reach cancer cells anywhere in the body with minimal aspired side effects (Tobis, Hochhauser & Souhami, 2010)

### 1.6 Medicinal Anti-Cancer Drugs

Over the preceding fifty years, the evolution of anticancer drugs has changed and diverged from conventional cytotoxicity, towards achieving rational designs of selective agents which act on specific cellular targets (DeVita and Chu, 2008, Hambley, 2009). Nevertheless, significant challenges remain, and the relationship between structural biology and chemistry may offer the most effective ways for discovering and improving upon novel anticancer agents (Neidle and Thurston, 2005).

### 1.6.1 DNA Reactive Agents

The full extent of cellular mechanisms relating to DNA reactive agents are yet to be completely determined. These mechanisms are essential to balance the efficacy and toxicity of the compounds. Furthermore, the use of many anticancer drugs is limited by dose-limiting toxicities, as well as the added issue of the development to drug resistance (Cheung-Ong, Giaever & Nislow, 2013). This makes it hard to use them efficiently. An example of a recognised family of DNA reactive agents are cisplatin and its derivatives including oxaliplatin and carboplatin (Fig 6), which act through the development of DNA-drug adducts leading to prevention of DNA replication and the initiation of apoptosis (Doak et al., 1998). These platinum derived compounds are found to be effective in treating many types of cancers such as ovarian, head, neck, and bladder. They have especially been effective in the treatment of testicular cancer with a rate of cure of 90% (Koster et al., 2010).

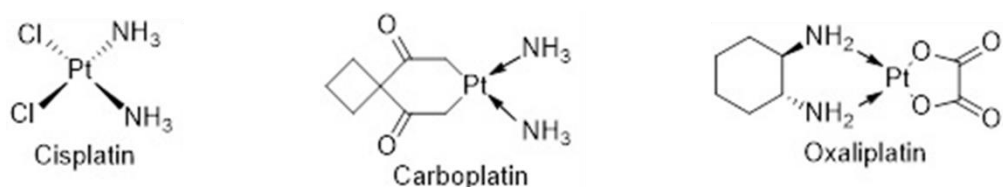


*Figure 6 Chemical structures of Platinum containing compounds, Cisplatin, Carboplatin and Oxaliplatin, which are widely used as anti-cancer agents*

There are several checkpoints on a cell cycle that generate the production of regulatory protein if the abnormalities such as irregular or damaged DNA are detected during the process of cellular replication. The development of adducts on the DNA will cause prevention in the replication of DNA during mitosis and thus instead trigger the process of apoptosis (Cavaliere et al., 2017). In comparison to Cisplatin, which was discovered in 1844 and licensed in 1978 for use, Carboplatin and Oxaliplatin are drugs which are seen as more recent and modern.

Even though all 3 drugs are used in chemotherapy to treat all cancers, either alone or in combination, each drug has a focused cancer target it is used for. For instance, the use of Carboplatin is mostly aimed at ovarian and lung cancer, whereas Oxaliplatin is more focused at bowel, stomach, pancreatic and oesophagus cancers. These differ from Cisplatin, which in turn is mostly aimed at testicular, ovarian, bladder, lung, and cervical cancer. Found within a literature-based study in the UK, it was shown that using platinum-based compounds in cancer treatments offers potential health gains over cancer treatment which does not include platinum compounds. In comparison to this, McWhinney, Goldberg & McLeod., (2008) reported that the benefit of all the three drugs mentioned is compromised by severe side effects including neurotoxicity. It was further found that neurotoxicity can result in both acute and chronic debilitation plus those patients treated with Oxaliplatin for colorectal cancer discontinue therapy more often because of peripheral neuropathy rather than tumour progression. This was backed by the Food and Drug Administration (FDA), that more than 70% of patients receiving Oxaliplatin are affected by some degree of sensory neuropathy. To conclude, neurotoxicity from Carboplatin administration is less frequent (4-6%) than that observed with Cisplatin or Oxaliplatin (15-60%).

#### 1.6.2 Platinum based Agents including Cisplatin

Carrying on from the claim laid down by Ott & Gust (2007), 'almost all drugs placed in the market are organic non-metal substances, Sumnthalalingam et al., (2012) report that currently many anti-cancer drugs in use or clinical trials are organic in nature, currently relying on mechanisms of action which involves the damage of nucleic acids (Glazer, 2013). Even though the modern use of pharmacologic agents to treat cancer began in the mid 1940's,

where the efficacy of nitrogen mustard in tumour bearing mice was highlighted by Alfred Gilman and Louis Goodman.

Discovered by Michele Peyrone in 1844, Cisplatin (cis-diamminedichloroplatinum(II)), was actually given world-wide recognition nearly a century later in 1960, when Barnett Rosenberg discovered the tumor-inhibiting characteristics it exhibited (Ndagi, Mhlongo, & Soliman, 2017). Aydin et al., (2014) further mention that the discovery of the anticancer activity in cisplatin helped trigger the development of novel drugs which contain metals such as platinum or ruthenium.

The location in the cell responsible for the activation of cisplatin is the cytoplasm. This is where chloride ions dissociate and are replaced by water molecules. Here the transformation of  $[\text{cis-Pt}(\text{Cl})_2(\text{NH}_3)_2]$  leads to the mono-aqua  $[\text{cis}-(\text{NH}_3)\text{Pt}(\text{Cl})_2(\text{OH})_2]^+$  and di-aqua  $[\text{cis-Pt}(\text{Cl})_2(\text{OH}_2)_2]^+$  complexes being formed. These hydrolysed forms of cisplatin have been shown to be 1000 times more reactive than normal cisplatin (Dasari & Tchounwou, 2014). The converted potent electrophile from the hydrolysed platinum complex reacts with the nucleotides available, such as the sulfhydryl groups present on proteins or nitrogen donor atoms existing on nucleic acids that make up DNA. The hydrolysed product of cisplatin forms covalent bonds to the N7 reactive centre on purine residues which causes DNA damage, the blocking of cell division, and triggering apoptosis (Dasari & Tchounwou, 2014, Bracht, Grünert & Bednarski, 2006).

Entering clinical experiments shortly after its 'discovery', the drug became highly active and popular amongst the world-wide audience in treating symptoms such as testicular, bladder and neck tumours in addition to ovarian carcinomas, with Ott & Gust (2007) labelling it the best-selling anticancer drug worldwide. Suntharalingam et al., (2012) agree with this

proposition, by adding that Cisplatin and its derivatives such as oxaliplatin and nedaplatin are widely used to treat cancers of all forms, with Platinum drugs being used ca. 50% in all chemotherapeutical treatment. This was a breakthrough since the tumours it attacked were mainly solid tumours. Initially it was observed that Cisplatin induced a filamentous growth in bacteria without it affecting any RNA or protein synthesis, which led to suggest that DNA was the primary target of the drug (Johnson, O'Dwyer, & Stevenson, 2006). However, the presence and development of side effects and drug resistance often leads to treatment failure (Bielefeld et al., 2013), with apparent clinical drawbacks including limited applicability, acquired resistance and side effects such as neurotoxicity and nephrotoxicity (Bruijninx & Sadler., 2008, Frezza et al., 2011). It has also been reported that it readily reacts with non-target tissues. In addition to this, cisplatin has limited solubility available in an aqueous solution thus restricting its administration intravenously whereby these shortcomings only occur due to the lack of tumour selectivity Cisplatin exhibits, leading the cause for new and novel compounds to be designed, which are therefore able to accumulate in specific target cells and help overcome the shortcomings and side effects found in cisplatin (Gabano, Ravera, & Osella, 2009)

Due to the presence of adducts, the formation of mono-adducts can also take place; intra- as well as interstrand crosslinks. Intrastrand crosslinks appear when the platinum adducts form on neighbouring bases on the same strand of DNA, while interstrand crosslinks occur when adducts form between two separate strands (Dasari & Tchounwou, 2014, Koster et al., 2013). Intrastrand adducts are projected to shape an approximate of 90% of adducts, whereas interstrand and monofunctional adducts are theorised to add to the toxicity of the platinum-based remedies (Koster et al., 2010). Adduct formation progresses towards destruction of DNA duplex as the intrastrand crosslinks curve the strand in the direction of the major groove

leading to the exposure of a lesser groove at which site several classes of protein bind, such as repair proteins (Alnajjar & Sweasy, 2019).

There are two cisplatin induced concentration types of death: necrosis and apoptosis. Necrosis is distinguished by cytosolic swelling with loss of the plasma membrane integrity and is associated with exposure to high concentrations exceeding 800  $\mu\text{M}$  of cisplatin. On the other hand, exposure to concentrations as low as 8.0  $\mu\text{M}$  over several consecutive days will cause apoptosis and thus, cell reduction, chromatin condensation and DNA fragmentation (Kim, He & Lemasters, 2003). The core response of closely monitored therapeutic treatments is apoptosis and has two adapted paths in mammals. One is the extrinsic pathway that includes the ligand binding to the tumour necrosis factor ( $\text{TNF-}\alpha$ ) which causes the adoption of caspase -3, -7, -8 and -9, these ultimately activate the associated death domain proteins to death receptors that cause cell death (Gonzalez, Hagerling & Werb, 2018). On the other hand, the intrinsic apoptotic pathway includes the adjustment of potential of the mitochondrial membrane causing the release of cytochrome c and the adjustment of apoptotic gene regulation. This process requires the upregulation of the pro-apoptotic gene Bax with synchronized downregulation of the anti-apoptotic gene Bcl-2, crucial in proliferation (Balkwill, 2009) (Gonzalez, Hagerling & Werb, 2018).

Theoretically, there are two main mechanisms associated with cisplatin uptake. In the instance of the platinum complex concentration increasing at a linear rate within the first hour of administration with a deficiency of saturation up to the concentration of 1.0 mM, the mechanism of passive diffusion is granted (Wang & Lippard., 2005, Balkwill., 2009). Complexes with platinum bases are assumed to utilise the CRT1 protein as a means of transport into the cell, replicating the way copper enters the cell. It has been found that when

the genetics of the CRT1 protein are mutated or deleted there has been an increase in resistance to platinum-based therapies, while upregulation of CRT1 intracellular levels lead to sensitisation of the cell (Wang & Lippard, 2005).

A growing issue is associated to the increase in the resistance of platinum-based drugs. There are two modes of resistance that are a main cause of concern, one being the deficiency of drug delivery to the target site and the other is the genetic and epigenetic alterations that affect sensitivity to the agent (Chen et al., 2013). There can be several factors responsible for the reduced concentration of the agent reaching the desired target site and therefore causing a limitation in the potential therapeutic effects of the administered drug. These can be poor bioavailability of the compound, an increase rate of metabolism, and an increase in the rate of excretion from the body (Chen et al., 2013). Cancer cells can become resistant through alteration of the drugs cellular target, upregulation of genes involved in the repair of drug induced damage especially to DNA, enhanced bypass of DNA adducts, increased tolerance to DNA damage, and increased levels of detoxification through increased cellular thiol production (Chen et al., 2013, Ohmichi et al., 2005). If resistance is displayed to one therapeutic agent, then cells may begin to present resistance to drugs that may be structurally and mechanically unrelated identified as a process called multidrug resistance (Ohmichi et al., 2005).

The foundation of the major drawbacks of platinum-based drugs are their side effects due to their highly toxic limiting the potential administration concentration. They also have the tendency to interact with non-target tissue and are highly neuro- and nephrotoxic (Wang & Lippard, 2005, Chen at al., 2013). The nephrotoxicity is speculated to be due to the intrinsic activation of protein kinases, the assembly of reactive oxygen species (ROS), and the stimulus

of fibrogenesis at the site of action (Ben Saad et al., 2017, Chen et al., 2013). The application of platinum-based chemotherapy has also been associated with tinnitus, hearing loss and peripheral neuropathies with the likes of loss of vibrational sense and weakness. These side effects are due to the unwanted cisplatin interaction with dorsal root ganglia and peripheral nerves leading to cisplatin induced apoptosis (Ohmichi et al., 2005).

The use of carboplatin has benefits due its properties of being the six-member ring conjugation with platinum, as it provides aqueous stability, which increases the half-life of the treatment while not impacting the clinical activity and demonstrating fewer side effects, from 1.5 to 3.6 hours to more than 30 hours. However, the administration does not override cisplatin resistance (Wang & Lippard, 2005). Additionally, Oxaliplatin form similar adducts on the same site on DNA as cisplatin, however, their structural differences cause a difference in identity by repair proteins, leading to oxaliplatin being able to overcome cisplatin resistance (Ben Saad et al., 2017).

### 1.7 Antimetabolites

Antimetabolites are a drug class referred to as one of the very first examples of rational design of a drug (Liu & Gerson, 2016). In 1946 by Spies it was discovered that with the intake of folic acids there was an escalation in the proliferation of lymphoblastic leukaemia cells, and this then led to its administration to patients experiencing megaloblastic anaemia. This is a condition where the bone marrow produces unusually large, structurally abnormal, immature red blood cells. It also shows how important the availability of folate is for the development of healthy red blood cells. Folate analogues like Aminopterin and Methotrexate (MTX) (Figure 7) were discovered to block folic acid thus, reducing proliferation rate (Cheung-Ong et al., 2013). MTX works by inhibiting the enzyme

dihydrofolate reductase (DHFR), which is converted in the synthesis of tetrahydrofolate.

MTX therefore inhibits the synthesis of DNA, RNA, and proteins.

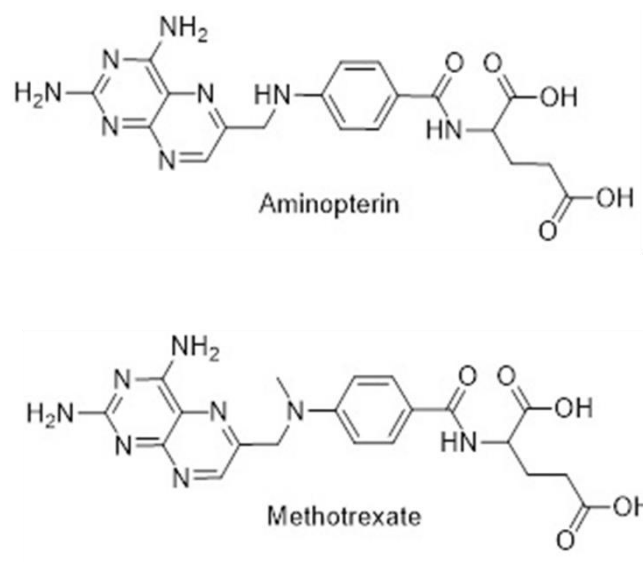


Figure 7 Chemical structures of Aminopterin and Methotrexate (MTX), which block the production of folic acid

Mammalian cells do not have the ability to produce folates *de novo*, these also do not possess the ability to cross the biological membrane through the process of diffusion due to their hydrophilic properties, causing the cells to be reliant on locating folates from a series of 1-carbon reactions (Matherly, Hou & Deng., 2007). To enhance the retaining volume, intracellular folate foylpolylglutamate synthetase (FPGS) combines glutamate to folate reducing its efflux from the cell and an identical process is undergone on MTX. MTX is converted to methotrexate polyglutamate (MTXPG) causing improved preservation in cells. As the polyglutamate metabolites are weak substrates for MTX efflux proteins, the reaction contributes to the efficacy of the MTX therapy (van de Steeg et al., 2009).

Antimetabolites imitate the behaviour of molecules found in the cell and hinders DNA replication with the aid of a DNA antagonist accountable for blocking nucleotide metabolism

pathways (Cheung-Ong et al., 2013). MTX is a common form of treatment for several cancers including leukaemia, non-small cell lung, bladder, neck and choriocarcinoma in which the rate of success exceeds 90%. Its mechanism of action arises inhibition of dihydrofolate reductase (DHFR) which catalyses the decline of dihydrofolate to tetrahydrofolate, essential in the production of DNA (van de Steeg et al., 2009, Xie et al., 2009). MTX interferes with purine and pyrimidine production which are crucial for the replication of DNA. MTX use causes a reduction in the amount of tetrahydrofolate and ultimately of the necessary nucleotides. This decline in nucleotide concentration leads to a decrease in cell population and the initiation of programmed apoptosis (van de Steeg et al., 2009).

Levels of DHFR expression can be an indicator for the level of response of MTX treatment, however, this is not always the case due to the establishment of a secondary mechanism. This secondary pathway includes stimulation of genetic injury through mechanisms such as: gene mutation, direct DNA damage, oxidative damage, and chromosomal aberration (Chatterjee & Walker., 2017). Xie and colleagues (2009) also explain that MTX demonstrates apoptosis through paths activated in response to DNA mismatch repair malfunctions, like the development of double strand breaks and the inhibition of homologous recombination that accompanies MTX use.

A common issue effecting MTX and other anti-folate drugs is that of drug resistance, which is a reduction in effectiveness of the medication. The resistance here arises from the loss or mutation of a cell surface receptor or target. In cases of such instance, anti-folates would be incapable of reducing the conversion of dihydrofolate to tetrahydrofolate, thus the production of nucleotides will not be affected causing the potential for uncontrolled DNA replication and cellular proliferation (Cheung-Ong et al., 2013).

## 1.8 Antimitotics

Antimitotics including the vinca alkaloids and taxoids are a further class of anticancer therapeutics. Vinca alkaloids were first extracted from the Madagascar periwinkle plant and are comprised of two multi-ring constructs (Mora et al., 2015, Douer, 2016).

Vincristine and vinblastine (Figure 8) are two most utilised vinca alkaloids entailing the mechanism where the prevention of formation of spindle microtubules during the cell cycle leads to ceasing replication progression (Douer, 2016).

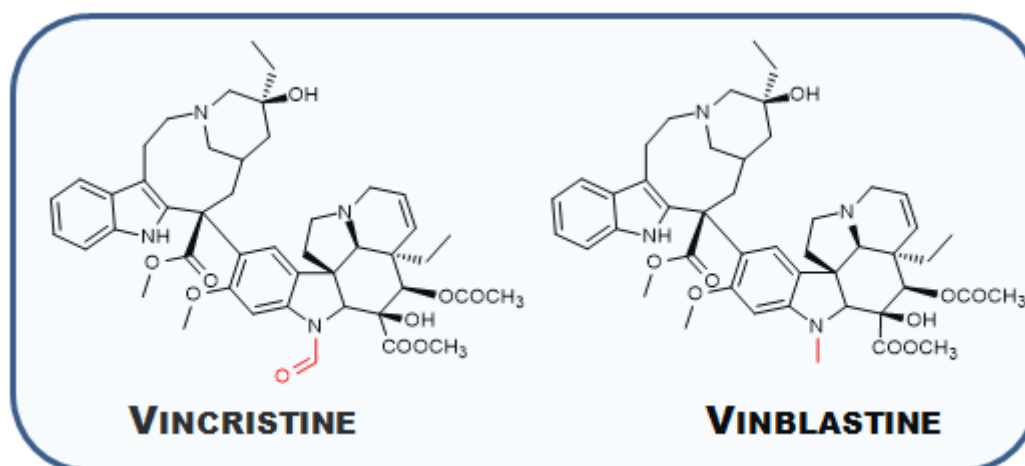


*Figure 8 Chemical structures of Vincristine and Vinblastine, common vinca alkaloids which inhibit the assembly of microtubules*

## 1.9 $\beta$ -Diketones

$\beta$ -Diketones have been a subject of study over a century and have been studied for properties in the treatment of osteoporosis, trauma, depression, and diabetes (Ara and Khan, 2014). It

is also regarded as an appropriate *Wnt* activator, a pathway that starts developing of malignant and benign breast cancer (Figure 9) (Wallace et al., 2013, Khan et al., 2018).

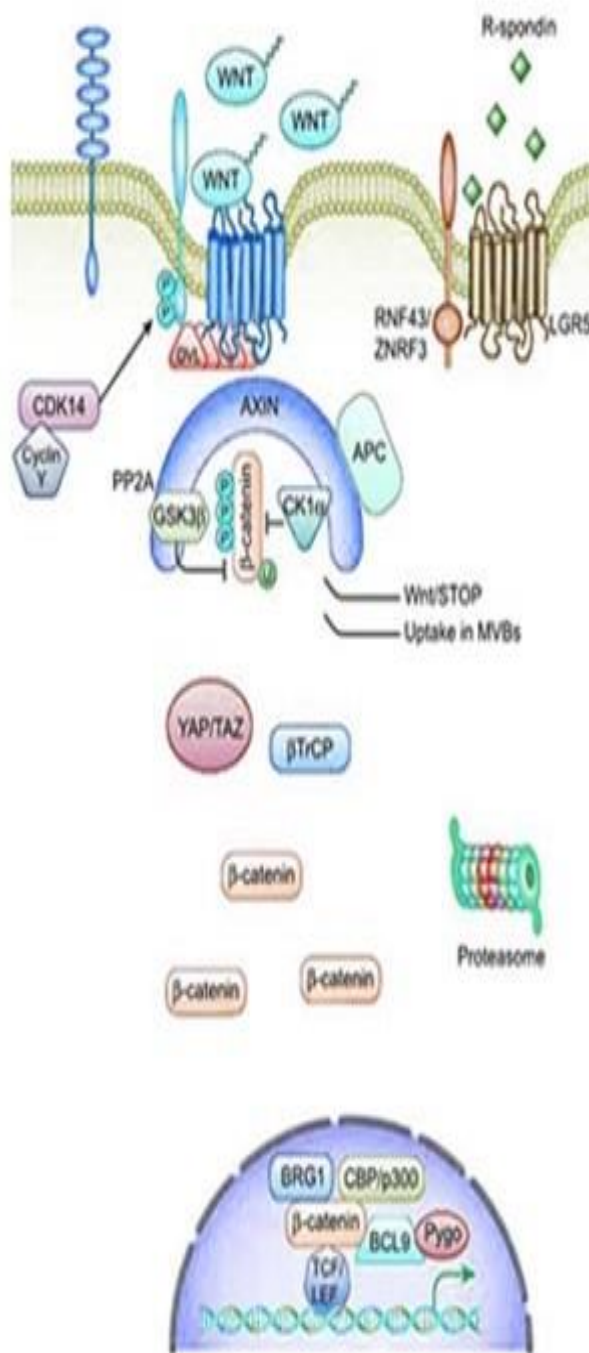


Figure 9: Wnt signalling is activated when secreted Wnt ligands bind to the seven-pass transmembrane receptor Fzd (dark blue) and the single-pass low-density lipoprotein receptor-related protein (LRP) (light blue). LRP is phosphorylated, leading to the recruitment and polymerisation of Dvl proteins (red) at the plasma membrane.

The Dvl polymer (active) inactivates the destruction complex; consisting of AXIN, adenomatous polyposis coli (APC), and GSK3 $\beta$ , leading to the stabilisation and cytoplasmic accumulation of  $\beta$ -catenin (orange) which then translocate to the nucleus.

When inside the nucleus,  $\beta$ -catenin forms a complex with T-cell factor (TCF) and lymphoid enhancer factor (LEF) (purple), acting as a transcriptional switch, that changes multiple cellular processes

Figure 9 Overview of the canonical Wnt signalling pathway (adapted from (Khan et al., 2018)

Commercially,  $\beta$ -diketone is used in the manufacture of a wide variety of synthetic polymer materials including polyvinyl chloride to acrylonitrile butadiene styrene (ABS).

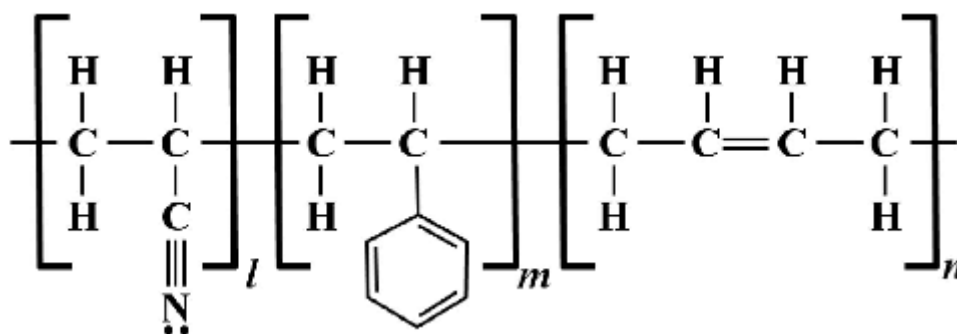


Figure 10 Structure of synthetic polymers which includes the common, acrylonitrile butadiene styrene (ABS). ([https://www.researchgate.net/figure/Formula-of-acrylonitrile-butadiene-styrene-ABS\\_fig1\\_307546266](https://www.researchgate.net/figure/Formula-of-acrylonitrile-butadiene-styrene-ABS_fig1_307546266))

### 1.9.1 Properties of $\beta$ -diketones

Given the stability, nontoxic and exceptional characteristics of  $\beta$ -diketones a huge number of applications have been studied by synthetic organic chemists, where the compounds are seen as promising scaffolds for the development of novel drug substances as well as carriers for metal-based drugs. Furthermore, due to their ability to form supramolecular organic as well as metal organic complexes, they are used as cages for contrast agents in diagnostic and medicinal imaging. In addition, the responsiveness, and synthetic strategies of several 1,3-diketones, allowed for them to be tested for therapeutic qualities within studies (Wallace et al., 2013). Members and derivatives of 1,3-diketones appear in numerous plants such as Eucalyptus leaves and liquorice. Additional long chain aliphatic 1,3-diketones are found in Sunflower pollen and vanilla beans and have powerful natural antioxidants and prominent anti-cancer properties with minimal toxicity (Radi et al., 2015).

In conjunction with the medicinal properties,  $\beta$ -diketones have also been utilised in sunscreen products in the United States (Andreassi, 2011). In addition, most  $\beta$ -diketones already known have an absorption wavelength in the range of  $\lambda = 300\text{-}400\text{nm}$  (Zawadiak et al., 2011)

$\beta$ -Diketones have exposed remarkable qualities given their structural orientation, especially due to the presence of the two carbonyl groups separated with a methylene group ( $\text{CH}_2$ ) (Urbaniak et al., 2011). Due to the presence of the less polar hydrogen atom on the enol-tautomer it is more favourable in inert solvents from the keto-tautomer which seems more dominant in the polar solvents (Simoni et al., 2008). Apart from the solvent as a factor influencing the equilibrium position of these compounds, substituents attached to the carbonyls also lead to equilibrium shift depending upon the nature of the substituting group as explained by Liang and colleagues (2008). The keto-enol property of  $\beta$ -diketones establish a resilient chelating property and possesses the ability to develop stable complexes together with different metals, comprising of transition metals and metals in the lanthanide series (Vigato, Peruzzo, & Tamburini, 2009).

#### 1.10 Absorption, Distribution, Metabolism and Excretion (A.D.M.E)

The development, description of new drugs and the safe use of approved drugs needs knowledge of the pharmacokinetics of the drug. Pharmacokinetics is the summation of the rates and scopes of four general processes or factors called absorption or introduction of the drug into the individuals' biological circulation, distribution or the drug administration progressing onto extravascular fluids and tissues, metabolism which causes the enzymatic changes in drug molecule structure and elimination or excretion which is primarily in urine or faeces (ADME) (Gu et al., 2018). A comprehensive understanding of the pharmacokinetics of

a drug is the foundation for modulating the most appropriate dose, route of administration, and intervals between doses to deliver the ideal concentrations of the active drug for an effective therapeutic effect (Bell et al., 2002).

The first is absorption with this being initiated once a drug is administered. This entails the process of transporting the drugs from the primary site which is the administration site to the systemic circulation (Undevia, Gomes-Abuin & Ratain, 2005).

The most immediate route of drug administration happens through intravenous administration; drugs provided through this method are considered to have 100% bioavailability. On the other hand, drugs administered orally are prone to absorption obstacles in the gastrointestinal tract (Undevia, Gomes-Abuin & Ratain, 2005). Undevia and colleagues in 2005 also explain that the absorption of oral drugs is regulated by various factors (Budha et al., 2012):

- I. The surface area of absorption of the drug administered
- II. the time needed to travel through the gastrointestinal tract
- III. Blood flow to the relevant site of absorption
- IV. Intestinal and gastric pH and successive pH dependent solubility
- V. Intestinal efflux and influx conveyance, for example the ATP binding cassette (ABC) gene products such as glycoprotein can inhibit the uptake of oral anticancer drugs)
- VI. The rate of intestinal metabolism, for example oral drugs are subject to intestinal metabolism by CYP3A4, a subclass of cytochrome p450 enzymes.

Proceeding from absorption, the administered drug distributes from the intravascular space to its target in the extravascular space (Budha et al., 2012). Most of the drugs administered

proceed to bind to the plasma proteins such as albumin. The amount of drug that proceeds to its target depends on the amount of drug that is successful in binding to plasma proteins, as only the fraction of the drug that is free in the body is pharmacologically active (Neidle, 2005).

Uptake of the drugs in the liver is mediated by one of two processes passive diffusion or active transport. Once the administered drug is in the liver, the anticancer drugs undergo phase I and phase II metabolic reactions (Undevia, Gomes-Abuin & Ratain, 2005). Phase I reactions cause a loss in the pharmacological activity or cause the activation of inactive prodrugs (Van Leeuwen et al., 2013). Whereas Phase II reactions usually cause inactive derivatives for the process of excretion. Even though this step is needed for the activation of pro drugs, like capecitabine and tamoxifen.

Drugs interactions linked with excretion are usually credited to renal impairment, which is resultant due to either a parent drug or due to co-administration with nephrotoxic agents (Undevia, Gomes-Abuin & Ratain, 2005). Majority of the kinase inhibitors undergo hepatic dismissal and faecal excretion with varying renal clearance (Landi et al., 2005). Thus, the main routes of drug excretion are through the biliary tract and kidneys (Neidle, 2011).

## 1.10 Protein coding and kinases

### 1.10.1 Proliferating Cell Nuclear Antigen (PCNA)

Genome instability is a significant hallmark of cancer which proceeds to cause mutations that deregulate cellular growth (Curtin, 2012). Mutations play a critical part in oncogenic transformation and can also be disastrous during mitosis (Forment, Kaidi & Jackson, 2012).

Venet, Dumont and Detours (2011) reported that the proliferating cell nuclear antigen (PCNA) DNA repair protein is extensively co-regulated in the genome. PCNA, which is a ring-like structural protein, assists as a co-factor for polymerase  $\delta$ , and surrounds DNA during strand synthesis to adopt proteins required for the replication and repair of DNA (Moldovan, Pfander & Jentsch, 2007). PCNA has been titled the 'ringmaster of the genome', as this 29-kDa protein has revealed to partake in several molecular pathways accountable for the life and death of the mammalian cell. PCNA as a single entity is not a tumour suppressor gene or oncogene, however, it is a proliferation encouraging protein whose expression is up-regulated for the duration of cell replication (Paunesku et al., 2001). It was identified by Ge and colleagues in 2007 that 131 mRNAs in 36 kinds of typical tissues, expression correlated  $r>0.65$  with expression of PCNA.

#### 1.10.2 Cyclin-dependent kinase 4 (CDK4)

Cyclin-dependent kinase 4 is an enzyme that is encoded by the CDK4 gene in humans. The protein determined by this gene is an associate of the Serine/Threonine (Ser/thr) protein kinase family. It is a catalytic subunit of the protein kinase composite that is vital for G1 phase progression of the cell cycle (Mori et al., 2019). The action of this kinase is limited to the G1-S phase, controlled by the regulatory subunits D-type cyclins and CDK inhibitor  $p16^{INK4a}$ . This kinase has revealed to be accountable for the phosphorylation of retinoblastoma (RB) gene product (Sangar et al., 2017).

Additionally, Ser/Thr-kinase element of cyclin D-CDK4 complexes that phosphorylate and inhibit members of the retinoblastoma protein family encompassing RB1 and adjust the cell-cycle during G1/S transition. Phosphorylation of RB1 permits dissociation of the transcription factor E2F from the RB/E2F complexes and the successive transcription of E2F

target genes that are liable for the development through the G1 phase (O'Leary, Finn & Turner, 2016). Moreover, Hypophosphorylation occurs of RB1 in early G1 phase, furthermore, Cyclin D-CDK4 complexes are chief integrators of several mitogenic and antimitogenic signals. Furthermore, the kinase is a component of the ternary complex, cyclin D/CDK4/CDKN1B which is required for the nuclear translocation and activity of the cyclin D-CDK4 complex (Xu et al., 2017).

Mutations in this gene and its associated proteins including D-type cyclins such as Rb and CDKN2A have been linked with tumorigenesis of a range of cancers. One specific mutation of CDK4 was identified in melanoma patients and the same mutation was also found in animal models (Sheppard & McArthur, 2013).

### 1.10.3 Cyclin-dependent kinase 6 (CDK6)

Cyclin dependent kinase 6 (CDK6) is a serine/threonine (Ser/thr) protein kinase entailed in the governing of the cell cycle and differentiation and encourages G1/S transition (Chen-Kiang et al., 2016). In addition, the ser/thr kinase is necessitated in the phosphorylation of pRB/RB1 and NPM1 and communicates with D-type G1 cyclins during interphase at G1 to form a pRB/RB1 kinase and controls the entrance into the cell cycle (Matushansky, Radparvar and Skoultchi, 2003). The kinase assists in the initiation and preservation of cell cycle exit for the period of differentiation, averts cell proliferation, and adjusts cell differentiation negatively, on the other hand, is mandatory for the proliferation of definite cell kinds such as erythroid and hematopoietic cells (Lucas, Domenico & Gelfand, 2004).

Furthermore, this kinase is crucial for cell proliferation within the dentate gyrus of the hippocampus and the sub-ventricular region of the lateral ventricles and is also needed during thymocyte growth.

The kinase aids in the changes in patterns of gene expression in astrocytes, also variations in the actin cytoskeleton as well as the depletion of stress fibres, and heightened motility during cell differentiation. CDK6 inhibits myeloid differentiation by interfering with RUNX1 and decreasing its transcription transactivation action, however, encourages proliferation of ordinary myeloid progenitors (Ohnishi et al., 2007).

CDK6 is over-expressed in some leukaemia's and malignancies including sarcoma, lymphoma, and melanoma which consequence due to neighbouring translocations (Jones et al., 2007).

## 1.11 Aims of the project

The aim of this project was to develop simple structural compounds as potential anti-cancer agents. Many synthesised compounds in trials or either at market such as Clozapine, Adalimumab and Bevacizumab are bulky in size. Some contain various functional groups whilst others exhibit significant responses for toxicity however many fail when tested within the pharmacological parameters. Therefore, looking at what natural products were already out there without the need of altering the substructure too much, Dibenzoylmethane, a derivative of Curcumin and a natural herb, was researched. Dibenzoylmethane was shown to already exert its chemical and biological activity on a range of different cells and illnesses. Without changing the skeletal structure of Dibenzoylmethane excessively, a plan was actioned to synthesise various analogues of the molecule. These derivatives however would only have minimal difference from Dibenzoylmethane, be easy to synthesise, not difficult to purify and provide enough activity to be tested under pharmacological conditions. It was decided that up to ten  $\beta$ -diketone derivatives plus a few other compounds with different organic functional groups, in this case 2-Azido Diketones, containing nitrogen atoms, and benzoyl-*N'*-phenylurea derivatives, which contain sulphur atoms. The rational thinking was to look at a theory of whether compounds which differ based on their molecular weight or functional group content would exert different activity whilst undergoing screening. The experiments looked at assays based around biological and metabolic concepts, these including cytotoxicity, plasma stability and liver metabolism. This was conducted using the MTT assay for cytotoxicity, determining plasma concentration for stability and calculating intrinsic clearance using the liver S9 fraction. In total, 16 compounds were tested on 5 different cancerous cell lines. Furthermore, since many proteins and enzymes within the body

are responsible for cell growth and death plus associated with DNA, it was interesting to see what gene expression levels would be for common protein kinases. This work was conducted using PCR and different primers involved.

All the work was carried out to test the hypothesis whether smaller or bigger structure molecules exhibited better activity on the cell lines to use as anti-cancer agents. This question was raised based on argument in current pharmaceutical thinking which looks at whether companies should synthesise new small molecular weight compounds or use biologics, which includes hormones, cytokines, vaccines and mono-clonal antibodies. It was expected that the benzoyl-*N'*-phenylurea derivatives would work the best across all the screening tests since they have a higher molecular weight content and contain a variety of functional groups such as Oxygen, Carbon, Sulphur and Nitrogen.

## 2 Material and Methods

### 2.1 Synthesis and purification

#### 2.1.1 General procedures for compound purification and determination

All the compounds described were synthesised within the laboratories at the University of Salford. The analysis and structural determination of the compounds were carried out by TLC (thin layer chromatography),  $^1\text{H}$ - and  $^{13}\text{C}$ -NMR (nuclear magnetic resonance spectroscopy), infrared spectroscopy (IR) and melting point analysis.

#### **Solvents and Reagents**

Anhydrous solvents for the reactions were obtained as follows:

Dry THF was obtained by distillation over sodium and benzophenone under argon atmosphere as required.

Dry toluene and acetonitrile were dried over activated 3 Å molecular sieves for a period of 24 hours.

Any other solvents and reagents used were purchased from Thermo Fisher Scientific.

#### **Chromatography**

Flash column chromatography was carried out on silica gel 60 Å pore size and a particle size of 40-63 µm purchased from Thermo Fisher Scientific. The column diameter size was determined via the amount of dry compound obtained after evaporation. Solvents were chosen according to TLC analysis, and mixed solvent systems utilised were in the v/v (volumetric ratio) form. The TLCs were carried out on pre-coated aluminium backed silica plates (0.2mm, 60 F254). Rf values determined were calculated to the nearest 0.01 decimal

place, and the development of the separated products on the plate were visualised at UV254 (short).

### **<sup>1</sup>H and <sup>13</sup>C-NMR**

All NMR spectra were obtained and recorded through the usage of a Bruker AC-400 spectrometer using CDCl<sub>3</sub> as an internal standard unless stated otherwise (7.26 ppm for <sup>1</sup>H NMR, 77.0 ppm for <sup>13</sup>C NMR). Chemical shifts ( $\delta$ ) are given in parts per million (ppm) relative to tetramethylsilane (TMS) in addition to the coupling constants (J), which are stated in Hertz (Hz) and reported to one decimal place. The solvent peaks were determined from tables giving typical solvent shifts in NMR spectroscopy available in the literature (gottlieb, Kotlyar & Nudelman, 1997).

### **Infra-red**

All spectra were obtained and recorded on Thermo Scientific Nicolet iS10, and the absorbance peaks of the compounds reported as wave numbers (cm<sup>-1</sup>).

### **Melting Point**

Melting points (MP) were recorded using a Stuart Melting Point SMP20.

## 2.1.2 General Procedures for synthetic approach

### **Procedure A**

Under an atmosphere of argon, Potassium tert-butoxide (1.40 eq, 3.49 g,  $3.10 \times 10^{-2}$  mol) was suspended in dry THF (50 mL) and cooled to 0°C whilst undergoing stirring, leading to the formation of a cloudy, white solution. Added dropwise over a period of 10 minutes was acetophenone/s (3.00 g,  $2.21 \times 10^{-2}$  mol) suspended in dry THF (50 mL), forming a yellow suspension.

The reaction mixture was then left to warm to room temperature whilst stirring for a period of 30 minutes before it was cooled to 0°C under ice. Benzoyl Chloride substituent/s (1.20 eq, 3.08 mL,  $2.65 \times 10^{-2}$  mol) was added dropwise using a glass syringe, which led to the formation of a yellow solution. The mixture was then left to stir at room temperature, under argon, for a period of up to 3 hours.

After being cooled down to 0°C, potassium tert-butoxide (1.40 eq, 3.49 g,  $3.10 \times 10^{-2}$  mol) was again added with stirring and refluxed for 12-24 hours overnight. The mixture was then cooled to 0°C before HCl (3M) was added until the desired pH level (2-3) was reached. Using DCM (3 x 50 mL), the reaction mixture was extracted with the resulting combined organic layers being washed with sodium bicarbonate (2 x 50 mL), water (2 x 50 mL) and brine (2 x 50 mL). Using MgSO<sub>4</sub>, the layers were dried and concentrated *in vacuo* leading to the formation of a coloured β-diketone compound.

### **Procedure B**

Sodium hydride (0.2 g, 7.5 mmol) was suspended in dry THF (20mL) and the appropriately substituted benzoate (0.7 g, 3 mmol) was added whilst stirring. The mixture was then placed to cool at 0 °C. The appropriately substituted acetophenone (0.5 g, 2.8 mmol) dissolved in anhydrous dry THF (20 mL) was added dropwise over 5-10 minutes. The reaction mixture was left to stir at RT for 30 minutes then refluxed for 16h before being cooled to RT. The obtained mixture was filtered through Celite, washed with ethanol (3 x 20 mL) and then acidified with HCl (10 %) until pH 2 was achieved. The product was extracted with EtOAc (2 x 30 mL), the organic layer then washed with brine, water and dried (MgSO<sub>4</sub>) and concentrated *in vacuo* before being further purified by flash column chromatography (silica, Hexane/EtOAc 4:6). The coloured product was obtained as a solid.

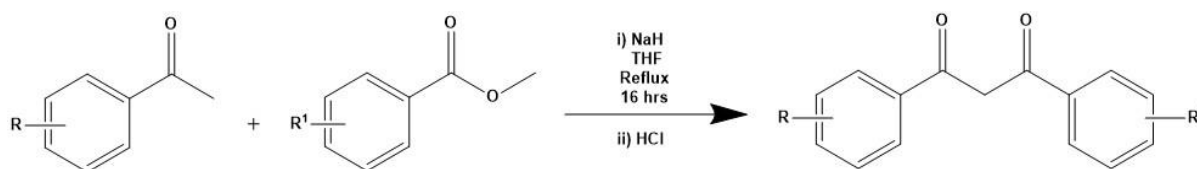


Figure 11 Scheme to show general synthetic route for 1,3-Diketone production using the base/acid method via reflux

### **Procedure C**

Into a thick microwave glass vessel was placed the starting acetophenone (0.25 g, 1.5 mmol) and the appropriately substituted benzoyl chloride (1 eq, 0.3 mL, 1.5 mmol) with a stirrer present. The vessel was allowed to irradiate under the microwave reactor under specific conditions (ie, 40 °C, 150MW, 30 minutes). The reaction mixture was allowed to cool before being poured onto crushed ice. HCl (10%) was added until a yellow precipitate had formed,

and the mixture was filtered. The contained product was extracted with DCM (2 x 25 mL), washed with brine, water and dried (MgSO<sub>4</sub>). Further purification was achieved by flash column chromatography (Pet Ether/EtOAc 8:2) to give a solid-coloured product.

#### **Procedure D**

To a solution of chloroimidazolium hexafluorophosphate (2.35 g, 7.8 mmol) dissolved in MeCN (8 mL), sodium azide (717 mg, 11 mmol) was added at 0 °C with the mixture then left to stir for 30 minutes. The mixture was filtered through a Celite pad, with the resulting filtrate concentrated in vacuo. The obtained residue was then dissolved in MeCN (ca. 2 mL) and the solution poured into Diethyl Ether (8mL) to form a precipitate, which was collected via suction filtration.

The resulting white solid (0.6 mmol) was dissolved in MeCN (0.5mL) and cooled to 0 °C. A solution of the required 1,3-dicarbonyl compound (0.5 mmol) and Triethylamine (1.0 mmol) in THF (2.0 mL) was added and the reaction stirred for a further 30 minutes. The reaction was quenched with H<sub>2</sub>O (5 mL), and the organic materials extracted with Dichloromethane (3 x 10 mL). The combined extracts were washed with brine (15 mL), and then dried over anhydrous Na<sub>2</sub>SO<sub>4</sub>. The solvent was removed in vacuo to afford the almost pure diazo compound. The crude material was purified by flash column chromatography (Ethyl Acetate:Hexane 10:2)

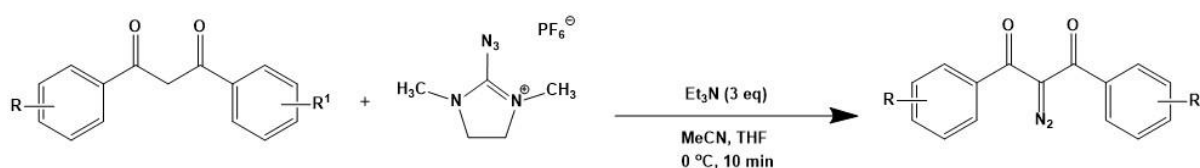


Figure 12 Scheme to show general synthetic route for 2-Azido-Diketone production

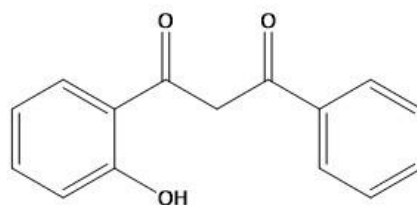
### **Procedure E**

To a solution of ammonium isothiocyanite (0.250g, 5 mmol) in 10 mL acetonitrile, 4-methoxy benzoyl chloride (0.64 g, 3.5 mmol) was added dropwise. The reaction mixture was stirred for 5 minutes until a white precipitate formed. A solution of appropriately substituted aniline (0.35g, 3 mmol) in acetonitrile (5 mL) was added gradually. The reaction mixture was stirred at room temperature for 4 hours and the solvent was evaporated *in vacuo*. The crude product was purified by column chromatography (hexane: ethylacetate, 8:3) to give a white product.

The final compounds were respectively synthesised using procedures A & B for the  $\beta$ -Diketone derivatives, procedure D for the 2-Azido-Diketone derivatives and procedure E for the *N*-benzoyl-*N'*-phenylurea derivatives. Based upon experimental requirements, it was decided that procedure C will not be used for any synthesis due to complications regarding low yield, purification issues, timing, and equipment limitations. Therefore, procedures A & B were utilised for the synthesis of the  $\beta$ -Diketone derivatives instead of procedure C, mainly based upon the fact that the final obtained yield was ca. 3-4 times more and easier to purify via flash column chromatography.

\*\* A table containing all the compounds which were synthesised are shown in **section 3.1**, **labelled table 3**. The compounds have been assigned numerically against the name of the compound synthesised.

### 2.1.3 Synthesis of $\beta$ -Diketone derivatives



Chemical Formula:  $C_{15}H_{12}O_3$

Molecular Weight: 240.26

**Figure 13: 1-(2-hydroxyphenyl)-3-phenylpropane-1,3-dione (1)**

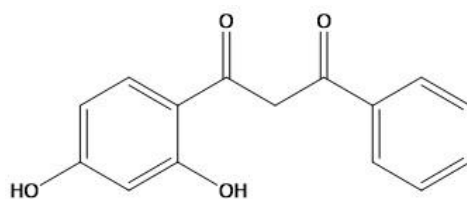
The above titled compound was prepared from 2-hydroxyacetophenone (3 g, 0.22 mmol) and benzoyl chloride (3.1mL, 0.26mmol) as per procedure A. Following flash column chromatography ( $SiO_2$ , Hexane:EtOAc 9:2) and recrystallization from methanol, compound 1 was isolated as a yellow solid (1.56 g , 67%)

**MP: 119 – 121 °C (lit. 120-122 °C)**

**$^1H$   $\delta$  ppm:** 3.95 (2H, s), 6.99 (1H, dd,  $J$  1.3, 8.3Hz), 7.36-7.58 (5H, 7.41 (t,  $J$  1.3 7.9Hz), 7.48 (t,  $J$  1.4 7.3Hz), 7.54 (dd,  $J$  1.4 7.9Hz), 7.53 (dd, 7.2, 1.3, 0.5 Hz)), 7.66 (1H, m), 7.97 (2H, dd  $J$  1.0, 8.5 Hz).

**$^{13}C$   $\delta$  ppm:**  $\delta$  114.4 (C1),  $\delta$  162.4 (C2),  $\delta$  118.6 (C3),  $\delta$  131.9 (C4),  $\delta$  123.4 (C5),  $\delta$  129.8 (C6),  $\delta$  199.2 (C7),  $\delta$  59.7 (C8),  $\delta$  195.1 (C9),  $\delta$  134.9 (C10),  $\delta$  128.6(C11),  $\delta$  128.5(C12),  $\delta$  128.5(C13),  $\delta$  128.5(C14),  $\delta$  128.6(C15)

**IR  $cm^{-1}$ :** 1885, 3100 (O-H), 1720 (C=O)



Chemical Formula:  $C_{15}H_{12}O_4$

Molecular Weight: 256.26

**Figure 14: 1-(2,4-dihydroxyphenyl)-3-phenylpropane-1,3-dione (2)**

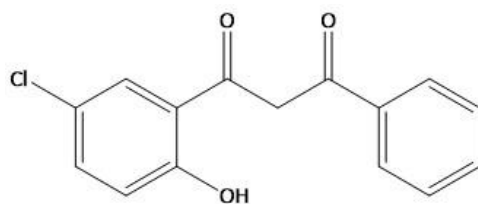
The above titled compound was prepared from 2,4-dihydroxyacetophenone (2.9 g, 0.18 mmol) and benzoyl chloride (3.1mL, 0.26mmol) as per procedure A. Following flash column chromatography ( $SiO_2$ , Hexane:EtOAc 9:2) and recrystallization from methanol, compound 2 was isolated as a yellow solid (1.26 g , 56%)

**MP: 164 – 168 °C**

**$^1H$   $\delta$  ppm:**  $\delta$  3.98 (2H, s), 6.56 (1H, dd,  $J$  1.8), 6.70 (1H, dd,  $J$  1.8, 7.6Hz), 7.53 (2H, dd,  $J$  1.3, 8.5Hz), 7.66 (1H, t,  $J$  1.5, 7.2Hz), 7.93-8.04 (3H, 8.01 (dd, 7.6 Hz), 7.97 (m,  $J$  1.9, 8.5Hz)

**$^{13}C$   $\delta$  ppm:**  $\delta$  102.79 (C1),  $\delta$  158.05 (C2),  $\delta$  98.73(C3),  $\delta$  125.56(C4),  $\delta$  159.74(C5),  $\delta$  101.3(C6),  $\delta$  197.66(C7),  $\delta$  63.22(C8),  $\delta$  189.22(C9),  $\delta$  127.58(C10),  $\delta$  126.87(C11),  $\delta$  125.84(C12),  $\delta$  123.66(C13),  $\delta$  121.42(C14),  $\delta$  121.18(C15)

**IR  $cm^{-1}$ :** 3049 (O-H), 1746 (C=O)



Chemical Formula: C<sub>15</sub>H<sub>11</sub>ClO<sub>3</sub>  
Molecular Weight: 274.70

**Figure 15: 1-(5-chloro-2-hydroxyphenyl)-3-phenylpropane-1,3-dione (3)**

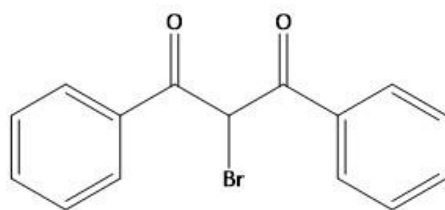
The above titled compound was prepared from 2'-Hydroxy-5'-chloroacetophenone (3.15 g, 0.29 mmol) and benzoyl chloride (3.1mL, 0.26mmol) as per procedure A. Following flash column chromatography (SiO<sub>2</sub>, Hexane:EtOAc 9:2) and recrystallization from methanol, compound 3 was isolated as a yellow solid (1.35 g , 62%)

**MP: 135-138 °C**

**<sup>1</sup>H δ ppm:** δ 4.00 (2H, s), 6.92 (1H, dd, 8.3Hz), 7.40 (1H, dd, *J* 1.7, 8.3Hz), 7.53 (2H, dd, *J* 1.3, 8.5Hz), 7.66 (1H, t, *J* 1.5, 7.2Hz), 7.97 (2H, dd, *J* 1.9, 8.5Hz), 8.06 (1H, d, *J* 1.7).

**<sup>13</sup>C δ ppm:** δ 119.5 (C1), δ 160.7 (C2), δ 120.0 (C3), δ 130.5 (C4), δ 129.3 (C5), δ 127.6 (C6), δ 199.2 (C7), δ 59.7 (C8), δ 195.1 (C9), δ 134.9 (C10), δ 128.6(C11), δ 128.5(C12), δ 128.9(C13), δ 128.5(C14), δ 128.6(C15)

**IR cm<sup>-1</sup>:** 1765, 3030 (O-H), 1756 (C=O), 720 (C-Cl)



Chemical Formula: C<sub>15</sub>H<sub>11</sub>BrO<sub>2</sub>  
Molecular Weight: 303.16

**Figure 16: 2-bromo-1,3-diphenylpropane-1,3-dione (4)**

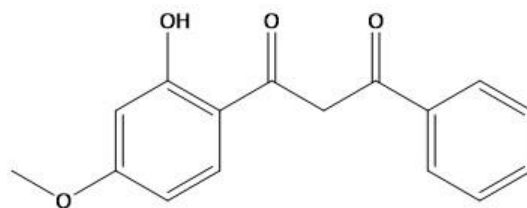
The above titled compound was prepared from 4-bromoacetophenone (1.8 g, 0.36 mmol) and benzoyl chloride (3.1mL, 0.26mmol) as per procedure A. Following flash column chromatography (SiO<sub>2</sub>, Pe:EtOAc 8:2) and recrystallization from methanol, compound 4 was isolated as a white solid (0.98 g , 52%)

**MP: 125 – 129 °C**

**<sup>1</sup>H δ ppm:** δ 5.98 (1H, s), 7.56 (4H, dd, *J* 1.4, 8.4Hz), 7.66 (2H, t, *J* 1.5, 7.4Hz), 7.97 (4H, m, *J* 1.9, 8.4Hz)

**<sup>13</sup>C δ ppm:** δ 135 (C1), δ 126.8 (C2), δ 128.8 (C3), δ 129.5 (C4), δ 128.8 (C5), δ 126.8(C6), δ 187 (C7), δ 57.3 (C8), δ 187 (C9), δ 135 (C10), δ 126.8(C11), δ 128.8(C12), δ 129.5(C13), δ 128.8(C14), δ 128.6(C15)

**IR cm<sup>-1</sup>:** 1685, 1742 (C=O), 503 (C-Br)



Chemical Formula: C<sub>16</sub>H<sub>14</sub>O<sub>4</sub>  
Molecular Weight: 270.28

**Figure 17: 1-(2-hydroxy-4-methoxyphenyl)-3-phenylpropane-1,3-dione (5)**

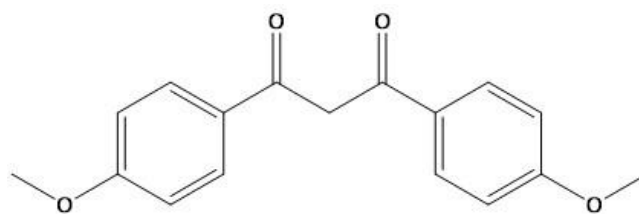
The above titled compound was prepared from 2-hydroxyacetophenone (2.2 g, 0.29 mmol) and 4-methoxybenzoyl chloride (3.1mL, 0.26mmol) as per procedure A. Following flash column chromatography (SiO<sub>2</sub>, Pe:EtOAc 10:1) and recrystallization from methanol, compound 5 was isolated as a white solid (0.88 g , 52%)

**MP: 121 – 128 °C**

**<sup>1</sup>H δ ppm:** δ 3.81 (3H, s), 3.95 (2H, s), 6.57 (1H, d, *J* 1.3, 6.64 (1H, d, *J* 1.3, 7.6Hz), 7.53 (2H, t, *J* 1.3 8.5Hz), 7.66 (1H, t, *J* 1.5,7.1Hz), 7.93-8.03 (3H, 8.00 (dd, 7.6Hz,)), 7.97 (dd, *J* 1.9,8.5Hz)

**<sup>13</sup>C δ ppm:** 114.4 (C1), δ 128.5 (C2), δ 111.3 (C3), δ 161.9 (C4), δ 101.3(C5), δ 164.7(C6), δ 199.7 (C7), δ 59.7 (C8), δ 195.1 (C9), δ 134.9 (C10), δ 128.6(C11), δ 128.5(C12), δ 128.9(C13), δ 128.5(C14), δ 128.6(C15) δ (C16)

**IR cm<sup>-1</sup>:** 1795, 3130 (O-H), 1680 (C=O), 1250 (-OCH)



Chemical Formula:  $C_{17}H_{16}O_4$   
Molecular Weight: 284.31

**Figure 18: 1,3-bis(4-methoxyphenyl)propane-1,3-dione (6)**

The above titled compound was prepared from 4-methoxyacetophenone (1.16 g, 0.18 mmol) and 4-methoxybenzoyl chloride (3.1mL, 0.26mmol) as per procedure A. Following flash column chromatography ( $SiO_2$ , Hexane:EtOAc 10:1) and recrystallization from methanol, compound 6 was isolated as a white solid (0.58 g , 46%)

**MP: 129 – 134 °C**

**$^1H$   $\delta$  ppm:**  $\delta$  3.80 (6H, s), 3.94 (2H, s), 7.05 (4H, dd,  $J$  1.2, 8.3Hz), 7.99 (4H, dd,  $J$  1.8,8.3Hz).

**$^{13}C$   $\delta$  ppm:** 134.9 (C1),  $\delta$  130.3 (C2),  $\delta$  114 (C3),  $\delta$  55.5 (C4),  $\delta$  114 (C5),  $\delta$  130.3(C6),  $\delta$  195.1 (C7),  $\delta$  59.7 (C8),  $\delta$  195.1 (C9),  $\delta$  134.9 (C10),  $\delta$  130.3(C11),  $\delta$  114(C12),  $\delta$  114(C13),  $\delta$  114(C14),  $\delta$  130.5(C15)  $\delta$  55.5(C16)  $\delta$  55.5(C17)

**IR  $cm^{-1}$ :** 1764, 1860 (C=O), 1186 (-OCH)

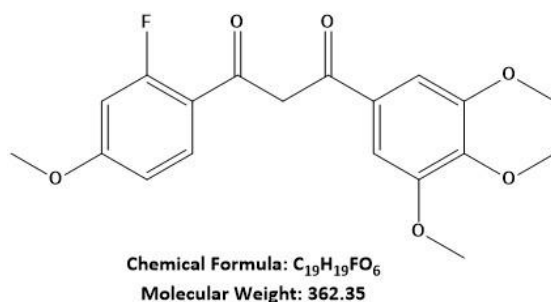


**Figure 19: 1-(3-(dimethoxydanyl)-4,5-dimethoxyphenyl)-3-(2-fluoro-4-methoxyphenyl)propane-1,3-dione (7)**

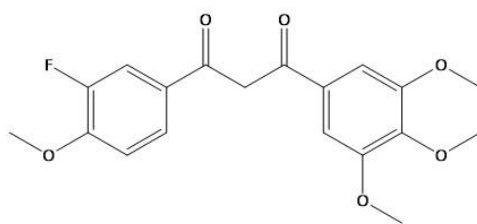
The above titled compound was prepared from methyl-3,4,5-trimethoxybenzoate (0.85 g, 2.3 mmol) and 3-fluoro-4-methoxyacetophenone (0.5 g, 2.6mmol) as per procedure B. Following flash column chromatography ( $SiO_2$ , Hexane:EtOAc 4:6) and recrystallization from methanol, compound 7 was isolated as a white solid (0.32 g , 68%)

**MP: 123-125 °C**

**$^1H$   $\delta$  ppm:**  $\delta$  3.77 (6H, s), 3.84 (2H, s), 3.87-3.88 (6H, 3.88 (s), 3.88 (s)), 6.87 (1H, dd,  $J$  2.3,7.6Hz), 7.23 (1H, dd,  $J$  2.3), 7.30 (2H, d,  $J$  1.8), 7.96 (1H, dd,  $J$  7.6).

**$^{13}C$   $\delta$  ppm:** 134.9 (C1),  $\delta$  125.7 (C2),  $\delta$  114.6 (C3),  $\delta$  163.9 (C4),  $\delta$  99.8 (C5),  $\delta$  158.7(C6),  $\delta$  195.1 (C7),  $\delta$  58.5 (C8),  $\delta$  199.2 (C9),  $\delta$  138.6 (C10),  $\delta$  108.2(C11),  $\delta$  152.1(C12),  $\delta$  139.8(C13),  $\delta$  152.1(C14),  $\delta$  107.5(C15)  $\delta$  57.6(C16)  $\delta$  60.3(C17)  $\delta$  60.3(C18),  $\delta$  57.6(C19)

**IR  $cm^{-1}$ :** 1843, 1769 (C=O), 1219 (-OCH), 1339 (C-F)



Chemical Formula: C<sub>19</sub>H<sub>19</sub>FO<sub>6</sub>  
Molecular Weight: 362.35

**Figure 20: 1-(3-(dimethoxydanyl)-4,5-dimethoxyphenyl)-3-(3-fluoro-4-methoxyphenyl)propane-1,3-dione (8)**

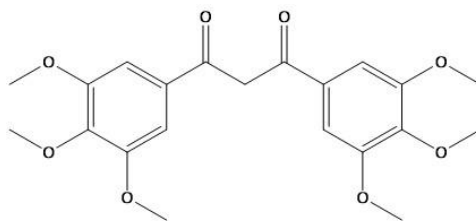
The above titled compound was prepared from methyl-3,4,5-trimethoxybenzoate (0.85 g, 2.3 mmol) and 2-fluoro-5-methoxyacetophenone (0.65 g, 3.1mmol) as per procedure B. Following flash column chromatography (SiO<sub>2</sub>, Hexane:EtOAc 4:6) and recrystallization from methanol, compound 8 was isolated as a white solid (0.37 g , 62%)

**MP: 123-125 °C**

**<sup>1</sup>H δ ppm:** δ 3.77 (6H, s), 3.88 (3H, s), 3.92 (3H, s), 3.95 (2H, s), 7.04 (1H, dd, 8.4Hz), 7.30 (2H, d, J 1.8), 7.71 (1H, dd, J 1.9, 8.4Hz), 7.78 (1H, dd, J 1.9)

**<sup>13</sup>C δ ppm:** 134.9 (C1), δ 129.5 (C2), δ 112 (C3), δ 152.8 (C4), δ 151.2 (C5), δ 115(C6), δ 195.3 (C7), δ 59.9 (C8), δ 194.5 (C9), δ 138.4 (C10), δ 108.5(C11), δ 153.8(C12), δ 138.6(C13), δ 152.8(C14), δ 108.4(C15) δ 56.6(C16) δ 61.3(C17) δ 57.4(C18), δ 57.4(C19)

**IR cm<sup>-1</sup>:** 1763, 1822 (C=O), 1053 (-OCH), 1156 (C-F)



Chemical Formula: C<sub>21</sub>H<sub>24</sub>O<sub>8</sub>  
Molecular Weight: 404.42

**Figure 21: 1-(3-(dimethoxydanyl)-4,5-dimethoxyphenyl)-3-(3,4,5-trimethoxyphenyl)propane-1,3-dione (9)**

The above titled compound was prepared from methyl-3,4,5-trimethoxybenzoate (0.69 g, 2.9 mmol) and 3,4,5-trimethoxyacetophenone (0.5 g, 2.38mmol) as per procedure B.

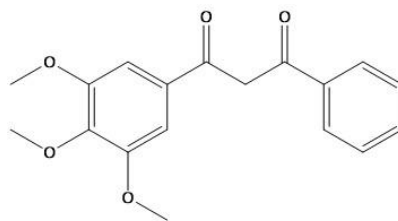
Following flash column chromatography (SiO<sub>2</sub>, Hexane:EtOAc 4:6) and recrystallization from methanol, compound 9 was isolated as a yellow solid (0.25 g , 32%)

**MP: 87 – 89 °C**

**<sup>1</sup>H δ ppm:** δ 3.77 (12H, s), 3.88 (6H, s), 3.95 (2H, s), 7.30 (4H, d, *J* 1.8 Hz).

**<sup>13</sup>C δ ppm:** 137.8 (C1), δ 109.5 (C2), δ 152.9 (C3), δ 139.8 (C4), δ 152.9 (C5), δ 109.5(C6), δ 195.1 (C7), δ 57.9 (C8), δ 195.1 (C9), δ 137.8 (C10), δ 109.5(C11), δ 152.9(C12), δ 139.8(C13), δ 152.9(C14), δ 109.5(C15) δ 60.9(C16) δ 60.9(C17) δ 56.2(C18), δ 56.2(C19), δ 56.2(C20) δ 56.2(C21)

**IR cm<sup>-1</sup>:** 1698, 1682 (C=O), 1365 (-OCH)



Chemical Formula: C<sub>18</sub>H<sub>18</sub>O<sub>5</sub>  
Molecular Weight: 314.34

**Figure 22: 1-(phenyl-3-(3,4,5-trimethoxyphenyl)propane-1,3-dione (10)**

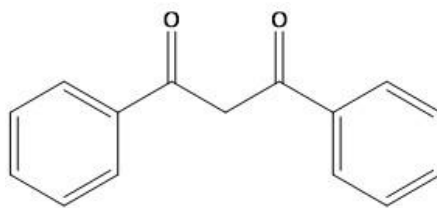
The above titled compound was prepared from methyl-3,4,5-trimethoxybenzoate (0.99 g, 2.4 mmol) and acetophenone (0.9 g, 2.38mmol) as per procedure A. Following flash column chromatography (SiO<sub>2</sub>, Hexane:EtOAc 4:6) and recrystallization from methanol, compound 10 was isolated as a yellow solid (0.45 g , 42%)

**MP: 87 – 89 °C**

**<sup>1</sup>H δ ppm:** δ 3.77 (6H, s), 3.88 (3H, s), 3.90 (2H, s), 7.23 (2H, d, *J* 1.8 Hz), 7.53 (2H, t, *J* 1.3, 8.5Hz), 7.66 (1H, t *J* 1.5,7.2Hz), 7.97 (2H, dd, *J* 1.9, 8.5Hz).

**<sup>13</sup>C δ ppm:** 138.6 (C1), δ 110.4 (C2), δ 151.9 (C3), δ 139.2 (C4), δ 151.9 (C5), δ 110.5(C6), δ 196.1 (C7), δ 59.9 (C8), δ 197.2 (C9), δ 134.8 (C10), δ 128.5(C11), δ 126.4(C12), δ 128.9(C13), δ 126.4(C14), δ 128.4(C15) δ 62.3(C16) δ 58.3(C17) δ 58.3(C18)

**IR cm<sup>-1</sup>:** 1639, 1752 (C=O), 1340 (-OCH)



Chemical Formula:  $C_{15}H_{12}O_2$

Molecular Weight: 224.26

**Figure 23: 1,3-diphenylpropane-1,3-dione (DBM)**

The above titled compound was prepared from acetophenone (2.6 g, 3.4 mmol) and Benzoyl chloride (3.5 mL, 3.38mmol) as per procedure A. Following flash column chromatography ( $SiO_2$ , Hexane:EtOAc 4:6) and recrystallization from methanol, DBM was isolated as a white solid (1.68 g , 73%)

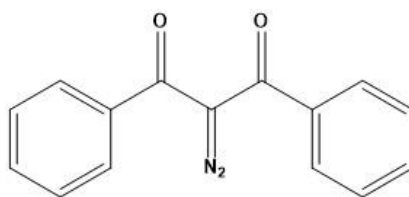
**MP: 115 – 117 °C**

**$^1H$   $\delta$  ppm:**  $\delta$  3.75 (2H, s), 7.53 (4H, dd,  $J$  1.3, 8.5Hz), 7.71 (2H, t,  $J$  1.5, 7.2Hz), 7.97 (4H, dd,  $J$  1.5, 8.5,Hz).

**$^{13}C$   $\delta$  ppm:** 136.7 (C1),  $\delta$  128.8 (C2),  $\delta$  128.6 (C3),  $\delta$  133.1 (C4),  $\delta$  128.6 (C5),  $\delta$  128.8 (C6),  $\delta$  190.4 (C7),  $\delta$  93.3 (C8),  $\delta$  190.1 (C9),  $\delta$  1346.7 (C10),  $\delta$  128.8(C11),  $\delta$  128.6(C12),  $\delta$  133.1(C13),  $\delta$  128.6(C14),  $\delta$  128.8(C15)

**IR  $cm^{-1}$ :** 1562, 1732 (C=O)

#### 2.1.4 Synthesis of 2-Azido-Diketone derivatives



Chemical Formula:  $C_{15}H_{10}N_2O_2$

Molecular Weight: 250.26

**Figure 24: 2-Azido-1,3-diphenylpropane-1,3-dione (11)**

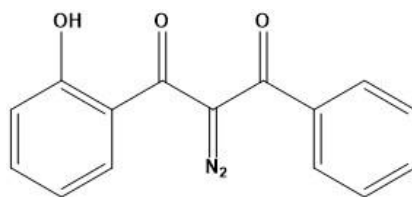
Using procedure D, the resulting white solid (1.24g, 0.6 mmol) was dissolved in MeCN (0.5mL) and cooled to 0 °C. A solution of 1,3-diphenylpropane-1,3-dione (2.4 g) and Triethylamine (1.0 mmol) in THF (2.0 mL) was added and the reaction stirred for a further 30 minutes. The reaction was quenched with H<sub>2</sub>O (5 mL), and the organic materials extracted with Dichloromethane (3 × 10 mL). The combined extracts were washed with brine (15 mL), and then dried over anhydrous Na<sub>2</sub>SO<sub>4</sub>. The solvent was removed in vacuo to afford the almost pure diazo compound (1.8 g, 87%). The crude material was purified by flash column chromatography (Ethyl Acetate:Hexane 10:2)

**MP: 149 – 153 °C**

**<sup>1</sup>H δ ppm:** δ 7.45 (4H, dd, *J* 1.4, 8.4Hz), 7.62 (2H, t, *J* 1.5, 7.4Hz), 7.98 (4H, m, *J* 1.9, 8.45 Hz).

**<sup>13</sup>C δ ppm:** 134.7 (C1), δ 130.3 (C2), δ 128.6 (C3), δ 129.5 (C4), δ 128.6 (C5), δ 130.8 (C6), δ 185.4 (C7), δ 153.3 (C8), δ 185.1 (C9), δ 134.7 (C10), δ 130.8(C11), δ 128.6(C12), δ 129.5(C13), δ 128.6(C14), δ 130.8(C15)

**IR cm<sup>-1</sup>:** 1420 (C=N), 1762 (C=O)



Chemical Formula: C<sub>15</sub>H<sub>10</sub>N<sub>2</sub>O<sub>3</sub>  
Molecular Weight: 266.26

**Figure 25: 2-Azido-1-(2-hydroxyphenyl)-3-phenylpropane-1,3-dione (12)**

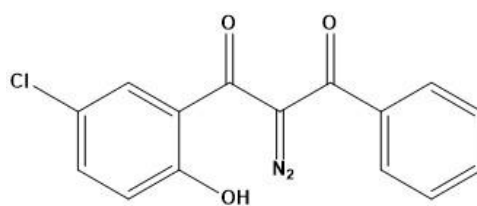
Using procedure D, the resulting white solid (1.24g, 0.6 mmol) was dissolved in MeCN (0.5mL) and cooled to 0 °C. A solution of 1-(2-hydroxyphenyl)-3-phenylpropane-1,3-dione (2.12 g) and Triethylamine (1.0 mmol) in THF (2.0 mL) was added and the reaction stirred for a further 30 minutes. The reaction was quenched with H<sub>2</sub>O (5 mL), and the organic materials extracted with Dichloromethane (3 × 10 mL). The combined extracts were washed with brine (15 mL), and then dried over anhydrous Na<sub>2</sub>SO<sub>4</sub>. The solvent was removed in vacuo to afford the almost pure diazo compound (1.48 g, 89%). The crude material was purified by flash column chromatography (Ethyl Acetate:Hexane 10:2)

**MP: 149 – 153 °C**

**<sup>1</sup>H δ ppm:** δ 6.90 (1H, t, *J* 1.3,8.3Hz), 7.33-7.53 (4H, 7.45 (m, *J* = 1.4, 8.4Hz), 7.50 (dd, *J* =1.4, 8.1Hz), 7.38 (dd, *J* = 1.3, 8.1Hz)), 7.49 (1H, t, *J* =1.4, 8.3Hz), 7.62 (1H, t, *J* 1.5, 7.4Hz), 7.98 (2H, dd, *J* 1.5, 8.4Hz).

**<sup>13</sup>C δ ppm:** 119.4 (C1), δ 160.4 (C2), δ 116.6 (C3), δ 133.9 (C4), δ 123.4 (C5), δ 129.8 (C6), δ 183.2 (C7), δ 159.7 (C8), δ 183.1 (C9), δ 132.9 (C10), δ 128.6(C11), δ 128.5(C12), δ 129.5(C13), δ 128.5(C14), δ 128.6(C15)

**IR cm<sup>-1</sup>:** 1635, 1430 (C=N), 1760 (C=O), 3430 (O-H)



Chemical Formula: C<sub>15</sub>H<sub>9</sub>ClN<sub>2</sub>O<sub>3</sub>

Molecular Weight: 300.70

**Figure 26: 2-Azido-1-(5-chloro-2-hydroxyphenyl)-3-phenylpropane-1,3-dione (13)**

Using procedure D, the resulting white solid (1.24g, 0.6 mmol) was dissolved in MeCN (0.5mL) and cooled to 0 °C. A solution of 1-(5-chloro-2-hydroxyphenyl)-3-phenylpropane-1,3-dione (1.86 g) and Triethylamine (1.0 mmol) in THF (2.0 mL) was added and the reaction stirred for a further 30 minutes. The reaction was quenched with H<sub>2</sub>O (5 mL), and the organic materials extracted with Dichloromethane (3 × 10 mL). The combined extracts were washed with brine (15 mL), and then dried over anhydrous Na<sub>2</sub>SO<sub>4</sub>. The solvent was removed in vacuo to afford the almost pure diazo compound (1.12 g, 85%). The crude material was purified by flash column chromatography (Ethyl Acetate:Hexane 10:2)

**MP: 163 – 172 °C**

**<sup>1</sup>H δ ppm:** δ 6.95 (1H, dd, 8.3Hz), 7.36-7.50 (3H, 7.39 (dd, *J* 1.7, 8.3Hz), 7.45 (dd, *J* 1.4, 8.4Hz), 7.62 (1H, t, *J* 1.5, 7.4Hz), 7.98 (2H, dd, *J* 1.5, 8.4Hz), 8.18 (1H, dd, *J* 1.7).

**<sup>13</sup>C δ ppm:** 121.5 (C1), δ 162.7 (C2), δ 120.0 (C3), δ 133.5 (C4), δ 128.3 (C5), δ 127.6 (C6), δ 186.2 (C7), δ 59.7 (C8), δ 183.1 (C9), δ 136.9 (C10), δ 130.6(C11), δ 129.5(C12), δ 127.9(C13), δ 128.5(C14), δ 130.6(C15)

**IR cm<sup>-1</sup>:** 1724, 1346 (C=N), 1800 (C=O), 3243 (O-H), 755 (C-Cl)

### 2.1.5 Synthesis of *N*-benzoyl-*N'*-phenylurea derivatives

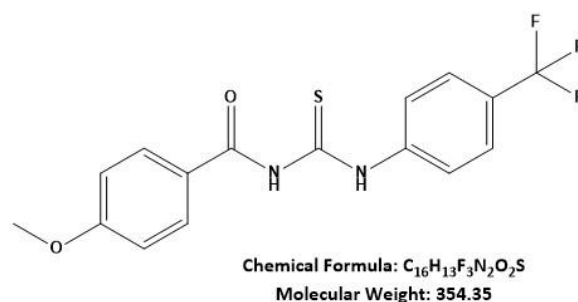


**Figure 27: 4-methoxy-*N*-((4-(trifluoromethyl)phenyl)carbamoithioyl)benzamide (14)**

As per Procedure E to a solution of ammonium isothiocyanite (0.250g, 5 mmol) in 10 mL acetonitrile, 4-methoxy benzoyl chloride (0.64 g, 3.5 mmol) was added drop-wise. The reaction mixture was stirred for 5 minutes until a white precipitate formed. A solution of 4-trifluoromethyl aniline (0.35g, 3 mmol) in acetonitrile (5 mL) was added gradually. The reaction mixture was stirred at room temperature for 4 hours and the solvent was evaporated *in vacuo*. The crude product was purified by column chromatography (hexane: ethylacetate, 8:3) to give a white product (0.28 g, 48%)

**MP: 120-124 °C**

**<sup>1</sup>H δ ppm:** δ 3.85 (3H, s), 7.04 (2H, dd, *J* 1.2, 8.3Hz), 7.11 (2H, dd, *J* 1.4, 8.2Hz), 7.57 (2H, dd, *J* 1.7, 8.2 Hz), 8.02 (2H, t, *J* 1.8, 8.3Hz).

**<sup>13</sup>C δ ppm:** 133.1 (C1), δ 131.2 (C2), δ 113.7 (C3), δ 160.4 (C4), δ 113.6 (C5), δ 131.2(C6), δ 167.3 (C7), δ 178.5 (C8), δ 137.7 (C9), δ 116.2 (C10), δ 127.9(C11), δ 129.1(C12), δ 127.9(C13), δ 116.8(C14), δ 124.3(C15) δ 54.2(C16)

**IR cm<sup>-1</sup>:** 1200 (C-N), 1239 (C-F), 1700 (C=O), 3340 (N-H), 1225 (-OCH), 650 (C-S)

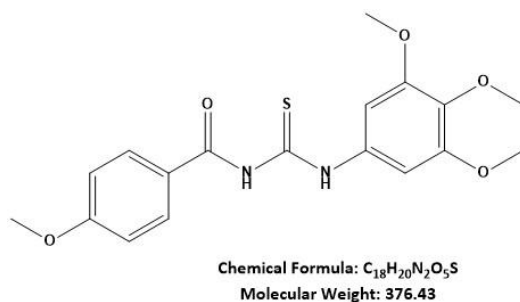


**Figure 28: 4-methoxy-N-((3,4,5-trimethoxyphenyl)carbamothioyl)benzamide (15)**

As per Procedure E to a solution of ammonium isothiocyanite (0.21g, 2.73 mmol) in 10 mL acetonitrile, 4-methoxy benzoyl chloride (0.46 g, 3.5 mmol) was added drop-wise. The reaction mixture was stirred for 5 minutes until a white precipitate formed. A solution of 3,4,5-trimethoxy aniline (0.43g, 2.4 mmol) in acetonitrile (5 mL) was added gradually. The reaction mixture was stirred at room temperature for 4 hours and the solvent was evaporated *in vacuo*. The crude product was purified by column chromatography (hexane: ethylacetate, 8:3) to give a white product (0.32 g, 44%)

**MP: 164- 172 °C**

**<sup>1</sup>H δ ppm:** δ 3.69 (3H, s), 3.81 (6H, s), 3.85 (3H, s), 6.31 (2H, d, *J* 1.5), 7.04 (2H, m, *J* 1.2, 8.3Hz), 8.02 (2H, dd, *J* 1.8, 8.3Hz).

**<sup>13</sup>C δ ppm:** 133.9 (C1), δ 132.6 (C2), δ 109.2 (C3), δ 161.2 (C4), δ 109.2 (C5), δ 132.6(C6), δ 165.3 (C7), δ 176.3 (C8), δ 140.5 (C9), δ 104.2 (C10), δ 154.5(C11), δ 134.2(C12), δ 154.3(C13), δ 104.2(C14), δ 62.9(C15) δ 56.2(C16) δ 56.2(C17) δ 55.8(C18)

**IR cm<sup>-1</sup>:** 1146 (C-N), 16130 (C=O), 3140 (N-H), 1163 (-OCH), 612 (C-S)

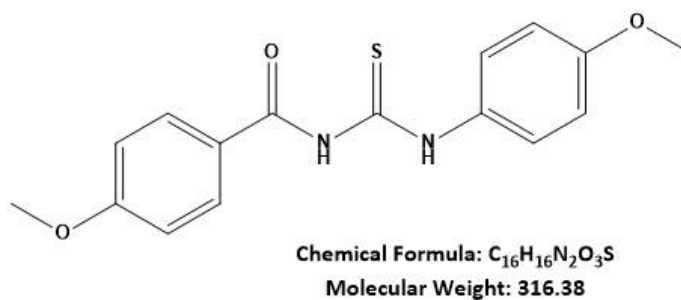


**Figure 29: 4-methoxy-N-((4-methoxyphenyl)carbamothioyl)benzamide (16)**

As per Procedure E to a solution of ammonium isothiocyanite (0.30g, 3.6 mmol) in 10 mL acetonitrile, 4-methoxy benzoyl chloride (0.46 g, 3.5 mmol) was added drop-wise. The reaction mixture was stirred for 5 minutes until a white precipitate formed. A solution of aniline (0.56g, 2.9 mmol) in acetonitrile (5 mL) was added gradually. The reaction mixture was stirred at room temperature for 4 hours and the solvent was evaporated *in vacuo*. The crude product was purified by column chromatography (hexane: ethylacetate, 8:3) to give a white product (0.42 g, 47%)

**MP: 164- 172 °C**

**$^1H$   $\delta$  ppm:**  $\delta$  3.76 (3H, s), 3.85 (3H, s), 6.69 (2H, dd,  $J$  2.7,8.8Hz), 7.04 (2H, dd,  $J$  1.2, 8.3Hz), 7.20 (2H, t,  $J$  2.2, 8.8Hz), 8.02 (2H, m,  $J$  1.8, 8.3Hz).

**$^{13}C$   $\delta$  ppm:** 130.9 (C1),  $\delta$  134.2 (C2),  $\delta$  113 (C3),  $\delta$  164.2 (C4),  $\delta$  113 (C5),  $\delta$  131.5(C6),  $\delta$  167.3 (C7),  $\delta$  178.6 (C8),  $\delta$  130.2 (C9),  $\delta$  121.5 (C10),  $\delta$  114.3(C11),  $\delta$  156.3(C12),  $\delta$  114.4(C13),  $\delta$  120.4(C14),  $\delta$  61.2(C15)  $\delta$  56.8(C16)

**IR  $cm^{-1}$ :** 1237 (C-N), 1785 (C=O), 3234 (N-H), 1236 (-OCH), 685 (C-S)

## 2.2 Experimental – Biological Assays

### 2.2.1 Subculture and cell maintenance

#### **Culture Media**

100mL of fresh culture media contained the following: RPMI-1640 (88mL), Foetal Bovine Serum (10mL), L-Glutamine (1mL) and Penicillin-Streptomycin (1mL)

#### **Thawing of adherent cells**

For this procedure, two T75 flasks were prepared per vial (ca. 1.5mL) of frozen cells. The following cells, HepG2, HeLa, A549, HCT-116 and CaCo-2 were used. The cryovial containing the frozen cell stocks were taken from liquid nitrogen or a freezer storage (-80°C), thoroughly cleaned using ethanol in sterile conditions and then allowed to thaw in a 37 °C water bath (ca 3 min). 0.6 mL of the cell suspension was then transferred and mixed into fresh culture media (ca 10 mL) and centrifuged at 1500rpm for 5 minutes to remove any excess DMSO. The pellet, obtained after the discarding of the media suspension, was mixed in fresh culture media (12 mL) and pipetted into the sterile T75 flasks. After an incubation period of 24 h, when microscopy showed that the cells had attached to the surface of the flask, the medium was removed and replaced with 12 mL of fresh culture medium to prepare the cells for sub-culturing.

#### **General subculture of adherent cells**

Adherent cells were sub-cultured from one T75 flask into 3 x T25 flasks. Firstly, the old medium from the T75 flask was discarded, and the cells on the surface of the flask were washed with sterile phosphate buffer (1x PBS v/w, 3 x 5mL for T25 / 3 x 8mL for T75). To detach the cells from the surface, trypsin-EDTA (2mL for T25/5mL for T75) was added before

the flask/s were incubated for 3-5 min at 37 °C. This step was confirmed using a light microscope. The cells, in the supernatant, were then re-suspended in fresh culture media (7 mL) to inactivate the trypsin-EDTA before being centrifuged at 1500rpm for 5 minutes. The obtained pellet, after discarding the supernatant, was mixed in fresh culture media (8mL) before ca. 2mL was pipetted into each T25 flask. The T25 flask was topped up using 6mL of fresh culture media, with the cells left to adhere and proliferate in a humidified incubator (37 °C, 5% CO<sub>2</sub>). The subculture of cells was routinely carried out every two to three days depending on the cell confluence and usage of the cells.

### **Freezing of adherent cell stock**

Three confluent T25 tissue culture flasks were prepared and used as cell stocks to be stored in liquid nitrogen. Cells were detached as per the subculture protocol and fresh culture media (5mL) was added to one of the T25 flasks. The cells were suspended, and the supernatant mixture transferred to the second T25 flask. Again, the mixed cell supernatant was transferred to the final T25 flask, whereby a concentrated cell supernatant was obtained. This was then centrifuged at 1500rpm for 7 minutes, and the supernatant discarded. The obtained pellet was then resuspended in foetal bovine serum (5mL containing 10% DMSO). Aliquots (1.5mL) were prepared in cryovials and transferred into an isopropanol freezing container to be frozen at -80°C overnight, before being stored in liquid nitrogen at -196°C to a long-term storage.

## 2.2.2 Cell Lines

The following cancer cell lines were used to screen the compounds; A549, Caco-2, HCT-116, HeLa and HepG2, with the incubation periods set as; 24, 48, 72 and 96 hours. The concentration dose range for all compounds whereby at the time of testing was; 3.125 $\mu$ M, 6.25 $\mu$ M, 12.5 $\mu$ M, 25 $\mu$ M, 50 $\mu$ M and 100 $\mu$ M.

### 2.2.2.1 HepG2

Renowned as one of the most widely used cell lines for the application of evaluating the toxicity of chemicals and drugs alike, is the human hepatocellular carcinoma cell line, HepG2. Known to possess 55 pairs of chromosomes with the ability to be grown successfully at a large scale and secrete various plasma proteins such as fibrinogen, transferrin and albumin, these cells are said to be adherent and epithelial like. HepG2 cells are conventionally cultured as a form of monolayer in a two-dimensional (2D) culture plate in small aggregates, stimulated with the aid of human growth hormones, which provides them with a doubling time of around 48 hours.

HepG2 cells were obtained from the biobank at the University of Salford, and sub-cultured as per the protocol (section 2.2.1) to be used as required. The cell line is derived from the liver tissue of a Caucasian American, aged 15 (Gerets et al., 2012). Originally established in 1979 by Barbara Knowles and fellow colleagues, HepG2 has been reported as a hepatocellular carcinoma (Aden et al 1979). As mentioned, HepG2 cells were subcultured every two to three days and grown in RPMI-1640 medium (Biosera.com) supplemented with FBS (10%), penicillin (100 units/mL), streptomycin (100 $\mu$ g/mL) and L-glutamine (2mM).

#### 2.2.2.2 HCT-116

Defined as a human colon cancer cell line, HCT 116 cells are found to be one of three colorectal carcinoma subpopulations from a single male human. The cell line is commonly used to study the biology of cancer due to its nature, whereby it is a growth factor independent cell line with a relatively low doubling time of approximately 21 hours. Although many researchers recommend the usage of McCoy's 5A medium for the growth of HCT 116 cells, HCT cells can efficiently grow in RPMI-1640. Therefore HCT 116 cells were grown in RPMI-1640 medium (Biosera.com) supplemented with FBS (10%), penicillin (100 units/mL), streptomycin (100µg/mL) and L-glutamine (2mM). In addition, the cell line is said to be highly aggressive human colorectal cell line with no known ability to differentiate and no expression of caudal type homeobox 1 (CDX1) coding gene. CDX1 is responsible for gene expression regulation such as that of intestinal alkaline phosphatase gene, which is responsible for dephosphorylation, and the inhibition of beta-catenin transcriptional activity, which is involved in cell adherence and gene transcription. It is also important in the differentiation of enterocytes (Yeung et al., 2010).

#### 2.2.2.3 HeLa

Obtained from the European Collection of Cell Cultures, the HeLa cell strain was first extracted from an epidermoid carcinoma of the cervix by George O. Gey from a patient named Henrietta Lacks in 1951 (Scherer & Syverton, 1952). Defined in science as an 'immortal' cell line, whereby it was the first strain to be grown successfully within cell culture laboratories, it is, along with HepG2, the most used in research studies till date due to its proficient, durable and prolific properties. Cell biologist, George Otto Gey, found that the culture survived indefinitely if given the correct nutrients and a suitable environment. In addition, researchers

believe that HeLa cells do not suffer programme death because they maintain a version of the enzyme, telomerase. The enzyme is reported to prevent the gradual shortening of telomeres of chromosomes. Telomere shortening is implicated in aging and death. The endothelial cell monolayers provide another quick doubling time of 24 hours, with HeLa cells typically sub-cultured every two days, and grown in RPMI-1640 medium (Biosera.com) supplemented with FBS (10%), penicillin (100 units/mL), streptomycin (100µg/mL) and L-glutamine (2mM).

#### 2.2.2.4 A549

A549 cells were obtained from the University of Salford. Typically grown as a monolayer, the adherent and epithelial like cell is derived from the lung. The cell line was first isolated in the year 1973 from a pulmonary adenocarcinoma, which is the removal and culture of cancerous lung tissue by D.J Giard and his team. Although A549 cells are a representative of the Alveolar type II pneumocyte of the human lung, the strain was derived from a 58-year-old male Caucasian and used for their speedy doubling time of approximately 22 hours. Again, the A549 cells were grown in RPMI-1640 medium (Biosera.com) supplemented with FBS (10%), penicillin (100 units/mL), streptomycin (100µg/mL) and L-glutamine (2mM).

#### 2.2.2.5 CaCo-2

The Caco-2 cell line is a differentiated cell line originally collected from a human, adult colon adenocarcinoma. They express cylindrical polarised morphology, tight junctions between adjacent cells and express hydrolase enzymes (Sambuy et al., 2005). The cells were grown in RPMI-1640 medium (Biosera.com.com) supplemented with FBS (10%), penicillin (100 units/mL), streptomycin (100µg/mL) and L-glutamine (2mM).

### 2.2.3 Drug Dilution

Drug candidates, including Cisplatin and Chlorpromazine, were prepared as concentration stocks in DMSO at **3.33 mM**

The following concentrations were prepared from the stock and stored at 4 °C; **100µM, 50µM, 25µM, 12.5µM, 6.25µM, 3.125µM**

The diluted concentrations were prepared using complete cell culture media into 1.5mL aliquots.

### 2.2.4 MTT Assay

MTT assays were performed for all synthesised compounds on all the cell lines which were grown, as described previously. As per the subculture protocol, cells were obtained and detached, ready to use. The pellet obtained was suspended in complete cell culture media (10mL) to obtain a homogeneous cell suspension. A volume of 10 µL was taken from the suspension mixture and the number of cells present within were counted on a C-Chip disposable haemocytometer slide (Neubauer improved grid). As a 96-well plate was being used for the assay, each well contained *ca.* 4000 cells per well, and was pipetted with 100 µL of the diluted cell suspension. The cell suspension was diluted to the required concentration dependant on the calculation of the number of cells present, coupled with the addition of fresh complete cell media. The diluted cell suspension (11mL), in a sterile reservoir, was pipetted using a multichannel pipette (100 µL per well) in to a flat-bottom treated 96-well plate. The plates were then stored to allow cell adherence in an incubator (37 °C, 5% CO<sub>2</sub>) for 24 h. The drug candidates in the diluted concentrations (100 µL) were then added onto the cells in each well of the 96-well plate in triplicate on duplicate plates, whereby the drug

concentration increased going down the plate. The plates were then incubated for specific time periods; 24 h, 48 h, 72 h and 96 h.

Following the incubation period, MTT solution (50  $\mu$ L; 3 mg/mL in PBS) was added to each well and the plate incubated for a further 3 h. The plate wells were then carefully aspirated to remove all the liquid, care being taken not to disrupt the cells or purple formazan crystals which had formed. DMSO (100  $\mu$ L per well) was added enabling the crystals to dissolve, whereby different shades of purple were observed, and the optical densities of the wells read on a spectrophotometer plate reader (Multiskan Ascent, Thermo LabSystems) at 540nm with 690nm set as a background reading. Data analysis on the collected readings allowed for mean values and the standard deviation to be calculated, thus enabling graphical plots to highlight dose response vs change in optical density to be plotted. The control sample, fresh cell culture media only, was normalised to 100 % cell growth. The obtained graphical plots allowed for the determination of the IC50 values (where 50 % of the cell growth was inhibited) for each drug candidate tested.

### 2.2.5 RNA isolation

#### **RNA Isolation and purification**

HepG2, HCT-116 and A549 cells were cultured and treated accordingly. Cells were harvested in 700 $\mu$ l TRIzol<sup>®</sup> reagent (Zymo Research #R2050-1-50) by scraping. These were either used immediately or stored at -80°C.

RNA isolation was conducted using the RNA Miniprep kit (Zymo Research #R2051). 100% ethyl ethanol was added to the TRIzol cell suspension at a ratio of 1:1 and mixed thoroughly. This suspension was added to the provided Zymo-spin IIC Column and centrifuged for 30 seconds at 13000g. All centrifugation occurred at 13000g for 30 seconds unless otherwise stated. The

cells were washed with 400µl of RNA wash buffer in the column and centrifuged. In order to remove DNA contamination, 5µl of DNase I was combined with 75µl DNA Digestion buffer to create a digestion enzyme buffer. This buffer was added onto the cells in the spin column and left at room temperature to incubate for 15 minutes.

After the digestion enzyme incubation, 400µl of RNA prewash was dispensed into the spin column and centrifuged. This stage was repeated to remove any enzyme traces. 700µl of the RNA washing buffer was then added into the spin column and centrifuged at 13000g until the wash buffer was completely removed from the spin column. To elute RNA, an Eppendorf tube free of RNA/DNA replaced the collection tube under the spin column and 35µl of RNase/DNase free water added into the spin column and centrifuged. The eluted RNA was re-added from the Eppendorf tube back into the spin column matrix and re-centrifuged to ensure optimal elution of RNA. RNA was stored at -80°C when not needed.

#### 2.2.5.1 RNA Quantification

The quality of the eluted RNA was analysed immediately as RNA degrades following multiple freeze/thaw cycles (Yu et al. 2017). A Nanophotometer (Implen P-class) was used to determine RNA concentration, A260/A280 and A260/A230 values. Pure RNA has an A260/A280 value of 2.0 where nucleic acids which are uncontaminated by phenols should show a ratio for A260/A280 of 1.8. The A260/A230 value is also used as a secondary measure for purity. This helps to determine the quantity of salt carryover. The A260/A230 value should read above 1.5, close to 2.0.

### 2.2.5.2 cDNA Synthesis

Isolated RNA was used to synthesise cDNA using the PCR Biosystems qPCR BIO cDNA Synthesis Kit (#PB30.11) (Table 1). The reaction conditions were followed according to manufacture guidelines: 42°C incubation for 30 minutes which was followed by 10 minutes incubation at 85°C to denature the RTase. The cDNA was stored at -20°C.

*Table 1 Reagents provided within the cDNA synthesis kit and the working volumes used. RTase was added prior to the addition of RNA as the RTase contains an RNase inhibitor within. The cDNA was created with a maximum RNA concentration of 200ng/μl.*

Reagent	20μl reaction
5 x cDNA synthesis mix	4.0μl
20x RTase	1.0μl
RNA	Xμl
PCR grade dH <sub>2</sub> O	Up to 20μl final volume

### 2.2.5.3 qRT-PCR

A 10μl reaction mixture was formed using 4μl of qPCR SyGreen HI-ROX Mix (PCR Biosystems #PB20.16), 1μl of 200ng/μl cDNA, 1μl 5μM F/R primer and 4μl of RNase/DNase free water. The primer sequence was determined using a primer bank (Harvard Med School (<https://pga.mgh.harvard.edu/primerbank/>)) which were optimised prior to their use.

The first cycle consisted of polymerase activation for 2 minutes at 95°C. This was followed with 40 repeated cycles of denaturation at 95°C for 5 seconds and primer annealing for 30 seconds (temperature dependant on primer). The Applied Biosystems SteponePlus Real-Time

PCR System was used for this purpose. The gradual heating of the PCR products produced a melt curve to determine dye dissociation from the dsDNA which would also confirm primer/dimer residue and specificity. The expression of genes was normalised using *human Gapdh* and  $\Delta\Delta Ct$  logged to calculate expression of genes for the compounds tested.

### Primer Optimisation

Primers were prepared at a final concentration of 5 $\mu$ M F/R in RNA/DNA free water from stock concentrations of 100 $\mu$ M. Reference human RNA was used to determine the optimal annealing temperature for the primers by conducting qPCR with the annealing temperatures for the primers set at 58°C, 59°C, 60°C, 61°C and 62°C. The oligonucleotide primers sets used for the amplification are shown below;

*Table 2 Primer sequences used for qRT-PCR.*

Gene ( <i>Human</i> )	Forward 5'	Reverse 5'	Annealing Temperature (°c)
GAPDH	AACCTGCCAAGTATGATGAC	ACCACCCTGTTGCTGTAG	58
PCNA	TTCCAGTCGGAAGTCTTGTGG	CCCGGATTAGGGCATGATTTCT	59
CDK4	ATGGCTACCTCTCGATATGAG	CATTGGGGACTCTCACACTCT	58
C			
CDK6	GCTGACCAGCAGTACGAATG	GCACACATCAAACAACCTGAC	60

## 2.3 Experimental – Pharmacological Assays

### 2.3.1 Plasma Stability Assay

One of the most challenging tasks in drug discovery is predicting the pharmacokinetic behaviour of a new chemical entity (NCE) in humans using data derived from *in vitro* model systems.

Conducted on over 200 top oral products a study revealed that an estimated 37% of drugs had very low solubilities, some less than 0.1mg/mL. The issue of poor solubility is one of the most important and common problems faced by scientists during the drug development phase. However, properties which give rise to these undesirable characteristics such as poor aqueous solubility, chemical instability, low half-life, toxicity and fast metabolism can be solved, and require the use of the prodrug approach. These are pharmacologically inactive compounds which can be readily converted *in vivo* to the active form, either enzymatically or nonenzymatically in order to exert their therapeutic effect. The term stability refers to the capacity of the drug to remain unchanged throughout time, and the effects can be studied under various environmental conditions such as light, temperature and chemical environment. The definition given by Skopp et al (2004) is, “capability of a sample material to retain the initial value of a measured quantity for a defined period within specific limits when stored under defined conditions.” Or “the chemical stability of an analyte in a given matrix under specific conditions for a given time interval.” (Shah et al, 1992). However, in pharmaceutical principles, stability looks at the storage time allowed before any degradation, which can be expressed scientifically as shelf life. In addition, Stability can be determined

through the continuous monitoring of the concentration of the analyte, be it in a stored solution or biological sample.

Von rauch et al (2004) mention that during the initial drug discovery stage, when a potential drug candidate is screened against any biological targets, the compounds in question need to display sufficient stability in the assay buffers for enzyme, receptor or even cell-based assays in order to reliably measure any form of biological activity. Plasma stability has been known to play an important role in the drug discovery and development phase, since it has been highlighted that rapid metabolism will lower the exposure a drug exhibits at the therapeutic targets, and combined with the instability of a compound, difficulties in obtaining accurate *in vitro* studies increases since such molecules continue to degrade even after samples have been evaluated. Within the human body, there are various ways a drug is broken down, and the metabolism of a drug or metabolite can occur in blood cells or within the fluid composites of blood itself, such as serum or plasma. Plasma is the largest part of blood, since it makes up more than half (~55%) of its content. Separated from blood as a light-yellow liquid, it mainly contains function water (~90%), salts and enzymes. Antibodies, clotting factors in addition to other biological matter such as nutrients, hormones and proteins (albumin and fibrinogen) are circulated too. Other components which can be easily carried or transported are drug metabolites, either in their pure, active or inactive forms. The process of metabolism, whereby the compound is broken down, can be referred to as metabolic instability, which is unique to the biological matrices, chemical instability due to the inherent properties of a compound such as oxidation, hydrolysis or isomerization. It has been studied that compounds with specific functional groups are more susceptible to these metabolic reactions than others. The main groups are the following esters, amides, lactones, lactams, carbamides,

sulphonamides, and these are more favourable targets for plasma enzymes such as hydrolases and esterase.

Since these functional groups are contained within the class derivatives synthesised, the plasma stability assay will investigate the effects of this and calculate the percentage of test compound remaining over how much has been degraded.

For each compound, from a stock solution (1mM) in DMSO (5 mL), 10 $\mu$ L of stock (1mM) was dissolved in 990  $\mu$ L of MeOH. This provided a final working standard of 1 $\mu$ M. Stock solutions were then stored at -20 °C. Human plasma (Sigma Aldrich), stored at -20 °C, was allowed to thaw at RT, before being centrifuged (12000rpm, 7 min) to remove any debris. Phosphate buffer (pH 7.4, 100 mL) was formulated by adding Na<sub>2</sub>HPO<sub>4</sub>·7H<sub>2</sub>O (2.02 g) to NaH<sub>2</sub>PO<sub>4</sub>·H<sub>2</sub>O (0.33 g) in a container with distilled water (80 mL). The pH of the solution was then adjusted using HCl or NaOH before being topped up with distilled water to a final volume of 100 mL. Eppendorf tubes (7 x 3 sets, 2mL) were labelled accordingly with the time intervals and placed in the fridge (4 °C) until use. The concentrations of plasma (50% and 100%) were made up using the phosphate buffer (pH 7.4). The conditions were as follows; Control (50  $\mu$ L of phosphate buffer), 50% plasma (25  $\mu$ L of phosphate buffer and 25  $\mu$ L of plasma) and 100% plasma (50  $\mu$ L of plasma). Time intervals (mins) were set as 0, 5, 15, 30, 45, 60 and 120

A total of 84 tubes for one compound were made and Rifampicin was used as a control drug.

Each compound (1  $\mu$ L) was added to each tube and mixed gently but firmly. The tubes were then placed in an incubation water bath at 37 °C for the time intervals mentioned above. Ice cold methanol (250  $\mu$ L) was added to each tube at the appropriate time interval to cease the activity of the reaction. The collected tubes were placed in a micro centrifuge (14000rpm, 20 min) and the supernatant removed, using a pipette, into new tubes, which were labelled

appropriately. The samples were stored at -80 °C until further use and analysed via HPLC to detect the change in concentration. This was then plotted as Percentage test compound remaining vs time to observed compound degradation.

The study was conducted in triplicate.

### 2.3.2 Liver S9 Fraction Stability Assay

Plenty of *in vitro* studies predominantly work on focussing their attention towards using compounds such as hepatocytes or specific subcellular hepatic fractions like S9 as in study reagents. More commonly these useful *in vitro* models are being used as a means of hepatic clearance as they contain many and various drug metabolising enzymes. One was mentioned above, the S9 fraction, with the other vital one being microsomes. These products of organ tissue homogenates are widely used in many biological assays thus the incubation of potential drug candidates with the addition of the S9 fraction can aid to help understand the metabolic fate of the compound in question or testing. This further provides a major advantage to using S9 fractions, which is a crude cell preparation, as in addition to containing a variety of Phase I and Phase II metabolising enzymes, the subcellular fractions are also sufficiently easy to prepare, use and store, for long periods of time, enabling cost efficiencies over whole cell models. Adding onto the advantages mentioned, the final point is that the subcellular fractions are said to be easily adaptable to high throughput screens, which then enables a huge number of compounds to be screened, at a rapid pace and inexpensive cost.

An important factor is that they contain both cytosolic enzymes like sulfotransferases, aldehyde oxidase and membrane-bound enzymes such as CYP450 (Varkhede et al, 2014). The cytosol part contains transferases, which are Phase II enzymes. The function of these is to transfer a functional group such as Hydroxyl or amine from one molecule to another. The

microsomes part contain the Cytochrome P450, which is a Phase I metabolite. These are a group of hemoproteins, which are involved in drug metabolism itself, accounting for approximately  $\frac{3}{4}$  of the total metabolism. The function is conducted when the heme group conducts oxidation on the substrates present. This is done by using protons derived for the NADH or NADPH substances, which act as co-factors to the S9, to split the oxygen present so that a single atom can be added to the substrate of the enzymes. Many drugs currently on the market today undergo their biotransformation via oxidations (Ogu & Maxa, 2000).

Subcellular fractions are mostly conducted using animals in order to estimate the risk of specific compounds causing cancer in humans, with the most common species used being *Rattus norvegicus* (Rat) and *Mus musculus* (Mouse). Prival and Mitchell, 1982, Lijinsky and Andrews, 1983, Nohmi et al., 1983 and Lin et al., 1985 all mention that the usage of these subcellular fractions, combined with or without enzymes, are considered very useful in the screening of mutagens from the viewpoints of their susceptibility to promutagens. This is further agreed by Maron and Ames (1983), Mortelmans and Zeiger (2000) who add that the effectiveness of the S9 fractions are because they effectively bioactivate the promutagens into mutagens, thus enabling them to be sufficiently good in mutagenicity screening test systems.

The S9 incubation assay helps to provide an understanding for the metabolism of compounds, in turn helping to predict pharmacological data such as *in vitro* intrinsic clearance, the intrinsic capability of the eliminating organ to remove the free drug from the body (Cl<sub>int</sub>). Furthermore, calculation could be made to determine the half-life of the compounds testing, with a view to see how the body eliminates such substances and how often. Like the plasma stability, RMP was used as an internal control, and all work was carried out in triplicate.

However, since a known compound which is unstable within these conditions was not used as a positive control, the data is presented within a preliminary stage of the study.

S9 fraction was obtained from the storage condition (-20 °C) and allowed to thaw carefully at RT. 1 mL of the stock S9 Fraction (20mg/mL) was removed carefully and placed into a new tube, with the stock returned to storage immediately. Warm Phosphate buffer (37 °C, pH 7.4, 18 mL) was added to the tube containing the S9 fraction and placed into an incubator (37 °C), with the standard working volume now at 1mg/mL. In a separate tube, NADPH (50mM) was prepared in phosphate buffer (2 mL, 7.4 pH).

Once again, Rifampicin was used as a control drug, and each compound had a total of 36 tubes prepared. Tubes were prepared as control (500 µL of phosphate buffer at 7.4 pH) and Treated (500 µL of freshly prepared S9 Fraction). The metabolic activity was studied at time intervals (min); 0, 5, 15, 30 and 45 at 37 °C.

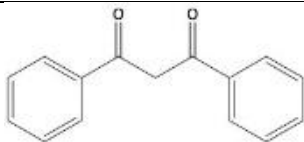
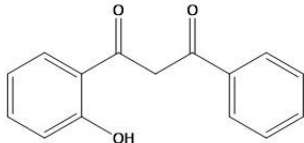
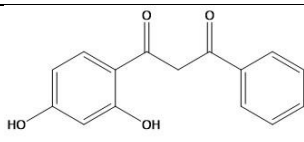
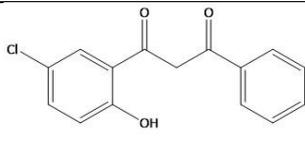
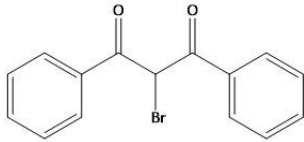
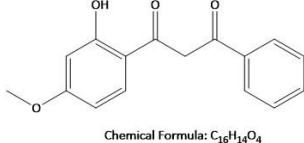
Each compound (1 µL) was added to each tube and mixed gently but firmly. 10 µL of the NADPH stock was added immediately and the tubes were then placed in an incubation water bath at 37 °C for the time intervals mentioned above. Ice cold methanol (750 µL) was added to each tube at the appropriate time interval to cease the activity of the reaction. In high-throughput stability assay for enzymatic reactions within biological matrices such as microsomes or plasma, organic solvents such as MeOH or ACN are readily used to stop the reaction by allowing the denaturation of the proteins (Di Li et al, 2003,2004). The collected tubes were placed in a micro centrifuge (14000rpm, 20 min) and the supernatant removed, using a pipette, into new tubes, which were labelled appropriately. The samples were stored at -80 °C until further use and analysed via HPLC to detect the change in concentration. A plot

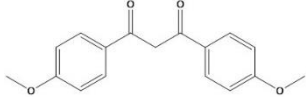
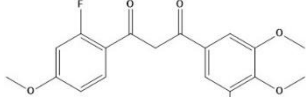
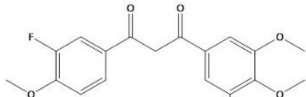
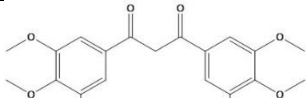
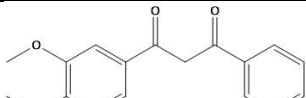
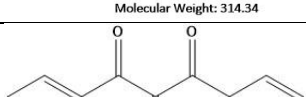
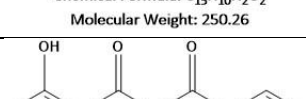
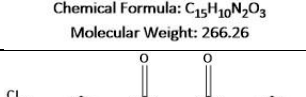
of Percentage compound remaining vs time was then analysed to calculate pharmacological values such as half-life ( $t_{1/2}$ ) and Intrinsic Clearance ( $Cl_{int}$ ).

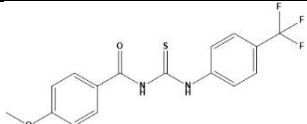
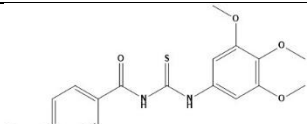
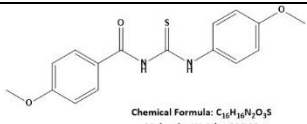
## 3 Results & Discussion

### 3.1 Synthesis of compounds and analogues

Table 3 Table shows the synthesised compounds as mentioned in the methods section 2.1.3, 2.1.4 & 2.1.5, including all  $\beta$ -Diketone, 2-Azido and Benzoylurea derivatives

Compound	Name	Structure
DBM	1,3-diphenylpropane-1,3-dione	 <p>Chemical Formula: <math>C_{15}H_{12}O_2</math> Molecular Weight: 224.26</p>
1	1-(2-hydroxyphenyl)-3-phenylpropane-1,3-dione	 <p>Chemical Formula: <math>C_{15}H_{12}O_3</math> Molecular Weight: 240.26</p>
2	1-(2,4-dihydroxyphenyl)-3-phenylpropane-1,3-dione	 <p>Chemical Formula: <math>C_{15}H_{12}O_4</math> Molecular Weight: 256.26</p>
3	1-(5-chloro-2-hydroxyphenyl)-3-phenylpropane-1,3-dione	 <p>Chemical Formula: <math>C_{15}H_{11}ClO_3</math> Molecular Weight: 274.70</p>
4	2-bromo-1,3-diphenylpropane-1,3-dione	 <p>Chemical Formula: <math>C_{15}H_{11}BrO_2</math> Molecular Weight: 303.16</p>
5	1-(2-hydroxy-4-methoxyphenyl)-3-phenylpropane-1,3-dione	 <p>Chemical Formula: <math>C_{16}H_{14}O_4</math> Molecular Weight: 270.28</p>

6	1,3-bis(4-methoxyphenyl)propane-1,3-dione	 <p>Chemical Formula: <math>C_{17}H_{16}O_4</math> Molecular Weight: 284.31</p>
7	1-(3-(dimethoxydanyl)-4,5-dimethoxyphenyl)-3-(2-flouro-4-methoxyphenyl)propane-1,3-dione	 <p>Chemical Formula: <math>C_{19}H_{18}FO_5</math> Molecular Weight: 362.35</p>
8	1-(3-(dimethoxydanyl)-4,5-dimethoxyphenyl)-3-3-flouro-4-methoxyphenyl)propane-1,3-dione	 <p>Chemical Formula: <math>C_{19}H_{18}FO_5</math> Molecular Weight: 362.35</p>
9	1-(3-(dimethoxydanyl)-4,5-dimethoxyphenyl)-3-(3,4,5-trimethoxyphenyl)propane-1,3-dione	 <p>Chemical Formula: <math>C_{21}H_{24}O_6</math> Molecular Weight: 404.42</p>
10	1-(phenyl-3-(3,4,5-trimethoxyphenyl)propane-1,3-dione	 <p>Chemical Formula: <math>C_{18}H_{18}O_5</math> Molecular Weight: 314.34</p>
11	2-Azido-1,3-diphenylpropane-1,3-dione	 <p>Chemical Formula: <math>C_{15}H_{10}N_2O_2</math> Molecular Weight: 250.26</p>
12	2-Azido-1-(2-hydroxyphenyl)-3-phenylpropane-1,3-dione	 <p>Chemical Formula: <math>C_{15}H_{10}N_2O_3</math> Molecular Weight: 266.26</p>
13	2-Azido-1-(5-chloro-2-hydroxyphenyl)-3-phenylpropane-1,3-dione	 <p>Chemical Formula: <math>C_{15}H_9ClN_2O_3</math> Molecular Weight: 300.70</p>

14	4-methoxy- <i>N</i> -((4-(trifluoromethyl)phenyl)carbamoithioyl)benzamide	 <p>Chemical Formula: C<sub>16</sub>H<sub>13</sub>F<sub>3</sub>N<sub>2</sub>O<sub>5</sub> Molecular Weight: 354.35</p>
15	4-methoxy- <i>N</i> -((3,4,5-trimethoxyphenyl)carbamoithioyl)benzamide	 <p>Chemical Formula: C<sub>18</sub>H<sub>20</sub>N<sub>2</sub>O<sub>8</sub> Molecular Weight: 376.43</p>
16	4-methoxy- <i>N</i> -((4-methoxyphenyl)carbamoithioyl)benzamide	 <p>Chemical Formula: C<sub>18</sub>H<sub>18</sub>N<sub>2</sub>O<sub>5</sub> Molecular Weight: 316.38</p>

### 3.1.1 Dibenzoylmethane

Dibenzoylmethane (DBM), (C<sub>6</sub>H<sub>5</sub>C(O))<sub>2</sub>CH<sub>2</sub>, is an organic compound and subsists as a 1,3-diketone, but the compound occurs primarily as the enol tautomer (Figure 30) (Thomas, Florence and Wilson, 2009). The interconversion concerning the diketones and the two corresponding enols is so swift that the difference is generally overlooked. DBM has the presence of a white solid, and the derivatives such as avobenzone have established applications such as sunscreen products (Zawadiak and Mrzyczek, 2010).

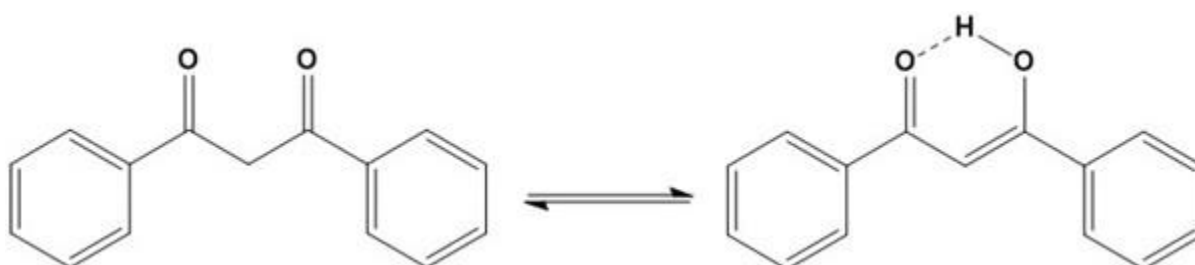


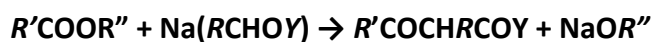
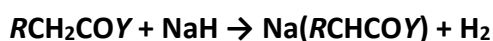
Figure 30 The equilibrium balance formed between the Keto and Enol Tautomer during rapid excitation

DBM is a natural phytochemical established as a minor component in the root extract of liquorice. DBM has shown to avert the formation of DNA-adducts encouraged by carcinogens in both *vivo* and *vitro* studies. DBM prompt apoptosis in human prostate and colon cancer cells, and cause cycle arrest in prostate cancer cells (Weng et al., 2009).

### 3.1.2 $\beta$ -Diketones and Synthesis

Over the past decade there have been several publications outlining the various techniques for the synthesis of  $\beta$ -diketones and their derivatives. There are some publications that mention a facile route to produce  $\beta$ -diketones as a precursor to targeted compounds like chalcones as well as some medicinal heterocyclic compounds (Sambaiah et al., 2017, Kel'in, 2003).

However, the most widespread and well-recognised procedure for the synthesis of  $\beta$ -diketones is one that involves Claisen acylation and carboethoxylation of ketones and esters in the presence of sodium hydride (Swamer & Hauser, 1950) (Scheme 1).



#### **Scheme 1: Claisen acylation and carboethoxylation of ketones (Swamer & Hauser, 1950)**

The technique is regulated by a typical Claisen method whereby an acyl group is bound to a ketone. The reaction in general is valid for 1,3-diketones, ketoaldehydes and ketoesters

having good yields (Swamer & Hauser, 1950, Sambaiah et al., 2017, Kel'in, 2003). Through intermolecular condensation, this technique produces good yield with methyl ketones and esters with the presence of metallic sodium. Modified procedures have been reported with the application of sodium methoxide and potassium *tert*-butoxide (Wai et al., 2000, Nandurkar et al., 2007)

The Claisen-condensation of ketones and esters is also an efficient way of obtaining aliphatic and aromatic  $\beta$ -diketones (Nadurkar et al., 2007). This is because of its flexibility and milder environments in the method, it is commercially adapted in the synthesis of 2,2,6,6-tetramethyl-3,5-heptanedione.

#### 3.1.2.1 Baker-Venkataraman Route

Baker-Venkataraman has been one of the most efficient mechanisms in place to make  $\beta$ -diketones and many classes of 'natural-product-like' compounds like flavones and chromones (Baker, 1933, Gomes et al., 2009, Lozano et al, 2012). This mechanism consumes *o*-benzoyloxyacetophenones undergoing base-catalysed intermolecular Claisen condensation of esters and ketones to generate *o*-hydroxydibenzoylmethanes (Ameen and Snape, 2015). This approach works well under microwave conditions as reported by Abdel Ghani and colleagues in 2008. With regards to the compounds synthesised in Procedure A, it has been suggested by Ares et al., (1993) to approach the methods using two ways. One of the variations to the method was suggested to be the addition of the hydroxyacetophenone and treat it with 2.2 equiv of potassium-*tert*-butoxide ( $\text{KO}^t\text{Bu}$ ).  $\text{KO}^t\text{Bu}$  is a strong base, which helps in the deprotonation of substrates and also the cyclization of compounds in order to form ring structures. The benzoyl chloride was then added, and after heating, the diketone was obtained. The second variation looks more closely and parallels the 5-methoxyflavone

synthesis. In this method, the hydroxyacetophenone was instead treated sequentially with 1.1 equiv of  $\text{KO}^t\text{Bu}$ , the benzoyl chloride, and then a second 1.1 equiv of  $\text{KO}^t\text{Bu}$ . After heating, the diketone was isolated.

A rapid method for the preparation of  $\beta$ -diketones is utilising a phenyl benzoate for dibenzoylation, which has been reported by Wallet and Gaydou (1996) as quite like the Baker-Venkataraman mechanism. This was acknowledged as fast and efficient because there is no heating procedure necessary throughout the process (Fig 31).

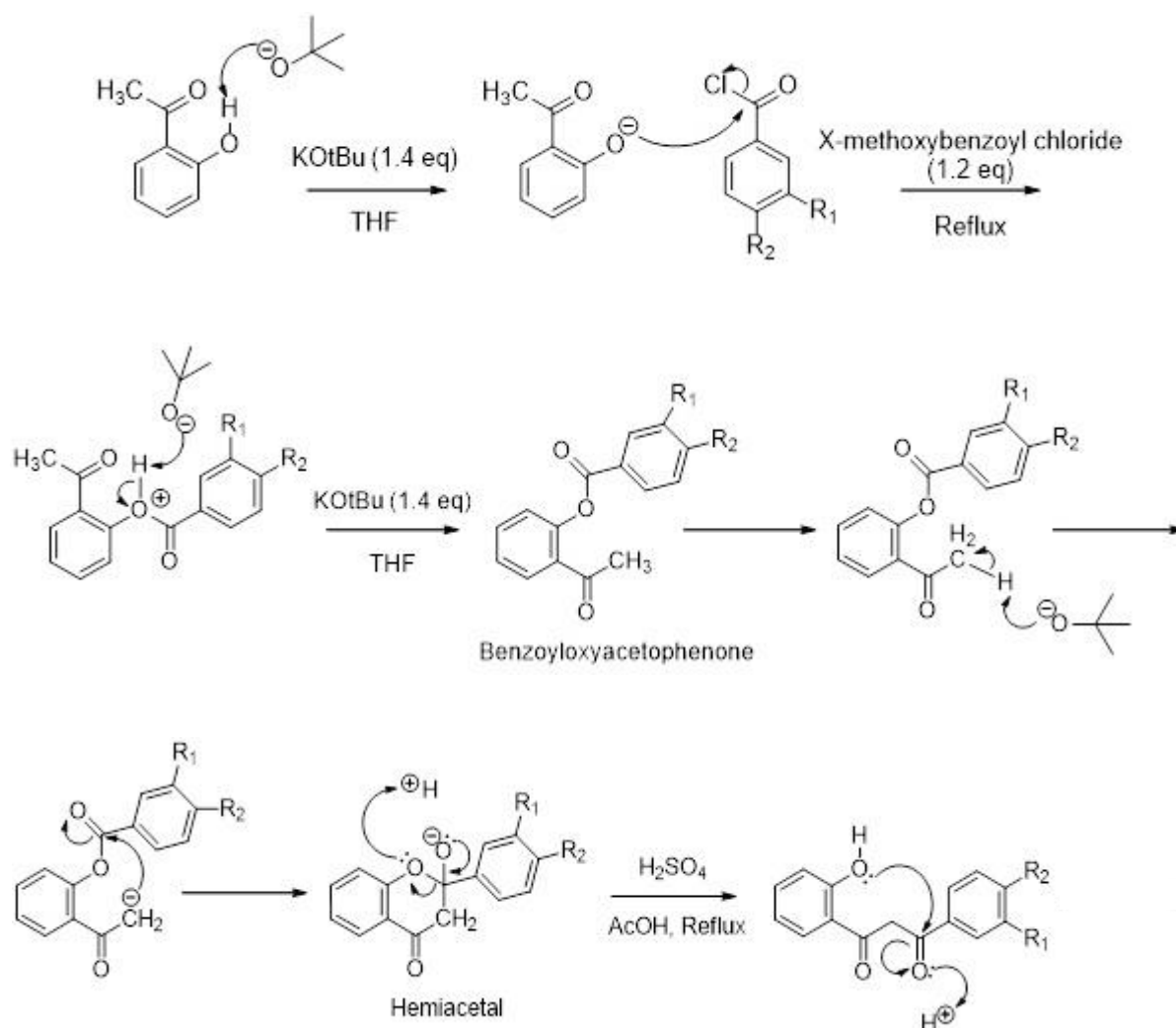


Figure 31 A modified mechanism of Baker-Venkataraman for the synthesis of  $\beta$ -diketones, highlighting ring closure

In Addition, substituted  $\beta$ -diketones (1-(2',4'-dihydroxy-5'-chlorophenyl) 3-aryl-propane-1,3-dione) have been produced by a speedy technique from acetophenones and aromatic acids to give the conforming benzoate, and with added dissolving in DMSO and sodium hydroxide followed by cooling in water (Sartape et al., 2015, Sheikh et al., 2009)

In 2005, Jae, Hwa and Mi developed a method carried out under argon starting with an acetophenone acid and a benzoyl cyanide as an alternative to an acyl chloride in the presence of lithium iso-propyl diamine (LDA) to produce the corresponding diketone with an excellent yield. The technique was also used to profit several  $\beta$ -diketone products with hydroxide, chloride and methoxy substitution (Salunkhe et al., 2015)

O-hydroxy by-products of  $\beta$ -diketone are also produced by refluxing O-hydroxyacetophenone with aroyl chlorides in acetone and dry potassium carbonate. Methoxy substituents containing O-hydroxyacetophenones are treated with similar constituents with potassium hydroxide or potassium carbonate dissolved in benzene in the existence of a phase transfer catalyst. The same reacting materials irradiate within the microwave (at 80°C) and in the presence of 2 equivalents of DBU heated for 16 hours yield  $\beta$ -diketones in sufficient amounts (Ghani et al., 2008)

A more efficient mechanism involves the development of the benzoate in pyridine starting from an acyl chloride. The product is then heated at 26°C for 2 hours with potassium hydroxide, to obtain the desired diketone in good yield (Bansal, 2017)

A parallel practise comprises of  $\beta$ -diketone in pyridine and crushed potassium hydroxide as a precursor to the synthesis of 3-benzoyl 6-methyl flavanone analogues (Haider & Haider, 2012). Despite this approach being simple and easy to formulate, the isolation of the compound from pyridine is a challenging task.

Additionally, Sambaiah and colleagues in 2017, reported the first aromatic nucleophilic ring opening and ring closure (ANRORC) reaction for the synthesis of 3-benzoyl chromone with benzamidines. The technique adapts numerous  $\beta$ -diketone derivatives as a facile method to produce 3-benzoyl-4H-chromen-4-one. The condensation of 2-methoxyacetophenone with 2-methoxymethyl benzoate in the presence of NaH, and the anhydride of 2-methoxy benzoic acid have reported to be ineffective in the synthesis of  $\beta$ -diketones (Jae et al., 2005, Blaskó, Xun & Cordell, 1988).

A different methodology was adopted in the effort to counter the complications in chemo-selective enolate formation of O- and C-acylated product of  $\beta$ -diketone. A series of bases and catalysts were used to investigate the efficacy of nitrogen heterocyclic carbene 'NHC-promoted (Fig 32) intermolecular aliphatic nucleophilic substitution reactions (Singh et al., 2011)

\*

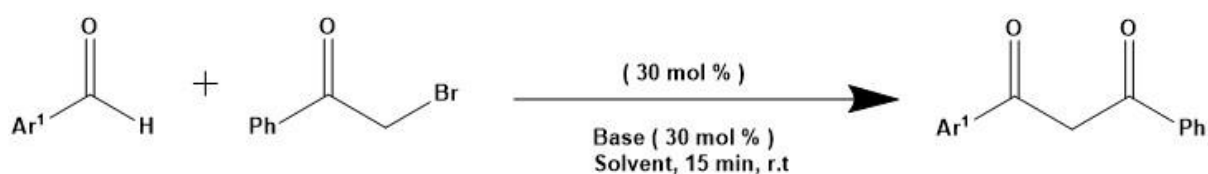


Figure 32 NHC stimulated synthesis of  $\beta$ -diketones (Singh et al., 2011).

Oxidation of hydroxyketones produces the conforming  $\beta$ -diketones (Barlett and Beaudry, 2011). Three oxidants have been studied; Dess-Martin-Periodinane (DMP), Swern oxidation and o-indoxybenzoic acid (IBX). The one to produce excellent yield was reported to be IBX compared to DMP and swern, accumulating poorer yield. Oxidation of alcohols to aldehydes

and ketones with IBX has proven to be effective despite its poor solubility (More and Finney, 2002).

An exceedingly regioselective and vastly yielding scheme gathering to about 98% for 1,3-diketones using microwave aided synthesis entails using enol ether of acetophenone and benzoyl halides or benzoyl cyanide. The reaction time of 20 minutes is heightened in comparison to the conventional methods which involve 24 hours for accomplishment with undesirable by-products (Wiles, Watts, Haswell & Pombo-villar, 2002) (Fig 33).

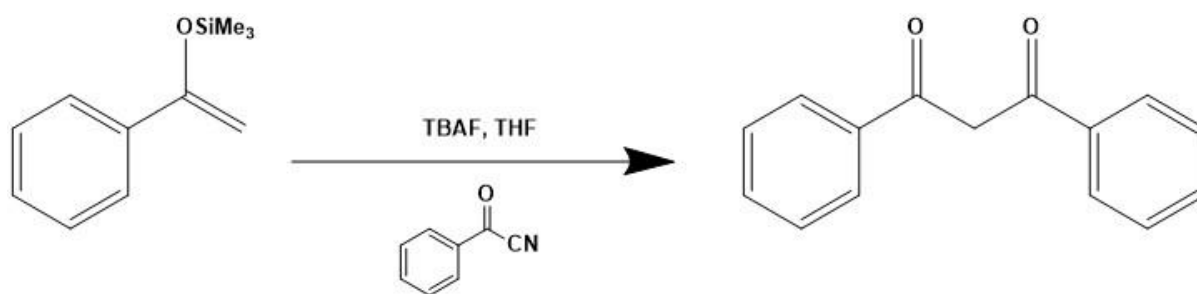


Figure 33 Microwave-assisted production of  $\beta$ -diketone with silyl enol ether (Wiles, Watts, Haswell & Pombo-villar, 2002)

### 3.1.3 $\beta$ -Diketones as scaffoldings for different targets

With the existing evolution in understanding the molecular foundation of cancer, attention has diverted to chemotherapy research, which aims to look at cancer through the diverse stages of its progression (Rayan et al., 2017). Over the past decades, different classes of compounds with diverse biological activity have been synthesised to inhibit cancer (Alam, 2018). Recently, non-synthetic agents have been extracted as potential chemotherapy agents.  $\beta$ -Diketone is one of the compounds known to have antibacterial, antiviral and antitumour properties (Sheikh, Ingle & Juneja, 2009).

A great quantity of  $\beta$ -diketone based compounds have been tested for cytotoxicity against tumour cells (Lin et al., 2011). Curcumin (*Curcuma longa* L) (Figure 34) is acknowledged as one of the most common naturally occurring compounds and possess different bioactive properties such as antioxidants (Nakano et al., 2004).

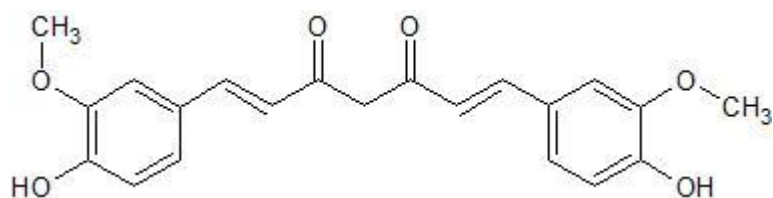


Figure 34 Naturally occurring  $\beta$ -Diketone, Curcumin, which has been tested for potential anti-cancerous activity

An analogue of Curcumin, 1,3-diphenyl propane-1,3-dione has been reported as anti-carcinogenic by conquering the growth of cells in various cell lines including COLO 205, A549, HL-60, RAW 264.7 and HeLa. Results of some studies have directed that the  $\beta$ -diketone, 1,3-propane-1,3-dione has a vastly potent activity and reduced the growth of mammary gland and uterine cells induced with 7,12-dimethylbenz[ $\alpha$ ]anthracene (DMBA) in mice (Miyata et al., 2001) (Sheikh et al., 2009).

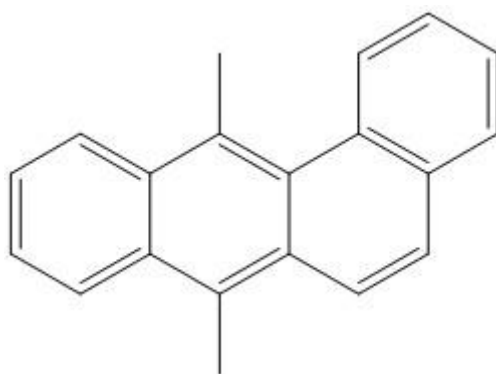


Figure 35 7,12-dimethylbenz[ $\alpha$ ]anthracene (DMBA)

### 3.1.4 Keto-Enol Tauterism

Due to their structural orientation, mainly the presence of the two carbonyl groups which are separated by a methylene group ( $\text{CH}_2$ ),  $\beta$ -Diketones have more than a few other interesting properties (Urbaniak et al 2011). One interesting property arises as ketones and other carbonyl compounds have the presence of a hydrogen located adjacent to the carbonyl group, which in turn leads to the creation of a state of an equilibrium with a constitutional isomer called an enol, an unstable isomer. This conversion due to the acidity of the  $\alpha$ -hydrogen on the carbonyl causes the phenomenon of a keto-enol interconversion or tautomerism, whereby two constitutional isomers are present in the equilibrium process. Distinguished mainly by the positioning and location of the double bond from the Alkene group combined with the different bonding location of the labile hydrogen atom, these continuous rapidly interconverted isomers are known as tautomers, either keto or enol. Although the above is a reversible reaction, the keto form is usually said to be dominant over the enol form as seen by acetone which is 99.9% a keto tautomer, once a stable equilibrium has been achieved, the concentrations of the contained ketone and enol can be measured. It has been researched through these reactions that even within one-sided equilibria, the evidence for the presence of the minor tautomer comes from the chemical behaviour of the compound.

When the parent keto form of a carbonyl containing organic molecule, such as a ketone or aldehyde, is converted into its enolic form, the process involves the transfer of a hydrogen atom or a proton from the  $\alpha$ -carbon of the carbonyl to the carbonyl oxygen functional group and is further accompanied by the saturation of the carbonyl double bond by an adjacent single bond. The conversion above can be catalysed one of two ways, either via an acid or a base whereby the traces are generally present in most samples, with most papers referring

to the keto-enol tautomeric equilibrium as an acid-base equilibrium. However, whether the catalysation is from an acid or base, a tautomerization process requires two main steps, protonation, and deprotonation, but the order of these step is dependent upon the conditions the reaction takes place in. The acid catalysed keto-enol tautomerism starts off by the initiation of the protonation of the carbonyl oxygen atom, which then in turn activates the  $\alpha$ -hydrogen/s. The result of the following steps results in one of the intermediates to lose one of the activated hydrogens thus yielding the enolic form of the compound. In comparison, the base catalysed keto-enol tautomerism however starts the equilibrium process with the deprotonation of the acidic  $\alpha$ -carbon to yield the enolate intermediate, which is then followed by the protonation of the carbonyl oxygen to again produce the enol form. As the enolate form is described as resonance stabilized, the carbonyl compound is stated to be usually a much stronger carbon acid than is the alkene. An illustrative example of this is said to be of acetone, whereby the pKa is around 40 units smaller than the given literature pKa value of ethane. For both reactions, in most cases, the second step is much slower than the first step.

It was previously mentioned above that the keto tautomer is much more dominant than the enol form, however Roger & Burdett (1965) say that owing to the presence of the less polar hydrogen atom which is located on the enol tautomer, this makes the mentioned form more favourable in inert solutions than the keto tautomer, which in contrast makes it much more dominant in polar solvents. Like the type of solvent used, there are many factors whereby which the balance of the equilibrium between a keto and enol form is affected. One major factor described by Cook et al., (2007) & Smith et al., (2016) which shifts the balance of equilibria between the tautomer's is said to be the potential substituents attached to the carbonyls and the shift is dependent on the nature of the substituting group. In addition, even though a carbonyl group is much more fundamentally stable than a converted enol group, the

presence of other functional groups, due to the rise of additional stabilization effects, can shift the balance of the equilibrium state from the much more dominant keto form to favour the enol form. A prime example of this concept coming to light is of Phenol, an aromatic organic compound consisting of a phenyl group to a hydroxy group, which is predominately much more stable than its corresponding keto tautomer, 2,4-cyclohexadienone, due to the basis of its aromaticity. The same concept has been found to be true for Dibenzoylmethane, which has been mentioned to exist exclusively in an enol form, which is chelated by an intramolecular hydrogen bond. Furthermore, other factors found to shift the balance of equilibria in research from the keto form to the enol form, or vice versa include electron withdrawing/donating groups, steric effects and temperature. Another important factor mentioned is due to a natural/physical property rather than chemical. As a rapid interconversion shifts the balance continuously, the tautomeric equilibria in the excited state of a compound can be very different than those which exist simultaneously within the ground state. Furthermore, in many cases which have been researched, it has been possible to induce an isomerisation between two existing tautomeric forms by light. Naumov and co-workers have recently applied the usage of time-resolved emission spectroscopy to highlight that the concept of photoexcitation can successfully induce the enolization of the given keto form of 6'-dihydroxyoxyluciferin. This is also in addition to the research conducted by Yankov et al., (2004), who have exclusively shown in their work that the keto form of Dibenzoylmethane, found to be relatively unstable in the ground state, is formed via the process of photoexcitation.

Even though the equilibria between a keto and enol form is rapid and can be measured through acid/base reactions, the effect can be identified in most of the NMR results and spectra, whereby the region of peaks at 190 ppm are attributed to the ketonic carbon, and

the peak at 175 ppm for the enolic carbon (Abdel Ghani., 2008). The following values are only for  $^{13}\text{C}$  NMR.

## 3.2 Biological Evaluation

The *in vitro* biological activity and pharmacological parameters of the synthesised compounds was assessed using a series of various assays. The first biological evaluation studied the cytotoxic ability of the drug candidates to determine growth inhibition of the cells using the MTT assay. Cisplatin, a chemotherapy medication used to treat several cancers, was used as a standard in order to enable the obtained data to be compared to that of an existing anti-cancer agent within literature. Following this, pharmacological parameters measuring the stability of the candidates, within different concentrations of Plasma and then S9 fraction over time were analysed using HPLC. Rifampicin, a semisynthetic macrocyclic antibiotic, was used as a standard control in order to determine data values such as % Compound remaining,  $t_{1/2}$  and  $CL_{int}$ . The pharmacological studies were conducted on a preliminary basis since a standard control was only used and no positive control compound, which was known to be unstable within the conditions tested.

### 3.2.1 Cytotoxicity – MTT Assay

The library of synthesised potential drug candidates was first screened using the MTT assay; with the anticancer activity of all the compounds of interest being tested on adherent *in vitro* cancer cell lines. The assay used allows for the determination of the half maximal inhibitory concentration (IC<sub>50</sub>), which effectively shows the required concentration of dose needed in order to inhibit the growth of cells by 50%. He and peers (2016) state that the determination

of the IC50 value is essential to understand the pharmacological and biological characteristics of a chemotherapeutic agent.

There are several assays available to determine cytotoxicity of available and newly formed compounds. First described by Mosmann in 1983, the usage throughout *in vitro* studies of the yellow tetrazolium salt, 3-[4,5-dimethyl-thiazol-2-yl]-2,5-diphenyltetrazolium bromide, or more commonly known as MTT, as an indicator for the viability of cells and their proliferation has increased. A traditional method for anti-cancer drug discovery and classical method for screening cytotoxic anti-cancer agents, the assay method is used widely to determine cytotoxicity, proliferation and activation of potential medicinal agents on the activity of mitochondrial dehydrogenase enzymes in cells (Scherliess, 2011). In addition, uses can also help evaluate cytotoxicity potential of drugs carried by liposomes (Angius and Floris, 2015). A liposome can be utilised as a multipurpose drug delivery vehicle for the administration of pharmaceutical drugs, whereby the system can undergo the process of alteration by either varying the size, lipid composition, electrical charge, membrane fluidity and finally the conjugation with surface-coating layers (Manconi et al, 2007). More specifically to cancer, it has been reported to be used to screen cytotoxic compounds during the development of chemotherapy or also to screen for unwanted cytotoxic effect during preclinical trials (Scherliess, 2011). The ease of the methodology, coupled with the speed at which results are obtained, makes MTT assays a useful operator-independent method for studying the number of cells (Lui, 2009). However, Hansen et al (1989) reports that since the formation of the test by Mosmann, it has been modified several times since.

MTT works on the principle that only viable cells have the ability to reduce a yellow aqueous solution, which is given by MTT, and convert it into Formazan, described as a dark purple-

violet colour, which is strongly lipophilic and water insoluble. This therefore can be detected colour metrically and the photometric assessment of the formazan concentration accounting for the number of viable cells (Van Meerloo et al, 2011). Fotakis and Timbell (2006) state 'Viable cells are able to reduce yellow MTT under tetrazolium ring cleavage to a...Formazan which precipitates in the cellular cytosol, whereas dead cells after damage, cannot transform MTT'. It was widely the concept that the amount of MTT formazan is directly proportional to the number of living cells (Van Meerloo et al, 2011), however according to Etxeberria et al (2011) this conclusion has now been seriously questioned.

Lui (2009) writes that the principle premise of the assay is the intrinsic ability of mitochondrial dehydrogenases and other reducing agents present in metabolically active cells to reduce the MTT compound. In addition, further research has provided biochemical evidence to indicate that MTT is mainly reduced in the cytoplasm of cells by NADH and other dehydrogenases associated to the endoplasmic reticulum (ER) (Berridge et al, 2005).

Even though the use of this assay is common, the technique does have several flaws to it. Lui (2009) states that the reduction of MTT may not be entirely dependent upon the number of cells but also upon the mitochondrial function and proliferation state. This means that the position of the cells within the wells of the plate at the time of testing may play a crucial role in the final reading results. An agglomeration of cells in certain positions of the well may show a lower number of cells counted than the actual number present. These may be positioned towards the upper end of the growth curve, where factors such as high cell densities and sub-optimal growth conditions would in turn hinder endogenous enzyme function. Further to this statement it says that since MTT values are attained from cells treated with drugs, then usually compared with results of those left untreated, it most likely will be the case that the

action of the drug studies maybe over-estimated. Normally another case for this is that fact that since the MTT assay is based on the reduction reaction of dyes resulting in colour changes, as the reduction is mediated enzymatically, other reduction substances still have the ability to interfere, as mentioned by Madesh and Balasubramanian (1998) where the effectors were stated to be Reactive Oxygen Species (ROS). In addition, research by Soenen and De Cuyper (2009) state other reduction process induced by liposomal preparations may affect the MTT assays. This was found by Angius and Floris (2015), where their study showed a direct interference of liposomes within the MTT assay, where observed cells treated with liposomes showed higher MTT absorbance values than the control used. In conclusion, Simms and Plattner (2009) concluded their study stating that the usage of the MTT assay was an inappropriate method for the means of testing the activity of drugs used for solid tumours.

### 3.2.2 Cytotoxicity – Cisplatin

Following on, Cisplatin was used as a basis for the comparison of the potential drug candidates, since the anti-cancer agent has been tested on various cell lines, which are mentioned in literature. IC50 values for the required cell lines were calculated as shown in Table 4 and then plotted as per Figure 36.

*Table 4 IC50 values calculated for Cisplatin. Cytotoxicity was observed on HepG2, HeLa, HCT-116, A549 and Caco-2 cell lines, with the standard deviation being calculated based on triplicate results*

Cell Line	IC50 [ $\mu$ M]			
	Cisplatin			
	24h	48h	72h	96h
<b>HepG2</b>	8.54 $\pm$ 1.54	7.26 $\pm$ 1.89	5.89 $\pm$ 2.42	5.37 $\pm$ 1.05
<b>HeLa</b>	7.72 $\pm$ 1.69	6.57 $\pm$ 1.96	5.71 $\pm$ 2.54	4.53 $\pm$ 2.47
<b>HCT-116</b>	10.30 $\pm$ 2.94	8.49 $\pm$ 1.89	6.64 $\pm$ 2.54	5.63 $\pm$ 1.65
<b>A549</b>	11.23 $\pm$ 1.54	9.11 $\pm$ 1.23	7.31 $\pm$ 1.28	6.04 $\pm$ 2.41
<b>Caco-2</b>	9.27 $\pm$ 2.39	7.97 $\pm$ 2.87	6.78 $\pm$ 2.69	5.75 $\pm$ 1.04

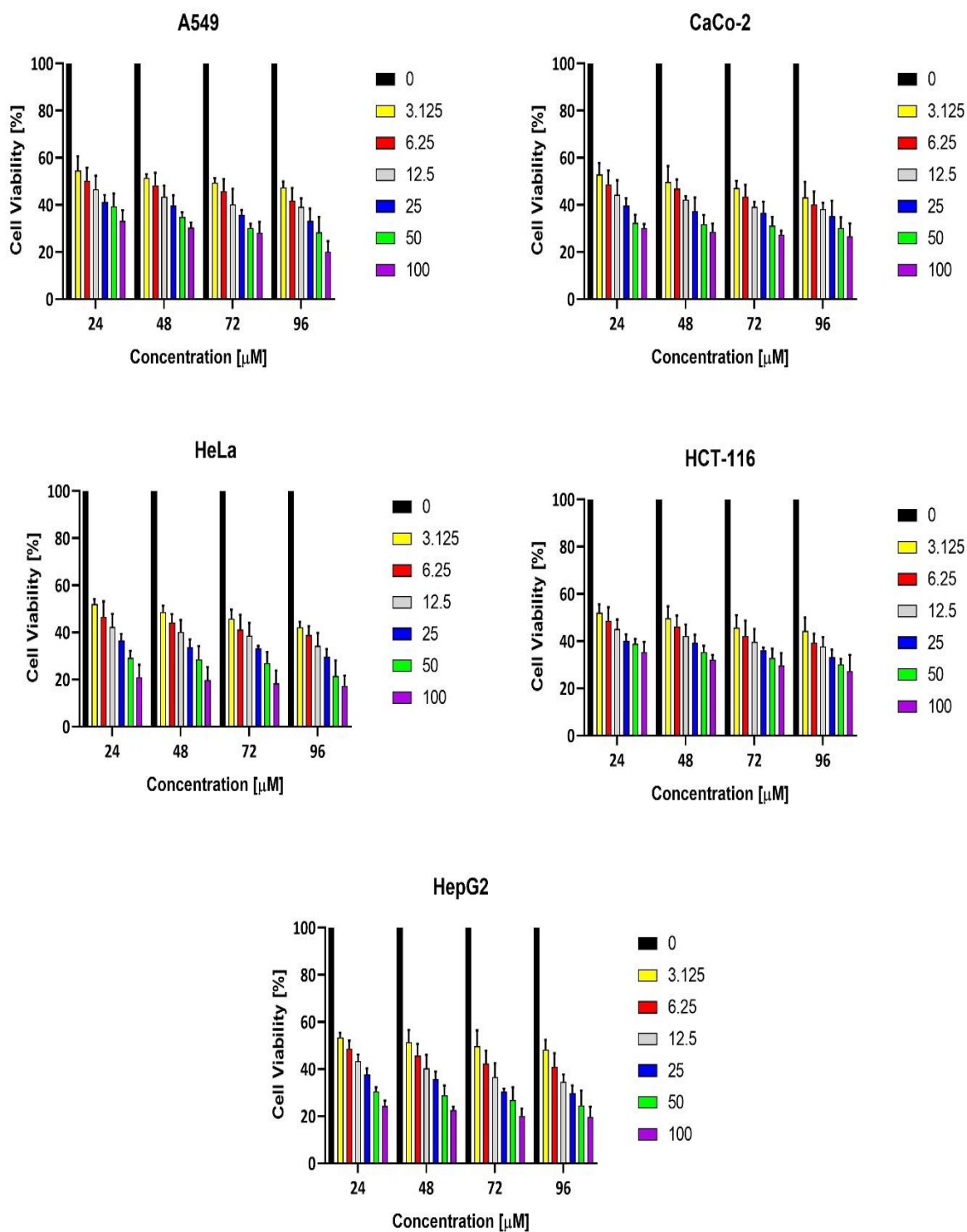


Figure 36 A graph showing the % Cell Viability of Cisplatin when tested on all 5 cells lines, which include HepG2, HeLa, HCT-116, A549 and Caco-2. Cells were incubated at periods of 24, 48, 72 and 96 hours, and dosed at concentrations; 100uM, 50uM, 25uM, 12.5uM, 6.25uM

### 3.2.3 Cytotoxicity - DBM and Derivatives (Compounds 1-10)

Tested in triplicates and over a period of 96 hours, the  $\beta$ -diketone derivatives showed an overall positive effect, in terms of cell death for all the cell lines which were used for screening. The general observation found was that as the incubation period increased, the average IC<sub>50</sub> values decreased, thus suggesting that as time progressed, cells which were treated were gradually destroyed.

Using the values from tables 5-7, a combined estimated average for the IC<sub>50</sub> values at the different incubation periods, 24h,48h,72h and 96h, could be calculated for all the  $\beta$ -diketone derivatives, and confirmed the theory that results obtained from the MTT assay were time dependant. As observed, the derivatives at the 24h incubation period for all cell lines had an average IC<sub>50</sub> value range from between 18.20 $\mu$ M to 27.81 $\mu$ M, whereby the range values decreased between 14.45 $\mu$ M – 21.27 $\mu$ M for the incubation period of 48hr. The IC<sub>50</sub> value range calculated for 72hr was 12.92 $\mu$ M – 19.09 $\mu$ M followed by 11.79 $\mu$ M – 19.00 $\mu$ M for 96hr, an apparent decrease over time. It has been known that a low IC<sub>50</sub> value is a positive characteristic of a potential drug candidate, whereby the low concentration threshold of the dose is seen a more potent.

Table 5 IC50 values of Beta-Diketone derivatives. Cytotoxicity was observed on HepG2 and HeLa cell lines, with the standard deviation being calculated based on triplicate results

Compound	IC50 [ $\mu$ M]							
	HepG2				HeLa			
	24h	48h	72h	96h	24h	48h	72h	96h
<b>DBM</b>	23.30 $\pm$ 1.89	16.22 $\pm$ 2.56	12.61 $\pm$ 1.02	11.76 $\pm$ 1.01	27.60 $\pm$ 1.89	22.63 $\pm$ 3.24	19.68 $\pm$ 2.46	18.45 $\pm$ 2.35
<b>1</b>	27.04 $\pm$ 2.54	18.49 $\pm$ 1.42	16.09 $\pm$ 0.23	14.54 $\pm$ 0.89	33.17 $\pm$ 2.84	18.31 $\pm$ 3.65	15.81 $\pm$ 3.89	14.90 $\pm$ 1.24
<b>2</b>	20.72 $\pm$ 1.57	12.47 $\pm$ 1.89	11.20 $\pm$ 1.28	10.46 $\pm$ 0.99	16.32 $\pm$ 1.82	11.23 $\pm$ 1.65	9.34 $\pm$ 2.69	9.12 $\pm$ 3.56
<b>3</b>	12.79 $\pm$ 1.09	11.28 $\pm$ 1.82	10.19 $\pm$ 1.68	8.99 $\pm$ 1.52	17.63 $\pm$ 0.78	15.94 $\pm$ 2.98	14.26 $\pm$ 1.45	12.49 $\pm$ 2.54
<b>4</b>	25.25 $\pm$ 3.65	22.88 $\pm$ 2.09	20.78 4.32	19.23 $\pm$ 1.47	18.25 $\pm$ 4.32	16.32 $\pm$ 3.05	14.61 $\pm$ 1.94	13.18 $\pm$ 4.32
<b>5</b>	25.13 $\pm$ 1.98	11.91 $\pm$ 2.65	10.03 $\pm$ 2.35	9.86 $\pm$ 1.36	10.04 $\pm$ 1.23	9.23 $\pm$ 1.56	8.44 $\pm$ 1.36	7.60 $\pm$ 1.23
<b>6</b>	28.2 $\pm$ 2.56	17.46 $\pm$ 3.65	14.00 $\pm$ 1.34	13.44 $\pm$ 3.89	17.13 $\pm$ 1.76	12.22 $\pm$ 1.49	12.45 $\pm$ 2.82	11.51 $\pm$ 4.23
<b>7</b>	11.13 $\pm$ 2.30	9.95 $\pm$ 1.12	8.56 $\pm$ 1.89	8.06 $\pm$ 2.49	16.33 $\pm$ 2.29	14.57 $\pm$ 1.60	12.94 $\pm$ 3.54	11.57 $\pm$ 2.35
<b>8</b>	13.12 $\pm$ 1.64	11.09 $\pm$ 1.93	9.80 $\pm$ 12.34	9.31 $\pm$ 2.19	15.81 $\pm$ 2.37	13.68 $\pm$ 1.14	12.48 $\pm$ 4.05	11.54 $\pm$ 1.45
<b>9</b>	26.01 $\pm$ 3.68	21.54 $\pm$ 2.61	19.48 $\pm$ 1.23	16.73 $\pm$ 1.25	13.06 $\pm$ 1.08	11.59 $\pm$ 2.59	10.31 $\pm$ 2.36	8.99 $\pm$ 1.67
<b>10</b>	21.78 $\pm$ 2.89	19.30 $\pm$ 1.51	17.60 $\pm$ 3.12	16.31 $\pm$ 2.14	14.86 $\pm$ 1.57	13.31 $\pm$ 2.45	11.89 $\pm$ 1.56	10.44 $\pm$ 2.54

Table 6 IC50 values of Beta-Diketone derivatives. Cytotoxicity was observed on A549 and HCT-116 cell lines, with the standard deviation being calculated based on triplicate results

Compound	IC50 [ $\mu$ M]							
	A549				HCT-116			
	24h	48h	72h	96h	24h	48h	72h	96h
<b>DBM</b>	24.44 $\pm$ 2.54	18.20 $\pm$ .56	14.55 $\pm$ 0.98	13.27 $\pm$ 1.87	18.28 $\pm$ 2.56	15.54 $\pm$ 3.24	13.77 $\pm$ 2.87	11.30 $\pm$ 2.45
<b>1</b>	24.75 $\pm$ 4.64	13.03 $\pm$ 4.87	11.42 $\pm$ 2.50	10.23 $\pm$ 1.26	16.92 $\pm$ 2.56	12.07 $\pm$ 4.25	10.36 $\pm$ 3.59	9.37 $\pm$ 2.57
<b>2</b>	21.21 $\pm$ 1.65	18.50 $\pm$ 1.56	15.37 $\pm$ 1.97	13.20 $\pm$ 2.89	24.19 $\pm$ 2.15	19.81 $\pm$ 2.58	17.79 $\pm$ 4.25	15.36 $\pm$ 3.81
<b>3</b>	28.09 $\pm$ 2.45	23.75 $\pm$ 1.57	21.65 $\pm$ 2.56	20.09 $\pm$ 1.89	11.67 $\pm$ 1.24	10.43 $\pm$ 2.56	8.82 $\pm$ 4.23	8.78 $\pm$ 2.18
<b>4</b>	24.78 $\pm$ 3.65	23.54 $\pm$ 3.12	21.05 $\pm$ 2.81	19.53 $\pm$ 1.89	19.01 $\pm$ 2.54	16.20 $\pm$ 3.02	14.55 $\pm$ 3.58	15.25 $\pm$ 3.41
<b>5</b>	28.20 $\pm$ 2.14	16.10 $\pm$ 1.84	14.64 $\pm$ 3.25	13.92 $\pm$ 3.68	25.04 $\pm$ 3.15	18.42 $\pm$ 3.18	16.81 $\pm$ 1.58	18.43 $\pm$ 2.45
<b>6</b>	17.28 $\pm$ 1.89	13.58 $\pm$ 1.36	12.66 $\pm$ 2.54	11.90 $\pm$ 2.10	24.11 $\pm$ 3.65	19.89 $\pm$ 4.85	17.38 $\pm$ 4.21	14.94 $\pm$ 3.54
<b>7</b>	25.31 $\pm$ 2.57	21.72 $\pm$ 1.98	19.76 $\pm$ 2.36	18.76 $\pm$ 5.41	48.17 $\pm$ 3.84	44.63 $\pm$ 2.41	39.63 $\pm$ 4.36	35.49 $\pm$ 1.28
<b>8</b>	16.36 $\pm$ 2.67	13.99 $\pm$ 2.34	12.58 $\pm$ 1.26	11.79 $\pm$ 3.45	48.50 $\pm$ 2.57	42.74 $\pm$ 3.14	39.93 $\pm$ 1.59	34.02 $\pm$ 2.14
<b>9</b>	28.06 $\pm$ 1.89	17.67 $\pm$ 1.59	14.83 $\pm$ 2.14	14.27 $\pm$ 2.36	40.78 $\pm$ 3.56	17.29 $\pm$ 2.48	15.88 $\pm$ 3.15	28.07 $\pm$ 4.56
<b>10</b>	28.10 $\pm$ 1.59	18.57 $\pm$ 1.12	16.77 $\pm$ 2.15	15.41 $\pm$ 1.75	29.27 $\pm$ 3.15	17.05 $\pm$ 2.18	15.08 $\pm$ 3.69	18.00 $\pm$ 4.20

Table 7 IC50 values of Beta-Diketone derivatives. Cytotoxicity was observed on the Caco-2 cell line, with the standard deviation being calculated based on triplicate results

Compound	IC50 [ $\mu\text{M}$ ]			
	Caco-2			
	24h	48h	72h	96h
<b>DBM</b>	25.72 $\pm 1.35$	22.02 $\pm 2.45$	18.53 $\pm 3.56$	15.76 $\pm 2.51$
<b>1</b>	16.52 $\pm 1.57$	14.58 $\pm 1.96$	13.08 $\pm 1.17$	11.11 $\pm 1.56$
<b>2</b>	20.37 $\pm 2.56$	17.27 $\pm 2.78$	15.30 $\pm 3.26$	12.88 $\pm 3.45$
<b>3</b>	19.25 $\pm 2.65$	17.23 $\pm 1.48$	16.84 $\pm 1.96$	15.16 $\pm 1.14$
<b>4</b>	14.6 $\pm 1.89$	13.14 $\pm 3.65$	11.74 $\pm 4.25$	10.98 $\pm 4.87$
<b>5</b>	17.23 $\pm 1.98$	15.22 $\pm 2.65$	15.10 $\pm 2.45$	14.95 $\pm 1.87$
<b>6</b>	18.90 $\pm 1.56$	17.62 $\pm 1.33$	16.32 $\pm 1.94$	15.23 $\pm 1.47$
<b>7</b>	23.60 $\pm 2.00$	21.14 $\pm 2.56$	20.74 $\pm 2.41$	18.98 $\pm 1.63$
<b>8</b>	22.90 $\pm 1.82$	21.01 $\pm 2.45$	20.54 $\pm 3.25$	18.29 $\pm 1.89$
<b>9</b>	25.64 $\pm 1.36$	23.31 $\pm 2.45$	21.67 $\pm 1.58$	19.60 $\pm 3.02$
<b>10</b>	24.60 $\pm 1.89$	22.34 $\pm 1.77$	20.37 $\pm 1.14$	19.28 $\pm 1.99$

Using the graphical plots for Log Concentration vs Cell viability, calculated IC<sub>50</sub> values highlighted that no  $\beta$ -diketone derivative was more effective than Cisplatin on any of the cell lines. It was noted however that the candidates which were screened did show positive potency effect on some cell line better than others. To start off with, DBM, which is commonly used in sunscreen and was used as an initial starting sub-structure for the derivatives displayed a steady response to all cell lines. It was seen that after the 24hr period, the effect of DBM in terms of IC<sub>50</sub> values shows a significant drop, which positively indicates a cytotoxic effect overall. Across all cell lines, the compound displayed a drop of around 10 $\mu$ M in terms of concentration for given IC<sub>50</sub> values. This can be seen on the HepG2 cell line where the IC<sub>50</sub> value for the 24hr incubation period of the cells studied was 23.30 $\mu$ M but dropped to 11.76 $\mu$ M at 96h, the same being seen for A549 and HCT-116, where the decrease was from 24.44 $\mu$ M to 13.27 $\mu$ M and 18.28 $\mu$ M to 11.30 $\mu$ M respectively.

When DBM was altered in order to provide the compounds 1 & 2, which contain extra Hydroxyl (-OH) groups at different aromatic positions, a difference in cell viability and IC<sub>50</sub> values was displayed across the cell lines. As before, IC<sub>50</sub> values after the 24-hour incubation period show a substantial response in terms of decrease, as exhibited by compound 1 on the HepG2, HeLa and A549 cell lines. Values from Table 5 show that at the 24hr incubation phase, the IC<sub>50</sub> values were 27.04 $\mu$ M, 33.17 $\mu$ M and 24.75 $\mu$ M, all higher than that of DBM. However, as the gradual treatment of the cells progressed over time, the values calculated at time 96hr were 14.54 $\mu$ M, 14.90 $\mu$ M and 10.23 $\mu$ M. An important thing to note in this finding is that bar one, all the IC<sub>50</sub> values of compound 1 after 96hr were found to be lower than that of DBM, thus suggesting that initially there may be a scope for delayed activity but the overall potency of the compound candidate is much greater over time. The same concept in terms of findings can be stated for compound 2, however once observed closely on individual cell lines, data

values indicate a proximity between the IC50 values at 72hr and 96hr for the HepG2 and HeLa cell lines. It seems like a plateau has been reached and no further cytotoxic effect will take place without a strong increase in dose concentration. The values which show this are as follows; HeLa - 9.34 $\mu$ M & 9.12 $\mu$ M, HepG2 – 11.20 $\mu$ M & 10.46 $\mu$ M.

Graphs showing the concentration vs cell viability at different time points across the cell lines can be seen in Figure 37-39 for DBM and compounds 1&2. As stated previously, as increase in cytotoxicity over time was observed.

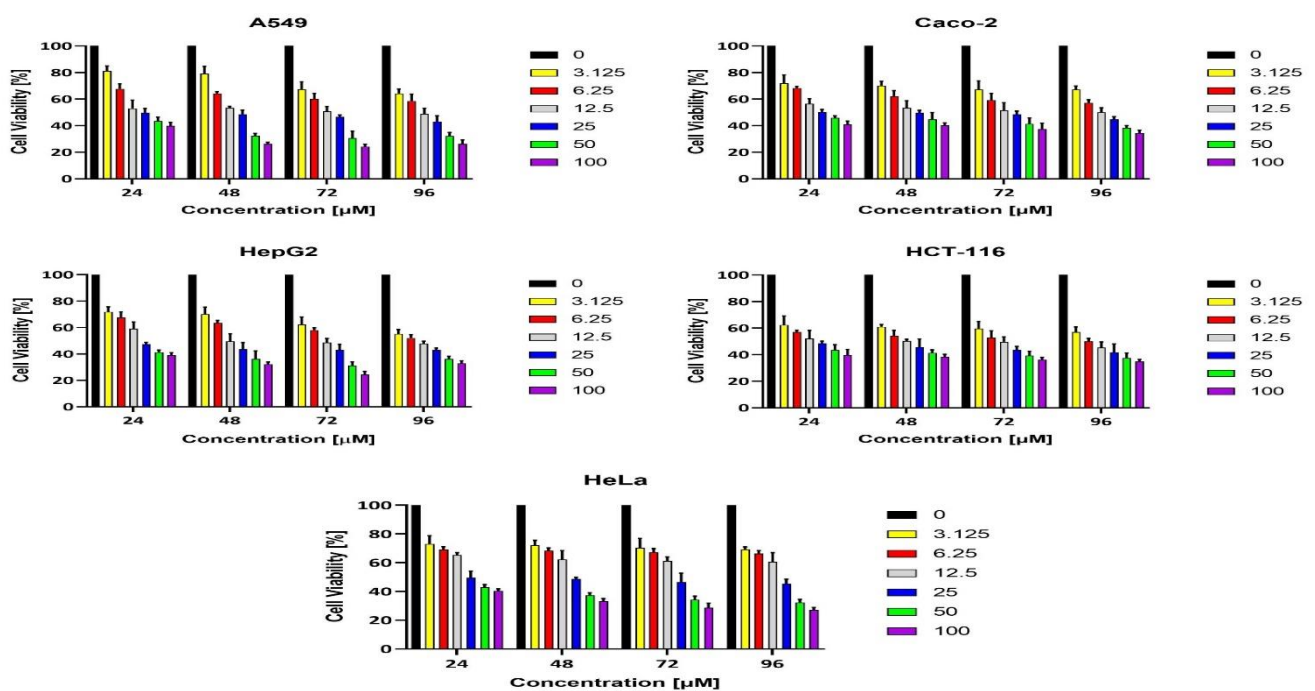


Figure 37 A graph showing the % Cell Viability of DBM when tested on all 5 cells lines, which include HepG2, HeLa, HCT-116, A549 and Caco-2. Cells were incubated at periods of 24, 48, 72 and 96 hours, and dosed at concentrations; 100 $\mu$ M, 50 $\mu$ M, 25 $\mu$ M, 12.5 $\mu$ M, 6.25 $\mu$ M and 3.125 $\mu$ M

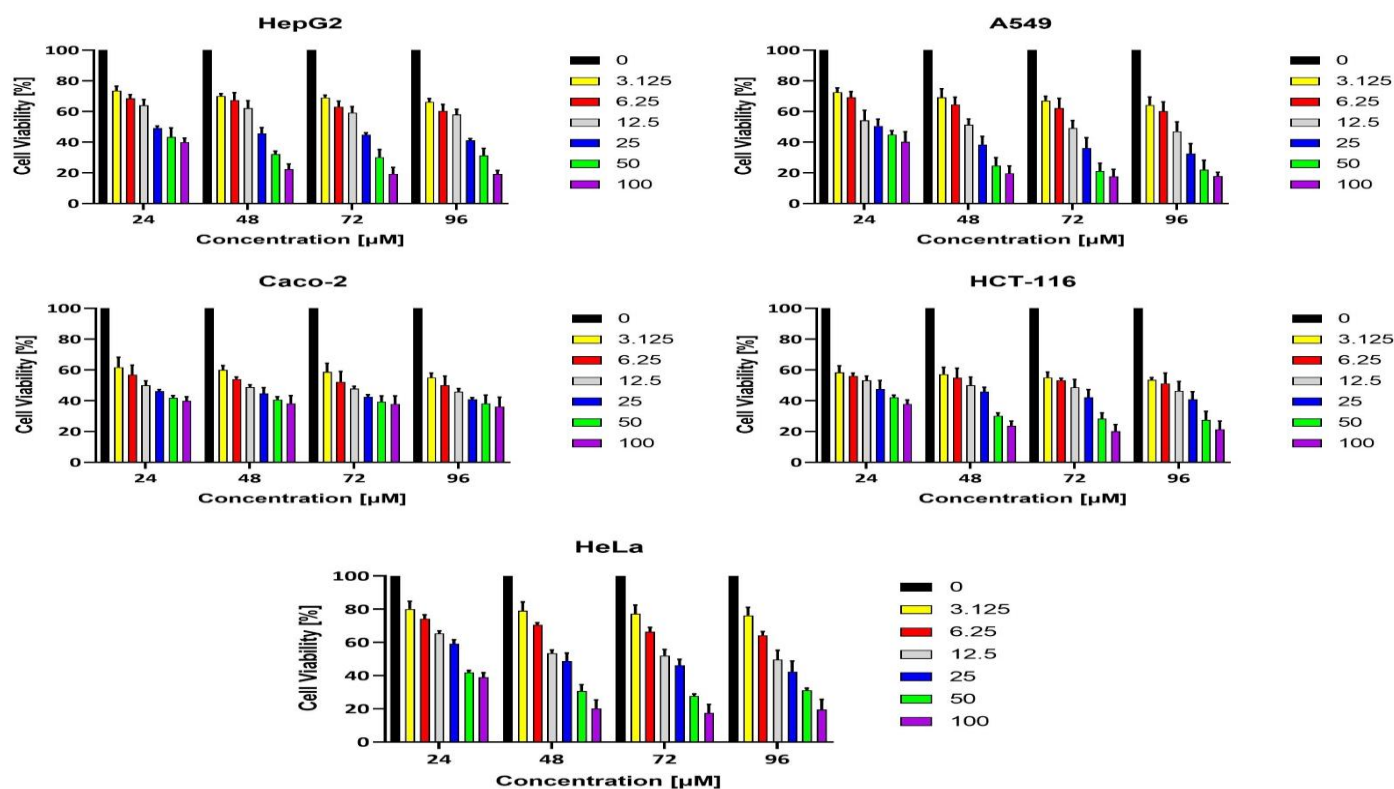


Figure 38 A graph showing the % Cell Viability of Compound 1 when tested on all 5 cells lines, which include HepG2, HeLa, HCT-116, A549 and Caco-2. Cells were incubated at periods of 24, 48, 72 and 96 hours, and dosed at concentrations; 100uM, 50uM, 25uM, 12.5uM, 6.25uM and 3.125uM

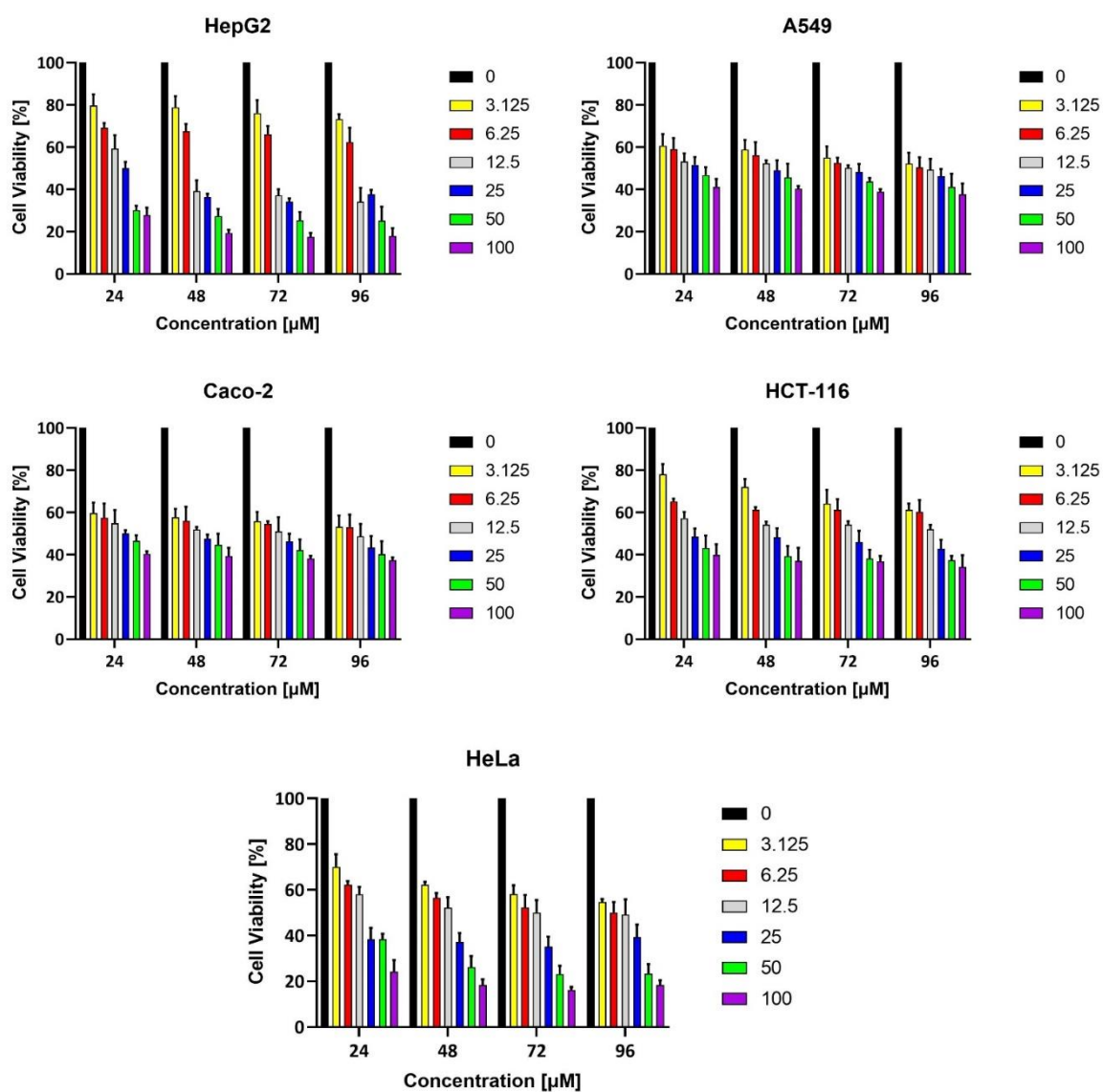


Figure 39 A graph showing the % Cell Viability of Compound 2 when tested on all 5 cells lines, which include HepG2, HeLa, HCT-116, A549 and Caco-2. Cells were incubated at periods of 24, 48, 72 and 96 hours, and dosed at concentrations; **100uM, 50uM, 25uM, 12.5uM, 6.25uM and 3.125uM**

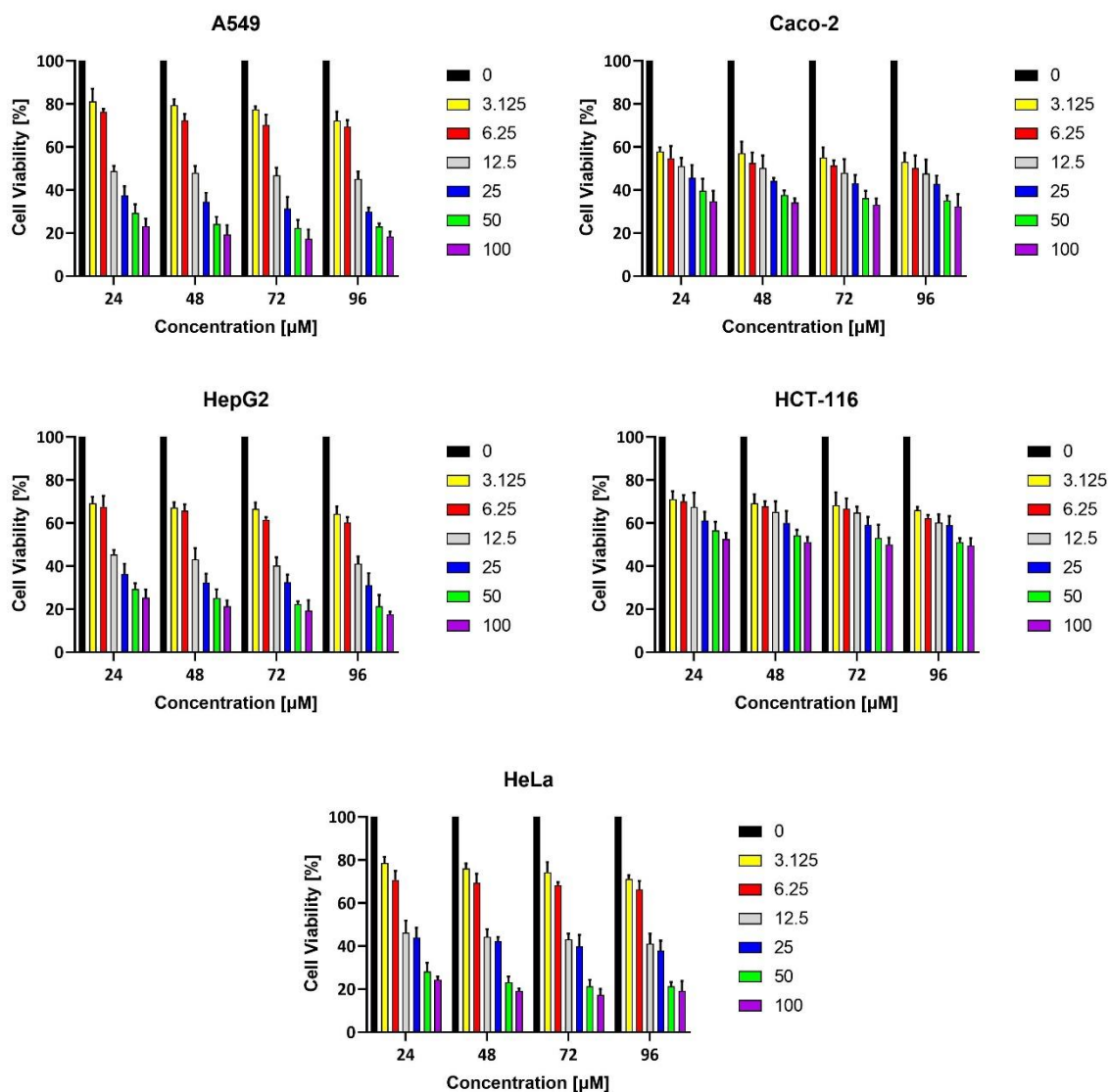


Figure 40 A graph showing the % Cell Viability of Compound 3 when tested on all 5 cells lines, which include HepG2, HeLa, HCT-116, A549 and Caco-2. Cells were incubated at periods of 24, 48, 72 and 96 hours, and dosed at concentrations; 100uM, 50uM, 25uM, 12.5uM,

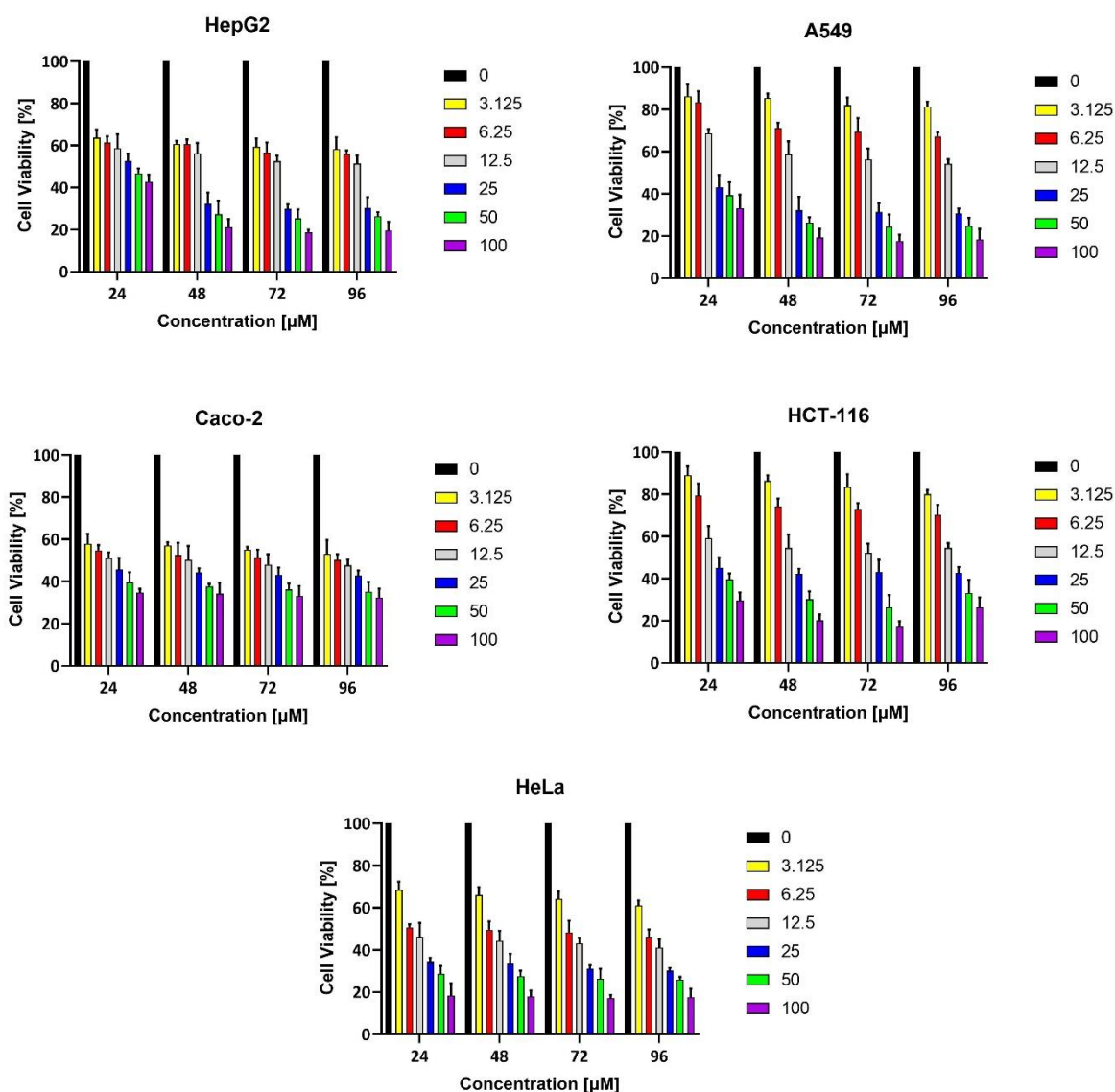


Figure 41 A graph showing the % Cell Viability of Compound 5 when tested on all 5 cells lines, which include HepG2, HeLa, HCT-116, A549 and Caco-2. Cells were incubated at periods of 24, 48, 72 and 96 hours, and dosed at concentrations; 100uM, 50uM, 25uM, 12.5uM,

When compounds 3 (Fig 40) & 5 (Fig 41) were investigated across all the cell lines, it was apparent that chemical substitution and position of functional groups plays a big role in the potency of the compounds to exhibit a form to cytotoxicity. To the general substructure of DBM, compounds 3 & 5 both contained the Hydroxyl (-OH) group at the *Ortho* position of the aromatic ring, however the relative substituents were positioned at the *Meta* (Cl) and *Para* (-

OCH<sub>3</sub>) respectively. Compared to compound 5, compound 3 initially shows a low IC<sub>50</sub> range between its values, with the greatest range being 8µM for the A549 cell line. On the other hand, the greatest range found for compound 5 was 16µM on the HepG2 cell line, an amount nearly double that of compound 3. Overall, the compounds follow the pattern discussed above of a time dependant response, however compound 5 exerts a much rapid response than that observed from compound 3. From the results, it can be deduced that both the compounds exhibit better cytotoxic effects than DBM on the HepG2 and HeLa cell lines, whereby the IC<sub>50</sub> values after 96h are in the low spectrum of values, however the response is not immediate, rather steady then rapid. As seen from compounds 1 & 2, the presence of the OH group plays a role in the IC<sub>50</sub> values being low, however it can be seen that the presence of a halogen group initially provides the platform for the compounds to have an immediate effect whereby the IC<sub>50</sub> values at 24h of the incubation period were lower than those exhibited by DBM, compound 1, 2 & 5 at all the cell lines bar one. Following this, the addition of a methoxy group in place of a halogen indicate that the functional group rather helps with the response exhibited over time than that off an immediate response. Comparing the values of compound 5 with 1 & 2, it was observed that a higher initial IC<sub>50</sub> value at 24h had decreased by a significant amount at 96h. This is shown where the IC<sub>50</sub> of compound 5 has been at 25.13µM (HepG2) and 28.20 µM (A549) but decreased to 9.86µM (HepG2) and 13.92µM. The data values were observed from tables 5-7.

Furthermore, the concept of a carbon or oxygen related group such as a Methyl or Methoxy to stabilise the compounds in order to exert their cytotoxic effects has further been strengthened by the findings of compound 4 being screen, in direct comparison with DBM. A very similar structure to that of DBM, compound 4 contains a bromine group, a halogen, attached to the central carbon between the 1,3 diketone, which understandably has replaced

the -CH<sub>2</sub> group. Findings have shown that the compound which contains the Br substituent has on average higher IC<sub>50</sub> values than DBM at the 96h incubation phase. This indicates that the presence of a group other than Oxygen or Carbon on the central carbon atom hinders the prospect of a compound exerting its cytotoxic activity. However, it is to be noted that compound 4 did have a better cytotoxic effect and potency on the Caco-2 cell line, a potential candidate for cancer affecting the colon since initial (24h) and final (96h) IC<sub>50</sub> values were calculated as 14.6μM and 10.98μM.

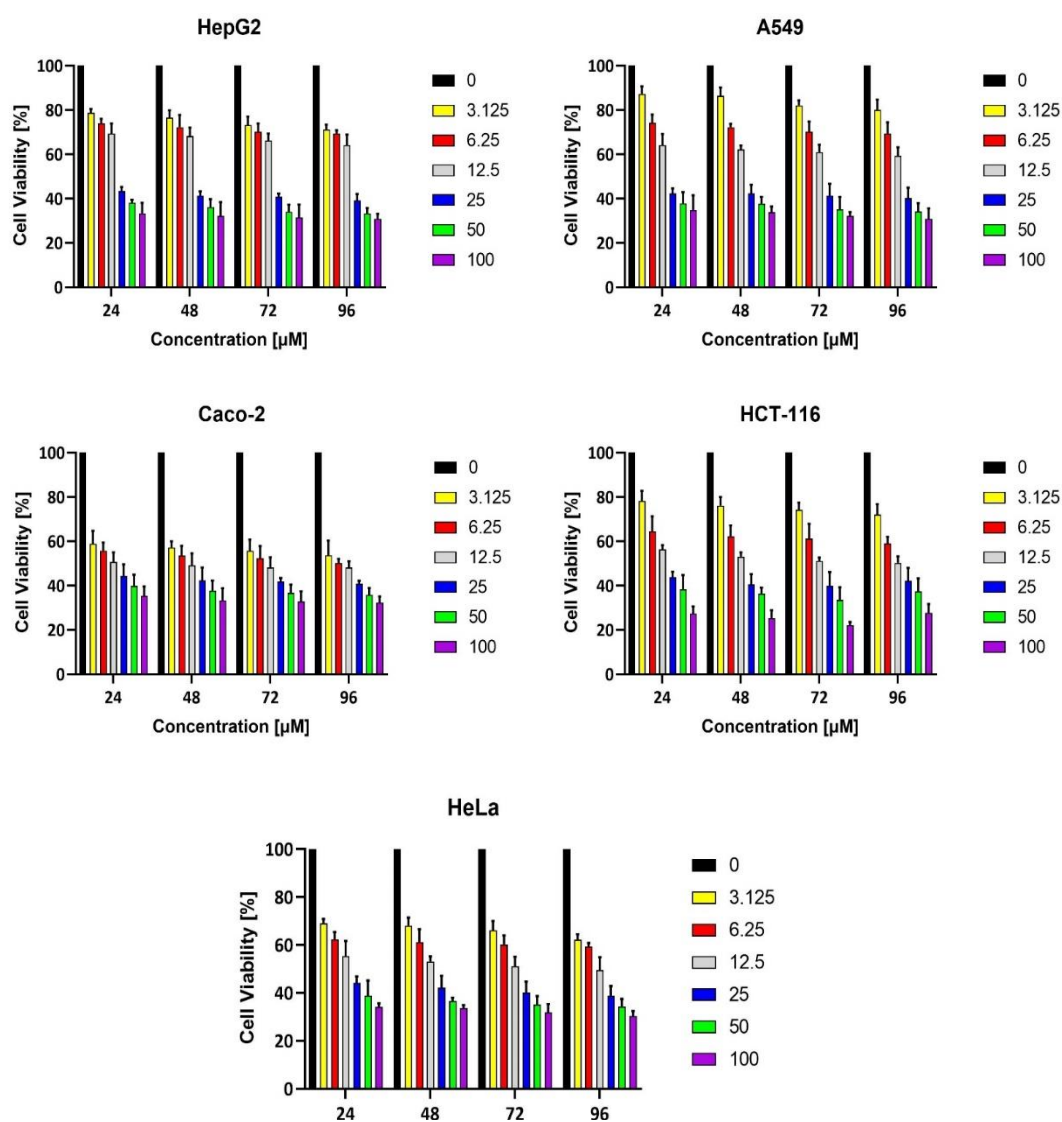


Figure 42 A graph showing the % Cell Viability of Compound 4 when tested on all 5 cells lines, which include HepG2, HeLa, HCT-116, A549 and Caco-2. Cells were incubated at periods of 24, 48, 72 and 96 hours, and dosed at concentrations; 100uM, 50uM, 25uM, 12.5uM, 6.25uM and 3.125uM

The graphs for compound 4 (Fig 42) highlight that the target compound maybe rendered unfavourable in contrast to other  $\beta$ -diketone derivatives tested. However, it should not be classed that the addition of halogen/s or related groups be counted out as unfavourable, since many derivatives work and exert their effects on one cell line but struggle to initiate a response against another. This was the case when compounds 7 & 8 were tested on the cell lines. Both compounds contain a Fluorine group substituted on the benzene aromatic ring, alongside bulky methoxy groups. Initially on the HepG2 and HeLa cell lines, it was seen that the compounds documented low IC<sub>50</sub> values, 11.13 $\mu$ M and 13.13 $\mu$ M (HepG2 at 24h) & 16.33 $\mu$ M and 15.81 $\mu$ M (HeLa at 24h) decreasing to 8.06 $\mu$ M and 9.31 $\mu$ M (HepG2 at 96h) & 11.57 $\mu$ M and 11.54 $\mu$ M (HeLa at 96h), however when screened on the other cell lines such as HCT-116, a cell line where other derivatives including compound 4 showed an IC<sub>50</sub> range of between 8.78 $\mu$ M – 18.43 $\mu$ M, the compounds in question displayed starting IC<sub>50</sub> values of 48.50 $\mu$ M & 48.17 $\mu$ M (24h) and final values of 35.49 $\mu$ M & 34.02 $\mu$ M (96h). These values were calculated to be the highest obtained for any  $\beta$ -diketone derivative.

The range of IC<sub>50</sub> values for compounds 7 & 8 can be seen in Fig 44-45. Even though high values have been calculated for the compounds, they have still shown to exert a cytotoxic effect on the tested cells.

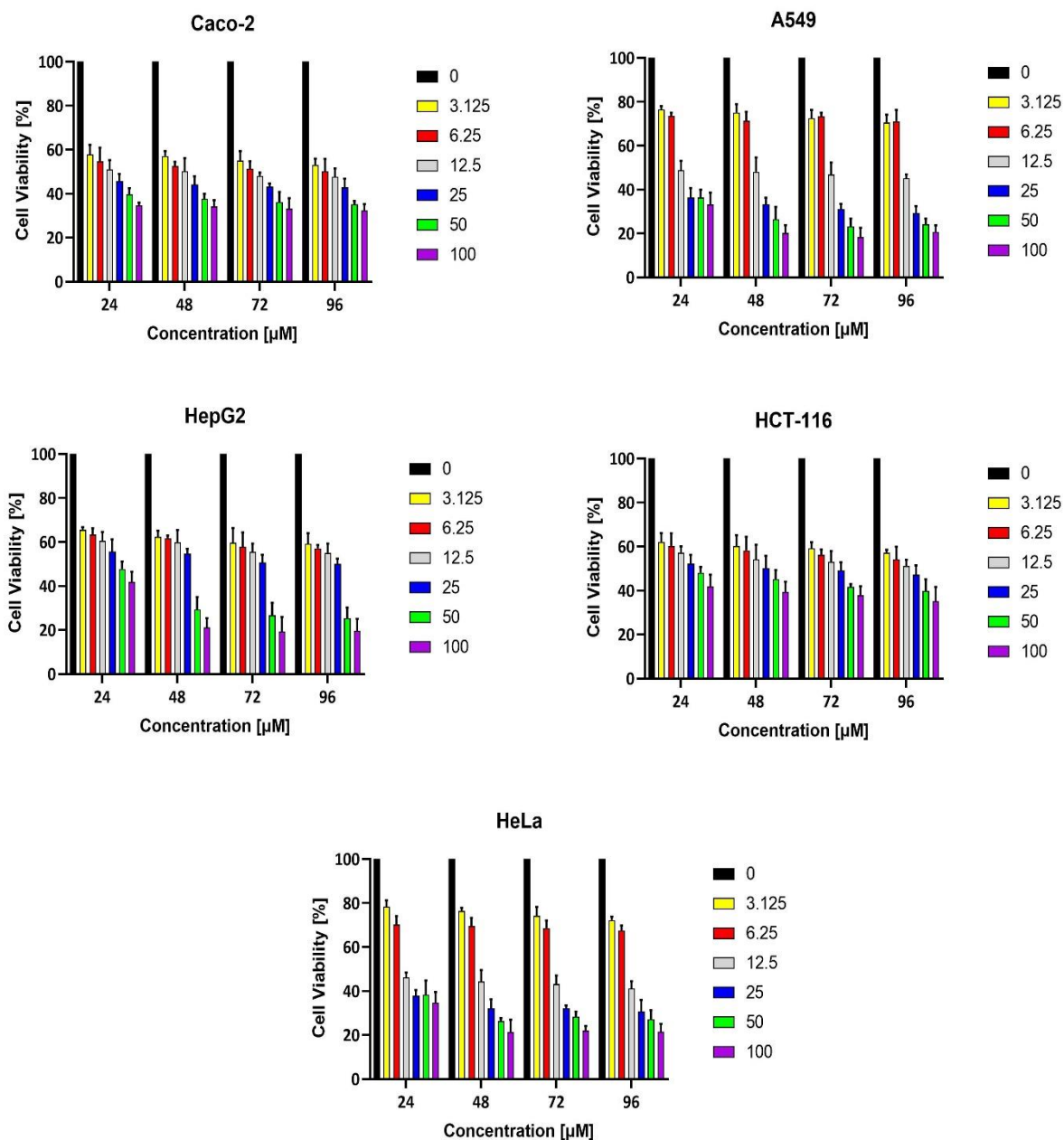


Figure 43A graph showing the % Cell Viability of Compound 6 when tested on all 5 cells lines, which include HepG2, HeLa, HCT-116, A549 and Caco-2. Cells were incubated at periods of 24, 48, 72 and 96 hours, and dosed at concentrations; 100uM, 50uM, 25uM, 12.5uM,

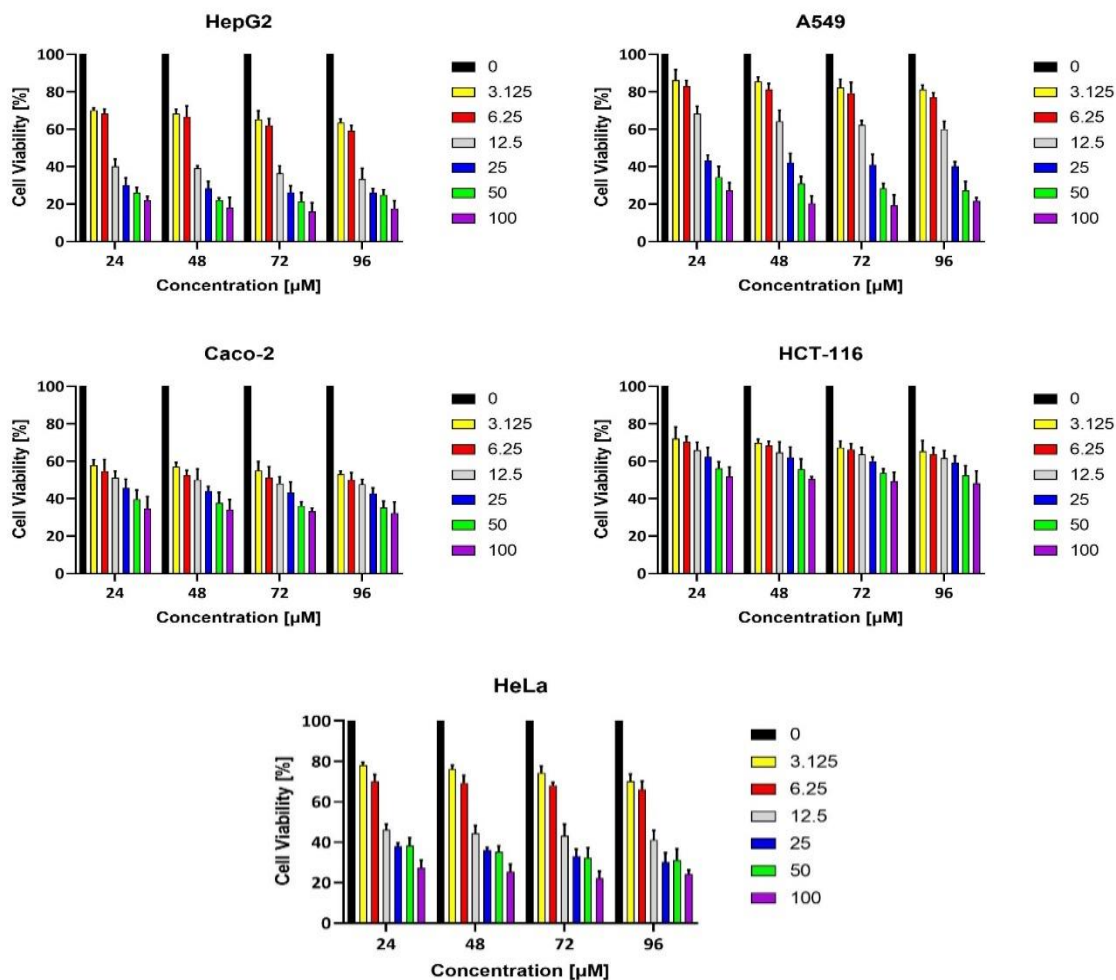


Figure 44 A graph showing the % Cell Viability of Compound 7 when tested on all 5 cells lines, which include HepG2, HeLa, HCT-116, A549 and Caco-2. Cells were incubated at periods of 24, 48, 72 and 96 hours, and dosed at concentrations; 100uM, 50uM, 25uM, 12.5uM, 6.25uM and 3.125uM

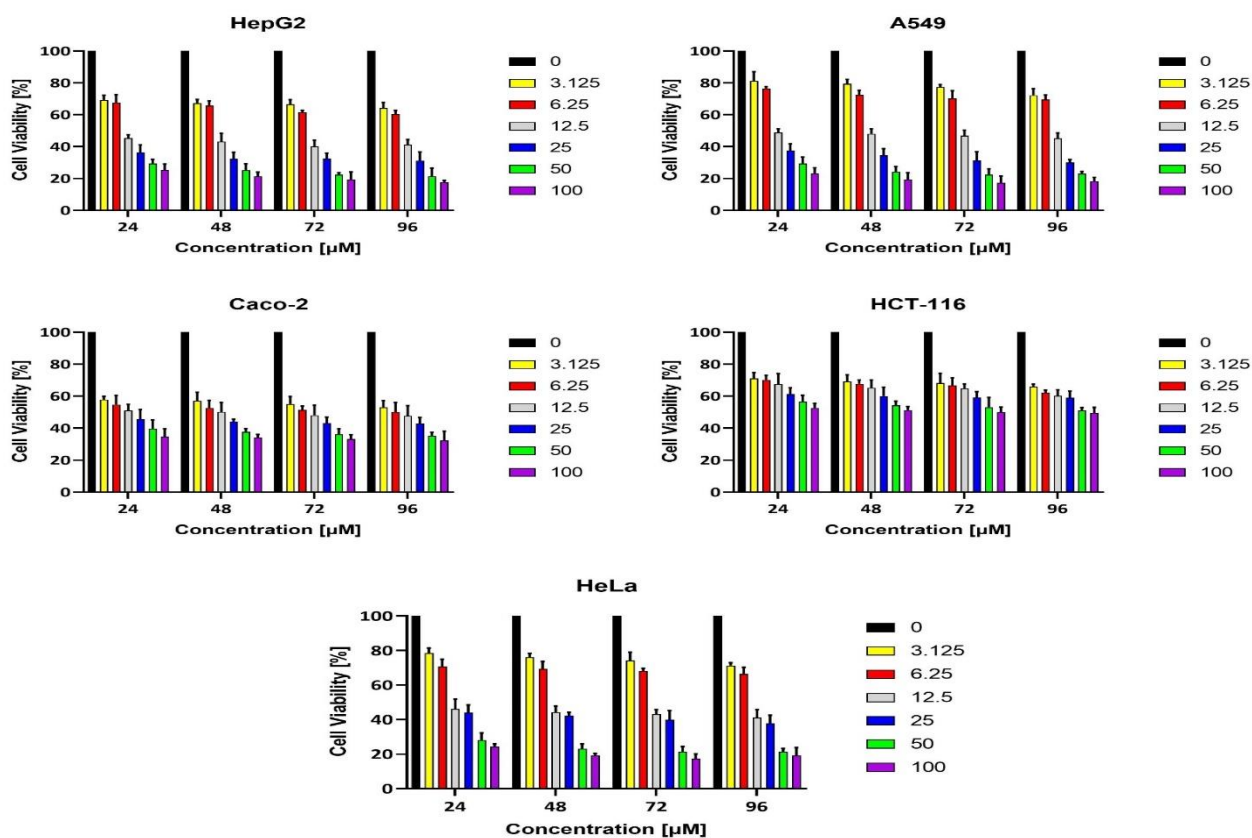


Figure 45 A graph showing the % Cell Viability of Compound 8 when tested on all 5 cells lines, which include HepG2, HeLa, HCT-116, A549 and Caco-2. Cells were incubated at periods of 24, 48, 72 and 96 hours, and dosed at concentrations; 100uM, 50uM, 25uM, 12.5uM, 6.25uM and 3.125uM

Containing methoxy groups in various positions on the aromatic ring, compounds 9 (Fig 46) and 10 (Fig 47) displayed properties which highlight their cytotoxic effect but also, for the first time in this investigation of  $\beta$ -diketone derivatives, a proliferation effect was seen. Even though the difference between both compounds is that 10 contains ether groups on one aromatic ring, whereas 9 has them present on both aromatic rings, a potent cytotoxic effect followed by a proliferating effect was observed on the HCT-116 cell line. This was observed after a significant response was registered from the 24h to 72h incubation period, however at 96h, the increase in IC50 values show the effect as either cytostatic or degradation and

metabolism were causing a reduction in efficacy. The increase in IC<sub>50</sub> values were from 15.88μM and 15.08μM at 72h to 28.07μM and 18.00μM at 96h. From this, compound 9 which contains a trimethoxy on each aromatic ring, shows a double increase in the IC<sub>50</sub> values, 12.19μM when compared to compound 10, which contains trimethoxy groups on one aromatic ring. The increase in IC<sub>50</sub> value seen here was 2.92μM.

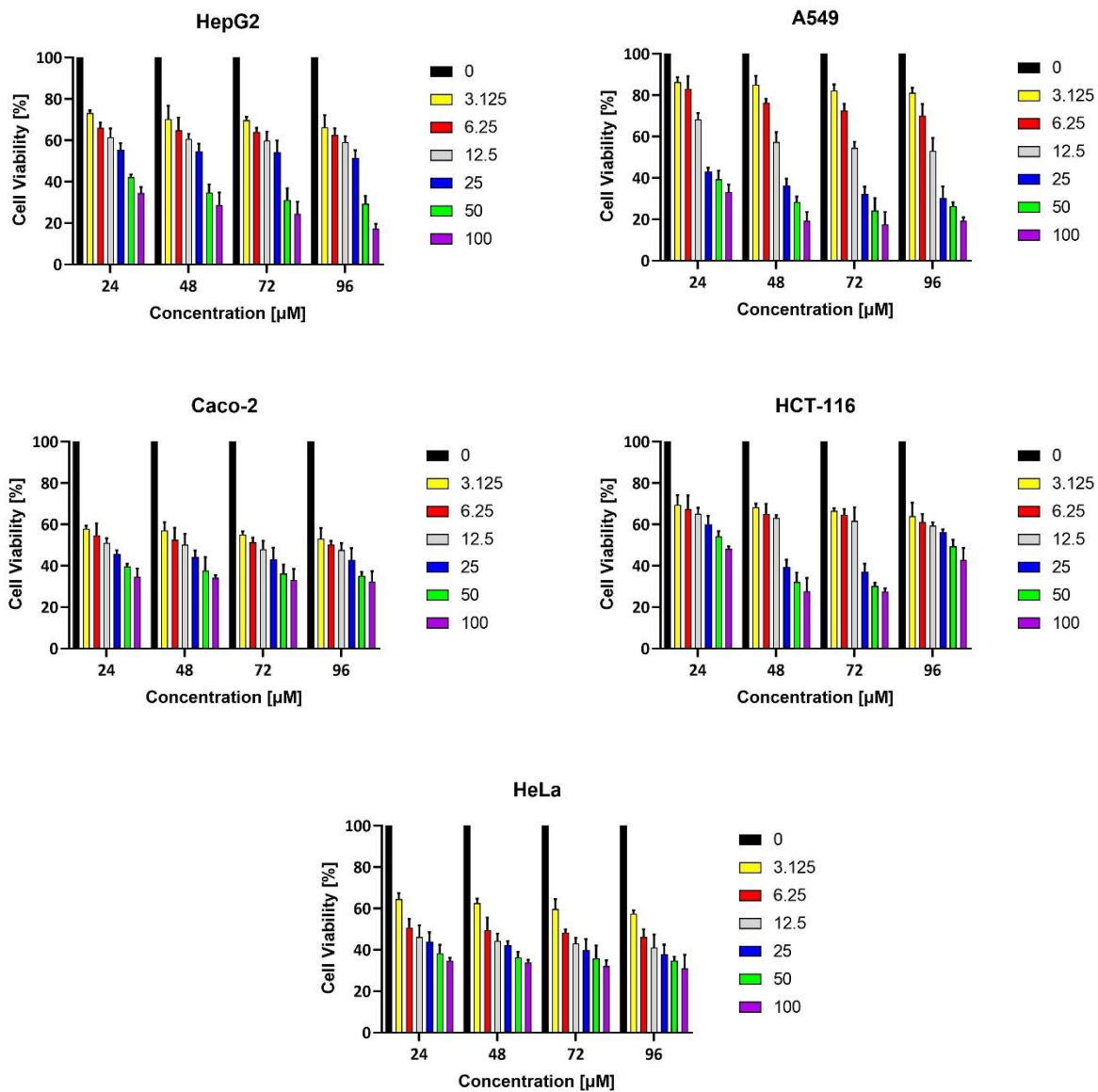


Figure 46A graph showing the % Cell Viability of Compound 9 when tested on all 5 cells lines, which include HepG2, HeLa, HCT-116, A549 and Caco-2. Cells were incubated at periods of 24, 48, 72 and 96 hours, and dosed at concentrations; 100uM, 50uM, 25uM, 12.5uM,

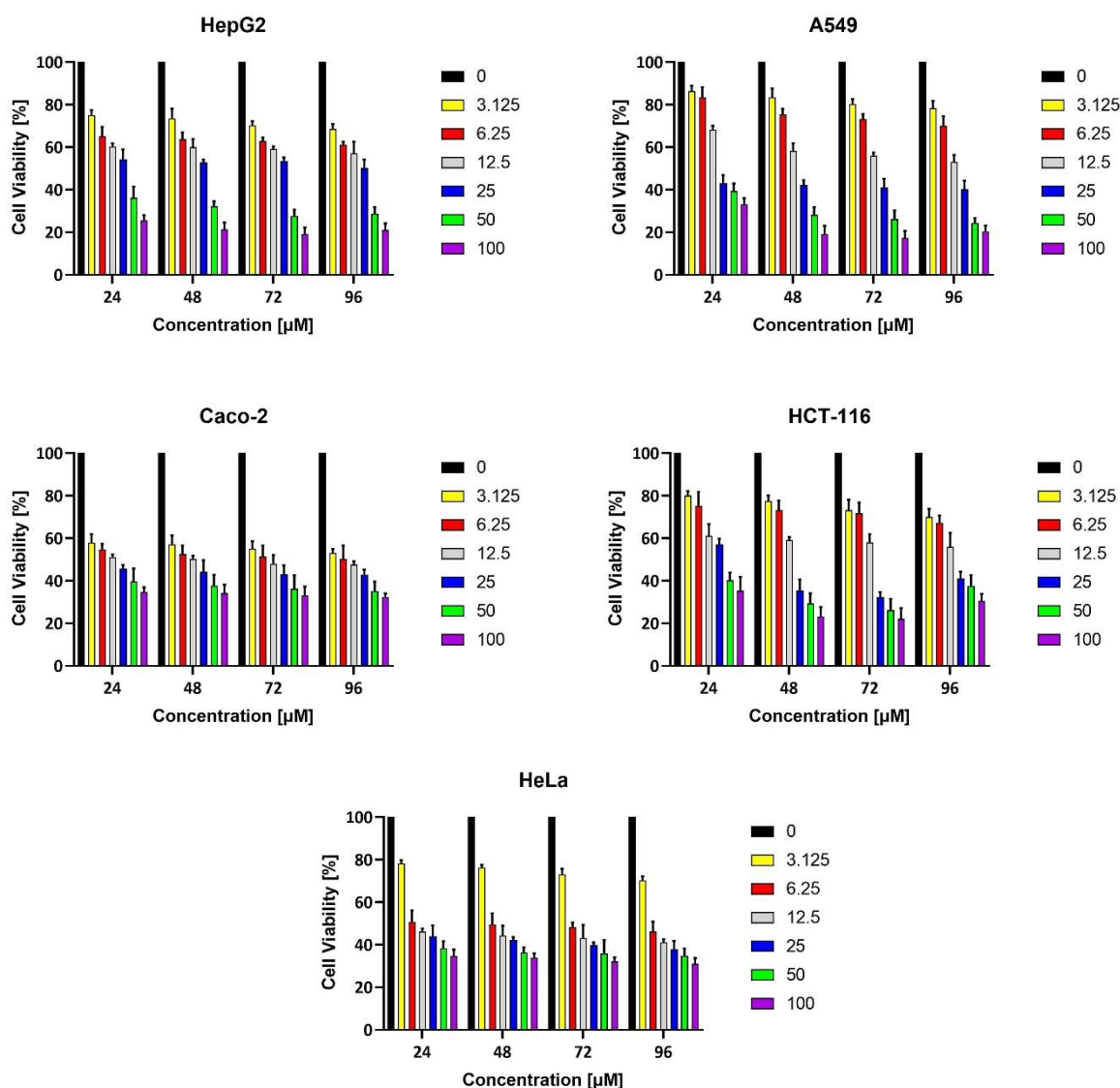


Figure 47 graph showing the % Cell Viability of Compound 10 when tested on all 5 cells lines, which include HepG2, HeLa, HCT-116, A549 and Caco-2. Cells were incubated at periods of 24, 48, 72 and 96 hours, and dosed at concentrations; 100uM, 50uM, 25uM, 12.5uM,

The tests on the  $\beta$ -diketone derivatives do indicate and confirm that the cytotoxic effect of the compounds on the cell lines is time and concentration dependant, whereby the potency of the candidates is found to be at concentration dose levels around the 17 $\mu$ M - 25 $\mu$ M mark. Moreover, no candidate was found to have a better effect on the cell lines than the internal control of Cisplatin.

### 3.2.4 Cytotoxicity - 2-Azido Derivatives (Compounds 11-13)

Calculated IC<sub>50</sub> values (Table 8-10) across all cell lines for the 2-Azido-diketone derivatives show the maximal dose required for 50% cell growth inhibition to be between the range of 16 $\mu$ M and 47 $\mu$ M. The values calculated were found to be higher than those of the  $\beta$ -diketone derivatives, especially DBM, 1 and 3, since the synthesised 2-Azido derivatives were based on a similar substructure. Like the  $\beta$ -diketones, the compounds did display a time dependant activity whereby the IC<sub>50</sub> would decrease over the time period as seen within Figures 48- 50, however the significance in response was seen to more than double. Compounds which exhibited effective cytotoxic potency was 11, on the HCT-116 cancer cell line. With a IC<sub>50</sub> concentration of 16.57 $\mu$ M at 24h, over time the value decreased at 96h to 12.34 $\mu$ M, a small but effect drop in terms of potency. Compounds 12 & 13, combined with 11, displayed steady decreases in IC<sub>50</sub> over the 24h-96h incubation treatment period, and changes in values did not exceed a 10 $\mu$ M range.

Table 8 IC50 values of 2-Azido-Diketone derivatives. Cytotoxicity was observed on HepG2 and HeLa cell lines, with the standard deviation being calculated based on triplicate results.

Compound	IC50 [ $\mu$ M]							
	HepG2				HeLa			
	24h	48h	72h	96h	24h	48h	72h	96h
<b>11</b>	36.05	31.28	30.79	29.83	26.87	24.54	23.46	22.78
	$\pm 2.15$	$\pm 4.25$	$\pm 1.26$	$\pm 2.54$	$\pm 3.26$	$\pm 1.25$	$\pm 3.64$	$\pm 1.87$
<b>12</b>	28.83	25.23	24.38	22.35	30.16	25.25	24.71	22.98
	$\pm 2.56$	$\pm 1.87$	$\pm 3.56$	$\pm 2.22$	$\pm 1.87$	$\pm 3.24$	$\pm 3.65$	$\pm 3.24$
<b>13</b>	46.54	39.55	36.00	32.32	25.57	21.37	21.16	20.59
	$\pm 4.54$	$\pm 4.33$	$\pm 3.54$	$\pm 4.21$	$\pm 2.32$	$\pm 1.24$	$\pm 3.65$	$\pm 4.21$

Table 9 IC50 values of 2-Azido-Diketone derivatives. Cytotoxicity was observed on A540 and HCT-116 cell lines, with the standard deviation being calculated based on triplicate results

Compound	IC50 [ $\mu$ M]							
	A549				HCT-116			
	24h	48h	72h	96h	24h	48h	72h	96h
<b>11</b>	32.20	28.32	27.20	27.00	16.57	14.87	13.33	12.34
	$\pm 2.15$	$\pm 3.65$	$\pm 4.21$	$\pm 1.25$	$\pm 2.56$	$\pm 1.98$	$\pm 3.14$	$\pm 1.24$
<b>12</b>	42.89	36.66	35.62	34.07	41.73	37.56	36.56	32.32
	$\pm 2.15$	$\pm 3.65$	$\pm 1.87$	$\pm 1.65$	$\pm 3.24$	$\pm 2.59$	$\pm 4.63$	$\pm 1.25$
<b>13</b>	35.95	25.78	23.34	24.42	43.55	40.01	39.22	36.48
	$\pm 3.65$	$\pm 2.24$	$\pm 1.36$	$\pm 3.24$	$\pm 1.24$	$\pm 0.87$	$\pm 2.35$	$\pm 2.50$

Table 10 IC50 values of 2-Azido-Diketone derivatives. Cytotoxicity was observed on the Caco-2 cell lines, with the standard deviation being calculated based on triplicate results

Compound	IC50 [ $\mu$ M]			
	Caco-2			
	24h	48h	72h	96h
<b>11</b>	39.37	34.37	32.37	33.03
	$\pm 1.25$	$\pm 0.98$	$\pm 4.25$	$\pm 4.12$
<b>12</b>	38.40	33.84	31.47	32.54
	$\pm 3.25$	$\pm 1.57$	$\pm 2.59$	$\pm 3.45$
<b>13</b>	41.72	35.60	30.96	32.37
	$\pm 1.25$	$\pm 2.56$	$\pm 3.26$	$\pm 2.98$

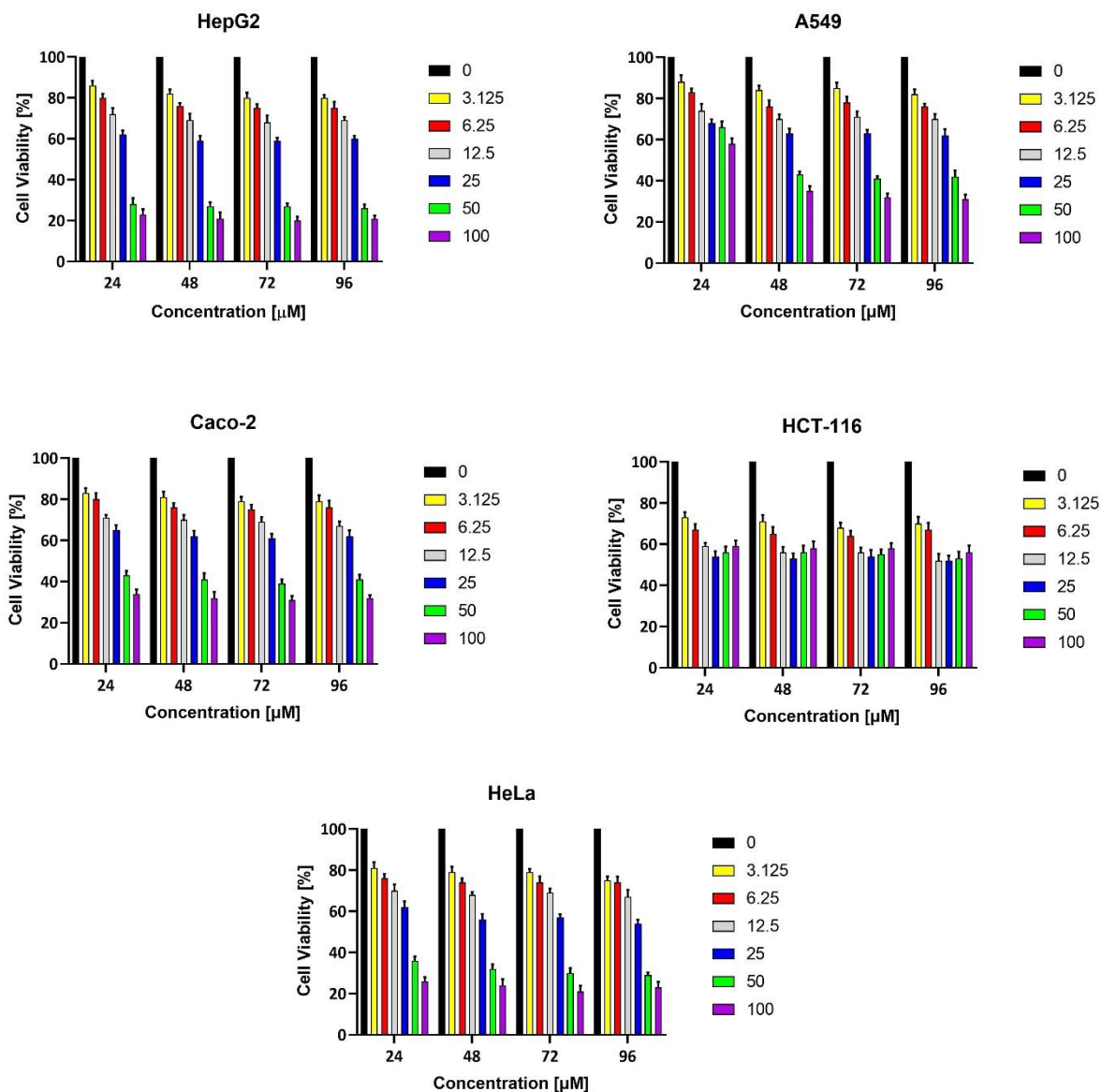


Figure 48 A graph showing the % Cell Viability of Compound 11 when tested on all 5 cells lines, which include HepG2, HeLa, HCT-116, A549 and Caco-2. Cells were incubated at periods of 24, 48, 72 and 96 hours, and dosed at concentrations; 100uM, 50uM, 25uM, 12.5uM,

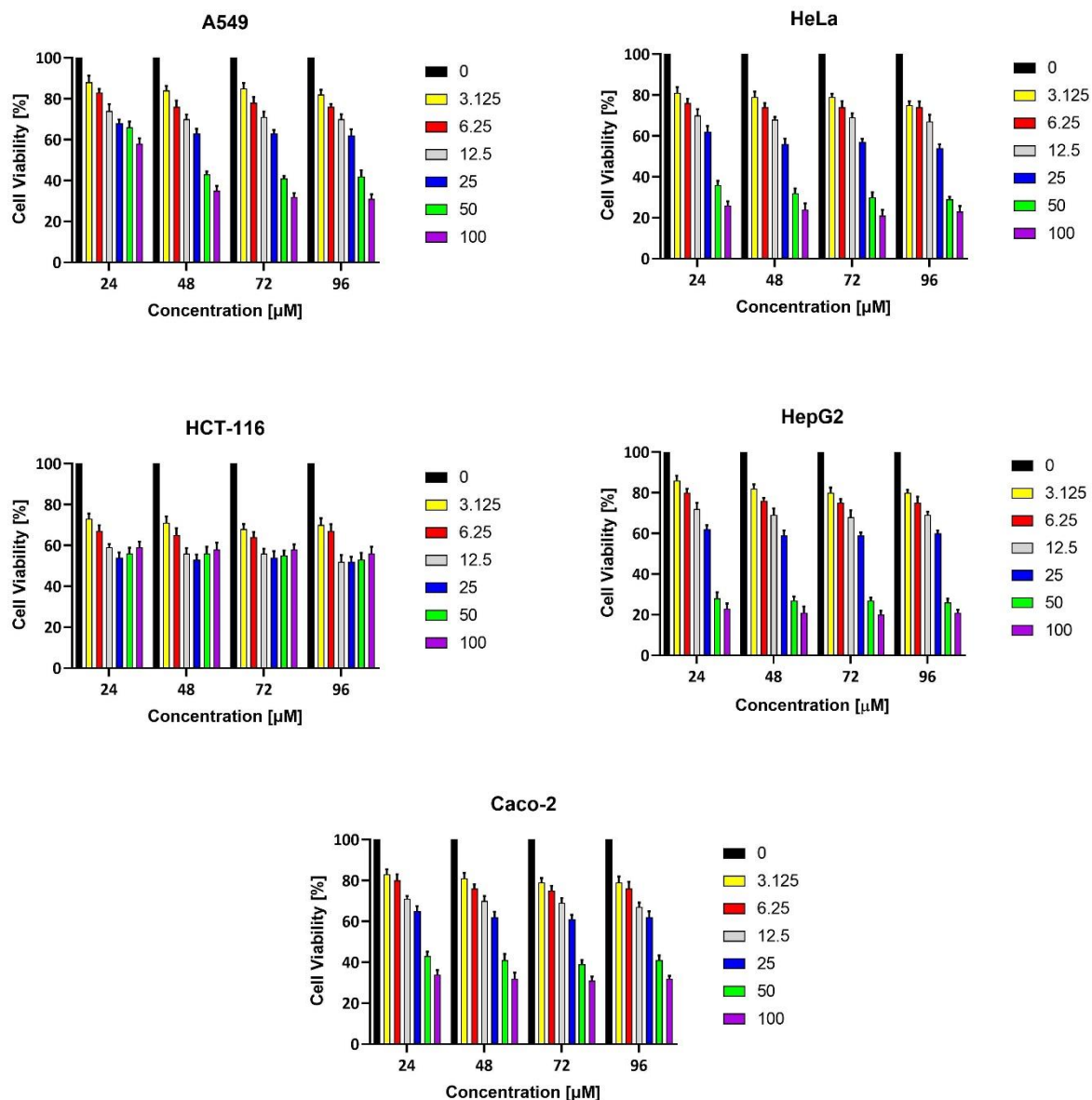


Figure 49 A graph showing the % Cell Viability of Compound 12 when tested on all 5 cells lines, which include HepG2, HeLa, HCT-116, A549 and Caco-2. Cells were incubated at periods of 24, 48, 72 and 96 hours, and dosed at concentrations; 100uM, 50uM, 25uM, 12.5uM

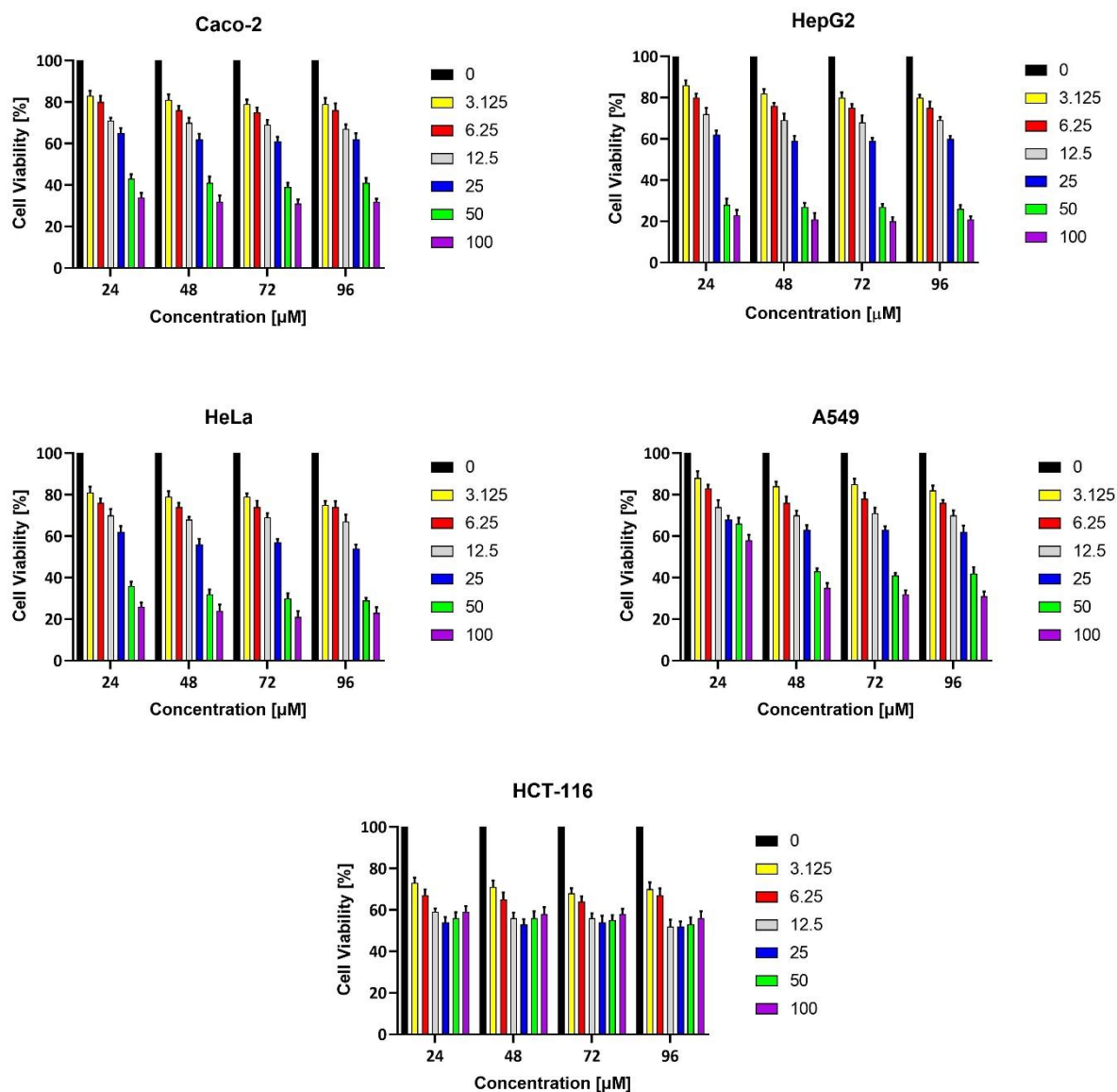


Figure 50 A graph showing the % Cell Viability of Compound 13 when tested on all 5 cells lines, which include HepG2, HeLa, HCT-116, A549 and Caco-2. Cells were incubated at periods of 24, 48, 72 and 96 hours, and dosed at concentrations; 100uM, 50uM, 25uM, 12.5uM

### 3.2.5 Cytotoxicity on Benzoylurea Derivatives (Compounds 14-16)

The cytotoxicity of benzoylurea derivatives was determined in contrast to  $\beta$ -diketone with an interest to see what the C=S bond within the compound instead of the C=O carbonyl bond will provide with regards to cytotoxic effect. The benzoylureas were screened on all the cell lines as before and over the same time period with the same concentration doses. It was found that the benzoylurea derivatives exhibited an aggressive response to that of the  $\beta$ -diketones in terms of expressing IC50 values, as some cell lines displayed very high IC50 values which dropped rapidly over time. Nearly all the IC50 values calculated were shown to be over 30 $\mu$ M except for the A549 cell line, which may suggest Benzoylurea derivatives to inhibit growth on breast cancer. This was shown where the IC50 values of compounds 14 (26.50 $\mu$ M), 15 (25.74 $\mu$ M) and 16 (26.18 $\mu$ M) at 24h and then at 96h, 17.66 $\mu$ M (14), 17.39 $\mu$ M (15) & 13.26 $\mu$ M (16) were calculated, ranges which were associated to the  $\beta$ -diketones.

It can be proposed that the Benzoylurea derivatives work better on an immediate basis, since the drop in IC50 after 24h had such a significant response. This is because such a huge drop was observed after 24h, which indicates that the majority of the cells tested had proliferation inhibited.

Table 11 IC50 values for the Benzoylurea derivatives. Cytotoxicity was observed on HepG2 and HeLa cell lines, with the standard deviation being calculated based on triplicate results.

Compound	IC50 [ $\mu$ M]							
	HepG2				HeLa			
	24h	48h	72h	96h	24h	48h	72h	96h
<b>14</b>	56.58 $\pm$ 3.26	26.15 $\pm$ 2.58	24.54 $\pm$ 3.24	25.93 $\pm$ 2.87	33.17 $\pm$ 2.99	22.33 $\pm$ 1.57	18.85 $\pm$ 3.65	18.28 $\pm$ 2.10
<b>15</b>	71.06 $\pm$ 2.65	38.71 $\pm$ 3.21	33.94 $\pm$ 1.68	26.36 $\pm$ 4.23	35.86 $\pm$ 3.45	28.12 $\pm$ 2.36	25.62 $\pm$ 1.54	24.70 $\pm$ 2.59
<b>16</b>	63.55 $\pm$ 3.24	36.06 $\pm$ 2.57	31.55 $\pm$ 1.24	28.93 $\pm$ 3.45	37.74 $\pm$ 3.99	27.97 $\pm$ 2.45	23.34 $\pm$ 3.68	22.41 $\pm$ 2.11

Table 12 IC50 values for the Benzoylurea derivatives. Cytotoxicity was observed on A549 and HCT-116 cell lines, with the standard deviation being calculated based on triplicate results.

Compound	IC50 [ $\mu$ M]							
	A549				HCT-116			
	24h	48h	72h	96h	24h	48h	72h	96h
<b>14</b>	26.50 $\pm$ 1.89	20.39 $\pm$ 2.65	19.01 $\pm$ 1.85	17.66 $\pm$ 2.45	135.50 $\pm$ 4.65	63.15 $\pm$ 2.31	55.21 $\pm$ 3.21	51.12 $\pm$ 1.98
<b>15</b>	25.74 $\pm$ 2.22	19.01 $\pm$ 3.56	17.00 $\pm$ 1.65	17.39 $\pm$ 2.45	88.40 $\pm$ 3.21	73.43 $\pm$ 2.58	68.22 $\pm$ 3.21	65.07 $\pm$ 2.57
<b>16</b>	26.18 $\pm$ 2.36	15.24 $\pm$ 4.21	13.42 $\pm$ 3.24	13.26 $\pm$ 2.45	78.29 $\pm$ 2.88	67.56 $\pm$ 1.65	63.72 $\pm$ 2.64	56.68 $\pm$ 4.23

Table 13 IC50 values for the Benzoylurea derivatives. Cytotoxicity was observed on the Caco-2 cell lines, with the standard deviation being calculated based on triplicate results.

Compound	IC50 [ $\mu$ M]			
	Caco-2			
	24h	48h	72h	96h
<b>14</b>	47.19	37.66	33.38	30.01
	$\pm 2.44$	$\pm 3.24$	$\pm 2.99$	$\pm 3.21$
<b>15</b>	50.11	37.96	33.26	33.06
	$\pm 2.15$	$\pm 3.24$	$\pm 5.36$	$\pm 2.54$
<b>16</b>	49.16	41.09	35.57	30.88
	$\pm 1.89$	$\pm 3.25$	$\pm 2.54$	$\pm 2.98$

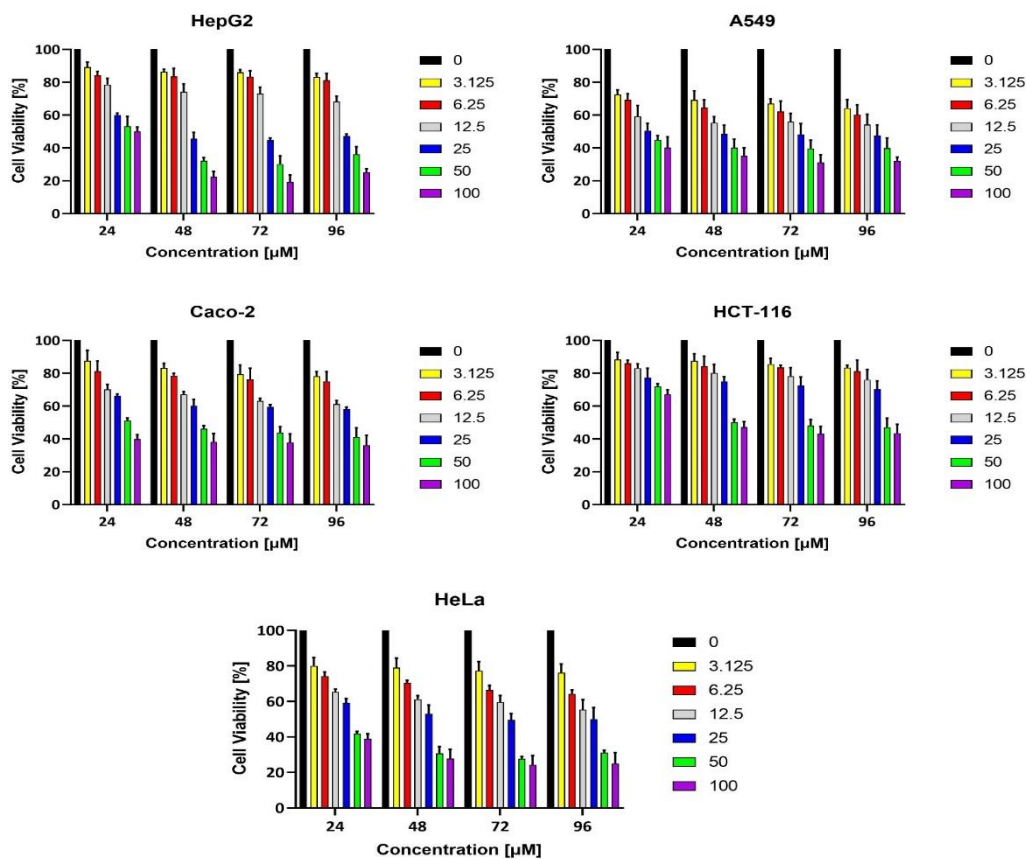


Figure 51 A graph showing the % Cell Viability of Compound 14 when tested on all 5 cells lines, which include HepG2, HeLa, HCT-116, A549 and Caco-2. Cells were incubated at periods of 24, 48, 72 and 96 hours, and dosed at concentrations; 100µM, 50µM, 25µM, 12.5µM, 6.25µM and 3.125µM

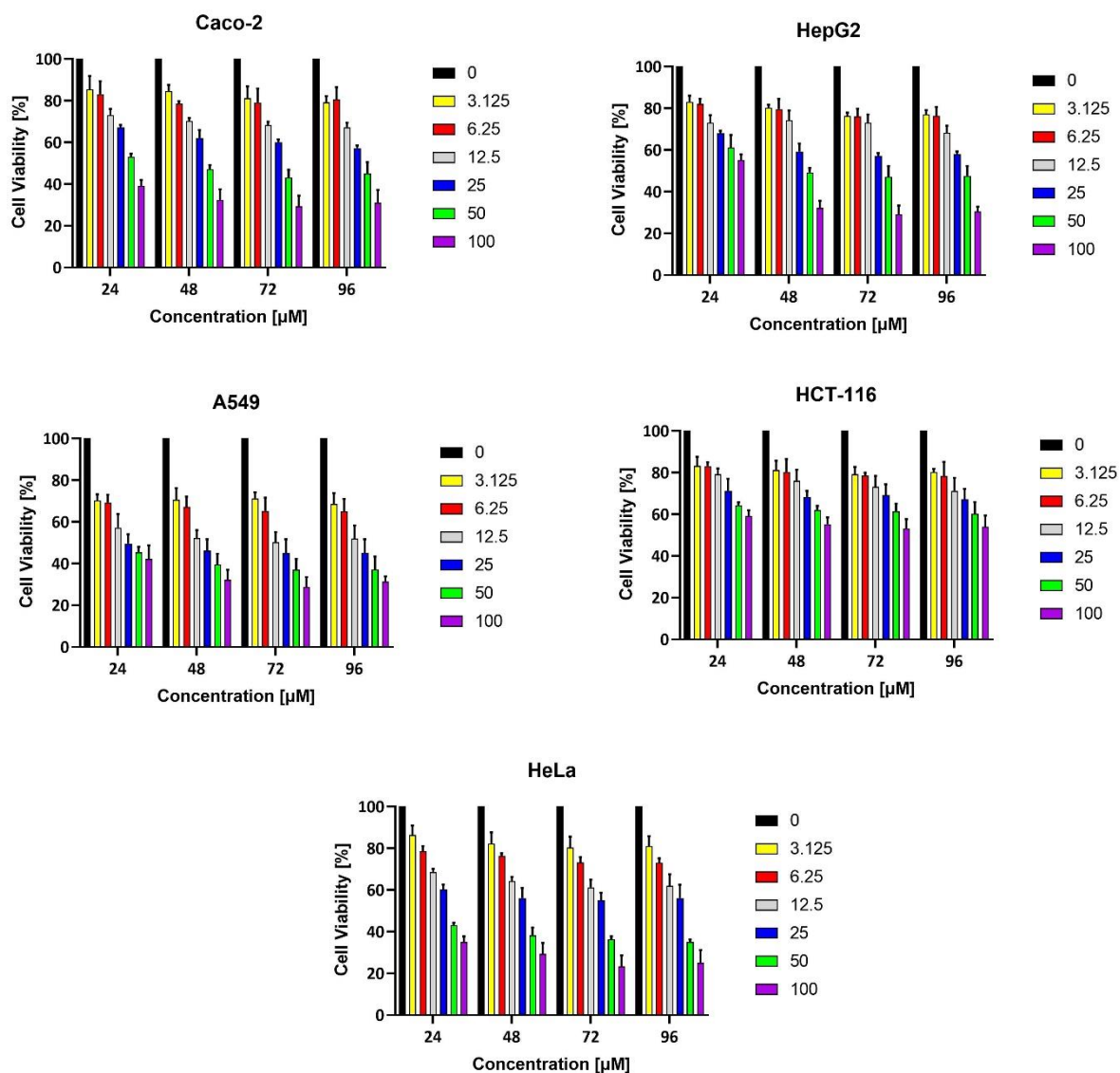


Figure 52 A graph showing the % Cell Viability of Compound 15 when tested on all 5 cells lines, which include HepG2, HeLa, HCT-116, A549 and Caco-2. Cells were incubated at periods of 24, 48, 72 and 96 hours, and dosed at concentrations; 100uM, 50uM, 25uM, 12.5uM

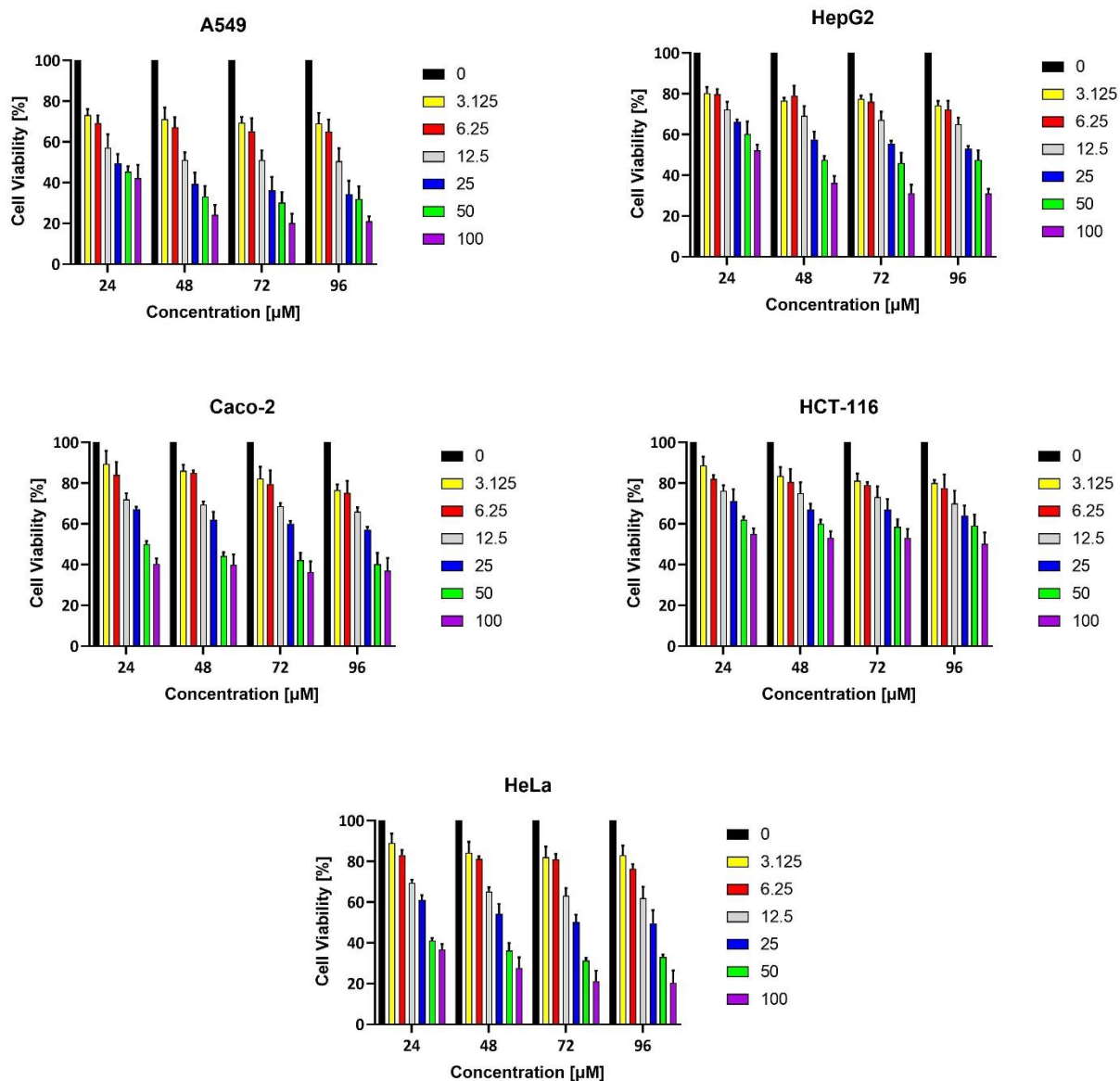


Figure 53A graph showing the % Cell Viability of Compound 16 when tested on all 5 cells lines, which include HepG2, HeLa, HCT-116, A549 and Caco-2. Cells were incubated at periods of 24, 48, 72 and 96 hours, and dosed at concentrations; 100uM, 50uM, 25uM, 12.5uM

The cell lines were selected to provide examples of several common tumour types in order to determine if the compounds exhibited cell line specific action or lead to consistent growth inhibition across multiple lines. It was found that activity was structurally and cell line dependent

### 3.3 Plasma Stability Assay

The plasma stability assay was conducted as a triplicate, whereby the conditions analysed the degradation of the potential drug candidates over a period of 120 mins. Conditions utilised by the assay included the usage of an internal control, Rifampicin, the temperature of the water bath at 37°C to replicate the human body, and the concentration of the plasma used at 50% and 100% respectively. The plasma concentration at 50% was diluted using phosphate buffer. The assay determines the stability of the new chemical entities in plasma vital since this will indicate the level of *in vivo* efficacy. Compounds were subjected to the plasma stability assay in order to determine the percentage of test compound remaining over different time intervals. Plots were visualised to show the difference in compound degradation for each synthesised candidate, and thus compared to RMP, which is stated to be relatively stable in a neutral pH of 7.4. Another control, whereby no plasma was present was also utilised for data analysis. Since a known compound which is unstable within these conditions was not used as a positive control, the data is presented within a preliminary stage of the study.

Table 14 Containing the data obtained from all compounds when tested at conditions containing 50% Plasma concentration, incubated over time intervals from 0 – 120 minutes. Data highlights % compound remaining from 100% and an overall % decrease from first incubation to last

Compound	Incubation on Plasma [50%]/min to show compound remaining (%)							Decrease from T0 to T120 (%)
	0	5	15	30	45	60	120	
<b>RMP</b>	100	98.7	96.6	94.4	91.7	87.9	84.1	15.9
<b>DBM</b>	100	98.1	90.3	84.3	80.2	75.6	69.2	30.8
<b>1</b>	100	98.5	93.4	90.3	86.8	81.6	75.8	24.2
<b>2</b>	100	98.9	95.3	91.4	87.6	83.6	78.9	21.1
<b>3</b>	100	96.7	92.5	90.8	86.3	81.7	73.5	26.5
<b>4</b>	100	94.6	89.3	86.1	80.2	74.3	68.7	31.3
<b>5</b>	100	97.4	92.7	88.3	84.1	79.2	73.1	26.9
<b>6</b>	100	95.7	89.3	81.2	76.2	73.6	69.9	30.1
<b>7</b>	100	94.1	89.4	81.3	74.6	68.3	64.3	35.7
<b>8</b>	100	95.1	90.3	80.6	75.2	67.3	63.9	36.1
<b>9</b>	100	92.1	87.3	78.3	71.2	64.3	62.8	37.2
<b>10</b>	100	91.5	88.3	79.1	71.4	65.2	63.0	37.0
<b>11</b>	100	84.1	73.5	66.5	59.4	50.1	46.3	53.7
<b>12</b>	100	88.9	79.2	72.5	64.3	57.2	50.7	49.3
<b>13</b>	100	86.2	77.3	70.8	62.3	55.6	49.1	50.9
<b>14</b>	100	98.2	97.1	93.2	90.3	86.1	82.3	17.7
<b>15</b>	100	98.6	96.4	92.3	91.3	84.3	80.1	19.9
<b>16</b>	100	97.6	95.3	91.5	91.3	83.6	81.2	18.8

Table 15 Containing the data obtained from all compounds when tested at conditions containing 100% Plasma concentration, incubated over time intervals from 0 – 120 minutes. Data highlights % compound remaining from 100% and an overall % decrease from first incubation to last.

Compound	Incubation on Plasma [100%]/min to show compound remaining (%)							Decrease from T0 to T120 (%)
	0	5	15	30	45	60	120	
<b>RMP</b>	100	97.7	95.6	91.2	87.6	84.3	82.4	17.6
<b>DBM</b>	100	93.7	86.7	81.3	74.6	69.2	62.3	37.7
<b>1</b>	100	94.1	91.6	84.5	78.3	71.8	65.6	34.4
<b>2</b>	100	94.8	92.4	87.6	81.3	75.8	68.3	31.7
<b>3</b>	100	92.6	90.4	82.3	76.8	70.1	64.2	35.8
<b>4</b>	100	82.3	79.4	69.2	58.3	55.6	50.2	49.8
<b>5</b>	100	94.2	90.3	83.4	76.3	70.8	63.4	36.6
<b>6</b>	100	93.1	86.2	79.3	71.2	67.8	59.3	40.7
<b>7</b>	100	92.1	86.5	78.3	71.3	64.2	59.1	40.9
<b>8</b>	100	91.9	85.4	79.3	72.4	64.6	60.3	39.7
<b>9</b>	100	90.1	84.3	74.2	69.2	60.2	56.2	43.8
<b>10</b>	100	91.2	86.1	75.2	69.4	61.3	56.2	43.8
<b>11</b>	100	78.3	65.3	52.7	43.1	35.8	28.3	71.7
<b>12</b>	100	83.6	70.5	61.3	52.	44.9	37.8	62.2
<b>13</b>	100	81.3	68.2	59.4	50.9	42.1	35.6	64.4
<b>14</b>	100	96.3	94.2	92.3	88.3	82.1	79.3	20.7
<b>15</b>	100	95.3	93.4	91.2	86.1	81.3	79.2	20.8
<b>16</b>	100	96.3	91.2	89.6	84.6	81.8	80.3	19.7

The values from tables 14-15 highlight that fact that when the plasma concentration is higher, the percentage of compound degradation is also much higher. This correlation factor is evident by looking at the tables, whereby values of the percentage compound remaining decrease from 100% over the 120 minute period. Used as a basis of control within the study, RMP exhibits a steady stable degradation within both concentrations of plasma. When RMP was incubated with 50% plasma, the degradation over 120 minutes was calculated to be a decrease of 15.9% overall since 84.1% of the compound was still remaining, and this stable degradation was also seen observed in a incubation of 100% plasma, where the percentage decrease now accounted for 17.6% since only 82.4% of the compound was present at the end. As mentioned previously, a stable compound provides for a better efficacy since the ADME process is much more balanced therefore the drug compounds can be absorbed steadily, distributed accordingly, metabolism slowly and then cleared quickly.

Graphs showing the percentage of test compound remaining vs time for both concentrations of plasma used for incubation further stresses the stability of the internal control.

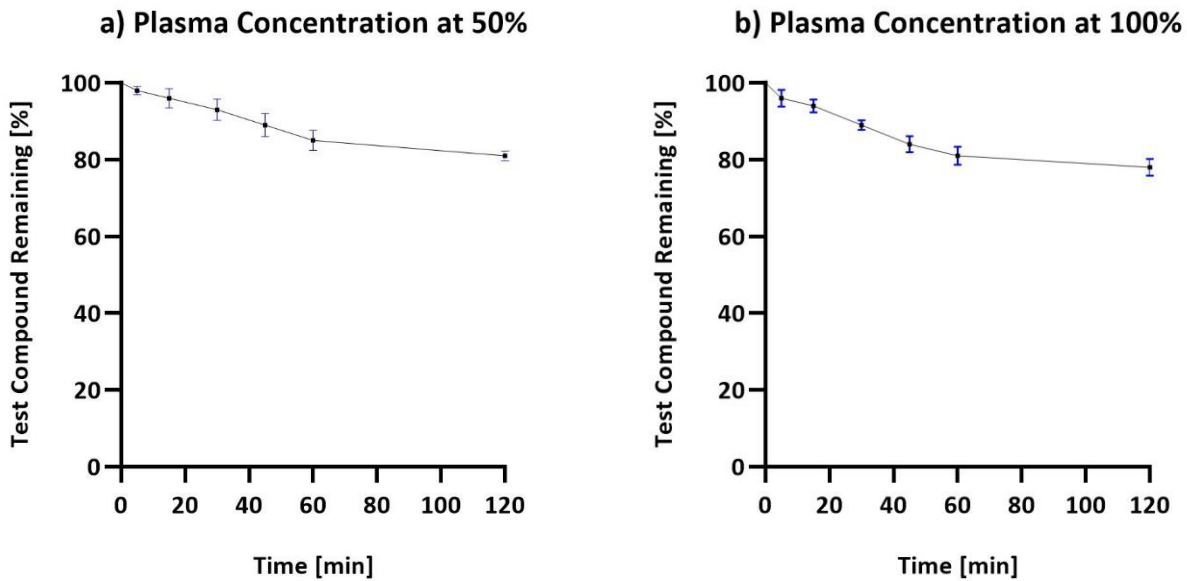
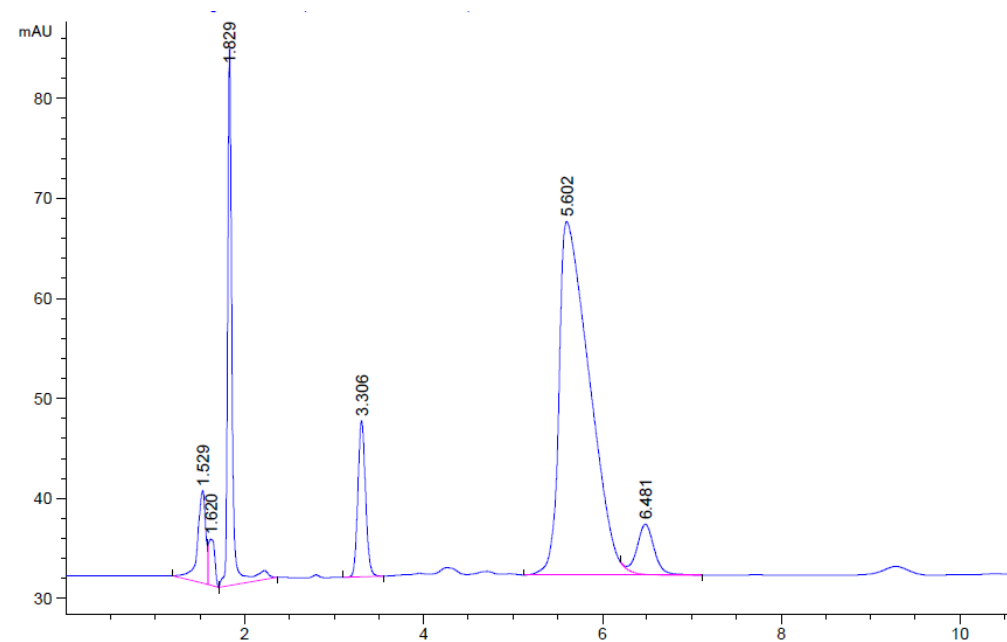


Figure 54 Above; Plotted data curves to show the % of RMP remaining over the different incubation periods, when tested with 50% and 100% Plasma concentrations. The graphs have been plotted using data from Table 14 & 15. Below; HPLC spectra obtained after running a sample containing RMP and 100% Plasma concentration after an incubation period of 120 minutes. HPLC system was injected with an 80:20 MeOH/H<sub>2</sub>O ratio



### 3.3.1 Plasma Stability – DBM and Derivatives (Compounds 1-10)

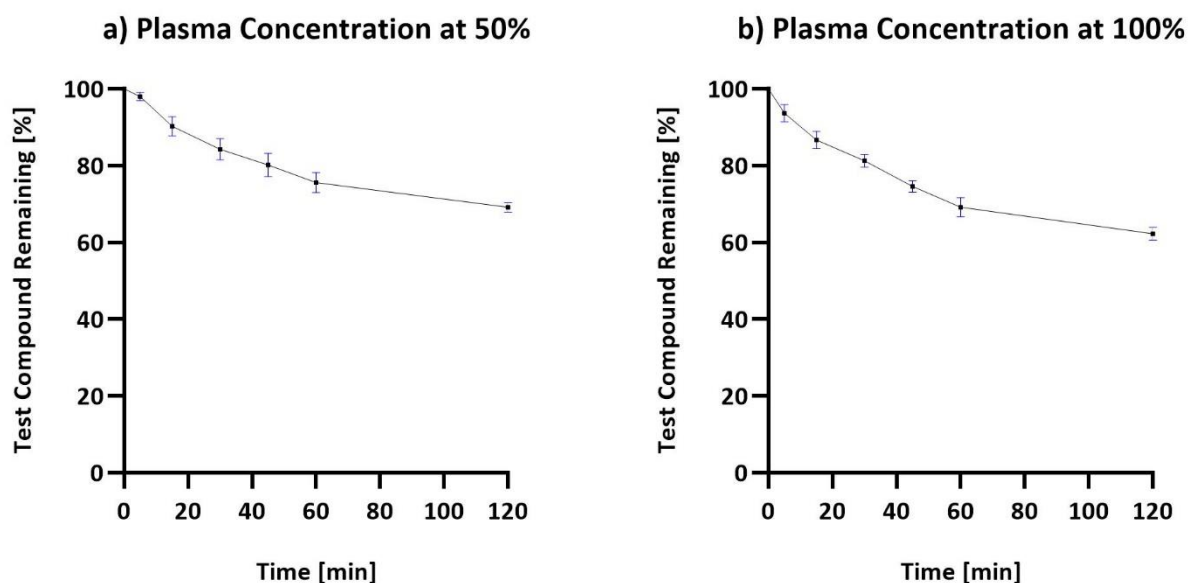


Figure 55 Plotted data curves to show the % of DBM remaining over the different incubation periods, when tested with 50% and 100% Plasma concentrations. The graphs have been plotted using data from Table 14 & 15

DBM has been stated to be a very stable compound till the 8h mark, however over a period of 120 minutes within this study, DBM was seen to degrade more than RMP. However, the concentration changes of plasma did not play a big role in the degradation since a percentage decrease of 30.8% was seen at 50% plasma compared to 37.7% within 100% plasma. This shows that the compound does not tend to undergo chemical changes such as hydrolysis or oxidation too much.

As seen with the MTT cytotoxicity assay, the  $\beta$ -diketone derivatives of DBM also underwent compound degradation, with results such as instability and stability being observed.

Candidates which contained the hydroxyl groups as part of their molecular substructure, Compounds 1,2, 3 and 5, all showed their ability to remain more stable than DBM in 50% plasma over a period of 120 minutes. Compound 2, which contained two hydroxyl groups was

the most stable out of all the derivatives, bringing into question the presence of more OH group, and the ability to form hydrogen bonds, since plasma contains water as a component. Compound 2, at a rate of 78.9% remaining, was followed by compound 1, which contained a sole hydroxyl group attached to the aromatic ring. This compound showed a 24.2% percentage decrease with 75.8% of compound available after degradation. Compounds 3 and 5, both which have additional functional groups attached in addition to the *Ortho* contained hydroxyl groups displayed close values in terms of the assay, as both compounds had 73.5% and 73.1% test compound remaining after 120minutes, a decrease of 26.5% and 26.9%. However, when the test conditions were changed to the usage of 100% plasma, the same compounds experienced degradation at a much higher rate, values which were equal to that of DBM. These values, calculated as percentage compound remaining were as follows; 65.6% (1), 68.3% (2), 64.2% (3) and 63.4% (5). These values were compared to that of DBM at 62.3%. From the plots below (Fig 56-59), it can be deduced that the stability of the compounds within 100% of plasma was much lower than that obtained from 50%. It was also noted that the compound, 2, which contained the most amount of hydroxyl groups, also experienced the most degradation. This maybe down to the effect of hydrolysis/oxidation taking place within the biological sample medium.

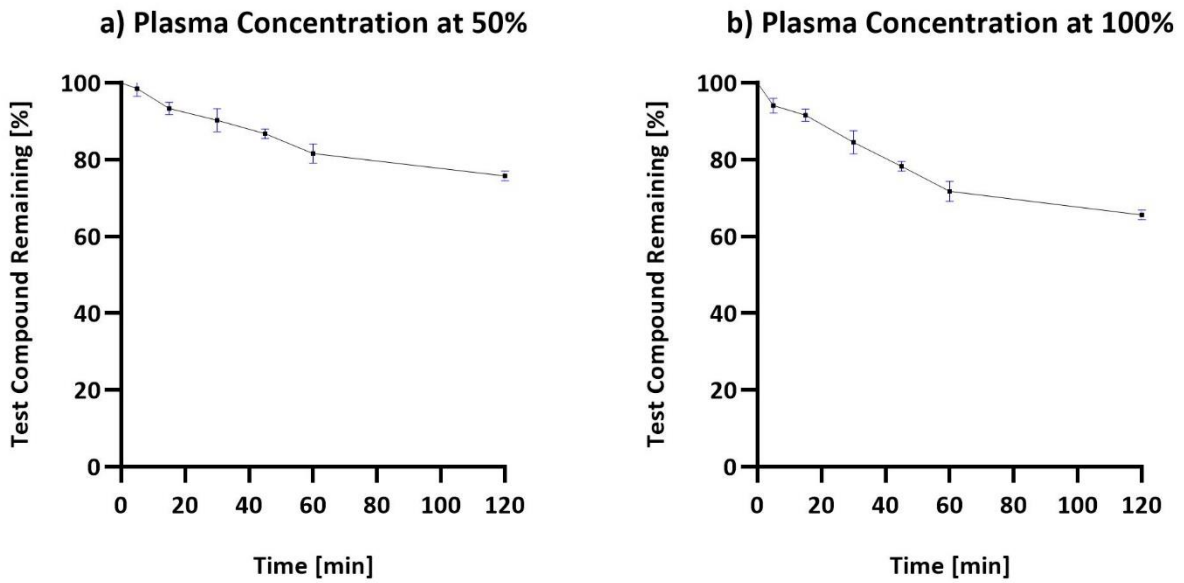
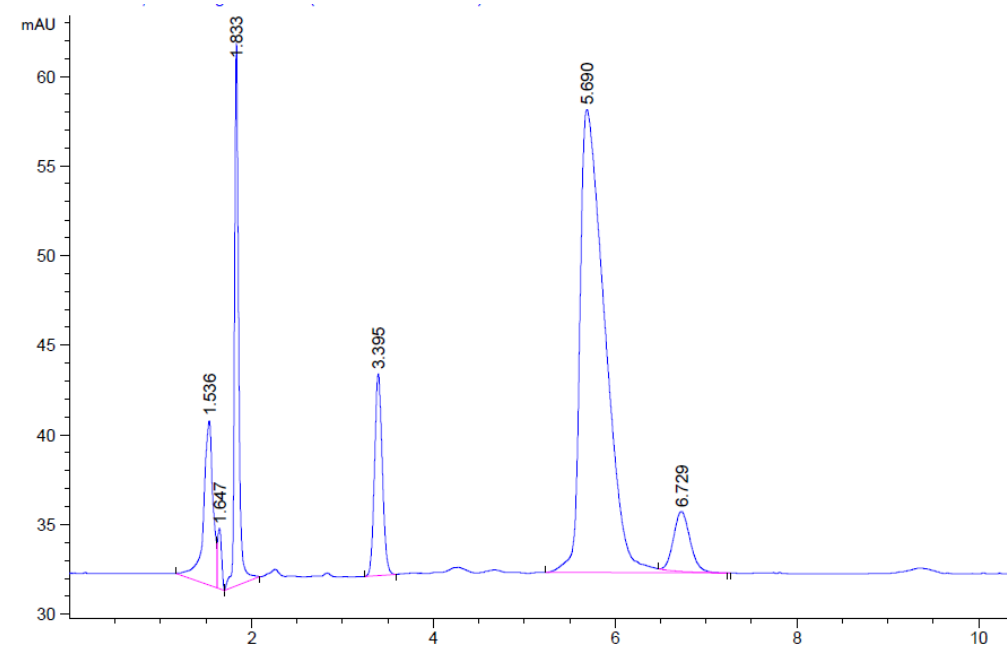


Figure 56 Plotted data curves to show the % of Compound 1 remaining over the different incubation periods, when tested with 50% and 100% Plasma concentrations. The graphs have been plotted using data from Table 14 & 15. Below; HPLC spectra obtained after running a sample containing Compound 1 and 50% Plasma concentration at incubation period 120 min. HPLC system was injected with an 80:20 MeOH/H<sub>2</sub>O ratio



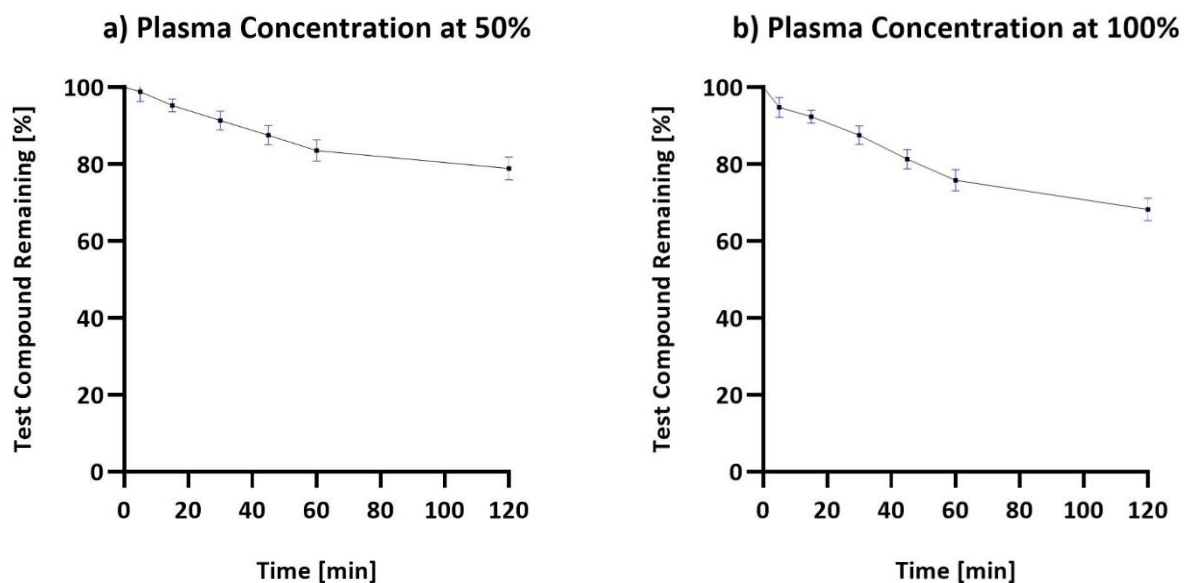
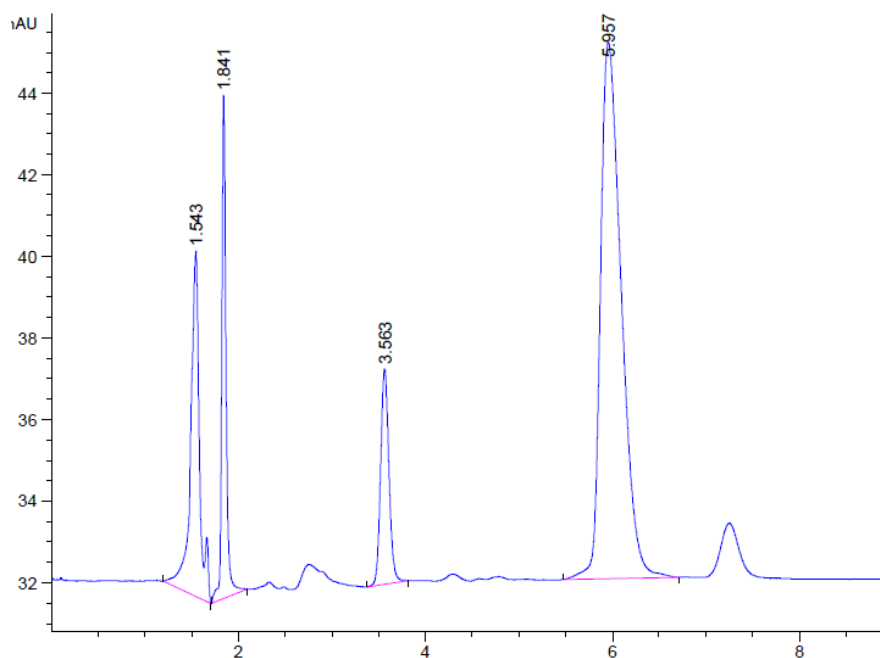


Figure 57 Plotted data curves to show the % of Compound 2 remaining over the different incubation periods, when tested with 50% and 100% Plasma concentrations. The graphs have been plotted using data from Table 14 & 15. Below; HPLC spectra obtained after running a sample containing Compound 2 and 100% Plasma concentration at incubation period 120 min. HPLC system was injected with an 80:20 MeOH/H<sub>2</sub>O ratio



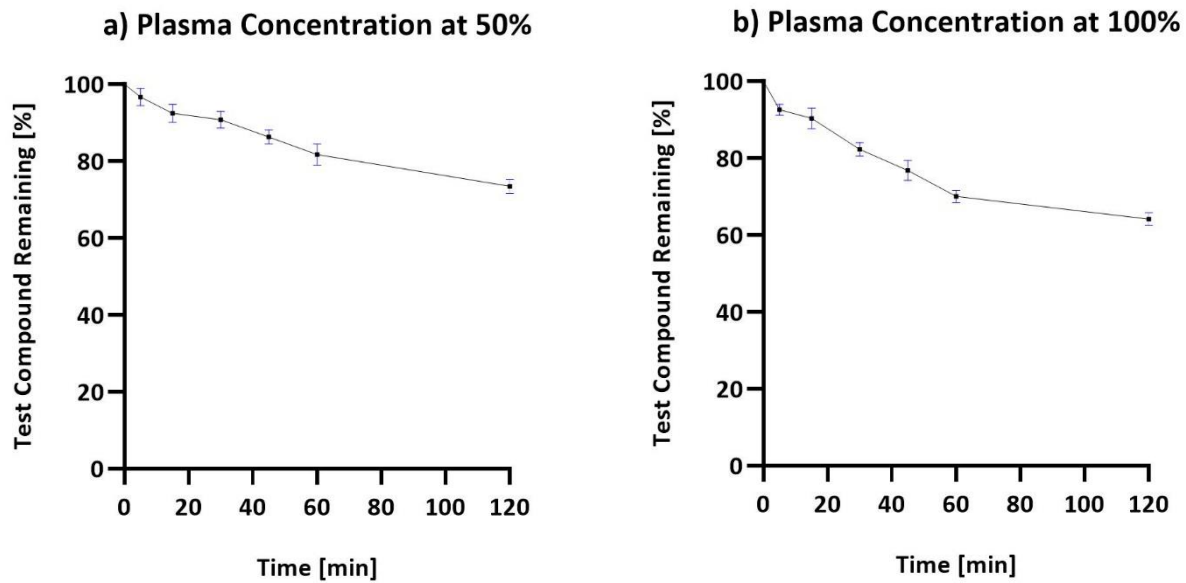
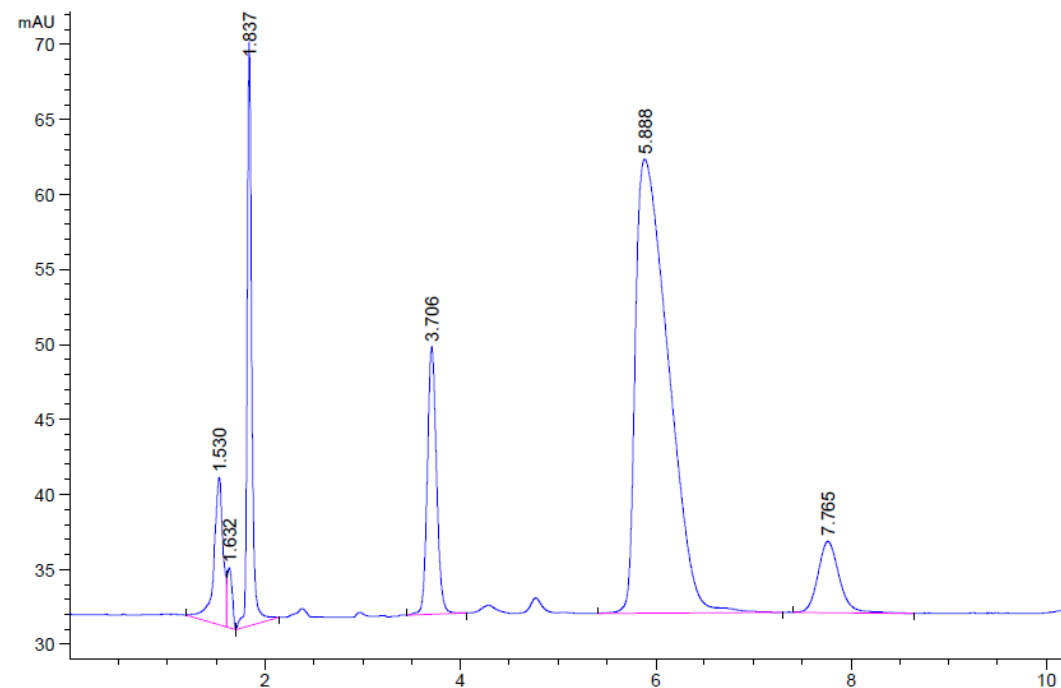


Figure 58 Plotted data curves to show the % of Compound 3 remaining over the different incubation periods, when tested with 50% and 100% Plasma concentrations. The graphs have been plotted using data from Table 14 & 15. Below; HPLC spectra obtained after running a sample containing Compound 3 and 50% Plasma concentration at incubation period 120 min. HPLC system was injected with an 80:20 MeOH/H<sub>2</sub>O ratio



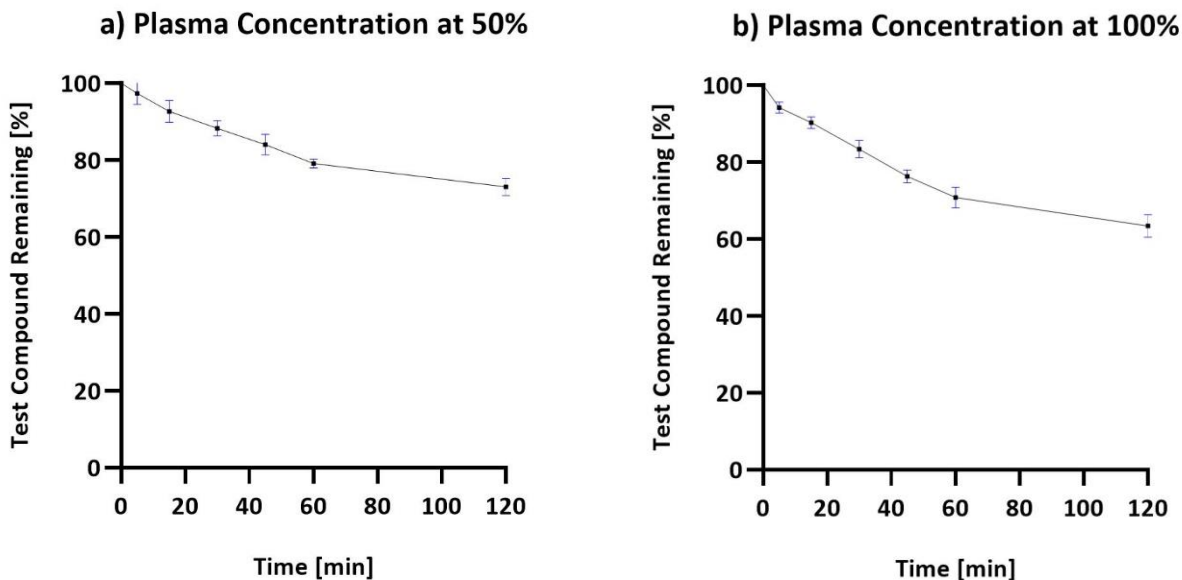
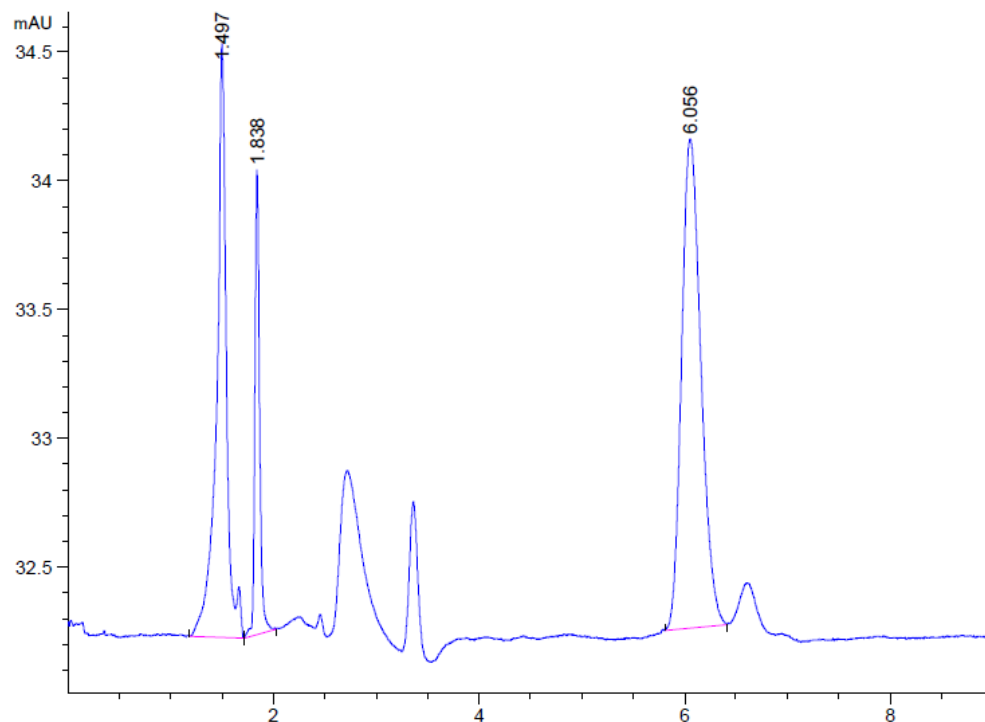


Figure 59 Plotted data curves to show the % of Compound 5 remaining over the different incubation periods, when tested with 50% and 100% Plasma concentrations. The graphs have been plotted using data from Table 14 & 15. Below; HPLC spectra obtained after running a sample containing Compound 5 and 100% Plasma concentration at incubation period 120 min. HPLC system was injected with an 80:20 MeOH/H<sub>2</sub>O ratio



Changing the group attached to the central carbon atom of the 1,3 diketone into a Br only showed a negative outcome, whereby the compound (4), was stable (68.7%) in 50% plasma, however rapidly degraded in 100% plasma (50.2%), a percentage decrease to be calculated at 49.8%. This further highlights the ability that a carbon, oxygen or nitrogen group attached to the central carbon can provide a stable effect. The rate the bromo containing compound degrades is shown below in Fig 60.

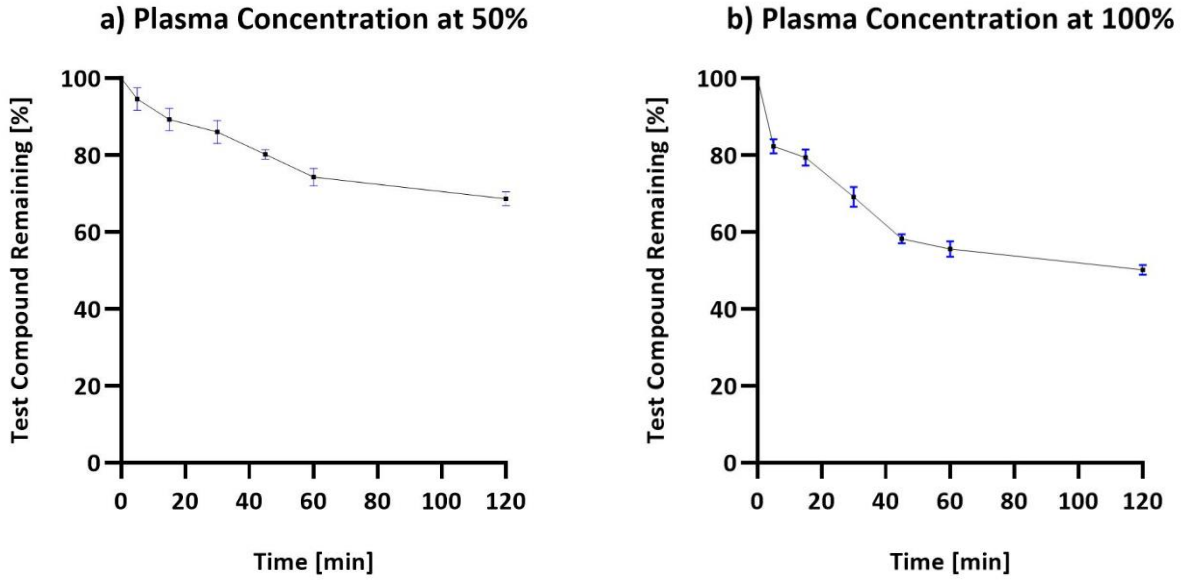
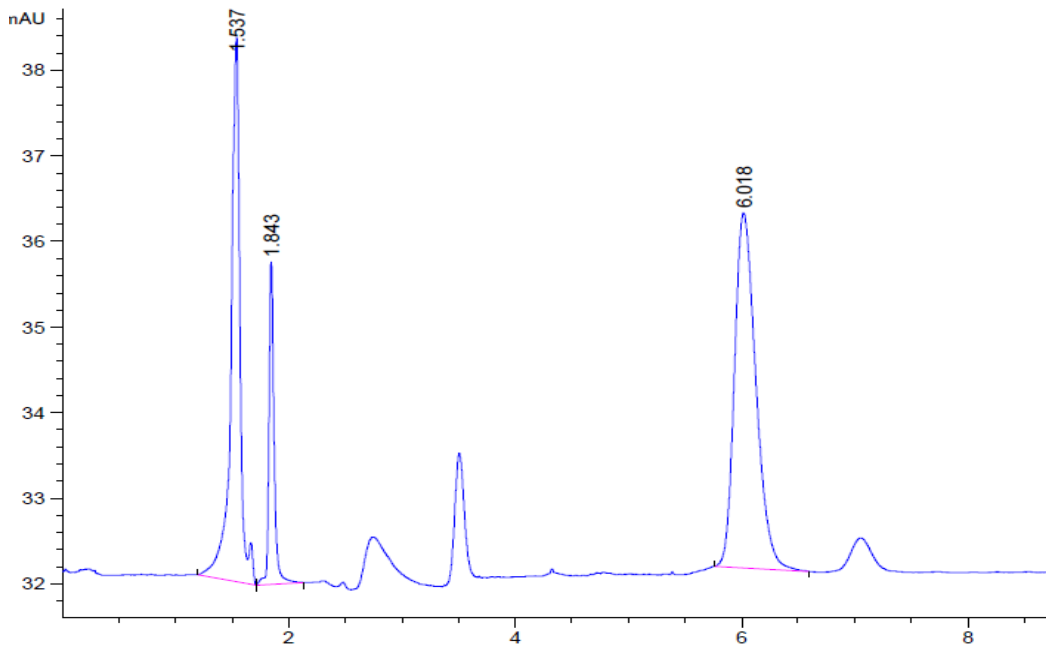


Figure 60 Plotted data curves to show the % of Compound 4 remaining over the different incubation periods, when tested with 50% and 100% Plasma concentrations. The graphs have been plotted using data from Table 14 & 15. Below; HPLC spectra obtained after running a sample containing Compound 4 and 50% Plasma concentration at incubation period 120 min. HPLC system was injected with an 80:20 MeOH/H<sub>2</sub>O ratio



Other  $\beta$ -diketone derivatives tested for stability under the conditions, were the methoxy containing compounds, 6, 9 and 10.

Compound 6 contains a simple methoxy group attached in the 4' *Para* position of the aromatic, which is then symmetrical, therefore gives rise to a 'Bis molecule. A  $\text{CH}_3$  group bond to the aromatic ring, with the help of an Oxygen, the methoxy group is classified as an ether, and is quite similar to an ester group. Ester's have been known to undergo rapid hydrolysis thus rendering themselves as relatively unstable. Compound 6 however seems to contradict this theory and remains quite stable when incubated in 50% plasma (69.9%), a value not far from DBM (69.2%). However, a steady degradation is observed when the conditions change to full concentration of plasma, whereby the compound remaining has been reduced to 59.3%. Again, when compared to DBM (62.3%), this change in value is minimal and rapid hydrolysis is not observed here. The same steady change of time, under both conditions is seen with compounds 9 & 10, whereby methoxy groups were present as a group or on both rings. Both these compounds are much alike compound 6, where the percentage decrease in 50% plasma went from 37.2% and 37% to 43.8% for both within 100% plasma.

When a fluorine group was added on the aromatic, with the methoxy groups still present, compounds 7 & 8 displayed the same activity as mentioned above, and a steady degradation of the compounds was observed in both 50% and 100% plasma conditions. The values calculated for both compounds in 50% plasma (64% and 63.9% remaining) and 100% (59.1% and 60.3%) was again relatively minimal in terms of rapid degradation.

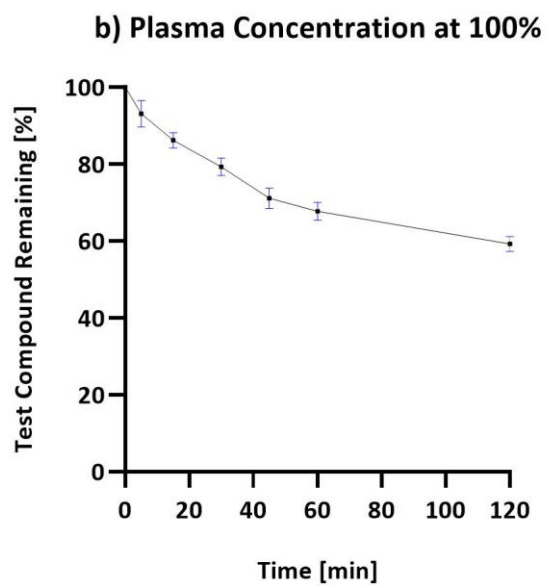
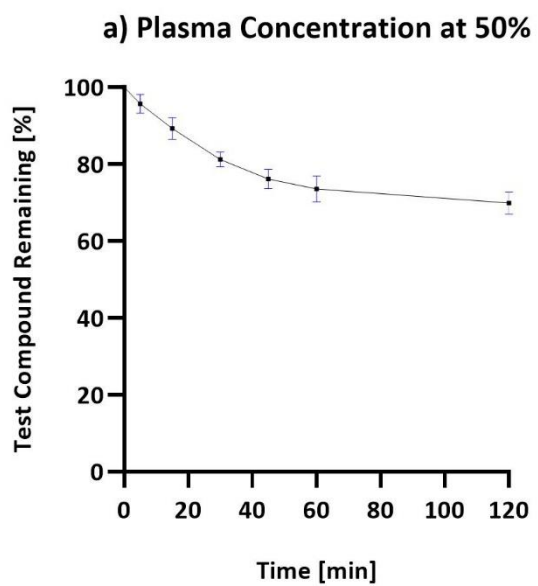


Figure 61 Plotted data curves to show the % of Compound 6 remaining over the different incubation periods, when tested with 50% and 100% Plasma concentrations. The graphs have been plotted using data from Table 14 & 15.

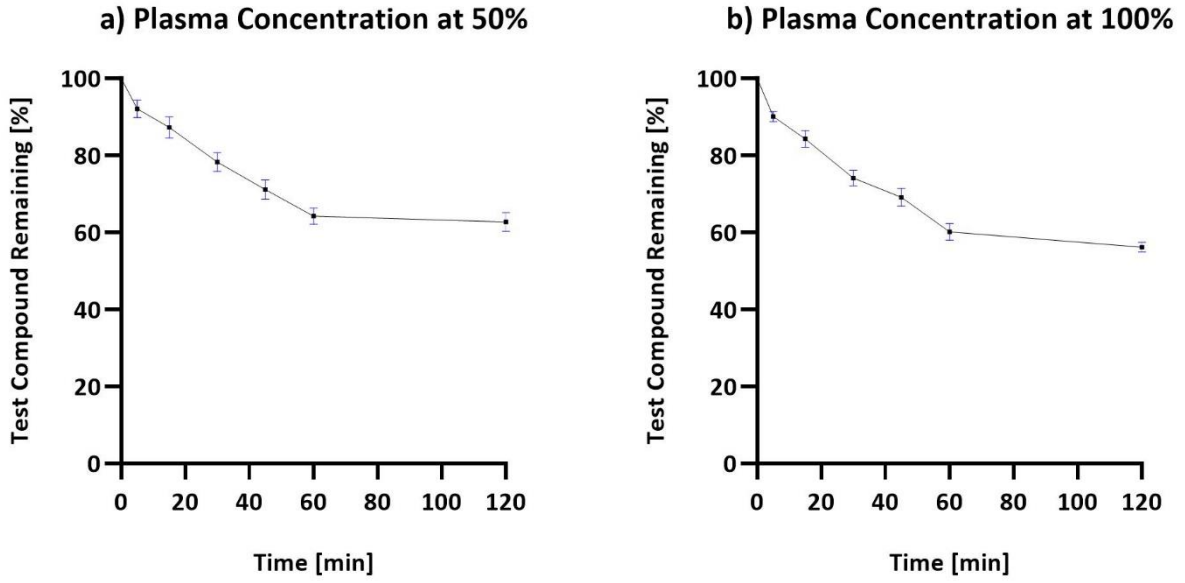
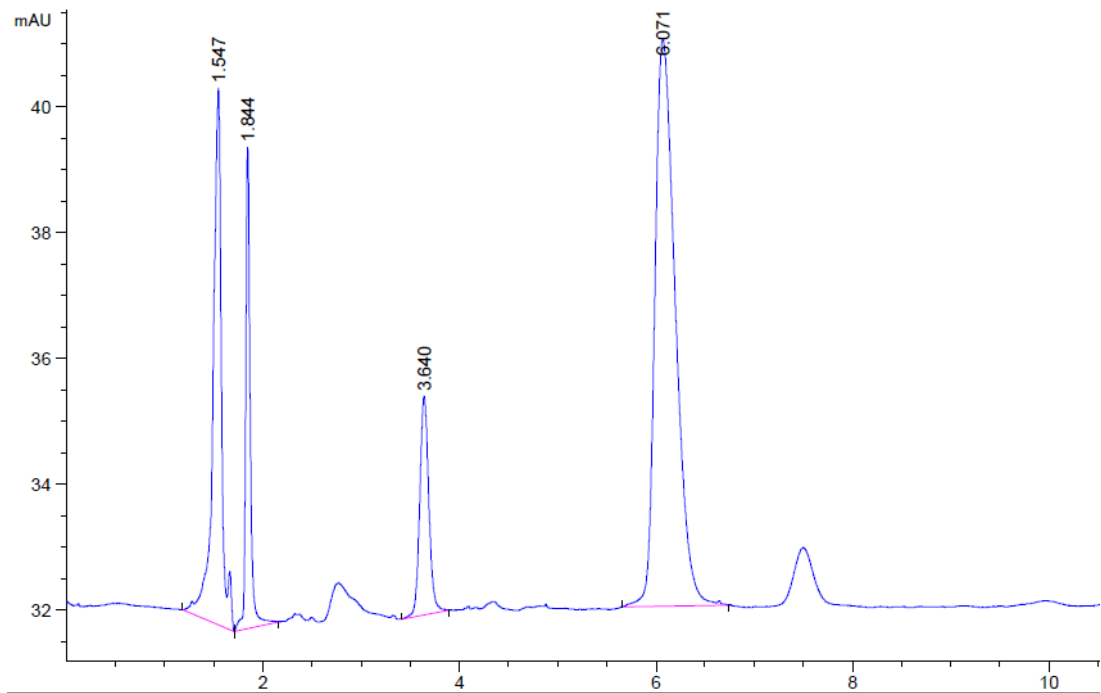


Figure 62 Plotted data curves to show the % of Compound 9 remaining over the different incubation periods, when tested with 50% and 100% Plasma concentrations. The graphs have been plotted using data from Table 14 & 15. Below; HPLC spectra obtained after running a sample containing Compound 9 and 50% Plasma concentration at incubation period 120 min. HPLC system was injected with an 80:20 MeOH/H<sub>2</sub>O ratio



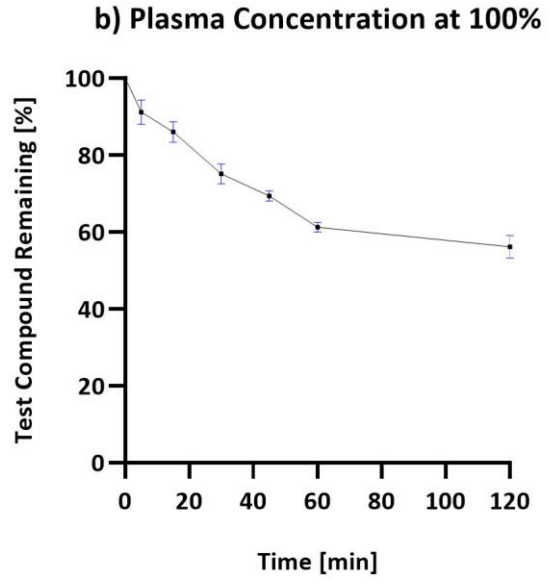
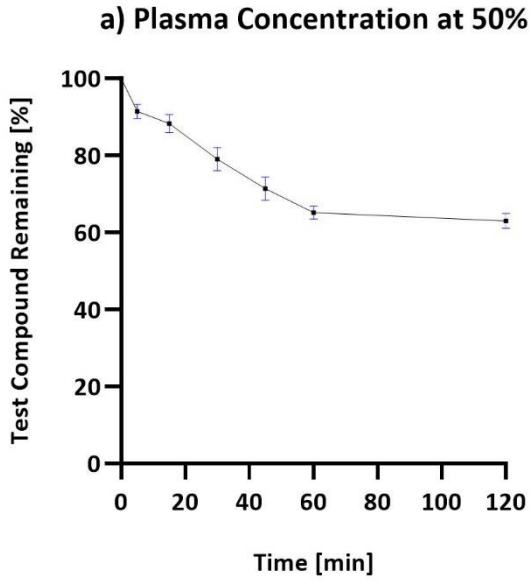


Figure 63 Plotted data curves to show the % of Compound 10 remaining over the different incubation periods, when tested with 50% and 100% Plasma concentrations. The graphs have been plotted using data from Table 14 & 15

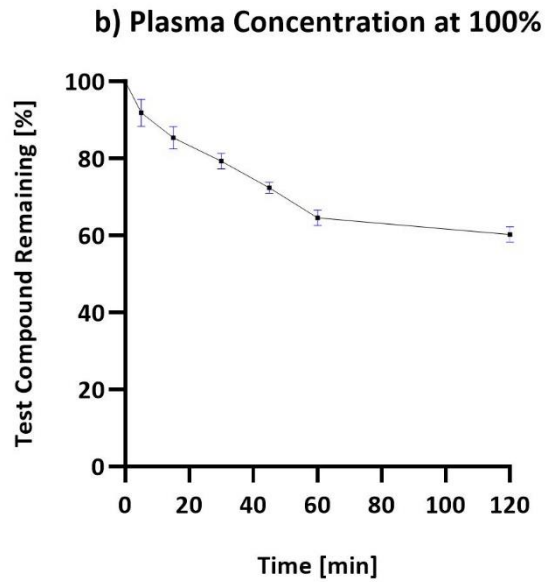
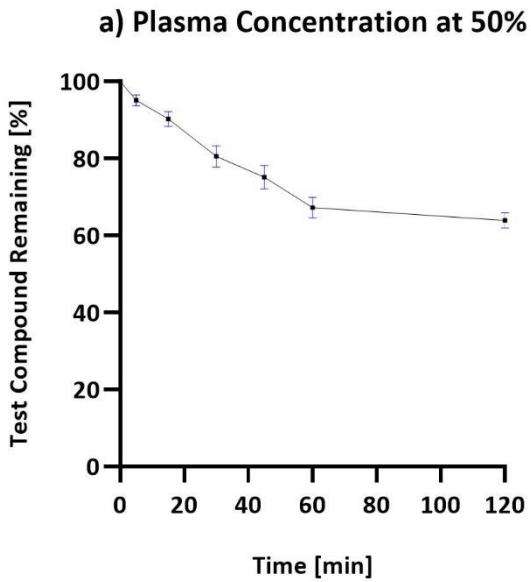


Figure 64 Plotted data curves to show the % of Compound 7 remaining over the different incubation periods, when tested with 50% and 100% Plasma concentrations. The graphs have been plotted using data from Table 14 & 15

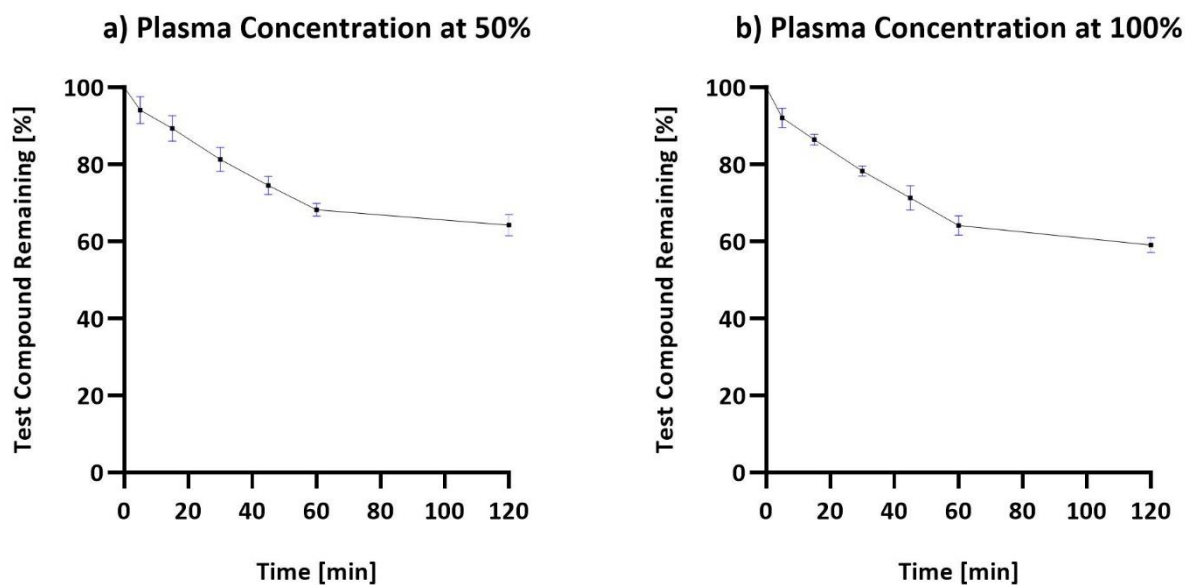
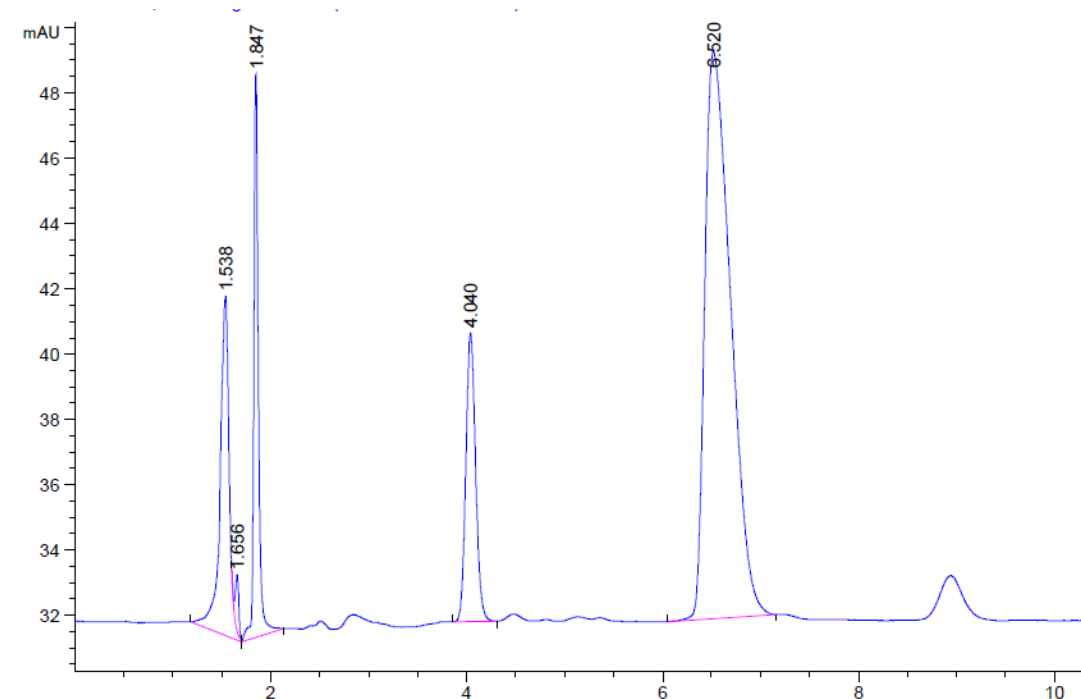


Figure 65 Plotted data curves to show the % of Compound 8 remaining over the different incubation periods, when tested with 50% and 100% Plasma concentrations. The graphs have been plotted using data from Table 14 & 15. Below; HPLC spectra obtained after running a sample containing Compound 8 and 50% Plasma concentration at incubation period 120 min. HPLC system was injected with an 80:20 MeOH/H<sub>2</sub>O ratio



The plots illustrated in Fig, 62-65 show the results where no rapid hydrolysis or compound degradation has taken place.

### 3.3.2 Plasma Stability – 2-Azido Derivatives (Compounds 11 -13)

Compounds 11,12 & 13 were synthesised with the option of allowing the  $\beta$ -diketone derivatives to contain a carbon, oxygen or nitrogen group at the central 1,3 diketone centre, in order to monitor the stability and efficacy of the bond. These nitrogen salt containing compounds should in theory provide a stable bond due to the ability of the nitrogen to openly bond, however this ideology has been proven wrong, since the data obtained shows the opposite effect taking place, ie compound instability. Table 14 shows the data values calculated for the percentage of compound which was remaining in 50% plasma, and all three compounds, 11,12 & 13 show a high level of instability where near less than half of the tested compound was remaining after 120 minutes. The values obtained 46.3% (11), 50.7% (12), 49.1% (13) were over 20% different from the compounds they were initially based upon in terms of substructure similarity (DBM, 1 and 3). Testing at 100% plasma, further rendered the use of the compounds negligible, since a rapid degradation trend was seen, whereby the compound/s remaining were less than 40%, this would show a percentage decrease of 60%. Compounds which contained some form of hydroxyl group, 12 (37.8%) and 13 (35.6) showed some stability in comparison to 11 (28.3%), which may not have lasted an assay of 4-8h of testing.

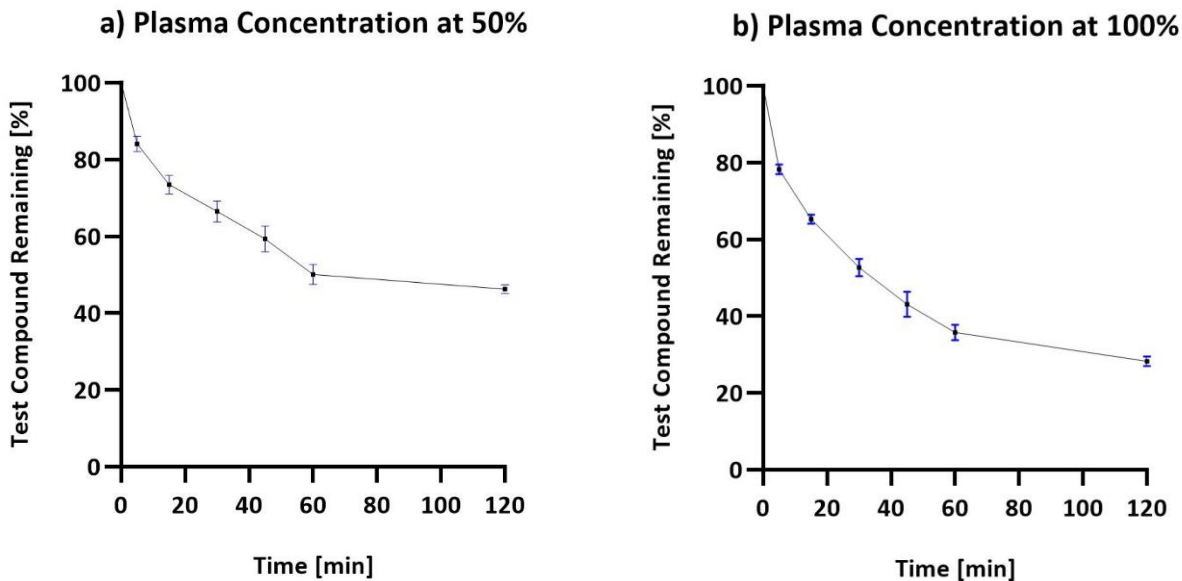
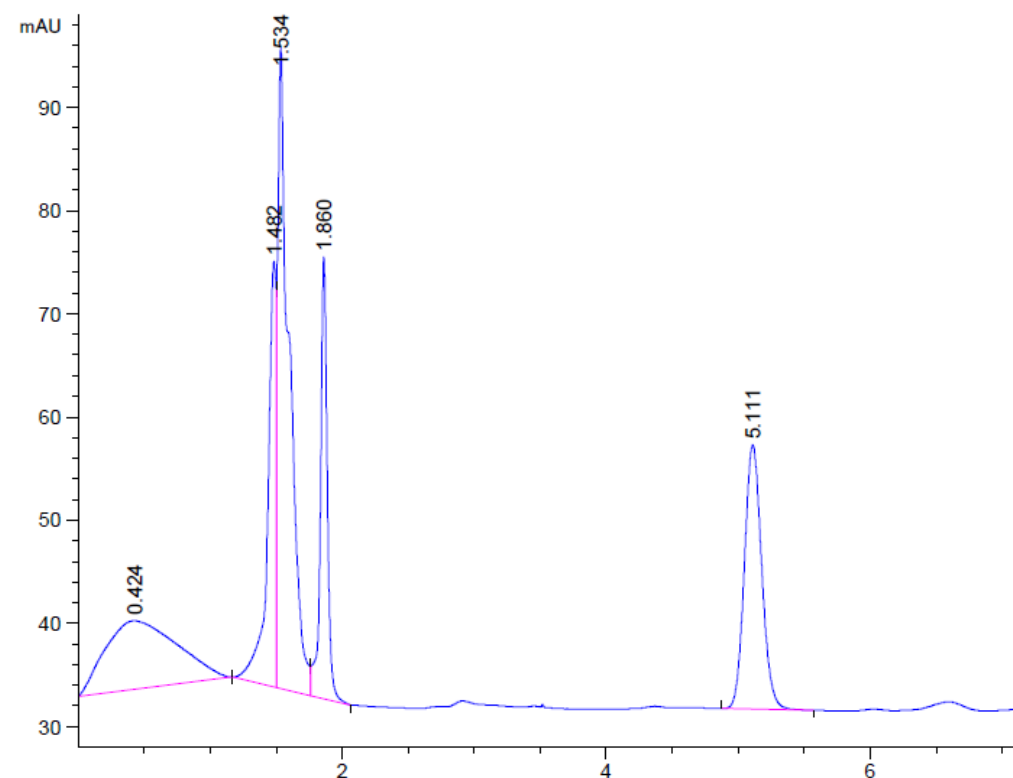


Figure 66 Plotted data curves to show the % of Compound 11 remaining over the different incubation periods, when tested with 50% and 100% Plasma concentrations. The graphs have been plotted using data from Table 14 & 15. Below; HPLC spectra obtained after running a sample containing Compound 11 and 100% Plasma concentration at incubation period 120 min. HPLC system was injected with an 80:20 MeOH/H<sub>2</sub>O ratio



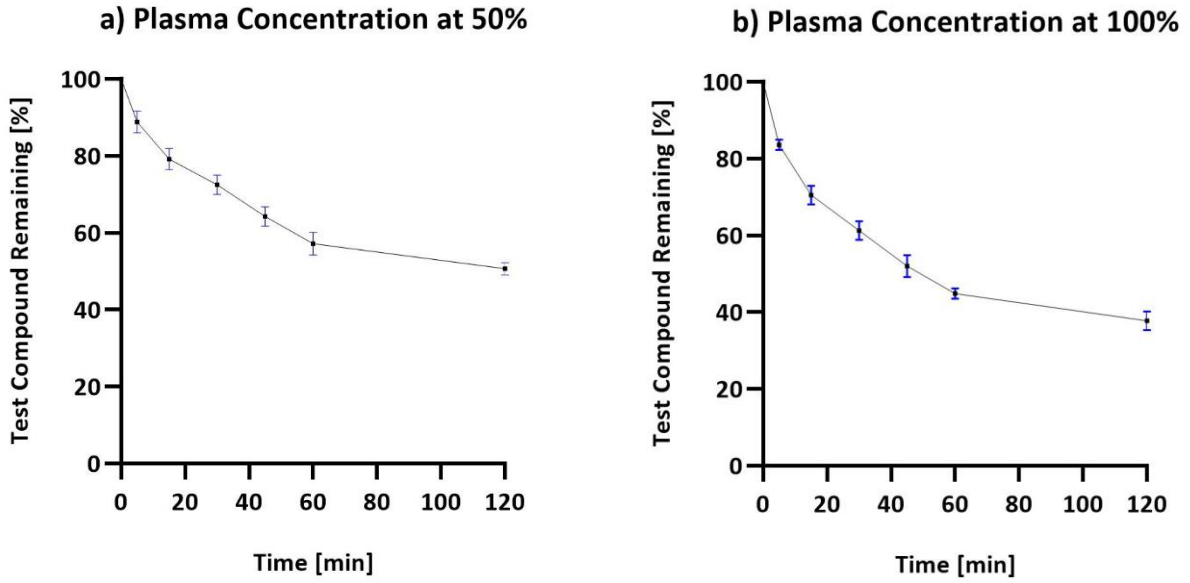
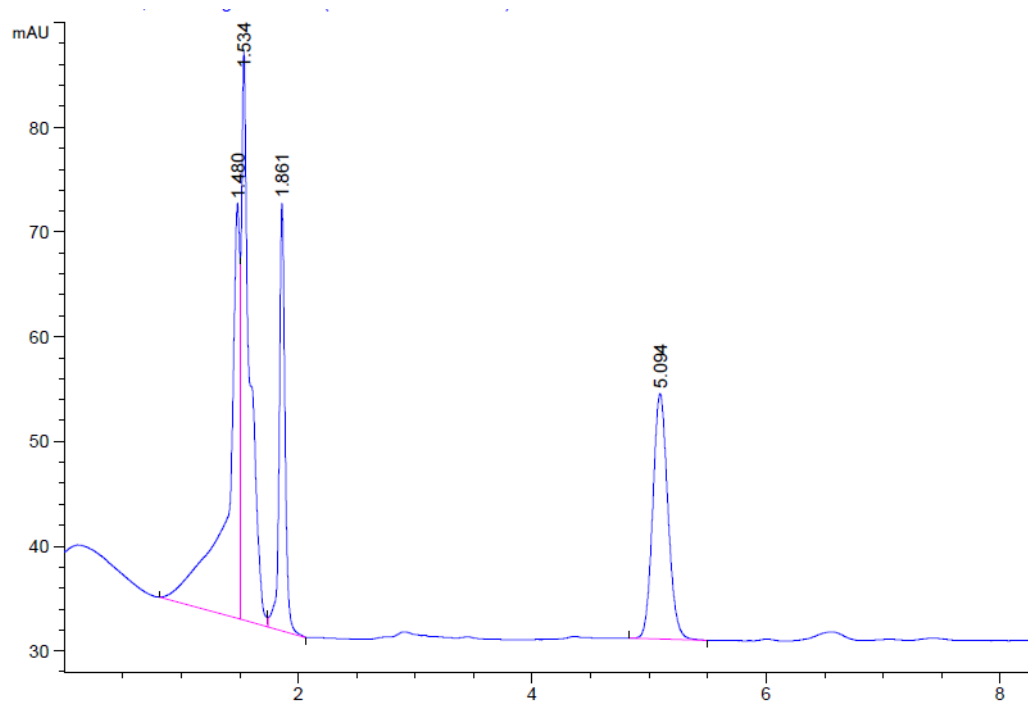


Figure 67 Plotted data curves to show the % of Compound 12 remaining over the different incubation periods, when tested with 50% and 100% Plasma concentrations. The graphs have been plotted using data from Table 14 & 15. Below; HPLC spectra obtained after running a sample containing Compound 12 and 100% Plasma concentration at incubation period 120 min. HPLC system was injected with an 80:20 MeOH/H<sub>2</sub>O ratio



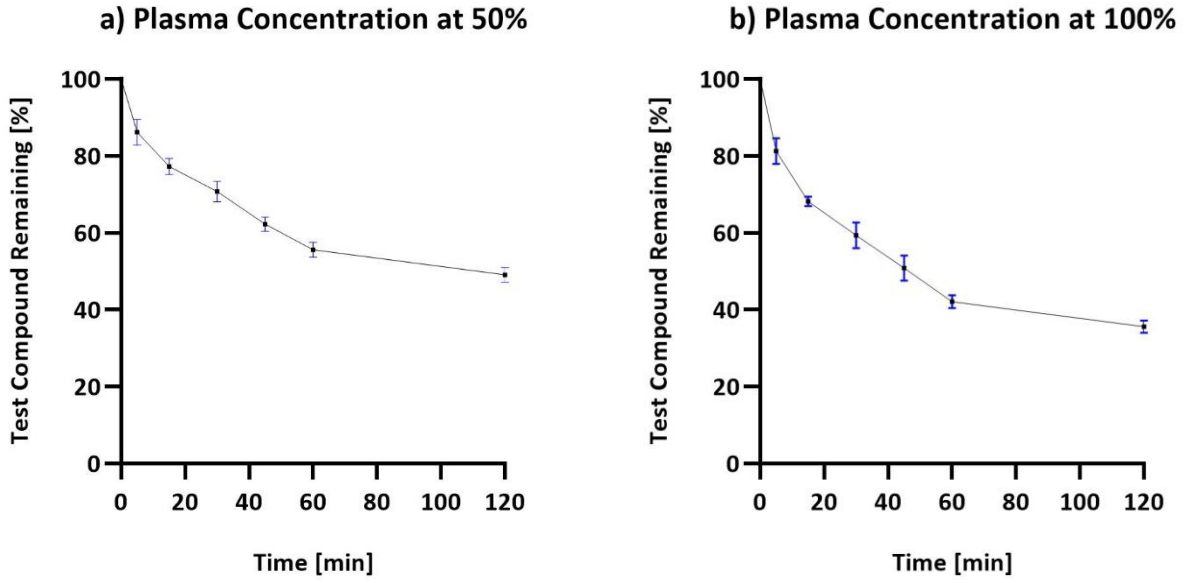
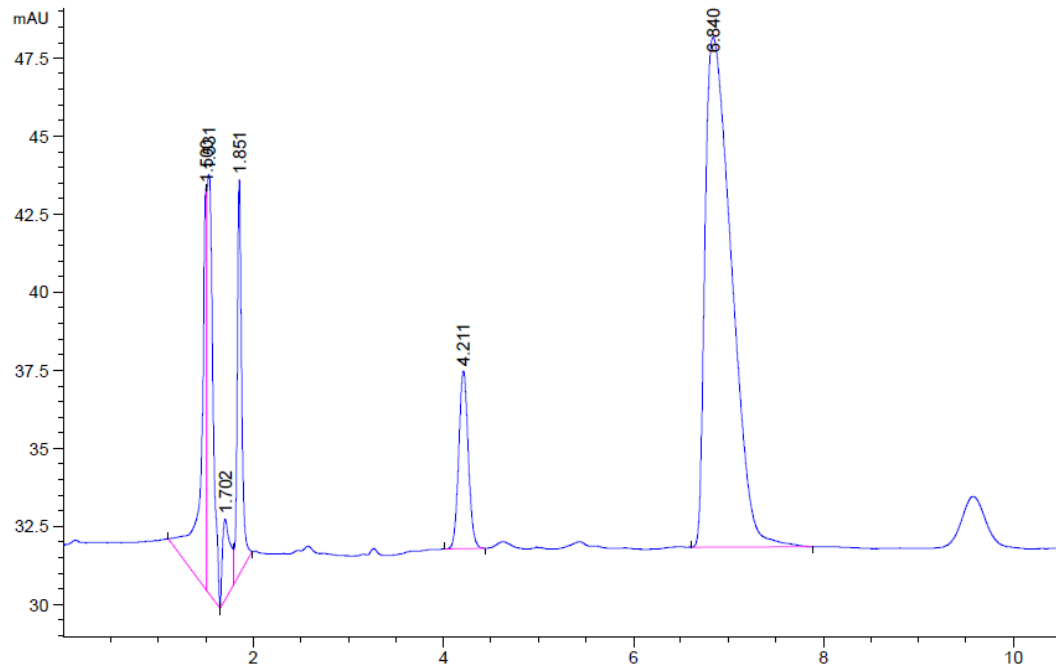


Figure 68 Plotted data curves to show the % of Compound 13 remaining over the different incubation periods, when tested with 50% and 100% Plasma concentrations. The graphs have been plotted using data from Table 14 & 15. Below; HPLC spectra obtained after running a sample containing Compound 13 and 50% Plasma concentration at incubation period 120 min. HPLC system was injected with an 80:20 MeOH/H<sub>2</sub>O ratio



The graphical plots further highlight the fact that the nitrogen salts did not favour the plasma conditions and may not provide the potential to be a future target compound.

### 3.3.3 Plasma Stability – Benzoylurea Derivatives (Compounds 14 - 16)

Benzoylurea's, which in contrast to the  $\beta$ -diketone derivatives and azido salts are bulky molecules with respect to containing several different functional groups and bonds, displayed excellent stability in both plasma conditions, with values near the internal standard, RMP. It may be down to the different properties contained within the benzoylureas, or the presence of certain bonds such as the amide (-NH) bond, all three compounds of this subclass, 14,15 and 16 showed a loss of no more than 20%, with the following values being obtained; 82.3% (14), 80.1% (15) and 81.2% (16) in 50% plasma, which then decreased slightly to 79.3% (14), 79.2 (15) and 80.3% (16) in 100% plasma. The minimal nominal changes experienced by the three compounds suggest that the bulkiness of the molecules, with the addition of different bonds, provides a platform for the compound to exhibit a higher level of stability within biological media. Due to this much required property, the ability of a drug to stay in the body in order to induce its maximal effects is seen as successful.

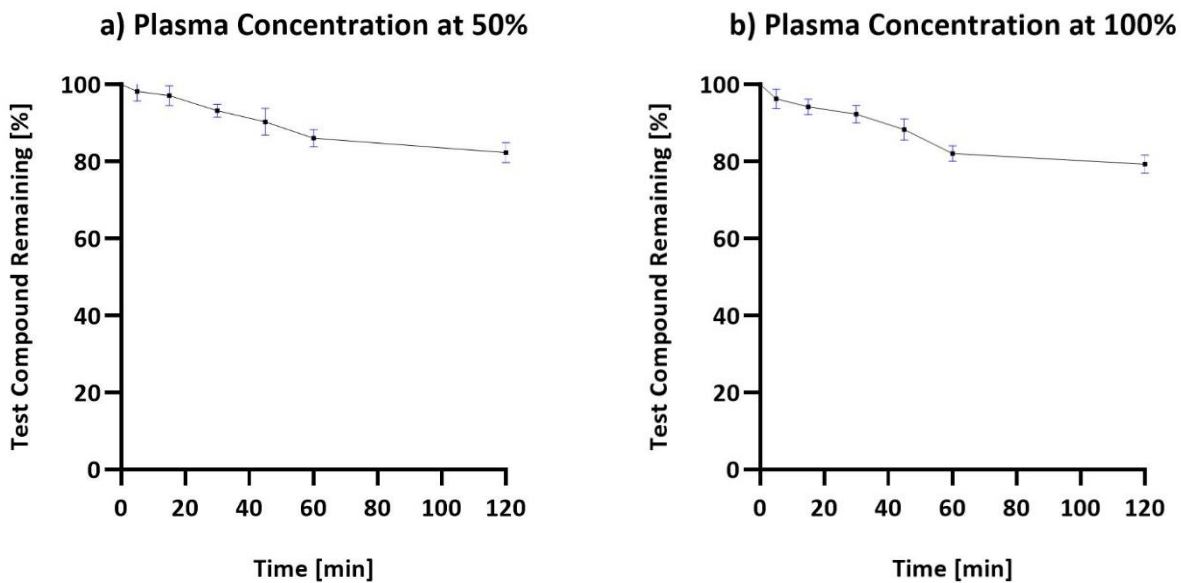
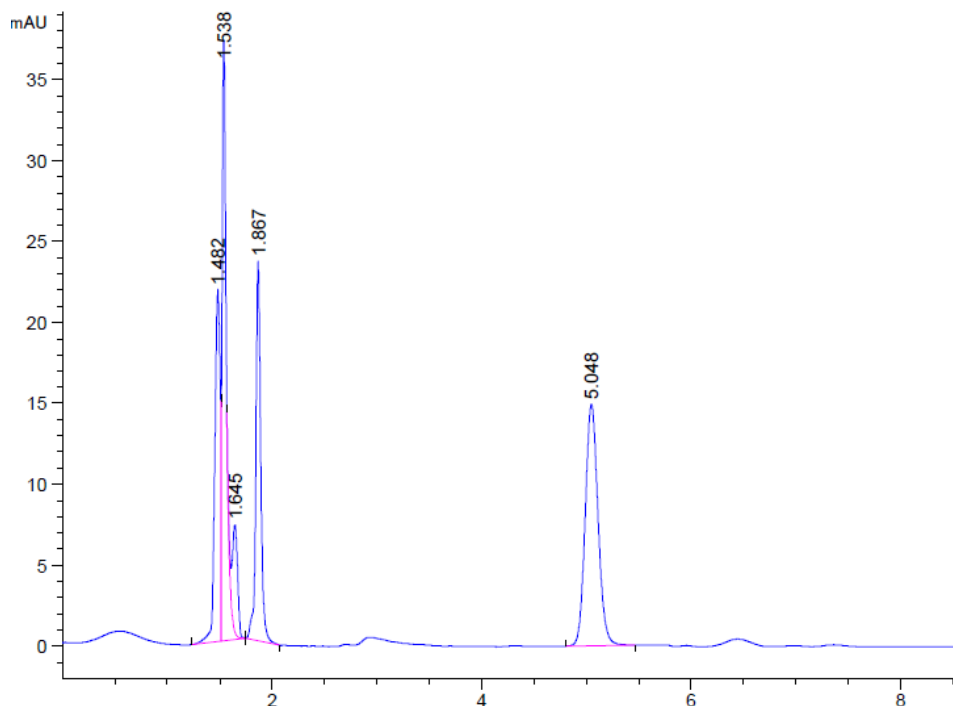


Figure 69 Plotted data curves to show the % of Compound 14 remaining over the different incubation periods, when tested with 50% and 100% Plasma concentrations. The graphs have been plotted using data from Table 14 & 15. Below; HPLC spectra obtained after running a sample containing Compound 14 and 100% Plasma concentration at incubation period 120 min. HPLC system was injected with an 80:20 MeOH/H<sub>2</sub>O ratio



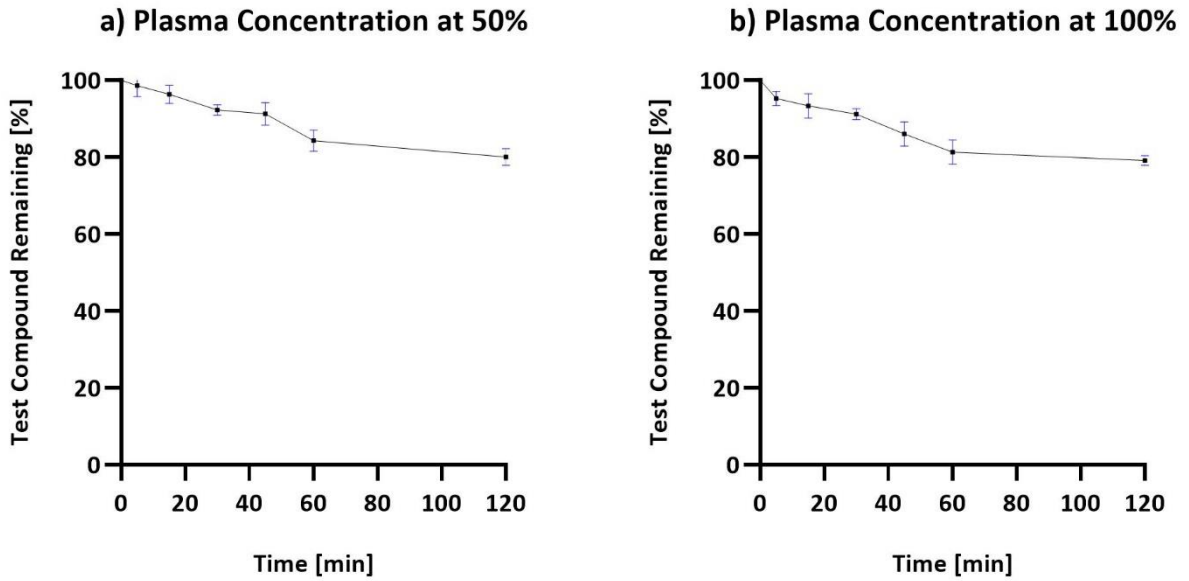
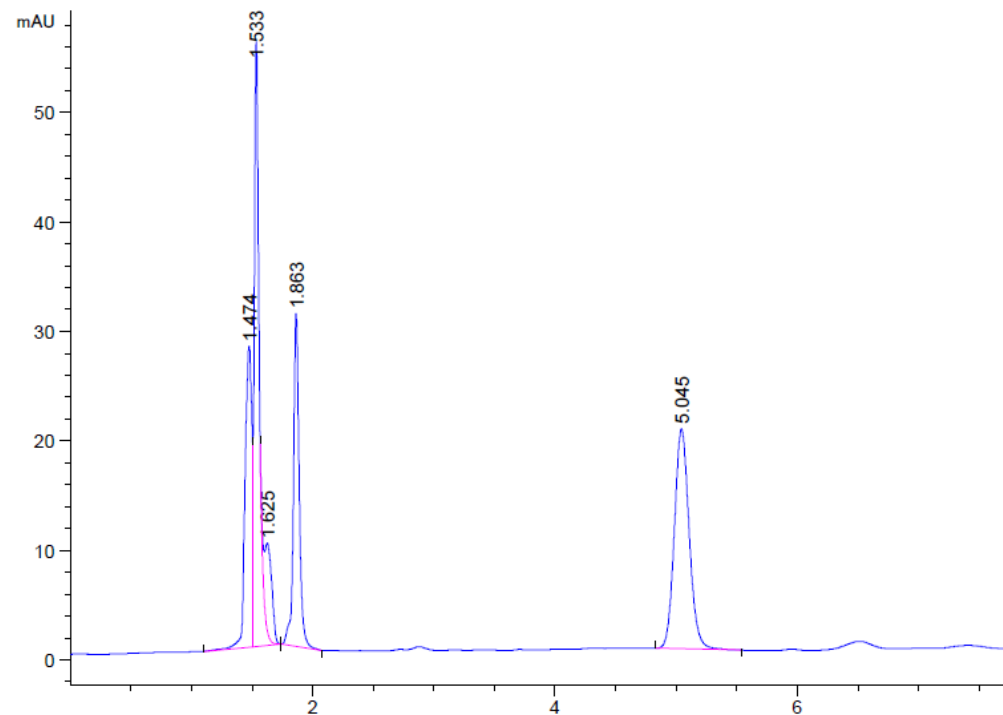


Figure 70 Plotted data curves to show the % of Compound 15 remaining over the different incubation periods, when tested with 50% and 100% Plasma concentrations. The graphs have been plotted using data from Table 14 & 15. Below; HPLC spectra obtained after running a sample containing Compound 15 and 100% Plasma concentration at incubation period 120 min. HPLC system was injected with an 80:20 MeOH/H<sub>2</sub>O ratio



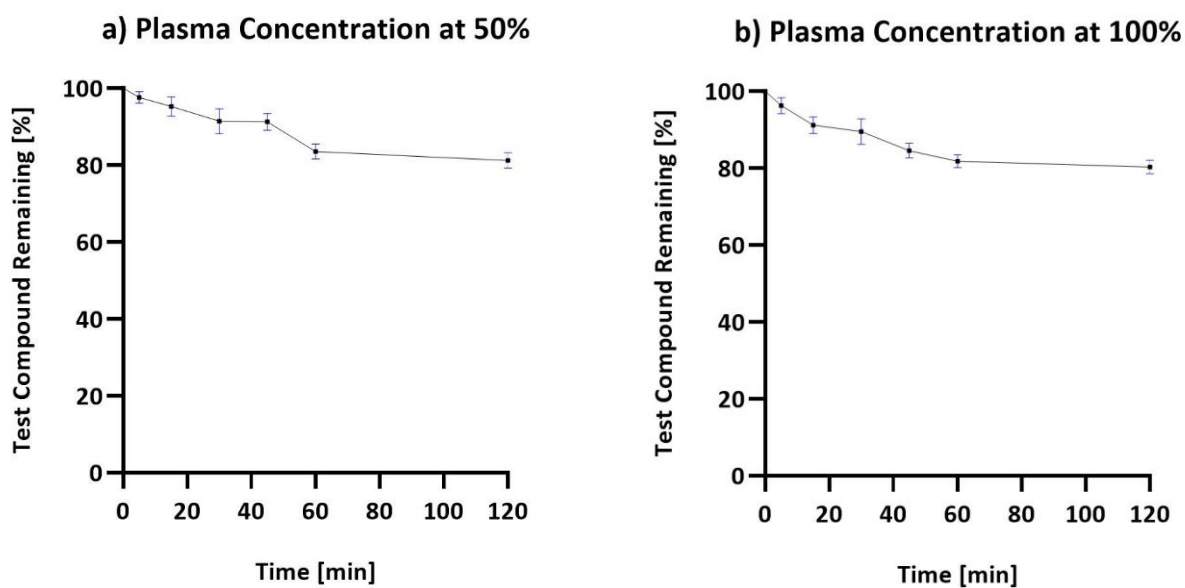
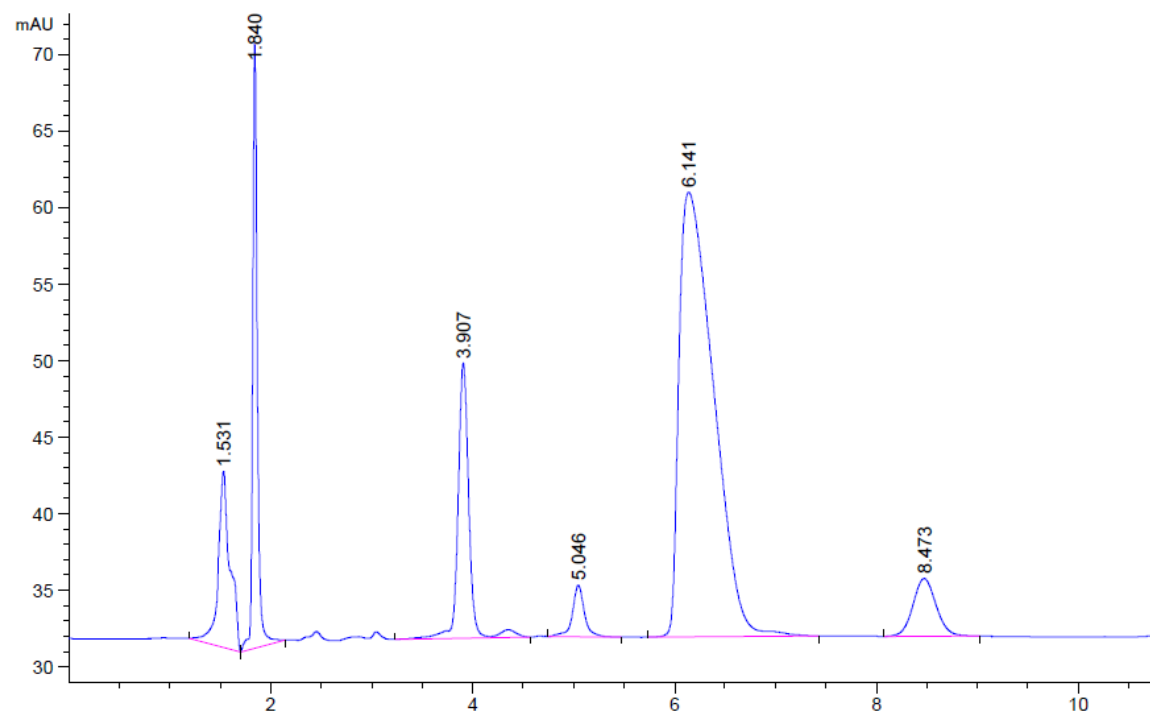


Figure 71 Plotted data curves to show the % of Compound 16 remaining over the different incubation periods, when tested with 50% and 100% Plasma concentrations. The graphs have been plotted using data from Table 14 & 15. Below; HPLC spectra obtained after running a sample containing Compound 16 and 50% Plasma concentration at incubation period 120 min. HPLC system was injected with an 80:20 MeOH/H<sub>2</sub>O ratio



Figs 69-71 plots showing the relative stability of all three benzoylurea compounds

It should be noted that the tested compounds, be it the active drug or their metabolites may at the time of testing not be relative to their initial concentration measured. This correlates with the fact that optimal conditions for the compounds in question are not maintained in terms of handling, storing or even processing the samples prior to their analysis and testing as mentioned by Reid., (2016). Due to this, the results obtained may not accurately reflect the concentration of the compound in the sample to when it was acquired prior to the testing phase. Since this may be the case, the analytes maybe unstable under the conditions they were exposed to, thus leading to an earlier and quicker degradation. The same can be said for the biological medium such as serum and plasma in addition to the compounds which were tested. Leading on this can be a factor within this study, since the plasma which was initially stored at  $-20^{\circ}\text{C}$ , was then thawed at room temperature and then frozen again. It has been suggested that in these circumstances where samples are thawed and stored, that the stability testing be run multiple times over freeze/thaw cycles. Toseland et al., (2010) advice that the best storage for the temperature of most drugs is at  $4^{\circ}\text{C}$  for short-term storage and at  $-20^{\circ}\text{C}$  for long-term storage. However, it should be considered that even though freezing and decreasing the temperature slows down both the rate of metabolic and chemical degradation, it does not absolutely stop those processes from occurring. Previous studies have reported the potential findings with regards to the stability of drugs *in vitro*. El Mahjob et al (2006) observed that the drugs Midazolam, Oxazepam, Clonazepam amongst others were found to be stable for a period of 1 year when optimal conditions were utilised such as storage at  $-80^{\circ}\text{C}$ . When compounds were stored at a lower temperature ( $-20^{\circ}\text{C}$ ), there was losses of 5% and 20% found for the high and low concentrations respectively. This further followed by the storage condition increasing in temperature to  $4^{\circ}\text{C}$ , whereby the effect of

refrigeration caused a decrease in concentration of 50% for the high dose concentration and more than 90% for the low concentration. Finally, when the study was conducted on compounds stored at RT, the losses at low concentration for all drugs were at 100% and 70% for the high concentration. This links to the  $\beta$ -diketone derivatives, where changes in temperature effect the equilibrium balance of the keto-enol tautomer. A change in the structure or bond between the functional group can cause different activity responses to be generated, which may have a fundamental effect on the assays, since a C=C double bond of the alkene is much less reactive due to electronegativity when compared with that of a C=O bond from the carbonyl. Both these forms are in equilibrium as discussed previously.

To try and overcome the effect of prolonged exposure whilst preparation steps are taking place, a traditional idea has been suggested by Clapton et al., (2017), with two different approaches that can be utilised. The first approach is to start the incubation period of each sample in the buffer at a different time right before the time of injection, whereas the second approach suggests that all the samples are frozen immediately after the reaction at  $-80^{\circ}\text{C}$  to stop the reaction from progressing. The samples will then be thawed on a one-by-one basis right before analysis, thus decreasing the exposure time.

Hydrolysis and oxidation are two of the prime mechanisms by how a compound will degrade in plasma. Hydrolysis is a process where a compound is split in two, or the breakdown of a compound when it reacts with water, whereas oxidation is a reaction whereby the transfer/loss of electrons and possible addition of oxygen has taken place. Since plasma mainly contains water, hydrolysis will therefore be the main process. As mentioned before, contained within the group which is susceptible to hydrolysis is amides. Synthesised as part of this study were a series of Benzoylurea derivatives, which contain a central urea amine linkage, neighboured by a carbonyl group (C=O) and a carbonothioyl (C=S) group. Accordingly,

the hydrolysis mechanism on an amide group has a very high potential to produce a carboxylic acid (-COOH) and an amine (-NH<sub>2</sub>).

From a medicinal chemistry point of view, different functional groups provide specific chemical properties and exhibit certain behaviours which further allow a drug molecule to exert its desired effect, both in terms of pharmacokinetics and pharmacodynamics. There is a big list of parameters in which a drug compound can play a significant role with regards to response, and the list includes factors such as water/lipid solubility, mechanism of action, route of metabolism and elimination and the ability to interact with biological targets. Due to the difference in the roles played by functional groups, some are classified as more significant than others. Since most drugs are small organic molecules, the only difference between them would be the type of functional groups present and the connectivity between these groups. The possibility to alter functional groups also allows to improve the activity, increase absorption, decrease potential side effect or in the long term, provide a better course of action for an alternative therapeutic effect.

When a single functional group is added to a specific molecule, wholesome changes will and can occur. This means affecting the overall balance of the molecule in terms of solubility and steric dimensions. An example of this will be the addition of a para hydroxyl group to an aromatic system, which potentially will influence the electron density of the aromatic ring through its ability to interact with the electrons present. The hydroxyl group has been a functional group which can affect the dynamics of a compound, since the focal addition of the -OH group will help to increase the water solubility of the compound, whereby the possibility of forming hydrogen bonds will increase significantly, and especially in plasma, since water makes up around 90% of it. As well as the ability to form hydrogen bonds, since the hydroxyl

group is off a larger size than the original hydrogen atom it replaced, the overall steric dimension of the compound is also affected. Another benefit of replacing a functional group with a hydroxyl, or even an aromatic amine, aromatic thiol or simple methoxy group is that these groups contain functional groups with lone pair, which are readily donated into the phenyl or aromatic ring system. Functional group substitution was observed during the synthesis of the  $\beta$ -diketones, where to the common DBM structure, functional groups such as hydroxyl, methoxy and halogens were added. This was in order to see if either these substitutions made significant effects on the compound with regards to plasma stability and degradation. As observed from the results, it was seen that the addition of hydroxyl groups provided a stable compound than the original DBM, however replacing with methoxy was not as successful. Oddly, the derivatives which contained the urea and amide groups exhibited a better stability in plasma than the  $\beta$ -diketones, especially since the hydrolysis of amides is common. However, since the compound contained a bulky structure with other functional groups present as a means of shielding, the compounds may have degraded in the long run. The idea here is of steric hindrance, a very common strategy which is used to block or slow a specific metabolic pathway. By using this approach, additional atoms are added adjacent to functional groups undergoing the metabolism in order to block the interaction of the drug molecule with the enzyme. Another reasonable explanation for the ability of Benzoylurea derivatives to be more stable than the 2-Azido-diketones or  $\beta$ -diketones would be the presence of the di-carbonyl functional groups instead of the one. Since oxygen can draw electrons towards itself much more efficient and strongly than carbon, the C=O becomes polarised, leaving the oxygen with a negative charge and in turn, the carbon with a positive charge. Due to the rise of this polarisation, the electrons on the oxygen of a water molecule are attracted to the slightly positive charge of the carbon atom, thus resulting in the process

of hydrolysis. This hydrolysis reaction is known to proceed more rapidly with esters than amides, and this would be the case where methoxy functional groups bonded to oxygen as an ether were shown to be less stable than DBM or any other hydroxyl containing compound. The reason for the difference in the rates of hydrolysis is down to the difference in structural differences between the two functional groups. The ester contains an oxygen atom, whereas the amide is attached to a nitrogen atom at the same position, and this difference brings in the ability of charge and attraction. As the carbonyl group is much more positively charged than that of the amide, this leads to a greater attraction between the carbon and water. Nitrogen on the other hand lessens that positive charge in the carbonyl atom, thus present less of an attraction to incoming water molecules, an observation made in the plasma stability assay, where the most stable compounds were the amide containing Benzoylurea derivatives. The same can be said for the 2-Azido-diketones, which even though contain an imine functional group, are said to degrade rapidly, a finding which was observed here. A finding by Sheikh et al., (2009) shows the structurally similar compound Curcumin to contain two phenolic hydroxyl groups, which when ionized causes a destabilization effect on curcumin, leading it towards oxidation and hydrolysis. Furthermore, it has been found that Curcumin is also very potent in cancer chemoprevention, but its plasma concentrations were found to be very low in rodents and human after oral administration probably due to low bioavailability (Jackson et al., 2002). Therefore, for further clinical application, the dietary chemo preventive compounds require more knowledge of *in vivo* pharmacokinetics including absorption, distribution, metabolism and excretion.

### 3.4 S9 Fraction Stability

All the compounds were tested via this S9 fraction assay to determine their metabolic stability in order to calculate half-life ( $t_{1/2}$ ) and Intrinsic Clearance ( $CT_{int}$ ), the amount of compound cleared/removed within a minute. Different time intervals were measured up until the 45-minute mark, with the natural log (ln) of the Percentage test compound remaining plotted against time. The former would then allow for a gradient to be calculated from the line, which would then help to determine the  $t_{1/2}$  and following this, the  $CT_{int}$ , measured in  **$\mu\text{L}/\text{min}/\text{mg}$  protein**. The following formulae were utilised to help with the calculations.

$$\text{Elimination rate constant (k)} = (- \text{gradient})$$

$$\text{Half Life (} t_{1/2} \text{) (min)} = 0.693/k$$

$$V (\mu\text{L}/\text{mg}) = \text{volume of incubation } (\mu\text{L}) / \text{protein in the incubation (mg)}$$

$$\text{Intrinsic Clearance (} CL_{int} \text{)} (\mu\text{L}/\text{min mg protein}) = V \times 0.693 / t_{1/2}$$

A scoring guide was used to consider whether the  $CT_{int}$  value calculated was either expressed as high or low in terms of human metabolism on the tested compound. The scale used for the analysis of the results is as follows;

**Low < 4.5**

**High > 24.6**

Table 16 Data values for all compounds calculating pharmacokinetic parameters such as Half life ( $t_{1/2}$ ) in minutes, Intrinsic Clearance and the overall % decrease of the starting compound tested with the S9 Fraction contained after an incubation period of 0-45 minutes

Compound	Half Life ( $t_{1/2}$ )/min	CT <sub>int</sub> ( $\mu\text{L}/\text{min}/\text{mg}$ protein)	% decrease from time 0 to 45 (min)
RMP	29.48 $\pm$ 2.31	12.00 $\pm$ 0.69	66.31 $\pm$ 0.69
DBM	27.94 $\pm$ 1.71	12.67 $\pm$ 0.76	68.70 $\pm$ 0.36
1	21.93 $\pm$ 1.72	16.14 $\pm$ 0.85	77.20 $\pm$ 0.71
2	21.06 $\pm$ 1.82	16.81 $\pm$ 0.61	79.00 $\pm$ 0.63
3	24.40 $\pm$ 2.39	14.51 $\pm$ 0.43	74.74 $\pm$ 0.45
4	34.13 $\pm$ 2.69	10.37 $\pm$ 0.84	60.80 $\pm$ 0.36
5	28.40 $\pm$ 2.16	12.46 $\pm$ 0.94	68.1 $\pm$ 0.21
6	31.93 $\pm$ 2.11	11.08 $\pm$ 0.35	65.3 $\pm$ 0.95
7	41.49 $\pm$ 1.64	8.53 $\pm$ 0.21	54.0 $\pm$ 0.61
8	44.42 $\pm$ 2.10	7.97 $\pm$ 0.65	51.5 $\pm$ 0.84
9	37.86 $\pm$ 2.01	9.35 $\pm$ 0.73	55.9 $\pm$ 0.71
10	36.09 $\pm$ 1.98	9.81 $\pm$ 0.36	59.4 $\pm$ 0.26
11	15.50 $\pm$ 1.30	22.84 $\pm$ 0.12	88.5 $\pm$ 0.23

<b>12</b>	14.68 ± 1.43	24.11 ± 0.45	89.7 ± 0.56
<b>*13</b>	16.04 ± 1.52	22.07 ± 0.36	88.0 ± 0.19
<b>14</b>	147.44 ± 1.47	2.40 ± 0.28	20.1 ± 0.54
<b>15</b>	128.33 ± 2.00	2.75 ± 0.46	21.7 ± 0.66
<b>16</b>	133.26 ± 1.24	2.65 ± 0.56	20.4 ± 0.15

From the Table 16, it is evident that all the compounds which were synthesised,  $\beta$ -diketones, 2-Azido-diketones and the Benzoylurea derivatives, all have intrinsic clearance whereby the values fall into the upper and lower ranges. The highest value found was just short of the scale used at 24.1192  $\mu\text{L}/\text{min}/\text{mg}$  protein however the lowest values calculated were under that of 4.5, averaging 2.6061  $\mu\text{L}/\text{min}/\text{mg}$  protein.

RMP was calculated to have a  $\text{CT}_{\text{int}}$  value of 12.0085, a value which falls between the halfway stage of 4.5 and 24.6. The same observations can be made with the  $\beta$ -diketone derivatives including DBM, where the values range from between a low of 7.97 to a high of 16.81. From the calculated values within the table, it has been observed that compounds 1,2,3 & 5, all which contain the hydroxyl groups have a higher clearance value. This was the case with both the  $\beta$ -diketones and the 2-Azido-diketones. The following observation was then linked to a correlation regarding  $t_{1/2}$ , through which it was seen that a candidate with a shorter half life had a high  $\text{CT}_{\text{int}}$ .

An example of this would be compound 1 and 12. Here a mono hydroxyl group is present on the  $\beta$ -diketone and the similar 2-Azido-diketone structure. The  $t_{1/2}$  of 1 was shown to be 21.93 min and off 12 to be 14.68 min. The  $CT_{int}$  values calculated were 16.1476 and 24.1192. This proves the theory above to be correct.

### 3.4.1 S9 Fraction Stability – DBM And Derivatives (Compounds 1 – 10)

Nearly all  $\beta$ -diketone derivatives displayed calculated values of both  $t_{1/2}$  and  $CT_{int}$  to be close to RMP, the internal control, however compounds which contained much bulkier functional groups such as compounds 7,8,9 & 10, where methoxy substituents amongst others were present, displayed a slightly higher half life and lower  $CT_{int}$ . Compounds 7 and 8, which contained the Fluorine group, had a  $t_{1/2}$  calculated of 41.49 and 44.42 in comparison to 29.48 of RMP and 27.94 of DBM. The  $CT_{int}$  values calculated also differed by approx. 66%, with 8.5337 (7) and 7.9716 (8) being calculated in contrast to 12.0085 (RMP) and 12.6728 (DBM).

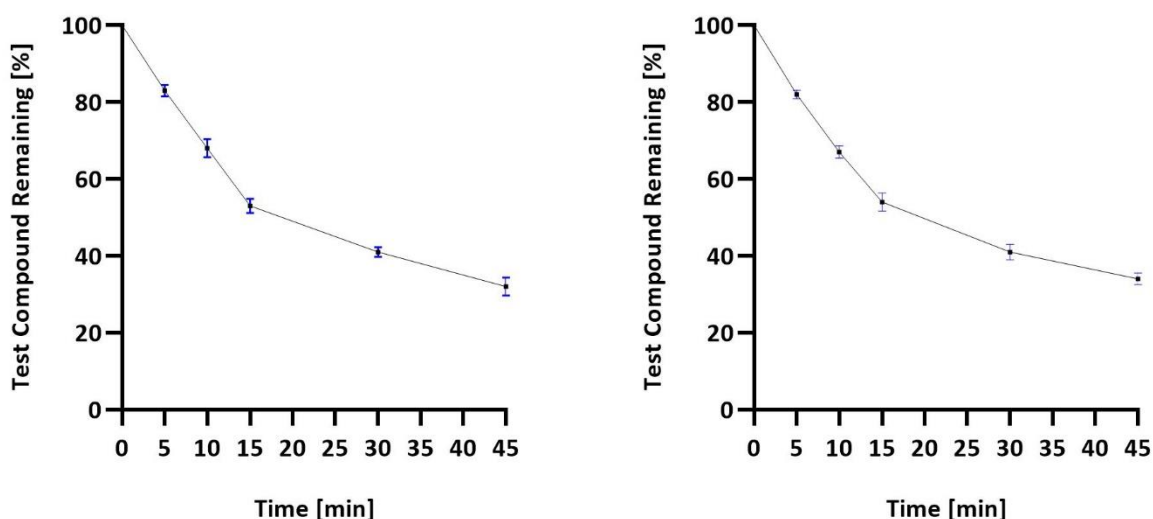
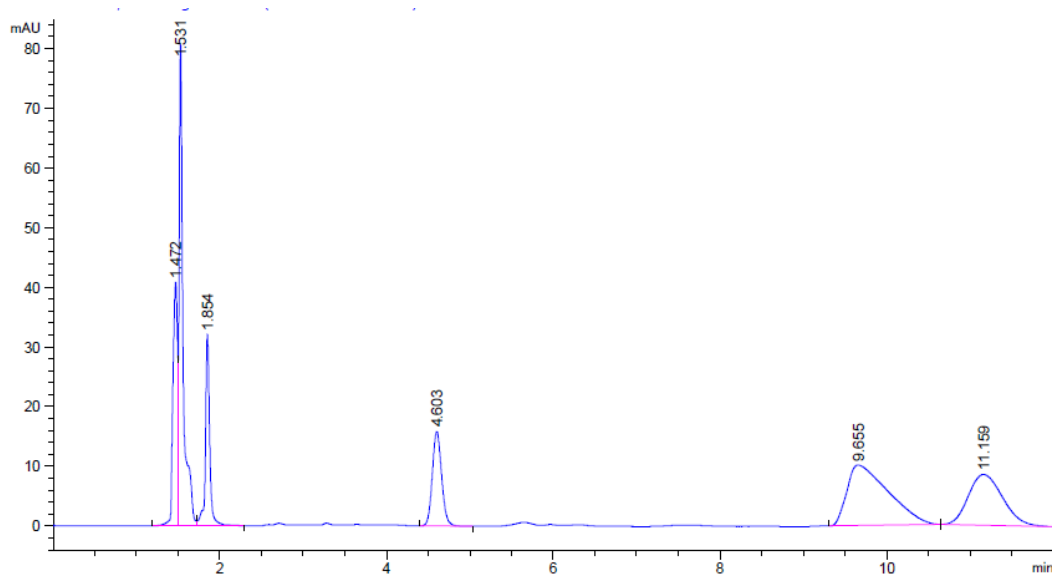
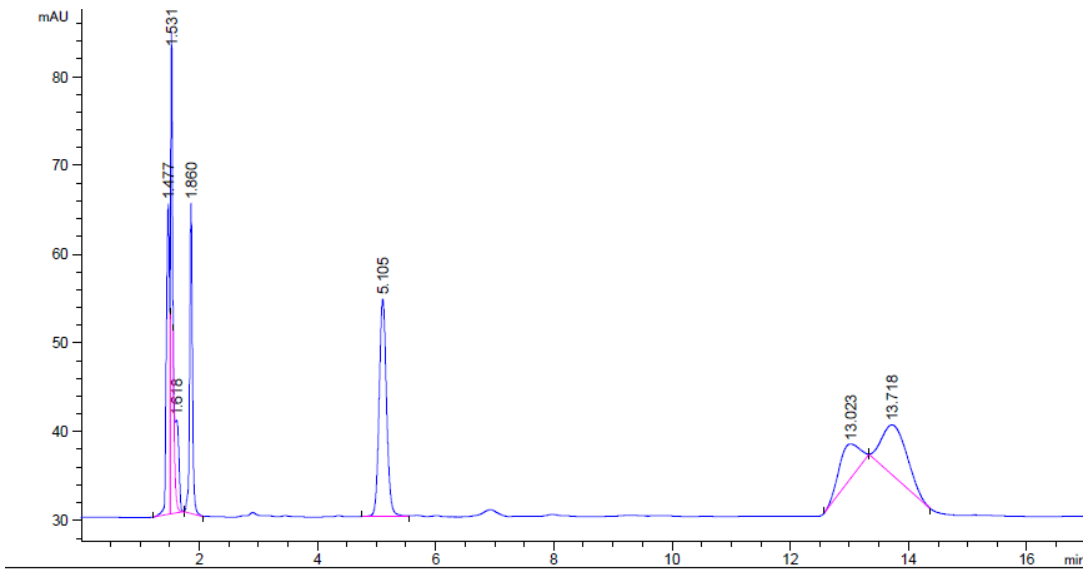


Figure 72 Plotted data curves to show the % of Compound RMP (left) and DBM (right) remaining over the different incubation periods, when tested in the presence of the S9 Fraction. Below; HPLC spectra obtained after running a sample containing RMP and S9 Fraction at time intervals of 10 min and 45 min respectively. HPLC system was injected with an 80:20 MeOH/H<sub>2</sub>O ratio



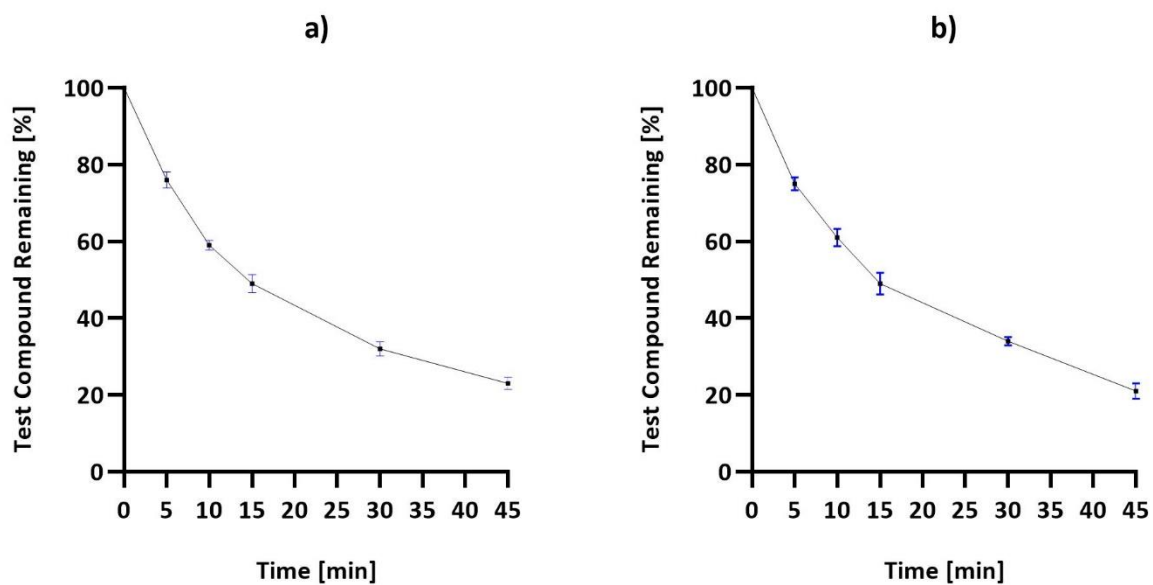
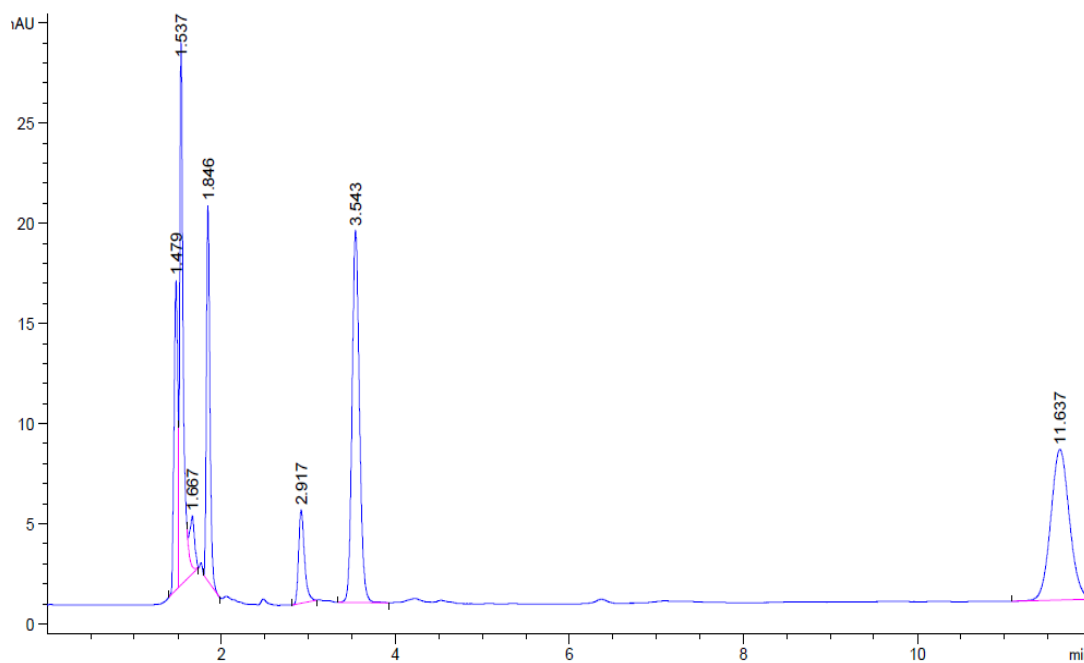


Figure 73 Plotted data curves to show the % of Compound 1 (a) and Compound 2 (b) remaining over the different incubation periods, when tested in the presence of the S9 Fraction. Below; HPLC spectra obtained after running a sample containing Compound 1 and S9 Fraction after an incubation period of 45 minutes. HPLC system was injected with an 80:20 MeOH/H<sub>2</sub>O ratio



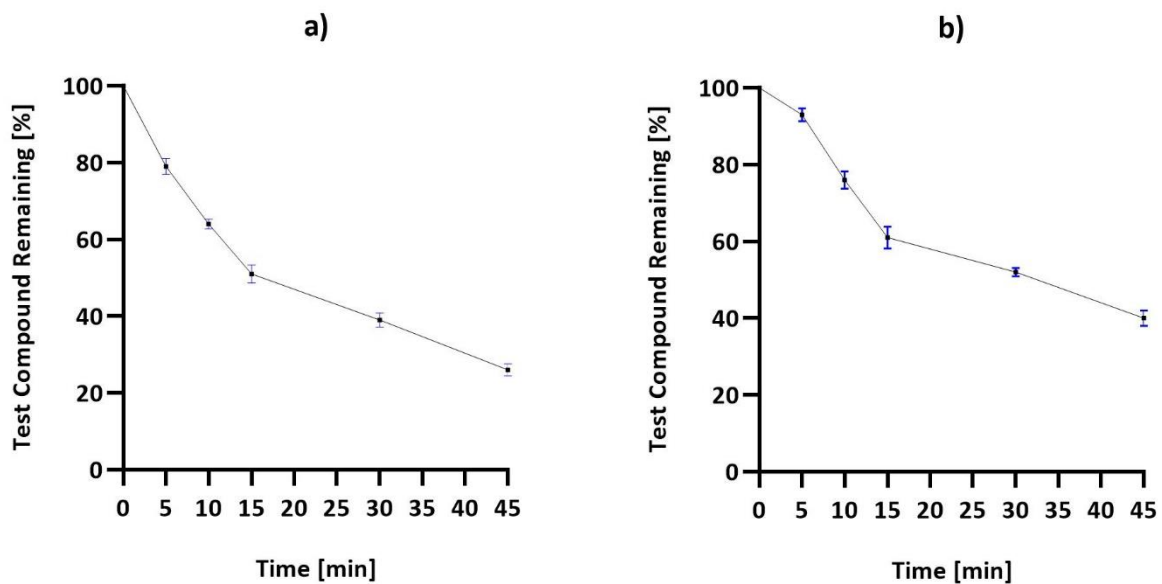
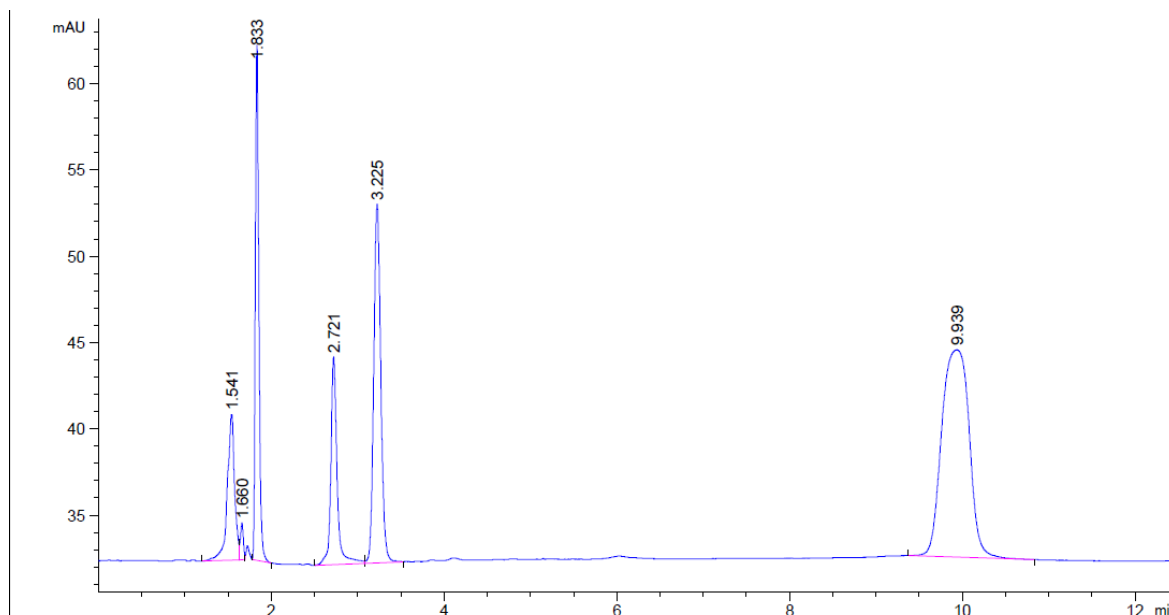


Figure 74 Plotted data curves to show the % of Compound 3 (a) and Compound 4 (b) remaining over the different incubation periods, when tested in the presence of the S9 Fraction. Below; HPLC spectra obtained after running a sample containing Compound 4 and S9 Fraction after an incubation period of 45 minutes. HPLC system was injected with an 80:20 MeOH/H<sub>2</sub>O ratio



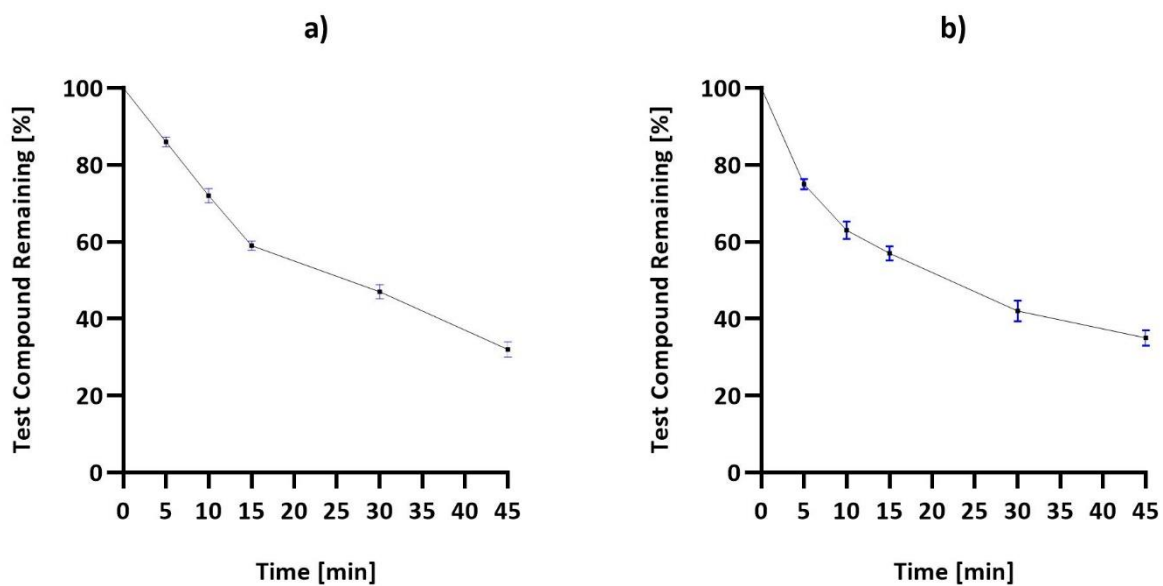
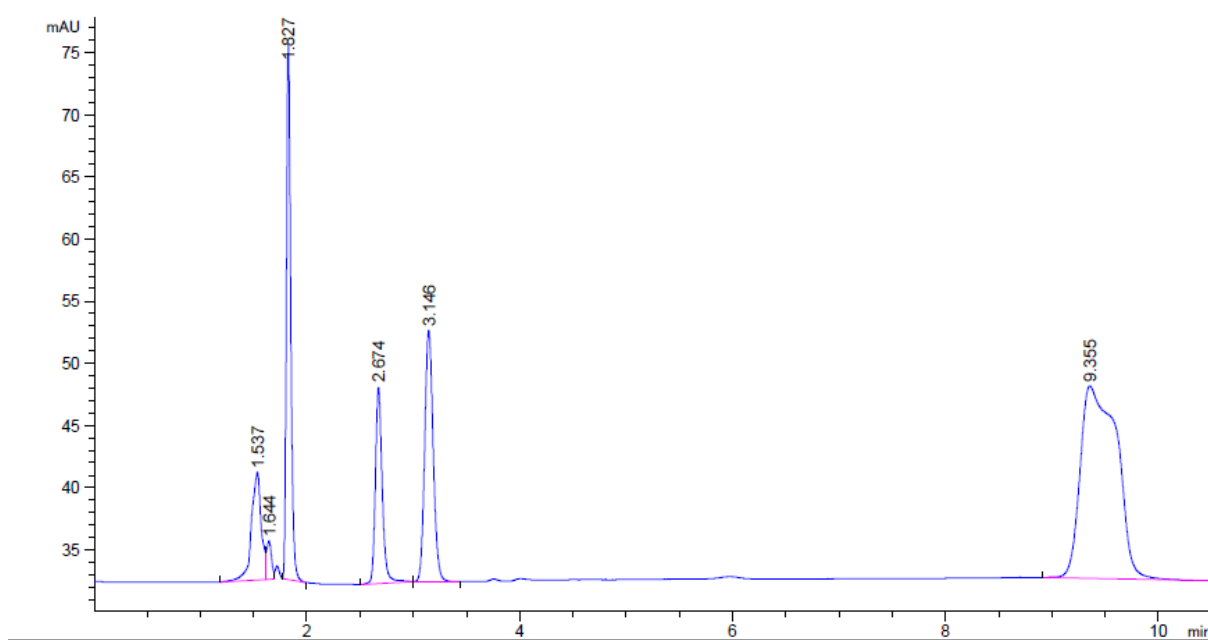


Figure 75 Plotted data curves to show the % of Compound 5 (a) and Compound 6 (b) remaining over the different incubation periods, when tested in the presence of the S9 Fraction. Below; HPLC spectra obtained after running a sample containing Compound 5 and S9 Fraction after an incubation period of 45 minutes. HPLC system was injected with an 80:20 MeOH/H<sub>2</sub>O ratio



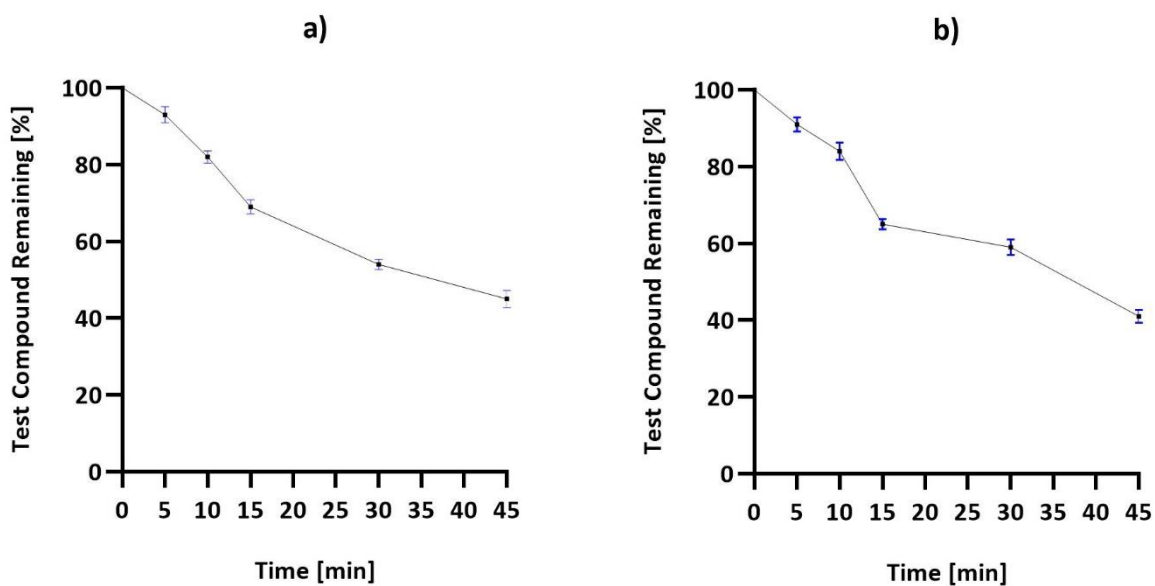
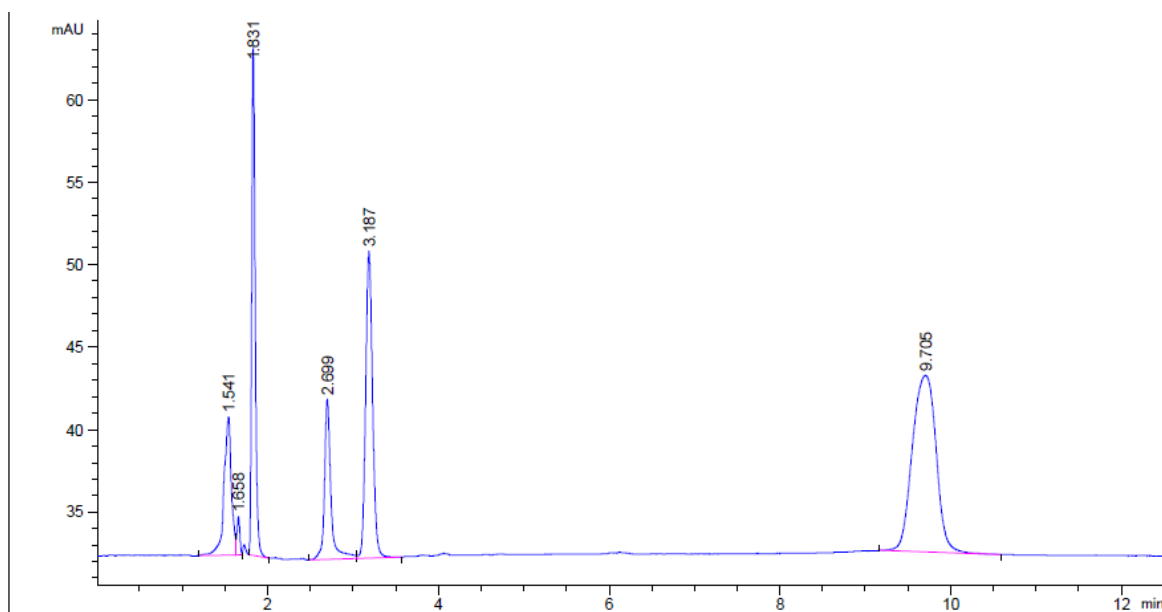


Figure 76 Plotted data curves to show the % of Compound 9 (a) and Compound 10 (b) remaining over the different incubation periods, when tested in the presence of the S9 Fraction. Below; HPLC spectra obtained after running a sample containing Compound 9 and S9 Fraction after an incubation period of 45 minutes. HPLC system was injected with an 80:20 MeOH/H<sub>2</sub>O ratio



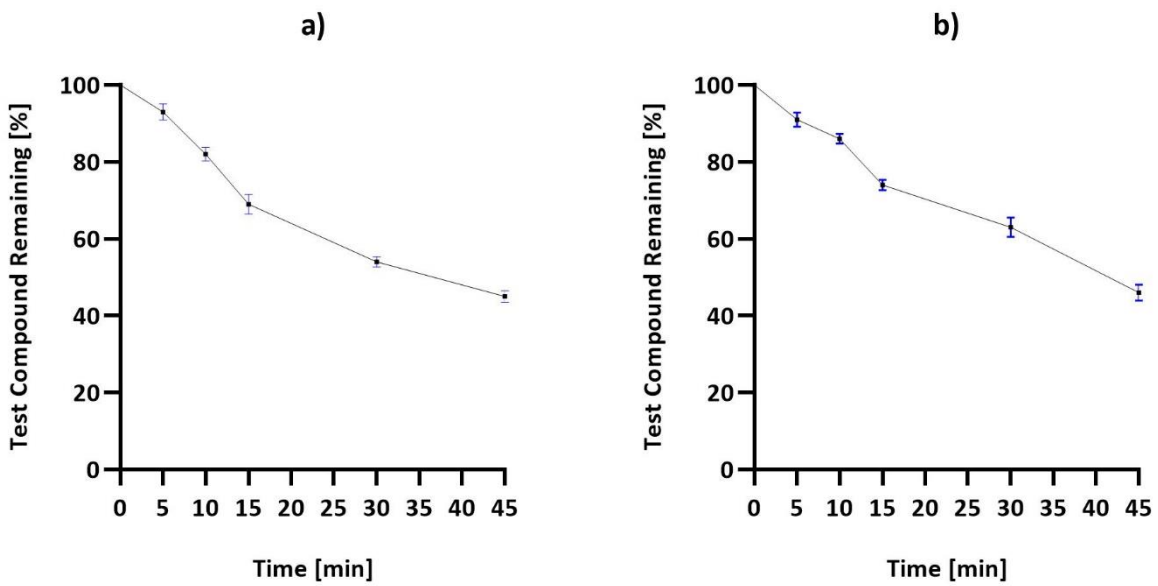
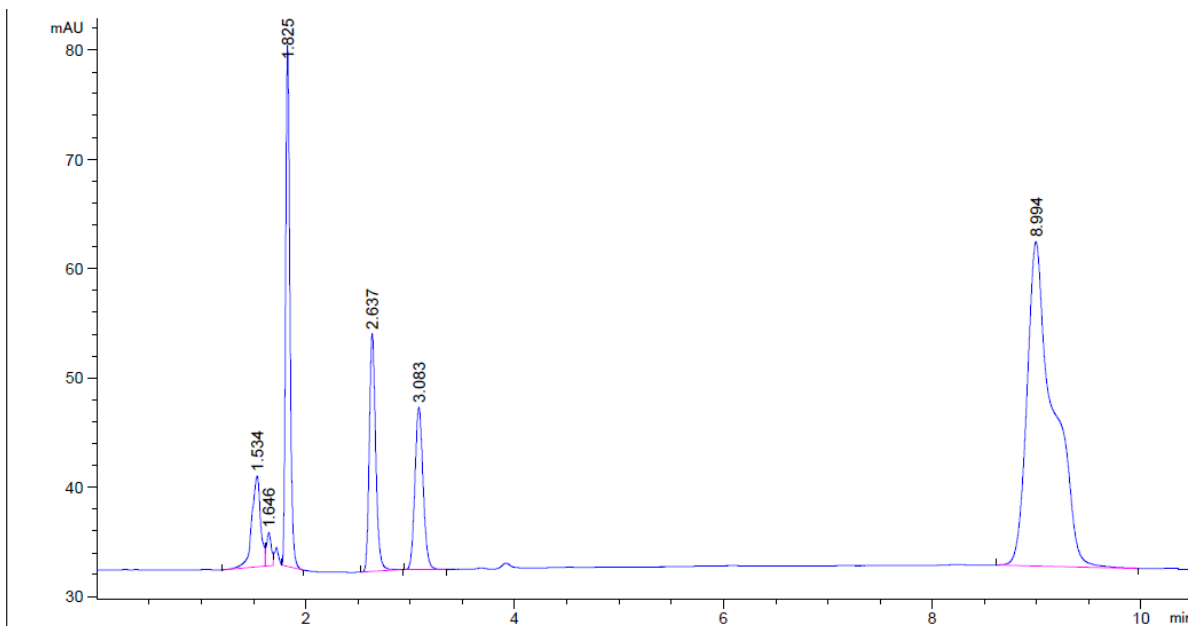


Figure 77 Plotted data curves to show the % of Compound 7 (a) and Compound 8 (b) remaining over the different incubation periods, when tested in the presence of the S9 Fraction. Below; HPLC spectra obtained after running a sample containing Compound 7 and S9 Fraction after an incubation period of 45 minutes. HPLC system was injected with an 80:20 MeOH/H<sub>2</sub>O ratio



### 3.4.2 S9 Fraction Stability – 2-Azido and Benzoylurea Derivatives (Compounds 11 – 16)

The plots in Fig 78-80 displayed the percentage of test compound which was remaining after the 45-minute incubation period with the S9 fraction. The overall percentage decrease value for each compound from T0 to T45 can be collected from table 16

Following further screening on the remainder of the derivatives, a major difference was found between the class of 2-Azido-diketones and Benzoylurea derivatives with regards to their stability in plasma. All three 2-Azido derivatives, 11,12 & 13, had relatively short  $t_{1/2}$  half life values of under 15 minutes, with  $CT_{int}$  values above 22.00. This finding therefore rendered the 2-Azido class of compounds as relatively instable and prone to a high level of metabolism by the biological enzymes, in comparison to the Benzoylurea derivatives, which displayed half life values of over 125 minutes, with very low  $CT_{int}$  values calculated such as 2.7594, 2.6572 and 2.4017 respectively. These values were regarded as low, if compared to the ranking scale used by Cyprotex. The increased metabolic stability can be down to the different types of functional groups and bonds present in the structure of the Benzoylurea derivatives when compared to the simple skeletal structures of both  $\beta$ -diketones and 2-Azido-diketone derivatives. When both the class of compounds are compared to the internal control, it can be deduced that the 2-Azido-diketones are less stable than RMP but on the other hand, the Benzoylurea derivatives are more stable.

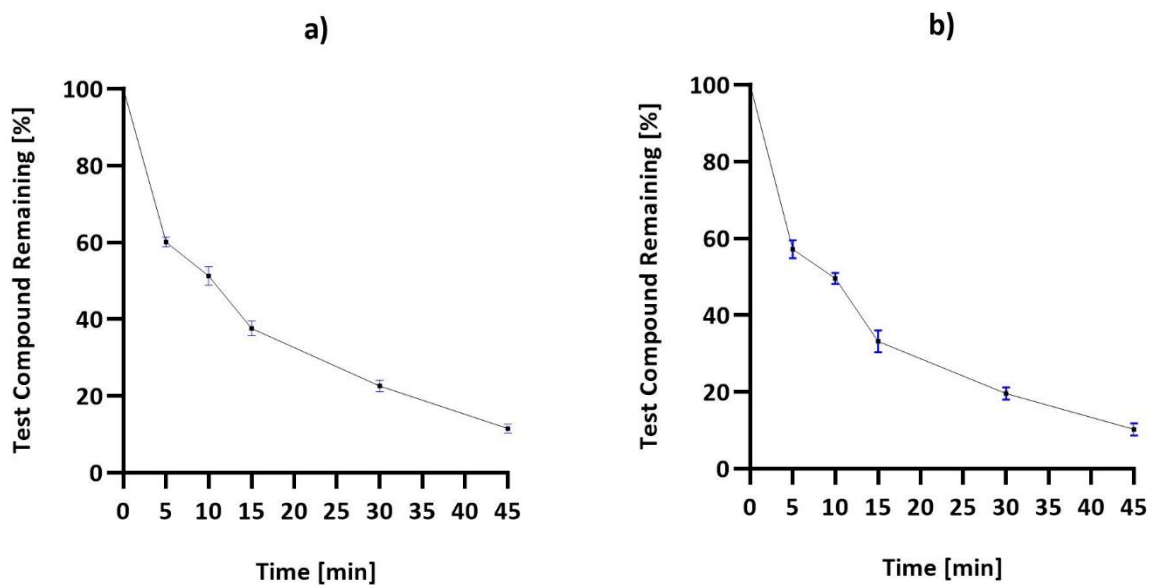
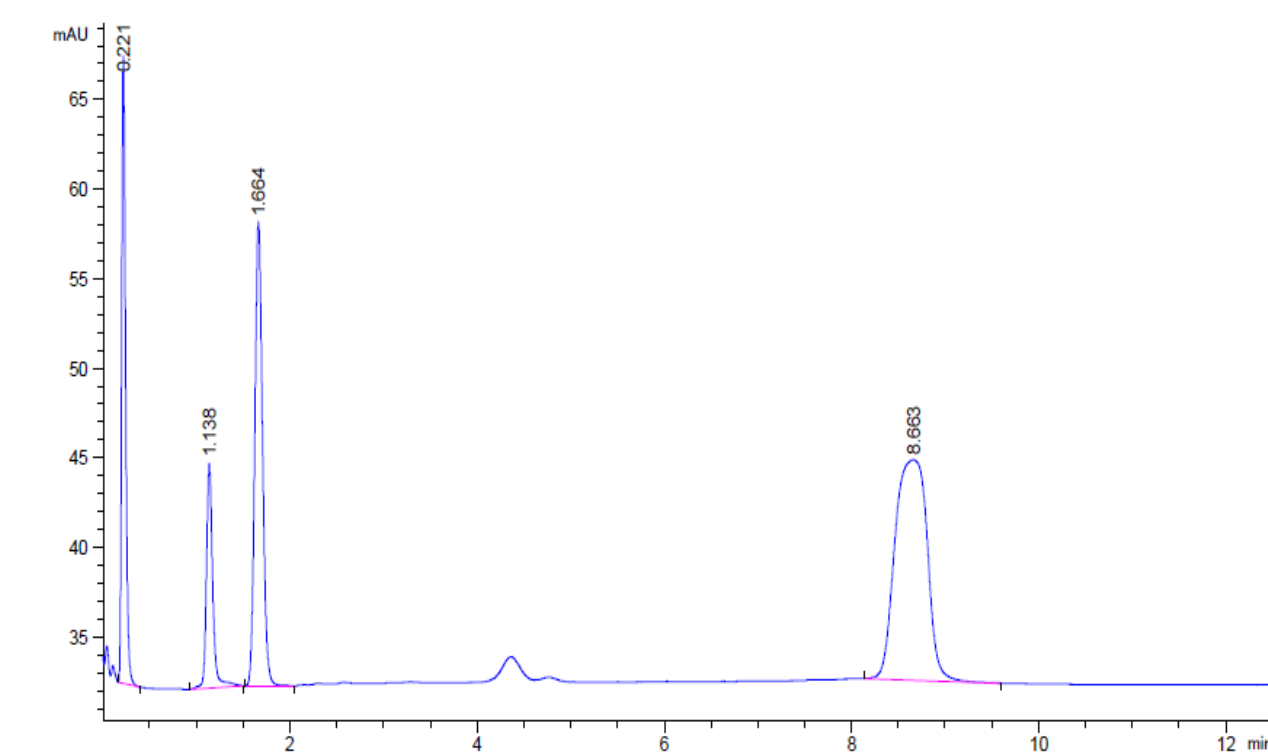


Figure 78 Plotted data curves to show the % of Compound 11 (a) and Compound 12 (b) remaining over the different incubation periods, when tested in the presence of the S9 Fraction. Below; HPLC spectra obtained after running a sample containing Compound 12 and S9 Fraction after an incubation period of 45 minutes. HPLC system was injected with an 80:20 MeOH/H<sub>2</sub>O ratio



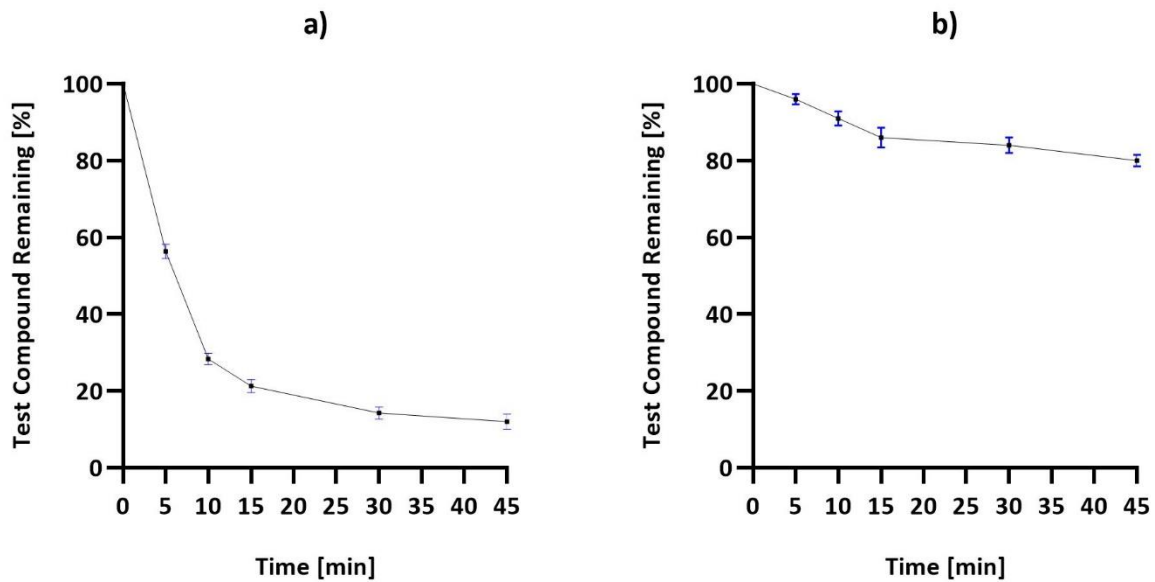
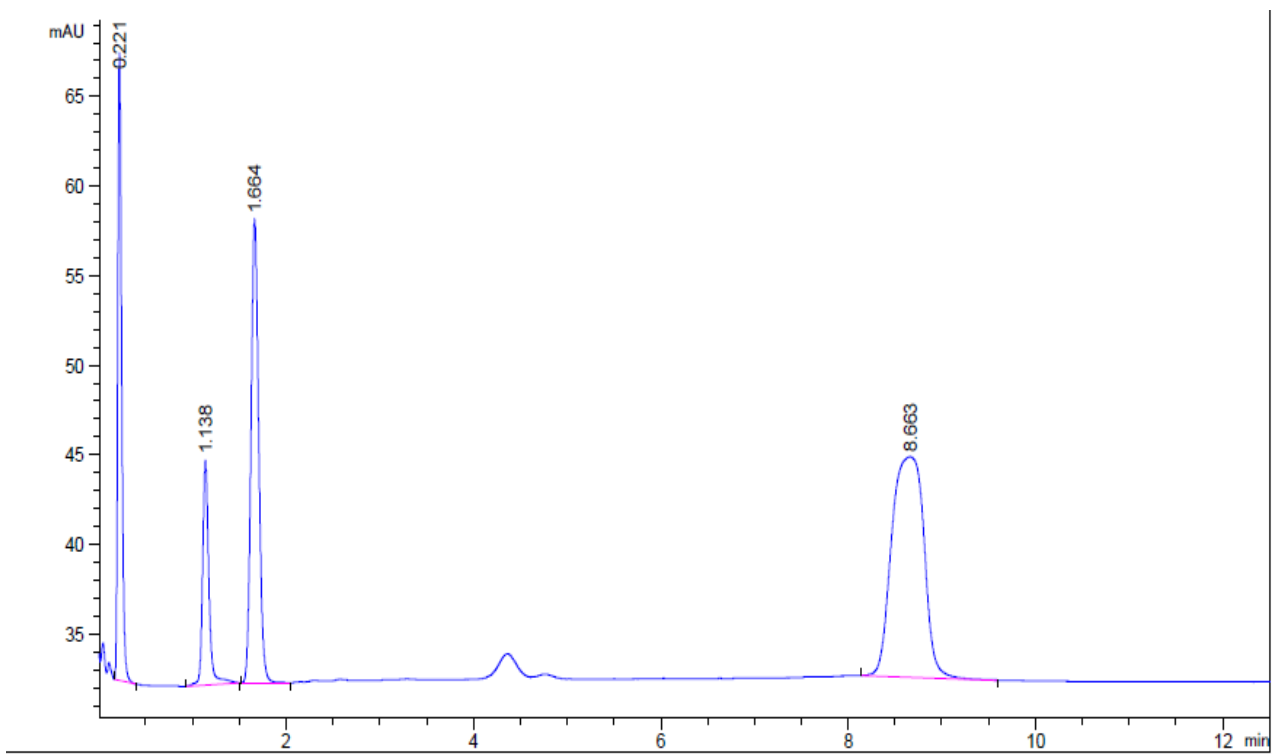


Figure 79 Plotted data curves to show the % of Compound 13 (a) and Compound 14 (b) remaining over the different incubation periods, when tested in the presence of the S9 Fraction. Below; HPLC spectra obtained after running a sample containing Compound 13 and S9 Fraction after an incubation period of 45 minutes. HPLC system was injected with an 80:20 MeOH/H<sub>2</sub>O ratio



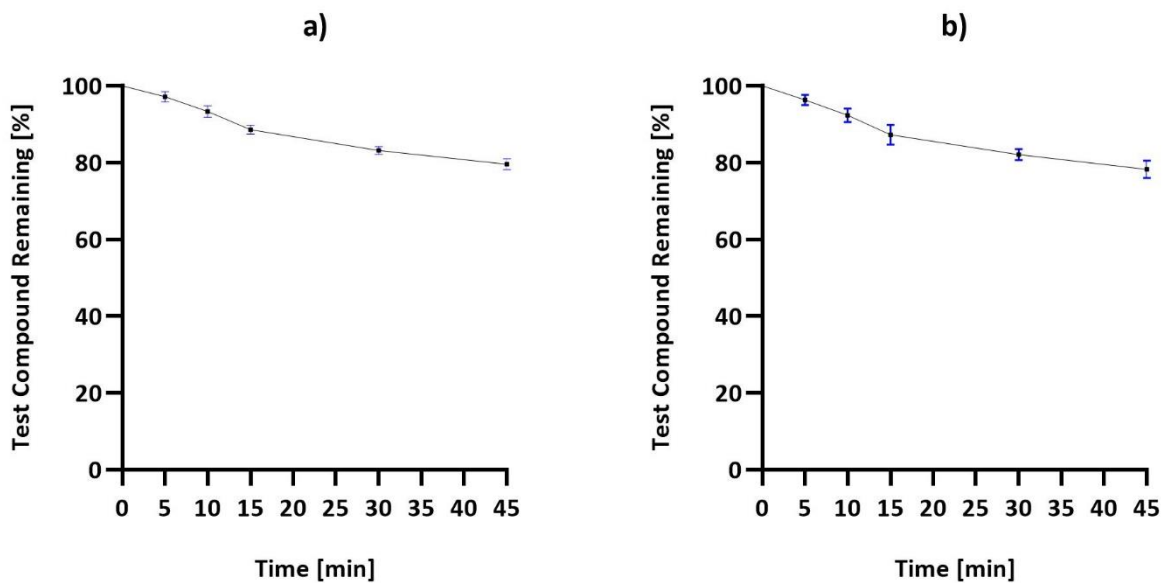
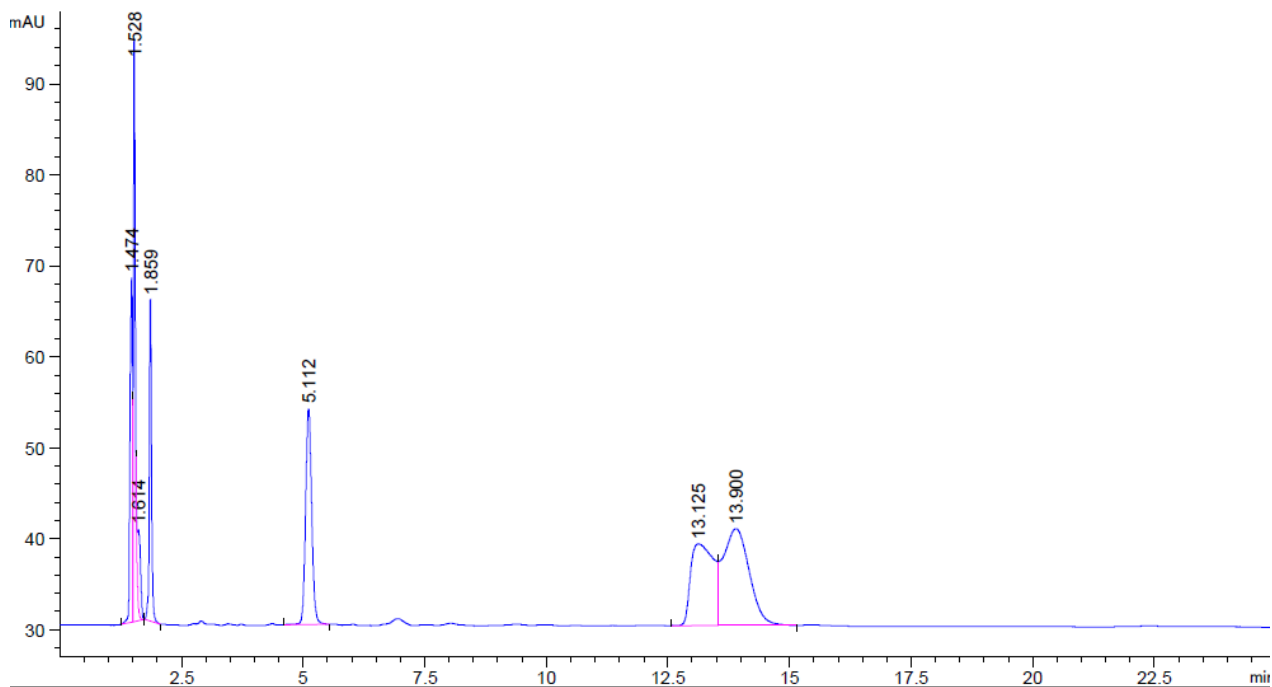


Figure 80 Plotted data curves to show the % of Compound 15 (a) and Compound 16 (b) remaining over the different incubation periods, when tested in the presence of the S9 Fraction. Below; HPLC spectra obtained after running a sample containing Compound 15 and S9 Fraction after an incubation period of 45 minutes. HPLC system was injected with an 80:20 MeOH/H<sub>2</sub>O ratio



The plots above shows the difference in the percentage compound remain for both the 2-Azido-diketone compounds and the Benzoylurea compounds. The ability of the benzoylurea compounds to be more stable is highlighted.

The role of ADME studies in drug discovery is critical in order to optimize the drug like properties exhibited by NCE thus helping to increase their level of success in the later stages of the drug discovery process. By using the concepts of *in vitro* metabolic stability, it allows for the prediction of clearance made from the body by the liver. By doing this allows for a greater understanding in prioritising the progression of a compound which exhibits and displays potentially favour results (Hartman., 2003). It has been theorised that intrinsic clearance obtained from *in vitro* metabolic studies can be used with the principal of predicting *in vivo* clearance. From the S9 fraction stability assay, the main concept is to obtain a compound which achieves low clearance, which in turn helps to reduce the dose, enhance the exposure of the compound, and prolong half-life. However, the ability of finding a low clearance compound through *in vitro* liver microsomal or hepatocyte assays is a big challenge since many low clearance compounds fail in clinic due to extremely long half-lives. This is because the liver is a primary site of metabolism, and like with every new tested drug, the drug metabolic transformations may have a significant impact on its safety and efficacy to clear and eliminate from the body. Due to this reason alone, the use of microsomes from either human or animal liver provide the platform to be used as useful models, which allow for the quick and inexpensive projection of hepatic clearance. Li Di et al (2015) mentions that a rapid and comprehensive metabolic stability serves as an effective gate in eliminating low value compounds. As mentioned above, the microsomes provide an inexpensive model to be used, however the enzymatic set up is limited to which is only contained in the endoplasmic reticulum. This means that the biological model only contains Phase I enzymes and results will

only allow for the information based on this. In contrast to this, the S9 liver fraction contains both phase I and II metabolic enzymes, which makes them more favourable and easier to use. This is also because the fractions are very easily obtained during the early stages of liver microsomal preparation but in addition contain both microsomal and cytosolic fractions that provide more metabolic information than microsomes alone. Contained as cytosolic fractions are the enzymes aldehydes oxidase, xanthine oxidase, sulfotransferases, methyltransferases, N-acetyl transferases and finally glutathione transferases, which have recently gained appreciation as a major contributor for the metabolism of certain chemotypes. Samantha et al further state that the fraction also contains phase I oxidative, reductive and hydrolytic enzymes, and as seen in the previous assay for the synthesised compounds, they are susceptible to hydrolysis, except the Benzoylurea derivatives. Since the S9 fraction contains CYP enzymes, particularly CYP1A2, CYP2C9, CYP2C19, CYP2D6 AND CYP3A4, these are responsible for the bulk of the metabolism of drugs in humans and are known for approximately 80% of oxidative drug metabolism. Since a relatively low number of studies have been published on the synthesised compounds and the assays conducted, judgements can be made on similar structures which have been studied intensively. DBM is said to be structurally similar to that of Curcumin, as mentioned previous, and studies shown for Curcumin highlight the fact that it has an unfavourable pharmacokinetic profile consisting of poor absorption, a quick rapid metabolism which render it as unstable, and following on, a rapid elimination, which leads to a short plasma half-life and low concentrations in target tissues. This may be down to the fact that cell uptake plays a rate-limiting role in metabolic clearance and research has shown the membrane permeability may limit the uptake of a compound and therefore its ability to reach the target. This would be possible when a high permeability compound can display slow intrinsic clearance due to the fact it has a slow

metabolic turnover after a rapid uptake initially. In order to overcome this barrier, assays such as octanol/water partitioning may be used as a model to see the hydrophilicity and lipophilicity of certain compounds. From the LogD values, it can be predicted how much of the compound will cross the membrane barrier. Moving on, it has been stated that compounds with half-lives under 30 minutes were binned as unstable in comparison to those with a half-life over 30 minutes, which were labelled as stable. From the results obtained and calculated it would be suggested that the Benzoylurea derivatives can be labelled as unstable due to a half-life of over 30 minutes and an intrinsic clearance of under 2.5, followed by the  $\beta$ -diketones derivatives which contained the hydroxyl groups. If the half life values are to be considered, then the hydroxyl containing compounds, including DBM and the 2-Azido-diketone would also fall under the unstable category. The compounds which were degraded quick within plasma, since they contained methoxy functional groups are deemed as the most stable, since they all have a half-life better than 30 minutes but also average intrinsic clearance values of around 10  $\mu\text{L}/\text{min}/\text{mg}$  protein.

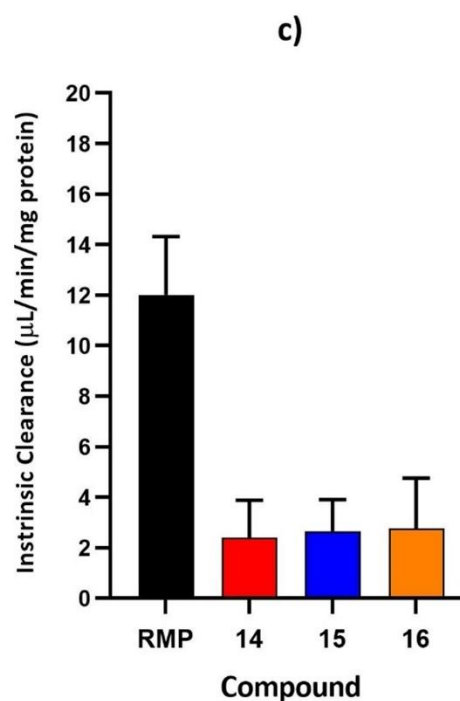
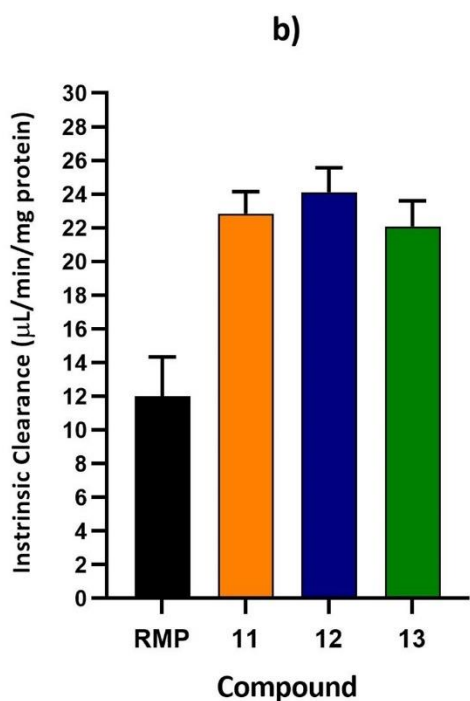
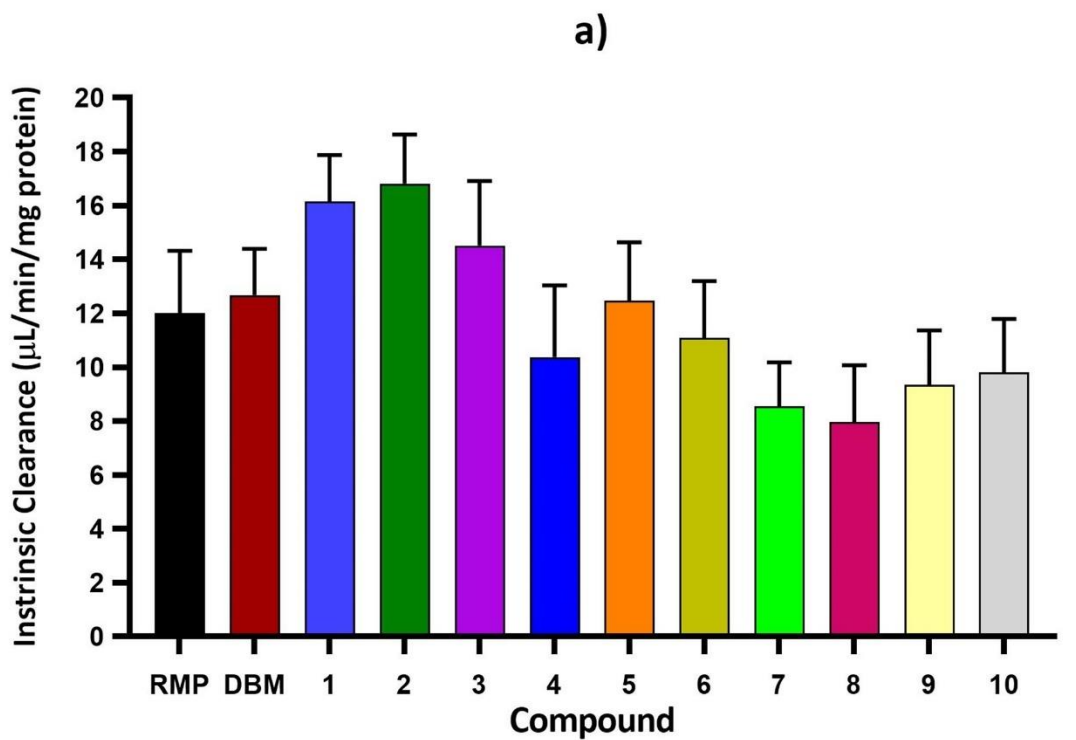


Figure 81 Graphical illustration/s plotted to show the Intrinsic Clearance for each compound tested in the presence of S9 Fraction. Graphs were plotted using data from Table 16 and show the following compounds respectively; a). RMP, DBM and derivatives b). RMP and the 2-Azido derivatives c) RMP and the Benzoylurea derivatives

## 3.5 PCR and qPCR

### 3.5.1 Polymerase Chain Reaction (PCR)

PCR is a biochemical technology in Molecular Biology, where a single or few copies of a piece of DNA are amplified across a magnitude to generate several copies, sometimes ranging from several thousand to a billion of a particular DNA sequence.

The technique works through a basis of basic steps such as separation and re-synthesis. After a sample containing double-stranded DNA has been input into the thermo cycler, a dsDNA strand is heated to a temperature of around 90-95°C to cause denaturation in the DNA molecule. Due to the presence of the heat, the hydrogen bonds between the Nucleic Acid bases are broken, thus collapsing the double-strand structure, and separating it into two single-strands. The following phase has the presence of an enzyme, a DNA polymerase such a Taq-Polymerase, and small primer sequences available. These substances allow the production of two new DNA single strands to be possible, however only work by using an original strand of the initial DNA molecule as a template. To make this possible, the temperature within the PCR machine must be automatically altered to a lower cooler range of 55-60°C, to gives the primers present a chance to anneal, which is basically just binding. After this process is complete, there is now a new molecule of DNA created, which now contains an original strand as well as the newly synthesised strand. These new strands which have been replicated can now be duplicated even further and form a cycle of denaturation and synthesis, which is repeated many times, such as 30-40 cycles, in order to obtain millions to billions of copies of DNA. However when this process of duplication is conducted, the temperature once again is elevated to roughly 75°C. All this is only possible due to the fact that when the Thermo cycler carries out the concept of performing the PCR reaction, it

is automatically programmed to alter and adjust the temperature regularly in order for the process of denaturation and synthesis to be carried out successfully and accordingly. PCR easily amplifies target regions of template DNA in a much shorter time (Saiki et al 1985). All this is down to the fact that the good stability of DNA at high temps makes PCR the only technique to determine species identification.

The method works mainly due to its use of utilising the Cytochrome B region of a gene, which is found in Mitochondrial DNA. mtDNA is inherited from the mother only unlike the other common Nuclear DNA. Upon entering a fertilised egg, sperm mitochondria is destroyed. While DNA is unique, the same cannot be said for mtDNA, as all maternal relatives have the identical mtDNA. However, this mtDNA is not the same between all population due to a lack of repair mechanism, which in turn means that it is susceptible to bases substitutions, making it highly prone to a high number of mutations. On average these are 10x times more than those linked to Nuclear DNA. Two reasons why this allows the techniques to be successful are since mtDNA can be found in abundance, therefore makes it a brilliant molecule to perform many a test on, and also that the Cytochrome B gene region contains sequence variation. This concept of sequence variation makes the Cytochrome B gene a common aspect to determine the evolutionary relationships between organisms and mammals. As stated before, this is due to the mutations which occur, and the variability provided by mtDNA means that the Short Variable Sections of the genes can be interrogated for this purpose.

However whilst the technique of PCR remains at a standard, there have been many other techniques which have been modified and designed to combat some weakness of the common PCR technique which exist.

### 3.5.2 Real-Time PCR

One modified technique is the recent Real-Time PCR or qPCR. Real-Time PCR analysis is a sensitive DNA quantification technique that has recently gained considerable attention in biotechnology, microbiology and molecular diagnostics (Guescini *et al.*, 2008).

The concept here with this technique is that it has the ability, in either one or more DNA samples, to detect and quantify DNA. The basis of quantification here is useful as it allows the Absolute number of copies of DNA obtained or the relative amount of DNA present to be calculated. The way qPCR reactions work differently to conventional PCR methods are by the means of using an inclusion of fluorescent reporter molecules in each of the reaction well present. The fluorescent dye is then detected and the overall theory is that an increase in the amount of fluorescence dye detected signifies that the amount of

DNA product present is also increasing. All this is only possible due to the fact that many thermocyclers are now fitted or equipped with fluorescence detection modules, which are currently used to monitor the increase or decrease in fluorescence signals omitted as the amplification of magnitude progresses.

The approach of qPCR and that of the conventional approach differ to an extent that whilst using the Real-Time PCR technique, the DNA which is amplified, the reaction is conducted and progresses in a real-time situation and is then quantified after each cycle to provide an approximate Threshold Cycle value (Ct Value) whilst when you compare this technique with the more standard and conventional approach of PCR, the product that you detect will only

be found at the end of the reaction. The basic choice in Real-Time PCR calculations is between absolute quantification, based on the standard curve, and relative quantification, based on PCR efficiency calculation (Guescini *et al.*, 2008), however absolute quantification can be achieved using a standard curve constructed by amplifying known amounts of target DNA (Rutledge *et al.*, 2003).

In addition another advantage of using the qPCR technique over the more conventional and standard PCR system, is that it allows you to determine the initial number of copies of the template DNA in question. This then further leads to the fact that since the reaction of the qPCR is conducted in a closed unified system, the opportunities available for issues and concerns regarding contamination and cross-reaction are ultimately reduced.

Using the technique, the cell lines HepG2, HeLa and A549 were monitored and analysed for the relative mRNA expression levels of CDK4, CDK6 and PCNA alongside an internal housekeeping control gene, Gapdh. The starved cells treated with the potential drug compounds (100 $\mu$ M) were incubated for 48h and 72h, since this interval was the most significant in terms of generating a response with the MTT cytotoxicity assay. Graphs plotting the level of gene expression ( $2^{-\Delta\Delta Ct}$ ) vs gene used were analysed for selected compounds from each sub class of derivatives. The plots were relative to the untreated sample vs treatment with a compound of choice.

Table 17 Gene expression was obtained on HepG2 cells after 48 hours with the standard deviation being calculated based on triplicate results.

	<b>Compounds</b>	<b>PCNA</b>	<b>CDK4</b>	<b>CDK6</b>
<b>HepG2 – 48h</b>	<b>Control</b>	6.32 ±1.02	1.27 ±0.10	0.36 ±0.00
	<b>DBM</b>	11.38 ±1.16	1.01 ±0.22	3.07 ±0.17
	<b>1</b>	5.46 ±1.12	0.56 ±0.02	9.32 ±0.53
	<b>2</b>	6.81 ±0.08	1.63 ±0.12	0.69 ±0.04
	<b>3</b>	6.71 ±0.00	0.86 ±0.08	3.75 ±0.21
	<b>4</b>	13.22 ±0.86	2.95 ±0.03	2.36 ±0.98
	<b>5</b>	7.36 ±1.23	0.79 ±0.06	5.41 ±0.33
	<b>6</b>	11.28 ±1.84	1.02 ±0.09	0.85 ±0.04
	<b>11</b>	7.23 ±1.12	0.92 ±0.12	0.88 ±0.01
	<b>12</b>	7.26 ±1.36	0.95 ±0.23	0.96 ±0.03
	<b>14</b>	4.53 ±0.14	3.35 ±0.01	4.36 ±0.00
	<b>15</b>	4.12 ±0.36	3.12 ±0.08	4.95 ±0.00

Table 18 Gene expression was obtained on HepG2 cells after 72 hours with the standard deviation being calculated based on triplicate results.

	Compounds	PCNA	CDK4	CDK6
HepG2 – 72h	Control	2.74 ±0.37	0.84 ±0.04	1.62 ±0.00
	DBM	4.89 ±0.24	1.15 ±0.09	0.55 ±0.03
	1	6.61 ±0.97	0.88 ±0.02	2.78 ±0.23
	2	8.76 ±0.23	0.98 ±0.05	0.50 ±0.02
	3	4.10 ±1.15	1.92 ±0.21	1.63 ±1.32
	4	11.54 ±0.93	2.45 ±0.06	4.65 ±0.89
	5	3.21 ±1.19	1.03 ±0.32	3.36 ±0.71
	6	6.04 ±0.98	0.88 ±0.08	4.60 ±0.26
	11	4.85 ±0.08	1.15 ±0.12	0.69 ±0.04
	12	4.75 ±0.00	0.95 ±0.08	0.55 ±0.21
	14	5.32 ±0.35	3.95 ±0.06	3.95 ±0.01
	15	4.75 ±0.45	3.36 ±0.01	3.65 ±0.02

Table 19 Gene expression was obtained on HeLa cells after 48 hours with the standard deviation being calculated based on triplicate results.

	<b>Compounds</b>	<b>PCNA</b>	<b>CDK4</b>	<b>CDK6</b>
<b>HeLa – 48h</b>	<b>Control</b>	0.55 ±0.05	1.95 ±0.01	1.98 ±0.00
	<b>DBM</b>	4.05 ±0.17	3.97 ±0.09	4.02 ±0.23
	<b>1</b>	1.89 ±0.26	0.52 ±0.01	0.61 ±0.03
	<b>2</b>	2.06 ±0.42	1.28 ±0.02	1.30 ±0.07
	<b>3</b>	3.27 ±0.13	1.12 ±0.10	2.90 ±0.16
	<b>4</b>	11.54 ±0.95	2.45 ±0.06	4.65 ±0.89
	<b>5</b>	3.21 ±1.19	1.03 ±0.32	3.36 ±0.71
	<b>6</b>	6.55 ±0.26	1.12 ±0.10	2.90 ±0.16
	<b>11</b>	8.65 ±0.97	1.26 ±0.02	1.68 ±0.23
	<b>12</b>	8.76 ±0.23	1.68 ±0.05	1.50 ±0.02
	<b>14</b>	3.23 ±0.53	1.32 ±0.88	3.65 ±0.13
	<b>15</b>	2.96 ±0.65	1.01 ±0.99	3.21 ±0.22

Table 20 Gene expression was obtained on HeLa cells after 72 hours with the standard deviation being calculated based on triplicate results.

	Compounds	PCNA	CDK4	CDK6
HeLa – 72h	Control	0.55 ±0.56	1.23 ±0.01	1.05 ±0.49
	DBM	5.73 ±0.24	7.07 ±0.17	12.22 ±1.38
	1	0.94 ±0.13	2.63 ±0.09	0.65 ±0.34
	2	2.06 ±0.42	6.47 ±0.10	8.92 ±2.57
	3	0.40 ±0.01	0.70 ±0.06	1.51 ±0.63
	4	11.54 ±0.95	2.45 ±0.06	4.65 ±0.89
	5	3.21 ±1.19	1.03 ±0.32	3.36 ±0.71
	6	1.63 ±0.06	1.41 ±0.13	0.78 ±0.40
	11	5.54 ±0.95	0.55 ±0.06	2.65 ±0.89
	12	4.21 ±1.19	0.63 ±0.32	2.36 ±0.71
	14	3.02 ±0.12	1.12 ±0.45	1.32 ±0.42
	15	2.75 ±0.32	1.23 ±0.47	1.12 ±0.36

Table 21 Gene expression was obtained on A549 cells after 48 hours with the standard deviation being calculated based on triplicate results.

	Compounds	PCNA	CDK4	CDK6
A549 – 48h	<b>Control</b>	3.52 ±0.36	1.23 ±0.01	3.15 ±0.00
	<b>DBM</b>	6.43 ±0.27	1.22 ±0.03	12.76 ±0.73
	<b>1</b>	6.02 ±0.84	0.65 ±0.02	3.89 ±0.22
	<b>2</b>	2.24 ±0.43	0.40 ±0.00	4.14 ±0.23
	<b>3</b>	1.82 ±0.83	0.70 ±0.06	1.15 ±0.06
	<b>4</b>	11.53 ±0.93	2.45 ±0.06	4.65 ±0.89
	<b>5</b>	3.21 ±1.19	1.03 ±0.32	3.36 ±0.71
	<b>6</b>	5.20 ±0.20	1.41 ±0.13	2.30 ±0.13
	<b>11</b>	1.06 ±0.42	3.47 ±0.10	2.92±2.57
	<b>12</b>	1.40 ±0.01	3.70 ±0.06	2.51 ±0.63
	<b>14</b>	6.21 ±0.36	1.64 ±0.03	6.53 ±0.33
	<b>15</b>	5.96 ±0.23	2.31 ±0.06	6.72 ±0.67

Table 22 Gene expression was obtained on A549 cells after 72 hours with the standard deviation being calculated based on triplicate results.

	<b>Compounds</b>	<b>PCNA</b>	<b>CDK4</b>	<b>CDK6</b>
<b>A549 – 72h</b>	<b>Control</b>	2.21 ±0.22	0.77 ±0.00	0.49 ±0.00
	<b>DBM</b>	4.05 ±0.17	0.78 ±0.01	1.00 ±0.05
	<b>1</b>	7.59 ±1.06	0.83 ±0.02	2.45 ±0.14
	<b>2</b>	2.13 ±0.85	1.02 ±0.01	0.65 ±0.03
	<b>3</b>	3.27 ±0.13	0.44 ±0.04	1.45 ±0.08
	<b>4</b>	11.54 ±0.93	2.45 ±0.06	4.65 ±0.89
	<b>5</b>	3.21±1.19	1.03 ±0.32	3.36 ±0.71
	<b>6</b>	3.11 ±0.52	1.78 ±0.17	0.72 ±0.04
	<b>11</b>	3.02 ±0.84	0.99 ±0.02	1.89 ±0.22
	<b>12</b>	3.24±0.43	0.99 ±0.00	1.14 ±0.23
	<b>14</b>	5.94 ±0.23	3.65 ±0.23	4.83 ±0.12
	<b>15</b>	5.71 ±0.36	2.94 ±0.12	4.12 ±0.20

Cyclin-dependent kinase 6 (CDK6) plays a vital role in regulating the progression of the cell cycle. More recently, CDK6 has also been shown to have a transcriptional role in tumor angiogenesis and whilst the Up-regulated CDK6 activity is associated with the development of several types of cancers., it should be known that CDK6 is over-expressed in various cancer cells (Bockstaele et al., 2006). The level of overexpression however has caused a positive effect for CDK6, since it has been found to be essential for cell proliferation in the pancreas, it has also been shown to reduce skin tumorigenesis and cell growth in fibroblasts. As seen from the results, it can be noted that the levels of expression of CDK6 are not high

nor are they low, with values averaging the same for all compounds on all cell lines. Studies conducted previously already show that DBM has ability to inhibit cell proliferation and has shown potent cancer hemopreventive effect in rat models of mammary tumorigenesis (Lin et al., 2011). In addition, DBM suppressed cell growth and caused cell cycle arrest in the prostate cancer cell lines (Khor et al., 2009) and also inhibited cell proliferation in human colon cancer cells, COLO 205. Cyclin-dependent kinase 4 (CDK4) and closely related CDK6 play key roles in mammalian cell proliferation, where they help to drive the progression of cells into the DNA synthetic (S) phase of the cell-division cycle, however from the results it does not seem like any compound inhibited any pathways for either proliferation or cell inhibition. Therefore the final conclusion would be that yes, the compounds provided successful in more assays than others, but they also lacked the complete biological and pharmacological activities and response required in order to challenge for a place on the pharma market. In order to do this, under strict conditions, the compounds will need to be tested on various biological and pharmacological basis before anything in the future is to be seen.

### 3.6 Conclusion and Future Work

In conclusion, based on the experimental studies conducted, it can be said that some synthesised compounds have shown more potential anti-cancer activity than other derivatives. However, no derivative showed great potential in each study completely as it was seen that if there was bias for a compound to show potential in a biological assay, then the same compound lacked that potential within the pharmacological assay. Overall, across all studies, the DBM and the diketone derivatives containing the OH hydroxyl groups performed much better in terms of cytotoxicity and stability than seen from the other compounds. This somewhat supports the theory that a compound does not need to be bulky to get the required response rather contain Functional groups which have an impact and cause activity. However, on the other hand, the much bulkier Benzoylurea derivatives showed good stability within the plasma stability assays but a low intrinsic clearance when subjected to the S9 Fraction. Furthermore, it should be noted that the 2-Azido derivatives did not show potential in both cytotoxicity and stability, and when going forward should either be disregarded or altered to enhance activity.

Going forward, the compounds need to be tested under much stricter conditions and utilising the correct controls, ie positive and negative. Once a full set of data is obtained within the studies such as the Plasma Stability and S9 Fraction stability assays, then further biological and pharmacological work can be carried out. These tests can include putting the compounds through flow cytometry, to see which phase/s of the cell cycle the compounds have activity in, thus rendering them cell cycle specific, determining the LogD value which highlights the ability to pass different barriers such as lipids. Furthermore, different genes can be tested via DNA/RNA extraction to see if the candidates respond to different gene expression. In

addition, there is further scope for the candidates to react with metals, mainly transition, to form metal complexes. By doing this, this may alter the structure of the compound and further enhance activity to get the required response that is needed from an anti-cancer agent.

## 4 References

Abdul, M., Santo, A. and Hoosein, N., 2003. Activity of potassium channel-blockers in breast cancer. *Anticancer research*, 23(4), pp.3347-3352.

Adati, R.D., Lima, S.A.M., Davolos, M.R. and Jafelicci Jr, M., 2006. A new  $\beta$ -diketone complex with high color purity. *Journal of alloys and compounds*, 418(1-2), pp.222-225.

Aden, D.P., Fogel, A., Plotkin, S., Damjanov, I. and Knowles, B.B., 1979. Controlled synthesis of HBsAg in a differentiated human liver carcinoma-derived cell line. *Nature*, 282(5739), pp.615-616.

Alnajjar, K.S. and Sweasy, J.B., 2019. A new perspective on oxidation of DNA repair proteins and cancer. *DNA repair*.

Anand, P., Kunnumakkara, A.B., Newman, R.A. and Aggarwal, B.B., 2007. Bioavailability of curcumin: problems and promises. *Molecular pharmaceutics*, 4(6), pp.807-818.

Andreassi, M., 2011. Sunscreens and photoprotection. *Expert Review of Dermatology*, 6(5), pp.433-435.

Baeza, A., Nájera, C., Sansano, J.M. and Saá, J.M., 2005. Asymmetric synthesis of O-benzoyl cyanohydrins by reaction of aldehydes with benzoyl cyanide catalysed by BINOLAM–Ti (IV) complexes. *Tetrahedron: Asymmetry*, 16(14), pp.2385-2389.

Balkwill, F., 2009. Tumour necrosis factor and cancer. *Nature reviews cancer*, 9(5), p.361.

Bansal, A. and Aggarwal, R., 2017. Effect of Reaction Conditions on the Outcome of the Reaction between 2-Hydrazino-4, 6-dimethylpyrimidine and Trifluoromethyl-beta-diketones. *Indian Journal of Heterocyclic Chemistry*, 27(4), pp.439-442.

Bartlett, S.L. and Beaudry, C.M., 2011. High-yielding oxidation of  $\beta$ -hydroxyketones to  $\beta$ -diketones using o-iodoxybenzoic acid. *The Journal of Organic Chemistry*, 76(23), pp.9852-9855.

Barua, S. and Mitragotri, S., 2013. Synergistic targeting of cell membrane, cytoplasm, and nucleus of cancer cells using rod-shaped nanoparticles. *ACS nano*, 7(11), pp.9558-9570.

Bassily, M.N., Wilson, R., Pompei, F. and Burmistrov, D., 2010. Cancer survival as a function of age at diagnosis: A study of the Surveillance, Epidemiology and End Results database. *Cancer epidemiology*, 34(6), pp.667-681.

Bell, I.M., Gallicchio, S.N., Abrams, M., Beese, L.S., Beshore, D.C., Bhimnathwala, H., Bogusky, M.J., Buser, C.A., Culberson, J.C., Davide, J. and Ellis-Hutchings, M., 2002. 3-Aminopyrrolidinone farnesyltransferase inhibitors: design of macrocyclic compounds with improved pharmacokinetics and excellent cell potency. *Journal of medicinal chemistry*, 45(12), pp.2388-2409.

Ben Saad, H., Gargouri, M., Kallel, F., Chaabene, R., Boudawara, T., Jamoussi, K., Magné, C., Mounir Zeghal, K., Hakim, A. and Ben Amara, I., 2017. Flavonoid compounds from the red marine alga *Alsidium corallinum* protect against potassium bromate-induced nephrotoxicity in adult mice. *Environmental toxicology*, 32(5), pp.1475-1486.

Berridge, M.V., Herst, P.M. and Tan, A.S., 2005. Tetrazolium dyes as tools in cell biology: new insights into their cellular reduction. *Biotechnology annual review*, 11, pp.127-152.

Bizzarri, M., Giuliani, A., Cucina, A., D'Anselmi, F., Soto, A.M. and Sonnenschein, C., 2011, June. Fractal analysis in a systems biology approach to cancer. In *Seminars in cancer biology* (Vol. 21, No. 3, pp. 175-182). Academic Press.

- Blaskó, G., Xun, L. and Cordell, G.A., 1988. Studies in the Thymelaeaceae, V. 2'-Hydroxyflavone from *Daphnopsis sellowiana*: Isolation and Synthesis. *Journal of natural products*, 51(1), pp.60-65.
- Bockstaele, L., Kooken, H., Libert, F., Paternot, S., Dumont, J.E., De Launoit, Y., Roger, P.P. and Coulonval, K., 2006. Regulated activating Thr172 phosphorylation of cyclin-dependent kinase 4 (CDK4): its relationship with cyclins and CDK "inhibitors". *Molecular and cellular biology*, 26(13), pp.5070-5085.
- Boffetta, P. and Nyberg, F., 2003. Contribution of environmental factors to cancer risk. *British medical bulletin*, 68(1), pp.71-94.
- Bosset, J.F., Collette, L., Calais, G., Mineur, L., Maingon, P., Radosevic-Jelic, L., Daban, A., Bardet, E., Beny, A. and Ollier, J.C., 2006. Chemotherapy with preoperative radiotherapy in rectal cancer. *New England Journal of Medicine*, 355(11), pp.1114-1123.
- Bracht, K., Grünert, R. and Bednarski, P.J., 2006. Correlations between the activities of 19 anti-tumor agents and the intracellular glutathione concentrations in a panel of 14 human cancer cell lines: comparisons with the National Cancer Institute data. *Anti-cancer drugs*, 17(1), pp.41-51.
- Browder, T., Butterfield, C.E., Kräling, B.M., Shi, B., Marshall, B., O'Reilly, M.S. and Folkman, J., 2000. Antiangiogenic scheduling of chemotherapy improves efficacy against experimental drug-resistant cancer. *Cancer research*, 60(7), pp.1878-1886.
- Budha, N.R., Frymoyer, A., Smelick, G.S., Jin, J.Y., Yago, M.R., Dresser, M.J., Holden, S.N., Benet, L.Z. and Ware, J.A., 2012. Drug absorption interactions between oral targeted

anticancer agents and PPIs: is pH-dependent solubility the Achilles heel of targeted therapy?. *Clinical Pharmacology & Therapeutics*, 92(2), pp.203-213.

Burdett, J.L. and Rogers, M.T., 1964. Keto-enol tautomerism in  $\beta$ -dicarbonyls studied by nuclear magnetic resonance spectroscopy. 1 I. Proton chemical shifts and equilibrium constants of pure compounds. *Journal of the American Chemical Society*, 86(11), pp.2105-2109.

Caraglia, M., Marra, M., Giuberti, G., D'alessandro, A.M., Budillon, A., Del Prete, S., Lentini, A., Beninati, S. and Abbruzzese, A., 2001. The role of eukaryotic initiation factor 5A in the control of cell proliferation and apoptosis. *Amino acids*, 20(2), pp.91-104.

Castonguay, A.L., Wrosch, C. and Sabiston, C.M., 2017. The roles of negative affect and goal adjustment capacities in breast cancer survivors: Associations with physical activity and diurnal cortisol secretion. *Health Psychology*, 36(4), p.320.

Cavalieri, E.L., Rogan, E.G. and Zahid, M., 2017. Critical depurinating DNA adducts: Estrogen adducts in the etiology and prevention of cancer and dopamine adducts in the etiology and prevention of Parkinson's disease. *International journal of cancer*, 141(6), pp.1078-1090.

Chan, D.S., Lau, R., Aune, D., Vieira, R., Greenwood, D.C., Kampman, E. and Norat, T., 2011. Red and processed meat and colorectal cancer incidence: meta-analysis of prospective studies. *PloS one*, 6(6), p.e20456.

Chee, C.F., 2011. *Synthesis of bioactive cyclohexenyl chalcones and flavonoid derivatives*/Chee Chin Fei (Doctoral dissertation, University of Malaya).

Chen, X., Wu, Y., Dong, H., Y Zhang, C. and Zhang, Y., 2013. Platinum-based agents for individualized Cancer Treatment. *Current molecular medicine*, 13(10), pp.1603-1612.

Chen-Kiang, S., Di Liberto, M. and Huang, X., Cornell University, 2016. *Targeting CDK4 and CDK6 in cancer therapy*. U.S. Patent 9,259,399.

Cheung-Ong, K., Giaever, G. and Nislow, C., 2013. DNA-damaging agents in cancer chemotherapy: serendipity and chemical biology. *Chemistry & biology*, 20(5), pp.648-659.

Chiu, C.C., Haung, J.W., Chang, F.R., Huang, K.J., Huang, H.M., Huang, H.W., Chou, C.K., Wu, Y.C. and Chang, H.W., 2013. Golden berry-derived 4 $\beta$ -hydroxywithanolide E for selectively killing oral cancer cells by generating ROS, DNA damage, and apoptotic pathways. *PLoS One*, 8(5), p.e64739.

Collins, D., Hogan, A.M. and Winter, D.C., 2011. Microbial and viral pathogens in colorectal cancer. *The lancet oncology*, 12(5), pp.504-512.

Cook, A.G. and Feltman, P.M., 2007. Determination of Solvent Effects on Keto—Enol Equilibria of 1, 3-Dicarbonyl Compounds Using NMR. *Journal of chemical education*, 84(11), p.1827.

Cory, S. and Adams, J.M., 2005. Killing cancer cells by flipping the Bcl-2/Bax switch. *Cancer cell*, 8(1), pp.5-6.

Croce, C.M., 2008. Oncogenes and cancer. *New England journal of medicine*, 358(5), pp.502-511.

Curtin, N.J., 2012. DNA repair dysregulation from cancer driver to therapeutic target. *Nature Reviews Cancer*, 12(12), p.801.

Danaei, G., Vander Hoorn, S., Lopez, A.D., Murray, C.J., Ezzati, M. and Comparative Risk Assessment collaborating group (Cancers, 2005. Causes of cancer in the world: comparative

risk assessment of nine behavioural and environmental risk factors. *The Lancet*, 366(9499), pp.1784-1793.

Danø, K., Behrendt, N., Høyer-Hansen, G., Johnsen, M., Lund, L.R., Ploug, M. and Rømer, J., 2005. Plasminogen activation and cancer. *Thrombosis and haemostasis*, 93(04), pp.676-681.

Dasari, S. and Tchounwou, P.B., 2014. Cisplatin in cancer therapy: molecular mechanisms of action. *European journal of pharmacology*, 740, pp.364-378.

Dawson, M.A. and Kouzarides, T., 2012. Cancer epigenetics: from mechanism to therapy. *Cell*, 150(1), pp.12-27.

Delaney, G., Jacob, S., Featherstone, C. and Barton, M., 2005. The role of radiotherapy in cancer treatment: estimating optimal utilization from a review of evidence-based clinical guidelines. *Cancer: Interdisciplinary International Journal of the American Cancer Society*, 104(6), pp.1129-1137.

DeVita, V.T. and Chu, E., 2008. A history of cancer chemotherapy. *Cancer research*, 68(21), pp.8643-8653.

Dittrich, N., Jung, E.K., Davidson, S.J. and Barker, D., 2016. An acyl-Claisen/Paal-Knorr approach to fully substituted pyrroles. *Tetrahedron*, 72(31), pp.4676-4689.

Doak, S.H., Jenkins, G.J., Johnson, G.E., Quick, E., Parry, E.M. and Parry, J.M., 2007. Mechanistic influences for mutation induction curves after exposure to DNA-reactive carcinogens. *Cancer research*, 67(8), pp.3904-3911.

Douer, D., 2016. Efficacy and safety of vincristine sulfate liposome injection in the treatment of adult acute lymphocytic leukemia. *The oncologist*, 21(7), pp.840-847.

El Mahjoub, A. and Staub, C., 2000. Stability of benzodiazepines in whole blood samples stored at varying temperatures. *Journal of pharmaceutical and biomedical analysis*, 23(6), pp.1057-1063.

Etxeberria, A., Mendarte, S. and Larregla, S., 2011. Determination of viability of *Phytophthora capsici* oospores with the tetrazolium bromide staining test versus a plasmolysis method. *Revista iberoamericana de micologia*, 28(1), pp.43-49.

Farber, S., Diamond, L.K., Mercer, R.D., Sylvester Jr, R.F. and Wolff, J.A., 1948. Temporary remissions in acute leukemia in children produced by folic acid antagonist, 4-aminopteroyl-glutamic acid (aminopterin). *New England Journal of Medicine*, 238(23), pp.787-793.

Finn, O.J., 2008. Cancer immunology. *New England Journal of Medicine*, 358(25), pp.2704-2715.

Forastiere, A.A., Goepfert, H., Maor, M., Pajak, T.F., Weber, R., Morrison, W., Glisson, B., Trotti, A., Ridge, J.A., Chao, C. and Peters, G., 2003. Concurrent chemotherapy and radiotherapy for organ preservation in advanced laryngeal cancer. *New England Journal of Medicine*, 349(22), pp.2091-2098.

Forment, J.V., Kaidi, A. and Jackson, S.P., 2012. Chromothripsis and cancer: causes and consequences of chromosome shattering. *Nature Reviews Cancer*, 12(10), p.663.

Formenti, S.C. and Demaria, S., 2013. Combining radiotherapy and cancer immunotherapy: a paradigm shift. *JNCI: Journal of the National Cancer Institute*, 105(4), pp.256-265.

Fotakis, G. and Timbrell, J.A., 2006. In vitro cytotoxicity assays: comparison of LDH, neutral red, MTT and protein assay in hepatoma cell lines following exposure to cadmium chloride. *Toxicology letters*, 160(2), pp.171-177.

Ge, W.W., Volkening, K., Leystra-Lantz, C., Jaffe, H. and Strong, M.J., 2007. 14-3-3 protein binds to the low molecular weight neurofilament (NFL) mRNA 3' UTR. *Molecular and Cellular Neuroscience*, 34(1), pp.80-87.

Gerets, H.H.J., Tilmant, K., Gerin, B., Chanteux, H., Depelchin, B., Dhalluin, S. and Atienzar, F.A., 2012. Characterization of primary human hepatocytes, HepG2 cells, and HepaRG cells at the mRNA level and CYP activity in response to inducers and their predictivity for the detection of human hepatotoxins. *Cell biology and toxicology*, 28(2), pp.69-87.

Gonzalez, H., Hagerling, C. and Werb, Z., 2018. Roles of the immune system in cancer: from tumor initiation to metastatic progression. *Genes & development*, 32(19-20), pp.1267-1284.

GRAHAM, D.Y., 2000. Helicobacter pylori infection is the primary cause of gastric cancer. *Journal of gastroenterology*, 35.

Gu, X., Xiao, Q., Ruan, Q., Shu, Y., Dongre, A., Iyer, R., Humphreys, W.G. and Lai, Y., 2018. Comparative untargeted proteomic analysis of ADME proteins and tumor antigens for tumor cell lines. *Acta pharmaceutica sinica B*, 8(2), pp.252-260.

Gudmundsson, J., Sulem, P., Gudbjartsson, D.F., Blondal, T., Gylfason, A., Agnarsson, B.A., Benediktsdottir, K.R., Magnusdottir, D.N., Orlygsdottir, G., Jakobsdottir, M. and Stacey, S.N., 2009. Genome-wide association and replication studies identify four variants associated with prostate cancer susceptibility. *Nature genetics*, 41(10), p.1122.

Guescini, M., Sisti, D., Rocchi, M.B., Stocchi, L. and Stocchi, V., 2008. A new real-time PCR method to overcome significant quantitative inaccuracy due to slight amplification inhibition. *BMC bioinformatics*, 9(1), pp.1-12.

Gundem, G., Van Loo, P., Kremeyer, B., Alexandrov, L.B., Tubio, J.M., Papaemmanuil, E., Brewer, D.S., Kallio, H.M., Högnäs, G., Annala, M. and Kivinummi, K., 2015. The evolutionary history of lethal metastatic prostate cancer. *Nature*, 520(7547), p.353.

Hambley, T.W., 2009. Is anticancer drug development heading in the right direction?. *Cancer research*, 69(4), pp.1259-1262.

Hanahan, D. and Weinberg, R.A., 2011. Hallmarks of cancer: the next generation. *cell*, 144(5), pp.646-674.

Hartman, D.A., 2002. Determination of the stability of drugs in plasma. *Current protocols in pharmacology*, 19(1), pp.7-6.

Hayflick, L. and Moorhead, P.S., 1961. The serial cultivation of human diploid cell strains. *Experimental cell research*, 25(3), pp.585-621.

He, Y., Zhu, Q., Chen, M., Huang, Q., Wang, W., Li, Q., Huang, Y. and Di, W., 2016. The changing 50% inhibitory concentration (IC50) of cisplatin: A pilot study on the artifacts of the MTT assay and the precise measurement of density-dependent chemoresistance in ovarian cancer. *Oncotarget*, 7(43), p.70803.

Hickok, J.T., Morrow, G.R., Roscoe, J.A., Mustian, K. and Okunieff, P., 2005. Occurrence, severity, and longitudinal course of twelve common symptoms in 1129 consecutive patients during radiotherapy for cancer. *Journal of pain and symptom management*, 30(5), pp.433-442.

Hochberg, M.E. and Noble, R.J., 2017. A framework for how environment contributes to cancer risk. *Ecology letters*, 20(2), pp.117-134.

Holick, M.F., 2008. Sunlight, UV-radiation, vitamin D and skin cancer: how much sunlight do we need?. In *Sunlight, Vitamin D and Skin Cancer* (pp. 1-15). Springer, New York, NY.

Hong, S.Y., Kim, Y., Park, Y., Choi, A., Choi, N.S. and Lee, K.T., 2013. Charge carriers in rechargeable batteries: Na ions vs. Li ions. *Energy & Environmental Science*, 6(7), pp.2067-2081.

Ikedioji, O.N., Davies, H., Bignell, G., Edkins, S., Stevens, C., O'Meara, S., Santarius, T., Avis, T., Barthorpe, S., Brackenbury, L. and Buck, G., 2006. Mutation analysis of 24 known cancer genes in the NCI-60 cell line set. *Molecular cancer therapeutics*, 5(11), pp.2606-2612.

Indolfi, P., Bisogno, G., Casale, F., Cecchetto, G., De Salvo, G., Ferrari, A., Donfrancesco, A., Donofrio, V., Martone, A., Di Martino, M. and Di Tullio, M.T., 2007. Prognostic factors in pleuro-pulmonary blastoma. *Pediatric blood & cancer*, 48(3), pp.318-323.

J Richardson, S., Bai, A., A Kulkarni, A. and F Moghaddam, M., 2016. Efficiency in drug discovery: liver S9 fraction assay as a screen for metabolic stability. *Drug metabolism letters*, 10(2), pp.83-90.

Jones, R., Ruas, M., Gregory, F., Moulin, S., Delia, D., Manoukian, S., Rowe, J., Brookes, S. and Peters, G., 2007. A CDKN2A mutation in familial melanoma that abrogates binding of p16INK4a to CDK4 but not CDK6. *Cancer research*, 67(19), pp.9134-9141.

Kareva, I., Waxman, D.J. and Klement, G.L., 2015. Metronomic chemotherapy: an attractive alternative to maximum tolerated dose therapy that can activate anti-tumor immunity and minimize therapeutic resistance. *Cancer letters*, 358(2), pp.100-106.

KC, S.K., Wallace, D.M., Hood, J. and Barroga, C.F., Samumed LLC, 2013.  *$\beta$ -and  $\gamma$ -diketones and  $\gamma$ -hydroxyketones as WNT/ $\beta$ -catenin signaling pathway activators*. U.S. Patent 8,609,717.

Kel'in, A.V. and Maioli, A., 2003. Recent advances in the chemistry of 1, 3-diketones: Structural modifications and synthetic applications. *Current Organic Chemistry*, 7(18), pp.1855-1886.

Khan, S.K., Yadav, P.S., Elliott, G., Hu, D.Z., Xu, R. and Yang, Y., 2018. Induced GnasR201H expression from the endogenous Gnas locus causes fibrous dysplasia by up-regulating Wnt/ $\beta$ -catenin signaling. *Proceedings of the National Academy of Sciences*, 115(3), pp.E418-E427.

Khor, T.O., Yu, S., Barve, A., Hao, X., Hong, J.L., Lin, W., Foster, B., Huang, M.T., Newmark, H.L. and Kong, A.N., 2009. Dietary feeding of dibenzoylmethane inhibits prostate cancer in transgenic adenocarcinoma of the mouse prostate model. *Cancer research*, 69(17), pp.7096-7102.

Kim, J.S., He, L. and Lemasters, J.J., 2003. Mitochondrial permeability transition: a common pathway to necrosis and apoptosis. *Biochemical and biophysical research communications*, 304(3), pp.463-470.

Koster, R., di Pietro, A., Timmer-Bosscha, H., Gibcus, J.H., van den Berg, A., Suurmeijer, A.J., Bischoff, R., Gietema, J.A. and de Jong, S., 2010. Cytoplasmic p21 expression levels determine cisplatin resistance in human testicular cancer. *The Journal of clinical investigation*, 120(10), pp.3594-3605.

Koster, R., Van Vugt, M.A.T.M., Timmer-Bosscha, H., Gietema, J.A. and De Jong, S., 2013. Unravelling mechanisms of cisplatin sensitivity and resistance in testicular cancer. *Expert reviews in molecular medicine*, 15.

Küppers, R., Engert, A. and Hansmann, M.L., 2012. Hodgkin lymphoma. *The Journal of clinical investigation*, 122(10), pp.3439-3447.

Kusmartsev, S., Eruslanov, E., Kübler, H., Tseng, T., Sakai, Y., Su, Z., Kaliberov, S., Heiser, A., Rosser, C., Dahm, P. and Siemann, D., 2008. Oxidative stress regulates expression of VEGFR1 in myeloid cells: link to tumor-induced immune suppression in renal cell carcinoma. *The Journal of Immunology*, 181(1), pp.346-353.

Lamb, J., Ramaswamy, S., Ford, H.L., Contreras, B., Martinez, R.V., Kittrell, F.S., Zahnow, C.A., Patterson, N., Golub, T.R. and Ewen, M.E., 2003. A mechanism of cyclin D1 action encoded in the patterns of gene expression in human cancer. *Cell*, 114(3), pp.323-334.

Lee, J.I., Son, H.S. and Jung, M.G., 2005. A novel synthesis of flavones from 2-methoxybenzoic acids. *Bulletin of the Korean Chemical Society*, 26(9), pp.1461-1463.

Lee, K.Y., Lee, M.J. and Kim, J.N., 2005. Facile synthesis of  $\alpha$ ,  $\beta$ -acetylenic ketones and 2, 5-disubstituted furans: consecutive activation of triple and double bond with ZnBr<sub>2</sub> toward the synthesis of furan ring. *Tetrahedron*, 61(36), pp.8705-8710.

Letai, A.G., 2008. Diagnosing and exploiting cancer's addiction to blocks in apoptosis. *Nature Reviews Cancer*, 8(2), p.121.

Liang, G., Li, X., Chen, L., Yang, S., Wu, X., Studer, E., Gurley, E., Hylemon, P.B., Ye, F., Li, Y. and Zhou, H., 2008. Synthesis and anti-inflammatory activities of mono-carbonyl analogues of curcumin. *Bioorganic & medicinal chemistry letters*, 18(4), pp.1525-1529.

- Lijinsky, W. and Andrews, A.W., 1983. The superiority of hamster liver microsomal fraction for activating nitrosamines to mutagens in *Salmonella typhimurium*. *Mutation Research/Fundamental and Molecular Mechanisms of Mutagenesis*, 111(2), pp.135-144.
- Lin, J.T., Griffith, O.M. and Corse, J.W., 1985. Subcellular fractionation of wheat leaf protoplasts by centrifugal elutriation. *Analytical biochemistry*, 148(1), pp.10-14.
- Lin, W., Hong, J.L., Shen, G., Wu, R.T., Wang, Y., Huang, M.T., Newmark, H.L., Huang, Q., Khor, T.O., Heimbach, T. and Kong, A.N., 2011. Pharmacokinetics of dietary cancer chemopreventive compound dibenzoylmethane in rats and the impact of nanoemulsion and genetic knockout of Nrf2 on its disposition. *Biopharmaceutics & drug disposition*, 32(2), pp.65-75.
- Liu, L. and Gerson, S., Case Western Reserve University, 2016. *Antimetabolite agent combinations in the treatment of cancer*. U.S. Patent 9,498,489.
- Liu, W.M. and Dalglish, A.G., 2009. MTT assays can underestimate cell numbers. *Cancer chemotherapy and pharmacology*, 64(4), p.861.
- Liu, Y., Miyoshi, H. and Nakamura, M., 2007. Nanomedicine for drug delivery and imaging: a promising avenue for cancer therapy and diagnosis using targeted functional nanoparticles. *International journal of cancer*, 120(12), pp.2527-2537.
- Lucas, J.J., Domenico, J. and Gelfand, E.W., 2004. Cyclin-Dependent Kinase 6 Inhibits Proliferation of Human Mammary Epithelial Cells<sup>1</sup> Supported in part by grants from the Denver Metropolitan Chapter of the Susan G. Komen Breast Cancer Foundation and the Cancer League of Colorado, American Cancer Society (grant IM-746), NIH (grants HL-36577

and AI-42246), and University of Colorado Cancer Center (grant CA46934). *Molecular Cancer Research*, 2(2), pp.105-114.

Manconi, M., Isola, R., Falchi, A.M., Sinico, C. and Fadda, A.M., 2007. Intracellular distribution of fluorescent probes delivered by vesicles of different lipidic composition. *Colloids and Surfaces B: Biointerfaces*, 57(2), pp.143-151.

Marijnen, C.A.M., Kapiteijn, E., Van de Velde, C.J.H., Martijn, H., Steup, W.H., Wiggers, T., Kranenbarg, E.K., Leer, J.W.H. and Cooperative Investigators of the Dutch Colorectal Cancer Group, 2002. Acute side effects and complications after short-term preoperative radiotherapy combined with total mesorectal excision in primary rectal cancer: report of a multicenter randomized trial. *Journal of clinical oncology*, 20(3), pp.817-825.

Maron, D.M. and Ames, B.N., 1983. Revised methods for the Salmonella mutagenicity test. *Mutation Research/Environmental Mutagenesis and Related Subjects*, 113(3-4), pp.173-215.

Marshall, D.C., Webb, T.E., Hall, R.A., Saliccioli, J.D., Ali, R. and Maruthappu, M., 2016. Trends in UK regional cancer mortality 1991–2007. *British journal of cancer*, 114(3), p.340.

Matherly, L.H., Hou, Z. and Deng, Y., 2007. Human reduced folate carrier: translation of basic biology to cancer etiology and therapy. *Cancer and metastasis reviews*, 26(1), pp.111-128.

Matushansky, I., Radparvar, F. and Skoultchi, A.I., 2003. CDK6 blocks differentiation: coupling cell proliferation to the block to differentiation in leukemic cells. *Oncogene*, 22(27), p.4143.

- Mayadev, J., Lim, J., Durbin-Johnson, B., Valicenti, R. and Alvarez, E., 2018. Smoking decreases survival in locally advanced cervical cancer treated with radiation. *American journal of clinical oncology*, 41(3), pp.295-301.
- Miller, A.J. and Mihm Jr, M.C., 2006. Melanoma. *New England Journal of Medicine*, 355(1), pp.51-65.
- Miyata, M., Furukawa, M., Takahashi, K., Gonzalez, F.J. and Yamazoe, Y., 2001. Mechanism of 7, 12-dimethylbenz [a] anthracene-induced immunotoxicity: role of metabolic activation at the target organ. *The Japanese Journal of Pharmacology*, 86(3), pp.302-309.
- Moldovan, G.L., Pfander, B. and Jentsch, S., 2007. PCNA, the maestro of the replication fork. *Cell*, 129(4), pp.665-679.
- Mora, M.C., Bassa, L.M., Wong, K.E., Tirabassi, M.V., Arenas, R.B. and Schneider, S.S., 2015. *Rhodiola crenulata* inhibits Wnt/ $\beta$ -catenin signaling in glioblastoma. *Journal of Surgical Research*, 197(2), pp.247-255.
- More, J.D. and Finney, N.S., 2002. A simple and advantageous protocol for the oxidation of alcohols with O-iodoxybenzoic acid (IBX). *Organic Letters*, 4(17), pp.3001-3003.
- Mori, Y., Kato, S., Fujisawa, Y., Ohnishi, S., Hiraku, Y., Kawanishi, S., Murata, M. and Oikawa, S., 2019. Mechanisms of DNA damage induced by morin, an inhibitor of amyloid  $\beta$ -peptide aggregation. *Free radical research*, 53(1), pp.115-123.
- Mortelmans, K. and Zeiger, E., 2000. The Ames Salmonella/microsome mutagenicity assay. *Mutation research/fundamental and molecular mechanisms of mutagenesis*, 455(1-2), pp.29-60.

Moyer, V.A., 2014. Screening for lung cancer: US Preventive Services Task Force recommendation statement. *Annals of internal medicine*, 160(5), pp.330-338.

Muirhead, R., Drinkwater, K., O'Cathail, S.M., Adams, R., Glynne-Jones, R., Harrison, M., Hawkins, M.A., Sebag-Montefiore, D. and Gilbert, D.C., 2017. Initial results from the Royal College of Radiologists' UK national audit of anal cancer radiotherapy 2015. *Clinical Oncology*, 29(3), pp.188-197.

NAKANO, K., NAKAYACHI, T., YASUMOTO, E., MORSHED, S.R.M., Hashimoto, K.E.N., KIKUCHI, H., NISHIKAWA, H., SUGIYAMA, K., AMANO, O., KAWASE, M. and SAKAGAMI, H., 2004. Induction of apoptosis by  $\beta$ -diketones in human tumor cells. *Anticancer research*, 24(2B), pp.711-718.

Nandurkar, N.S., Bhanushali, M.J., Bhor, M.D. and Bhanage, B.M., 2007. Y (NO<sub>3</sub>)<sub>3</sub>·6H<sub>2</sub>O: A novel and reusable catalyst for one pot synthesis of 3, 4-dihydropyrimidin-2 (1H)-ones under solvent-free conditions. *Journal of Molecular Catalysis A: Chemical*, 271(1-2), pp.14-17.

Neidle, S. and Thurston, D.E., 2005. Chemical approaches to the discovery and development of cancer therapies. *Nature Reviews Cancer*, 5(4), p.285.

Nishida, N., Yano, H., Nishida, T., Kamura, T. and Kojiro, M., 2006. Angiogenesis in cancer. *Vascular health and risk management*, 2(3), p.213.

Nishida-Aoki, N. and Ochiya, T., 2015. Interactions between cancer cells and normal cells via miRNAs in extracellular vesicles. *Cellular and Molecular Life Sciences*, 72(10), pp.1849-1861.

Nohmi, T., Yoshikawa, K., Nakadate, M. and Ishidate Jr, M., 1983. Species difference in the metabolic activation of phenacetin by rat and hamster liver microsomes. *Biochemical and biophysical research communications*, 110(3), pp.746-752.

- Nossal, G.J.V., 1994. Negative selection of lymphocytes. *cell*, 76(2), pp.229-239.
- Ogu, C.C. and Maxa, J.L., 2000, October. Drug interactions due to cytochrome P450. In Baylor University Medical Center Proceedings (Vol. 13, No. 4, pp. 421-423). Taylor & Francis.
- Ohmichi, M., Hayakawa, J., Tasaka, K., Kurachi, H. and Murata, Y., 2005. Mechanisms of platinum drug resistance. *Trends in pharmacological sciences*, 26(3), pp.113-116.
- Ohnishi, M., Katsuki, H., Fujimoto, S., Takagi, M., Kume, T. and Akaike, A., 2007. Involvement of thrombin and mitogen-activated protein kinase pathways in hemorrhagic brain injury. *Experimental neurology*, 206(1), pp.43-52.
- O'Leary, B., Finn, R.S. and Turner, N.C., 2016. Treating cancer with selective CDK4/6 inhibitors. *Nature reviews Clinical oncology*, 13(7), p.417.
- Pantel, K., Brakenhoff, R.H. and Brandt, B., 2008. Detection, clinical relevance and specific biological properties of disseminating tumour cells. *Nature Reviews Cancer*, 8(5), p.329.
- Parkin, D.M., Boyd, L. and Walker, L.C., 2011. 16. The fraction of cancer attributable to lifestyle and environmental factors in the UK in 2010. *British journal of cancer*, 105(S2), p.S77.
- Pastan, I., Hassan, R., FitzGerald, D.J. and Kreitman, R.J., 2007. Immunotoxin treatment of cancer. *Annu. Rev. Med.*, 58, pp.221-237.
- Paun, B.C., Cassie, S., MacLean, A.R., Dixon, E. and Buie, W.D., 2010. Postoperative complications following surgery for rectal cancer. *Annals of surgery*, 251(5), pp.807-818.

Paunesku, T., Mittal, S., Protić, M., Oryhon, J., Korolev, S.V., Joachimiak, A. and Woloschak, G.E., 2001. Proliferating cell nuclear antigen (PCNA): ringmaster of the genome. *International journal of radiation biology*, 77(10), pp.1007-1021.

Pennathur, A., Gibson, M.K., Jobe, B.A. and Luketich, J.D., 2013. Oesophageal carcinoma. *The Lancet*, 381(9864), pp.400-412.

Plati, J., Bucur, O. and Khosravi-Far, R., 2011. Apoptotic cell signaling in cancer progression and therapy. *Integrative biology*, 3(4), pp.279-296.

Polk, D.B. and Peek Jr, R.M., 2010. Helicobacter pylori: gastric cancer and beyond. *Nature Reviews Cancer*, 10(6), p.403.

Pradhan, J. and Goyal, A., 2015.  $\beta$ -diketones: Important Intermediates for Drug Synthesis. *International Journal of Pharmaceutical Research & Allied Sciences*, 4(2).

Prasad, S., Tyagi, A.K. and Aggarwal, B.B., 2014. Recent developments in delivery, bioavailability, absorption and metabolism of curcumin: the golden pigment from golden spice. *Cancer research and treatment: official journal of Korean Cancer Association*, 46(1), p.2.

Prival, M.J. and Mitchell, V.D., 1982. Analysis of a method for testing azo dyes for mutagenic activity in Salmonella typhimurium in the presence of flavin mononucleotide and hamster liver S9. *Mutation Research/Environmental Mutagenesis and Related Subjects*, 97(2), pp.103-116.

Pui, C.H., Robison, L.L. and Look, A.T., 2008. Acute lymphoblastic leukaemia. *The Lancet*, 371(9617), pp.1030-1043.

Radi, S., Tighadouini, S., Feron, O., Riant, O., Bouakka, M., Benabbes, R. and Mabkhot, Y., 2015. Synthesis of novel  $\beta$ -keto-enol derivatives tethered pyrazole, pyridine and furan as new potential antifungal and anti-breast cancer agents. *Molecules*, 20(11), pp.20186-20194.

Rahbar, A., Orrego, A., Peredo, I., Dzabic, M., Wolmer-Solberg, N., Strååt, K., Stragliotto, G. and Söderberg-Nauclér, C., 2013. Human cytomegalovirus infection levels in glioblastoma multiforme are of prognostic value for survival. *Journal of Clinical Virology*, 57(1), pp.36-42.

Rayan, A., Raiyn, J. and Falah, M., 2017. Nature is the best source of anticancer drugs: Indexing natural products for their anticancer bioactivity. *PLoS One*, 12(11), p.e0187925.

Rutledge, R.G. and Cote, C., 2003. Mathematics of quantitative kinetic PCR and the application of standard curves. *Nucleic acids research*, 31(16), pp.e93-e93.

Saiki, R.K., Scharf, S., Faloona, F., Mullis, K.B., Horn, G.T., Erlich, H.A. and Arnheim, N., 1985. Enzymatic amplification of  $\beta$ -globin genomic sequences and restriction site analysis for diagnosis of sickle cell anemia. *Science*, 230(4732), pp.1350-1354.

Salunkhe, R.R., Ahn, H., Kim, J.H. and Yamauchi, Y., 2015. Rational design of coaxial structured carbon nanotube–manganese oxide (CNT–MnO<sub>2</sub>) for energy storage application. *Nanotechnology*, 26(20), p.204004.

Sambaiah, M., Raghavulu, K., Kumar, K.S., Yennam, S. and Behera, M., 2017. Synthesis of novel fused chromone–pyrimidine hybrids and 2, 4, 5-trisubstituted pyrimidine derivatives via ANRORC rearrangement. *New Journal of Chemistry*, 41(18), pp.10020-10026.

Sambuy, Y., De Angelis, I., Ranaldi, G., Scarino, M.L., Stammati, A. and Zucco, F., 2005. The Caco-2 cell line as a model of the intestinal barrier: influence of cell and culture-related factors on Caco-2 cell functional characteristics. *Cell biology and toxicology*, 21(1), pp.1-26.

Sangar, M.L.C., Genovesi, L.A., Nakamoto, M.W., Davis, M.J., Knobluagh, S.E., Ji, P., Millar, A., Wainwright, B.J. and Olson, J.M., 2017. Inhibition of CDK4/6 by palbociclib significantly extends survival in medulloblastoma patient-derived xenograft mouse models. *Clinical Cancer Research*, 23(19), pp.5802-5813.

Sartape, A.S., Patil, S.A., Patil, S.K., Salunkhe, S.T. and Kolekar, S.S., 2015. Mahogany fruit shell: a new low-cost adsorbent for removal of methylene blue dye from aqueous solutions. *Desalination and Water Treatment*, 53(1), pp.99-108.

Scharovsky, O.G., Mainetti, L.E. and Rozados, V.R., 2009. Metronomic chemotherapy: changing the paradigm that more is better. *Current oncology*, 16(2), p.7.

Scherer, W.F., Syverton, J.T. and Gey, G.O., 1953. Studies on the propagation in vitro of poliomyelitis viruses: IV. Viral multiplication in a stable strain of human malignant epithelial cells (strain HeLa) derived from an epidermoid carcinoma of the cervix. *The Journal of experimental medicine*, 97(5), pp.695-710.

SCHERLIEß, R., 2011. The MTT assay as tool to evaluate and compare excipient toxicity in vitro on respiratory epithelial cells. *International journal of pharmaceutics*, 411(1-2), pp.98-105.

Shaffi, S.M., Shah, M.A., Bhat, I.A., Koul, P., Ahmad, S.N. and Siddiqi, M.A., 2009. CYP1A1 polymorphisms and risk of lung cancer in the ethnic Kashmiri population. *Asian Pac J Cancer Prev*, 10(4), pp.651-656.

Shah, M.A., Kojima, T., Hochhauser, D., Enzinger, P., Raimbourg, J., Hollebecque, A., Lordick, F., Kim, S.B., Tajika, M., Kim, H.T. and Lockhart, A.C., 2019. Efficacy and safety of pembrolizumab for heavily pretreated patients with advanced, metastatic adenocarcinoma

or squamous cell carcinoma of the esophagus: the phase 2 KEYNOTE-180 study. *JAMA oncology*, 5(4), pp.546-550.

Shah, V.P., Midha, K.K., Dighe, S., McGilveray, I.J., Skelly, J.P., Yacobi, A., Layloff, T., Viswanathan, C.T., Cook, C.E., McDowall, R.D. and Pittman, K.A., 1992. Analytical methods validation: bioavailability, bioequivalence, and pharmacokinetic studies. *Journal of pharmaceutical sciences*, 81(3), pp.309-312

Sheikh, J.I., Ingle, V.N. and Juneja, H.D., 2009. Synthesis of Novel Antibacterial Agents: 1-(2', 4'-Dihydroxy-5'-chlorophenyl)-3-arylpropane-1, 3-Diones. *Journal of Chemistry*, 6(3), pp.705-712.

Sheppard, K.E. and McArthur, G.A., 2013. The cell-cycle regulator CDK4: an emerging therapeutic target in melanoma.

Shirzadfar, H., Riahi, S. and Ghaziasgar, M.S., 2017. Cancer imaging and brain tumor diagnosis. *J Bioanalysis and Biomedicine*, 9, pp.1-2.

Siegel, R.L., Miller, K.D. and Jemal, A., 2015. Cancer statistics, 2015. *CA: a cancer journal for clinicians*, 65(1), pp.5-29.

Simoni, D., Rizzi, M., Rondanin, R., Baruchello, R., Marchetti, P., Invidiata, F.P., Labbozzetta, M., Poma, P., Carina, V., Notarbartolo, M. and Alaimo, A., 2008. Antitumor effects of curcumin and structurally  $\beta$ -diketone modified analogs on multidrug resistant cancer cells. *Bioorganic & medicinal chemistry letters*, 18(2), pp.845-849.

Singh, S., Singh, M.K., Agarwal, A., Hussain, F. and Awasthi, S.K., 2011. (2E)-1-(4-Aminophenyl)-3-(2, 4-dichlorophenyl) prop-2-en-1-one. *Acta Crystallographica Section E: Structure Reports Online*, 67(7), pp.o1616-o1617.

Siviero, A., Gallo, E., Maggini, V., Gori, L., Mugelli, A., Firenzuoli, F. and Vannacci, A., 2015. Curcumin, a golden spice with a low bioavailability. *Journal of Herbal Medicine*, 5(2), pp.57-70.

Skeel, R.T. and Khleif, S.N. eds., 2011. *Handbook of cancer chemotherapy*. Lippincott Williams & Wilkins.

Skopp, G., 2004. Preanalytic aspects in postmortem toxicology. *Forensic science international*, 142(2-3), pp.75-100

Smith, A., Howell, D., Patmore, R., Jack, A. and Roman, E., 2011. Incidence of haematological malignancy by sub-type: a report from the Haematological Malignancy Research Network. *British journal of cancer*, 105(11), p.1684.

Smith, S. and Prewett, S., 2017. Principles of chemotherapy and radiotherapy. *Obstetrics, Gynaecology & Reproductive Medicine*, 27(7), pp.206-212.

Spies, T.D., 1946. Effect of folic acid on persons with macrocytic anemia in relapse. *Journal of the American Medical Association*, 130(8), pp.474-477.

Thomas, L.H., Florence, A.J. and Wilson, C.C., 2009. Hydrogen atom behaviour imaged in a short intramolecular hydrogen bond using the combined approach of X-ray and neutron diffraction. *New Journal of Chemistry*, 33(12), pp.2486-2490.

Tobias, J.S., Hochhauser, D. and Souhami, R.L., 2010. *Cancer and its management*. Oxford: Wiley-Blackwell.

Tward, A.D., Jones, K.D., Yant, S., Cheung, S.T., Fan, S.T., Chen, X., Kay, M.A., Wang, R. and Bishop, J.M., 2007. Distinct pathways of genomic progression to benign and malignant

tumors of the liver. *Proceedings of the National Academy of Sciences*, 104(37), pp.14771-14776.

Umar, S., Kumar, A., Sajad, M., Zargan, J., Ansari, M.M., Ahmad, S., Katiyar, C.K. and Khan, H.A., 2013. Hesperidin inhibits collagen-induced arthritis possibly through suppression of free radical load and reduction in neutrophil activation and infiltration. *Rheumatology international*, 33(3), pp.657-663.

Undevia, S.D., Gomez-Abuin, G. and Ratain, M.J., 2005. Pharmacokinetic variability of anticancer agents. *Nature Reviews Cancer*, 5(6), p.447.

Urbaniak, W., Jurek, K., Witt, K., Goraczko, A., Staniszewski, B. and Mickiewicz, A., 2011. Properties and application of diketones and their derivatives. *Chemik*, 65(4), p.273.

van de Steeg, E., van der Kruijssen, C.M., Wagenaar, E., Burggraaff, J.E., Mesman, E., Kenworthy, K.E. and Schinkel, A.H., 2009. Methotrexate pharmacokinetics in transgenic mice with liver-specific expression of human organic anion-transporting polypeptide 1B1 (SLCO1B1). *Drug Metabolism and Disposition*, 37(2), pp.277-281.

Van Leeuwen, R.W.F., Brundel, D.H.S., Neef, C., van Gelder, T., Mathijssen, R.H.J., Burger, D.M. and Jansman, F.G.A., 2013. Prevalence of potential drug–drug interactions in cancer patients treated with oral anticancer drugs. *British journal of cancer*, 108(5), p.1071.

Van Meerloo, J., Kaspers, G.J. and Cloos, J., 2011. Cell sensitivity assays: the MTT assay. In *Cancer cell culture* (pp. 237-245). Humana Press.

Varkhede, N.R., Jhajra, S., Ahire, D.S. and Singh, S., 2014. Metabolite identification studies on amiodarone in in vitro (rat liver microsomes, rat and human liver S9 fractions) and in vivo (rat feces, urine, plasma) matrices by using liquid chromatography with high-resolution

mass spectrometry and multiple-stage mass spectrometry: Characterization of the diquinone metabolite supposedly responsible for the drug's hepatotoxicity. *Rapid Communications in Mass Spectrometry*, 28(4), pp.311-331.

Venet, D., Dumont, J.E. and Detours, V., 2011. Supplementary analysis for: Most random gene expression signatures are significantly associated with breast cancer outcome.

Vigato, P.A., Peruzzo, V. and Tamburini, S., 2009. The evolution of  $\beta$ -diketone or  $\beta$ -diketophenol ligands and related complexes. *Coordination Chemistry Reviews*, 253(7-8), pp.1099-1201.

Vogelstein, B. and Kinzler, K.W., 2004. Cancer genes and the pathways they control. *Nature medicine*, 10(8), p.789.

Von Rauch, M., Schlenk, M. and Gust, R., 2004. Effects of C2-Alkylation, N-Alkylation, and N,N'-Dialkylation on the Stability and Estrogen Receptor Interaction of (4 R, 5 S)/(4 S, 5 R)-4,5-Bis (4-hydroxyphenyl)-2-imidazolines. *Journal of medicinal chemistry*, 47(4), pp.915-927.

WALLET, J.C. and GAYDOU, E.M., 1996. A Practical Synthesis of Dibenzoylmethanes. *Synthetic communications*, 26(22), pp.4097-4103.

Wang, D. and Lippard, S.J., 2005. Cellular processing of platinum anticancer drugs. *Nature reviews Drug discovery*, 4(4), p.307.

Wang, W., Vellaisamy, K., Li, G., Wu, C., Ko, C.N., Leung, C.H. and Ma, D.L., 2017. Development of a long-lived luminescence probe for visualizing  $\beta$ -galactosidase in ovarian carcinoma cells. *Analytical chemistry*, 89(21), pp.11679-11684.

Watts, P., Wiles, C., Haswell, S.J. and Pombo-Villar, E., 2002. Solution phase synthesis of  $\beta$ -peptides using micro reactors. *Tetrahedron*, 58(27), pp.5427-5439.

Webber, K. and Friedlander, M., 2017. Chemotherapy for epithelial ovarian, fallopian tube and primary peritoneal cancer. *Best Practice & Research Clinical Obstetrics & Gynaecology*, 41, pp.126-138.

Weng, C.J., Yang, Y.T., Ho, C.T. and Yen, G.C., 2009. Mechanisms of apoptotic effects induced by resveratrol, dibenzoylmethane, and their analogues on human lung carcinoma cells. *Journal of agricultural and food chemistry*, 57(12), pp.5235-5243.

Woodhead, C., Cunningham, R., Ashworth, M., Barley, E., Stewart, R.J. and Henderson, M.J., 2016. Cervical and breast cancer screening uptake among women with serious mental illness: a data linkage study. *BMC cancer*, 16(1), p.819.

Wust, P., Hildebrandt, B., Sreenivasa, G., Rau, B., Gellermann, J., Riess, H., Felix, R. and Schlag, P.M., 2002. Hyperthermia in combined treatment of cancer. *The lancet oncology*, 3(8), pp.487-497.

Xie, Y., Bagby, T.R., Cohen, M.S. and Forrest, M.L., 2009. Drug delivery to the lymphatic system: importance in future cancer diagnosis and therapies. *Expert opinion on drug delivery*, 6(8), pp.785-792.

Xu, H., Yu, S., Liu, Q., Yuan, X., Mani, S., Pestell, R.G. and Wu, K., 2017. Recent advances of highly selective CDK4/6 inhibitors in breast cancer. *Journal of hematology & oncology*, 10(1), p.97.

Yankov, P., Saltiel, S. and Petkov, I., 1986. Photoketonization of dibenzoylmethane in polar solvents. *Chemical physics letters*, 128(5-6), pp.517-520.

Yeung, T.M., Gandhi, S.C., Wilding, J.L., Muschel, R. and Bodmer, W.F., 2010. Cancer stem cells from colorectal cancer-derived cell lines. *Proceedings of the National Academy of Sciences*, 107(8), pp.3722-3727.

Zawadiak, J. and Mrzyczek, M., 2010. UV absorption and keto–enol tautomerism equilibrium of methoxy and dimethoxy 1, 3-diphenylpropane-1, 3-diones. *Spectrochimica Acta Part A: Molecular and Biomolecular Spectroscopy*, 75(2), pp.925-929.

Zawadiak, J., Mrzyczek, M. and Piotrowski, T., 2011. Synthesis and properties of aromatic 1, 3-diketones and bis-(1, 3-diketones) obtained from acetophenone and phthalic acids esters. *European Journal of Chemistry*, 2(3), pp.289-294.

## Appendix A

Raw Data –  $^1\text{H}$ NMR spectra

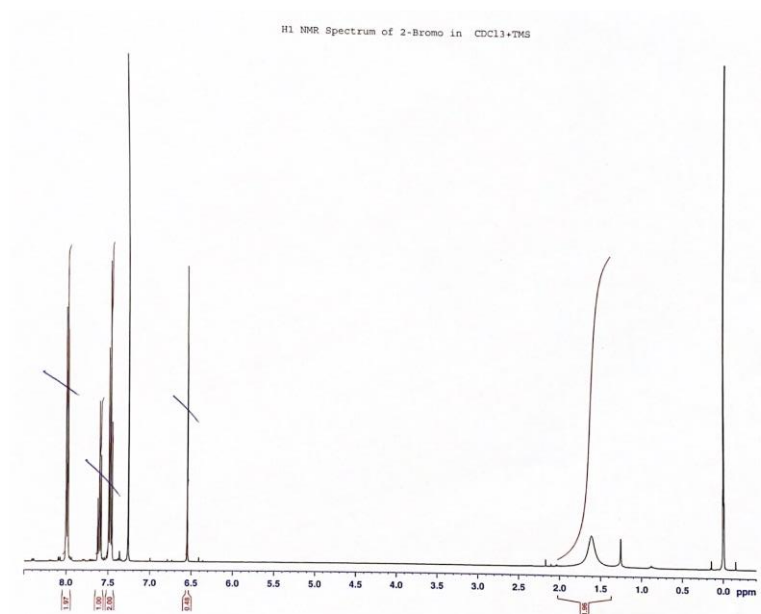


Figure 82 –  $^1\text{H}$  NMR spectra for 2-bromo-1,3-diphenylpropane-1,3-dione (4)

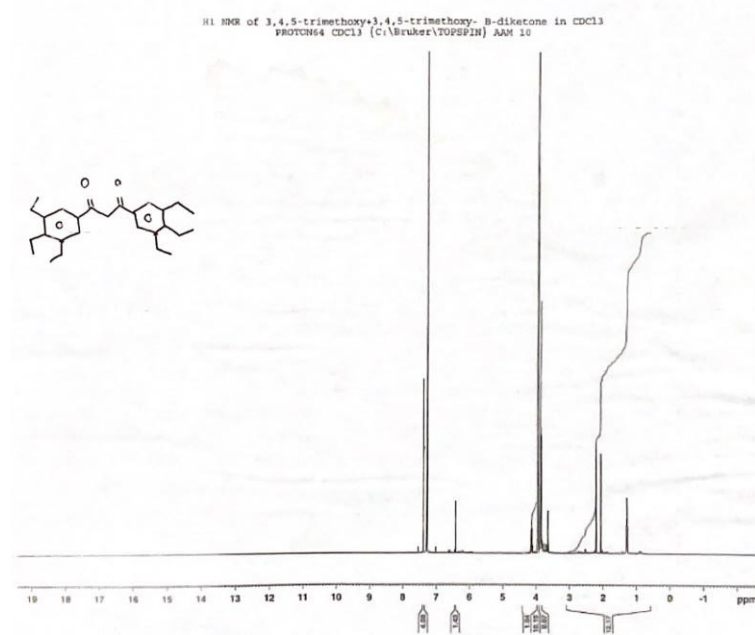
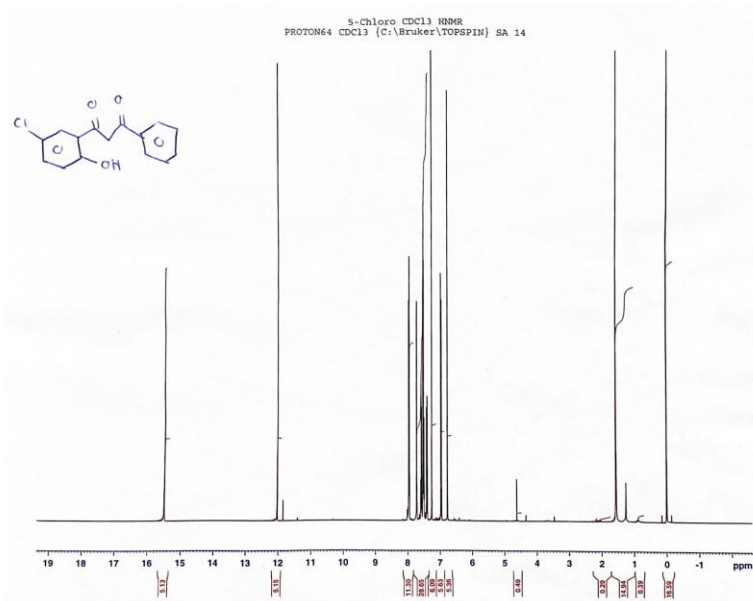
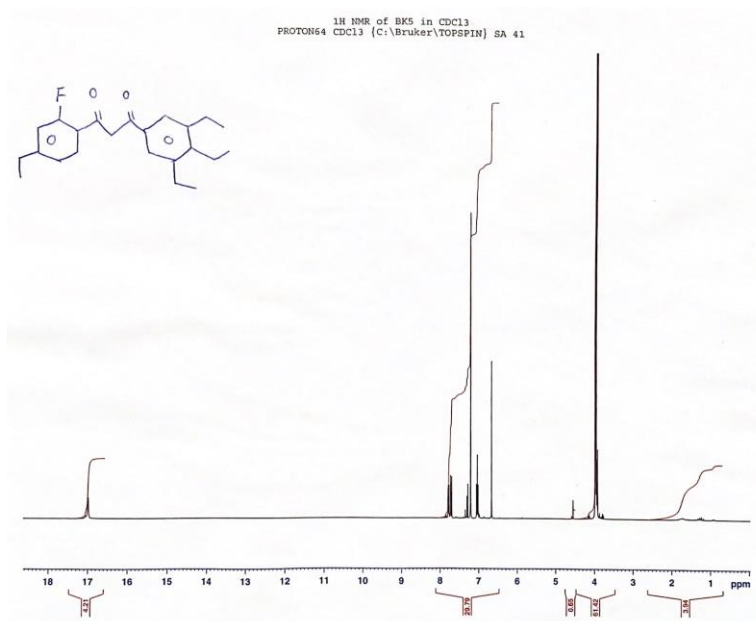
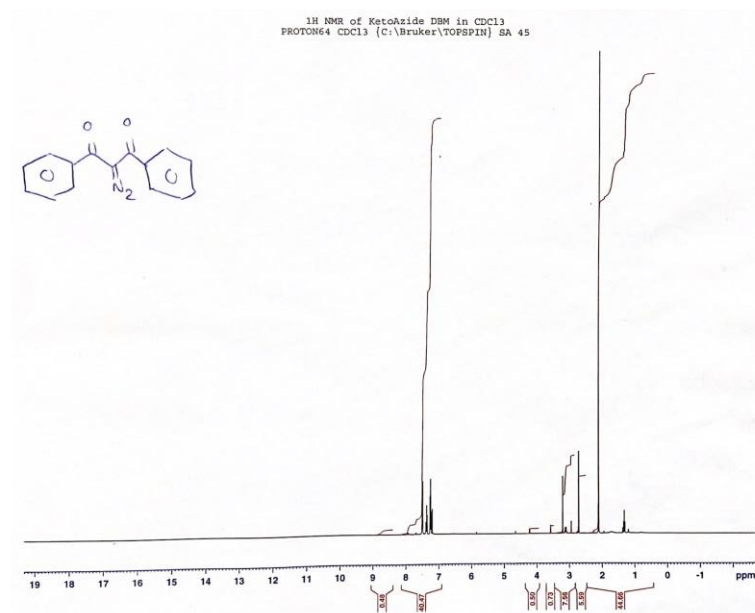
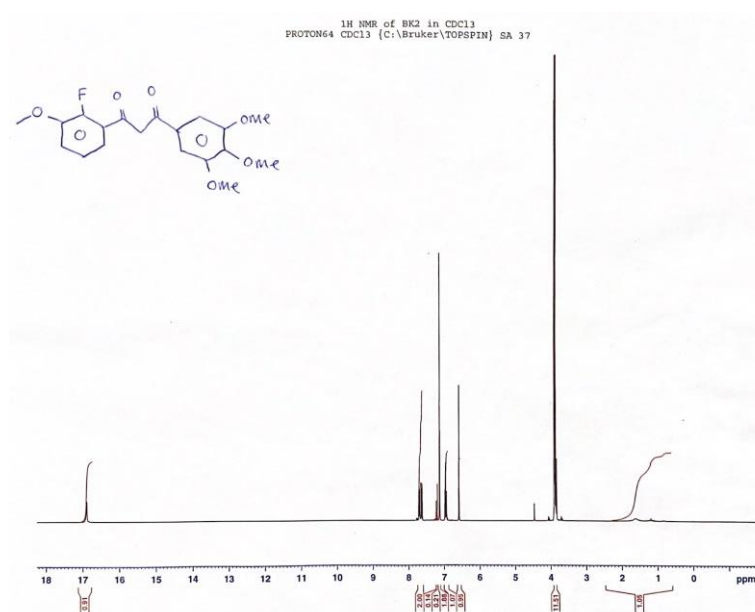
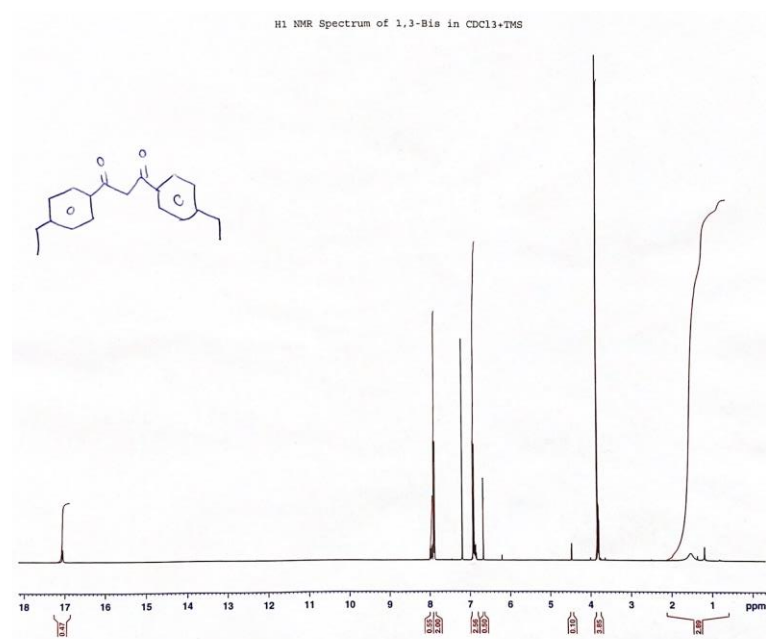
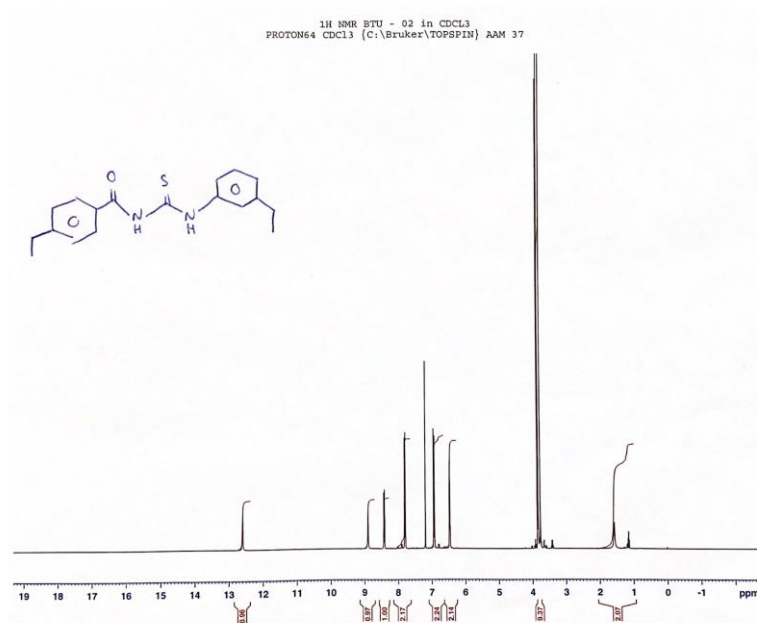


Figure 83 -  $^1\text{H}$  NMR spectra for 1-(3-(dimethyloxidanyl)-4,5-dimethoxyphenyl)-3-(3,4,5-trimethoxyphenyl)propane-1,3-dione (9)







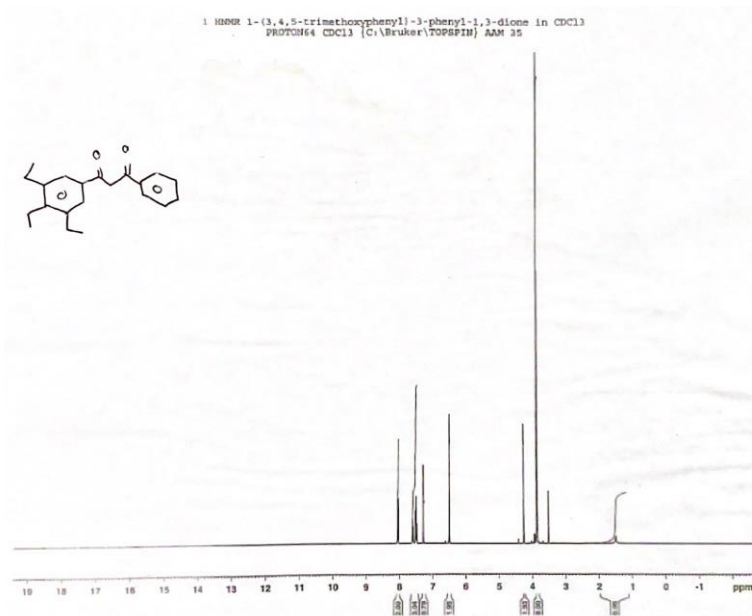


Figure 90 -  $^1\text{H}$  NMR spectra for 1-(phenyl-3-(3,4,5-trimethoxyphenyl)propane-1,3-dione) (10)

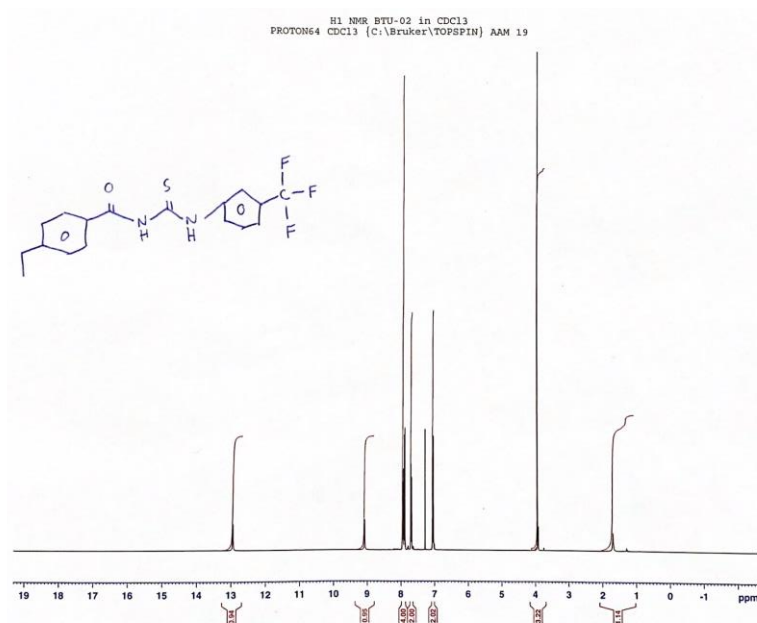
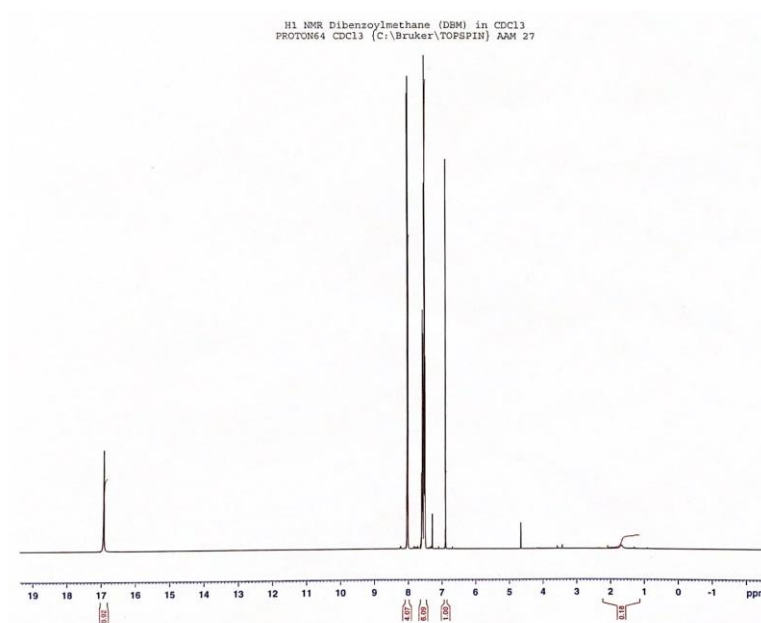
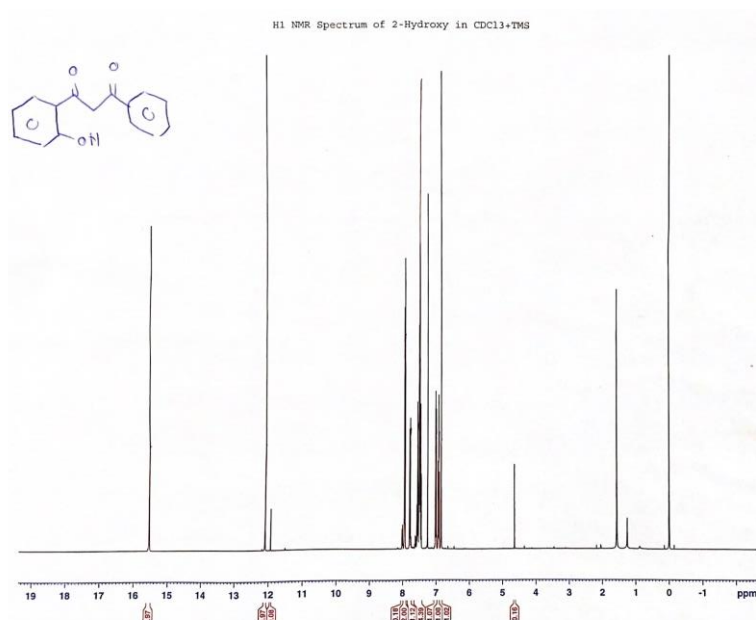


Figure 91 -  $^1\text{H}$  NMR spectra for 4-methoxy-N-(4-(trifluoromethyl)phenyl)carbamothioylbenzamide (14)



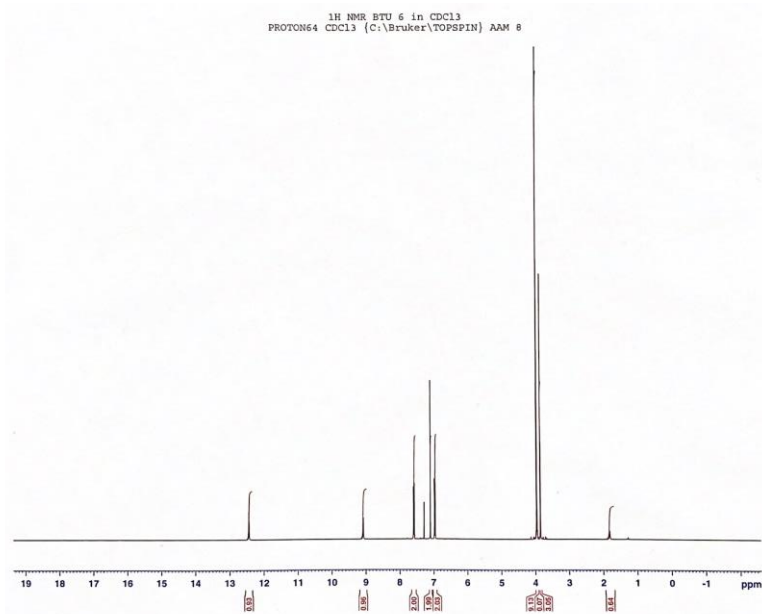


Figure 94 -  $^1\text{H}$  NMR spectra for 4-methoxy-N-((3,4,5-trimethoxyphenyl)carbamothioyl)benzamide (15)

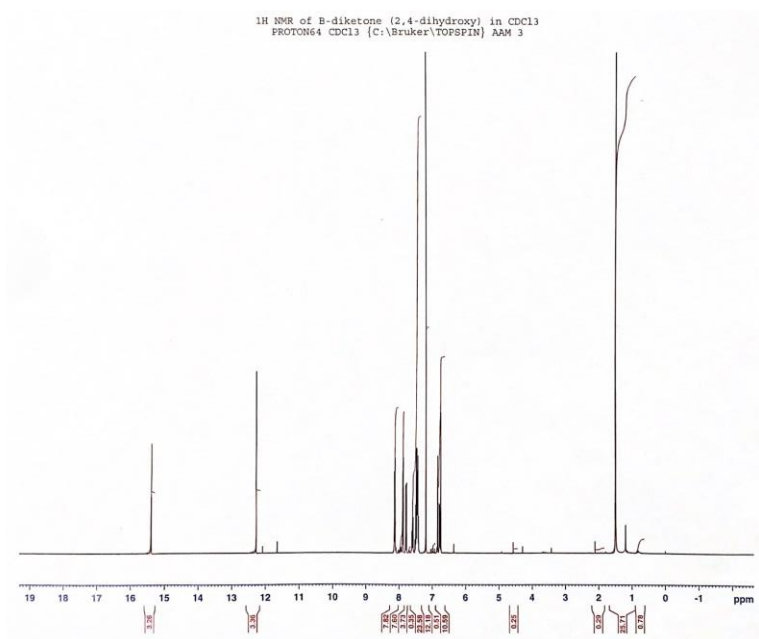


Figure 95 -  $^1\text{H}$  NMR spectra for 1-(2,4-dihydroxyphenyl)-3-phenylpropane-1,3-dione (2)

## Raw Data – IR Spectra

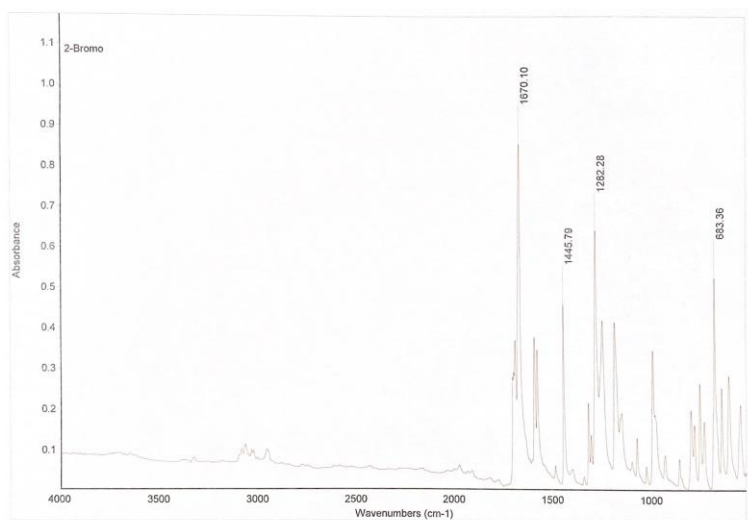


Figure 96 – Infrared Spectroscopy (IR) for 2-bromo-1,3-diphenylpropane-1,3-dione (4)

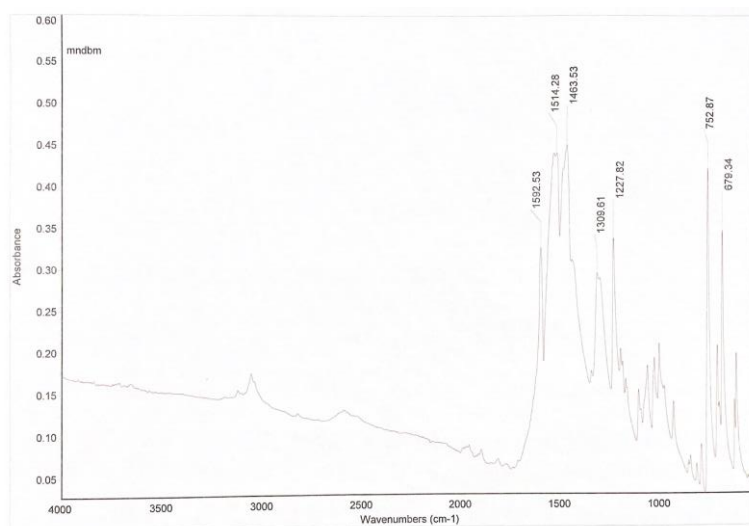


Figure 97 - Infrared Spectroscopy (IR) for 2-Azido-1-(2-hydroxyphenyl)-3-phenylpropane-1,3-dione (12)

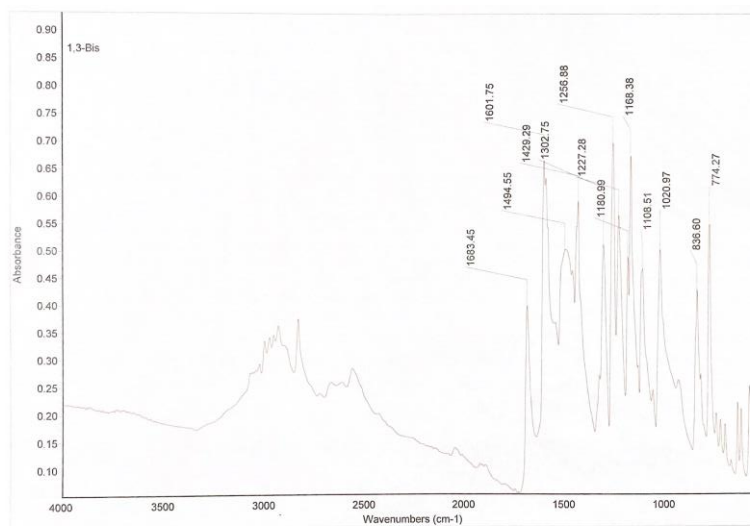


Figure 98 - Infrared Spectroscopy (IR) for 1,3-bis(4-methoxyphenyl)propane-1,3-dione (6)

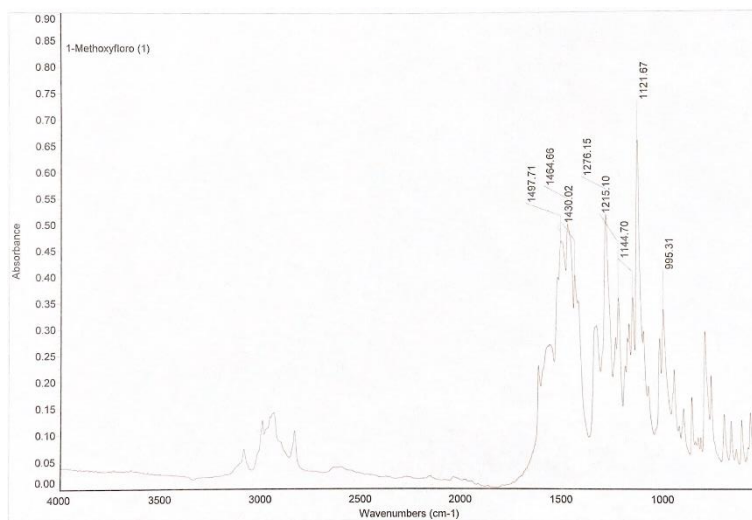


Figure 99 - Infrared Spectroscopy (IR) for 1-(3-(dimethoxydanyl)-4,5-dimethoxyphenyl)-3-3-flouro-4-methoxyphenyl)propane-1,3-dione (8)

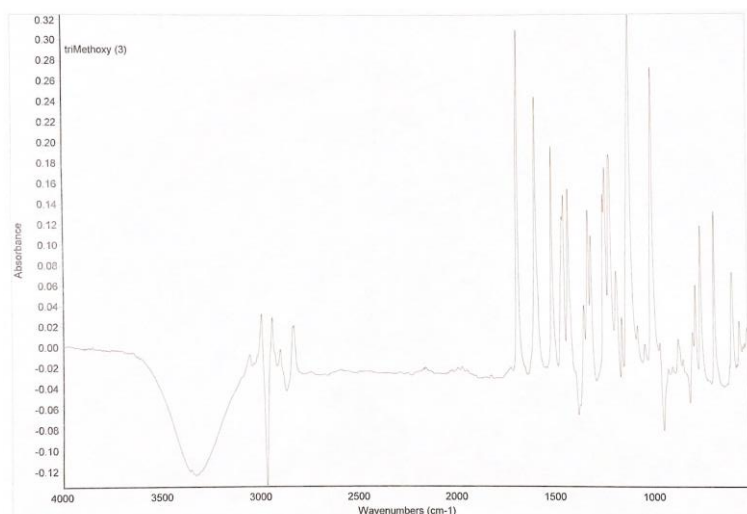


Figure 100 - Infrared Spectroscopy (IR) for 1-(3-(dimethoxydanyl)-4,5-dimethoxyphenyl)-3-(3,4,5-trimethoxyphenyl)propane-1,3-dione (9)

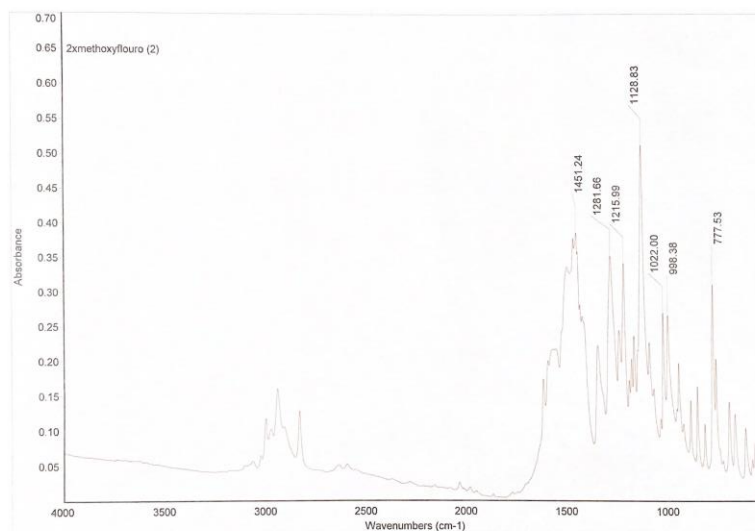


Figure 101 - Infrared Spectroscopy (IR) for 1-(3-(dimethoxydanyl)-4,5-dimethoxyphenyl)-3-(2-flouro-4-methoxyphenyl)propane-1,3-dione (7)

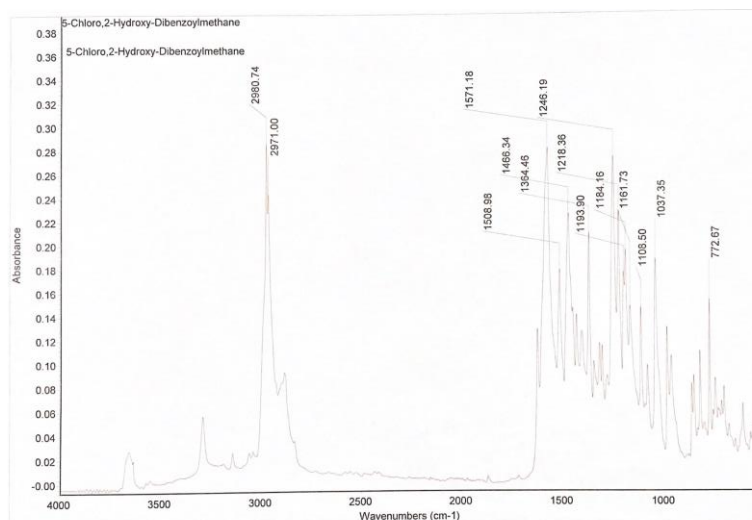


Figure 102 - Infrared Spectroscopy (IR) for 1-(5-chloro-2-hydroxyphenyl)-3-phenylpropane-1,3-dione (3)

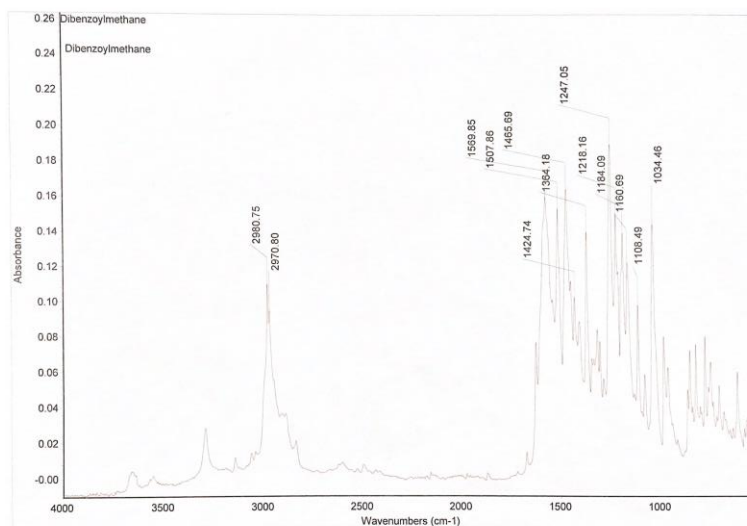


Figure 103 - Infrared Spectroscopy (IR) for 1,3-diphenylpropane-1,3-dione (DBM)

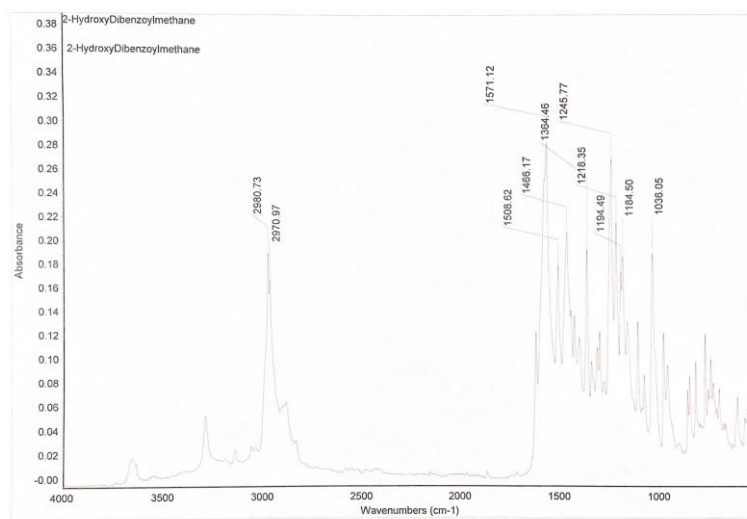


Figure 104 - Infrared Spectroscopy (IR) for 1-(2-hydroxyphenyl)-3-phenylpropane-1,3-dione (1)